Developing Biophysical and Structural Methods for Characterisation of Small Molecule Modulators of K2P Potassium Channels

Submitted in partial fulfilment of the requirements for the degree of Doctor of Philosophy

Jit Hang Jackie Ang

Wolfson College, University of Oxford

Hilary 2017

Authorship Declaration

This thesis and the work presented in it were completed at the University of Oxford (Nuffield Department of Medicine, Department of Physics and Department of Biochemistry) between October 2013 and April 2017, under the supervision of Prof. Liz Carpenter and Prof. Stephen Tucker. All contributions made by others have been stated clearly in the text. This work has not been submitted in full or partial fulfilment of any other degree.

Jit Hang Jackie Ang

April 2017

Abstract: Developing Biophysical and Structural Methods for Characterisation of Small Molecule Modulators of K2P Potassium Channels

Biophysical techniques are widely used to determine the structure, function and ligand binding properties of a protein. However, their application to membrane proteins has been limited due to the difficulty of obtaining sufficient purified sample.

In this work, I use such methods to examine the thermostability and ligand binding properties of TREKs, two members of the family of tandem pore domain K^+ channels important for the regulation of cellular excitability. Structures of TREK1 and TREK2 are available and thus when combined with such approaches may help guide the design of better ligands.

I first successfully optimised the DSF method using the CPM dye for the detection of TREK ligands and found this to be a viable approach. In addition, direct binding detection methods such as SPR, ITC and Biolayer Interferometry were also investigated.

A test case of 351 compounds derived from an FDA-approved pharmaceutical agent library were then screened against a range of K2P channels using the CPM assay. Several compounds were identified that appeared to thermostabilize the TREKs. These initial hits were further assessed using label-free DSF and functional studies on channel activity. Two compounds, cilnidipine and rimonabant were identified as a novel inhibitor and activator of TREK2 and TREK1 respectively. The findings are significant for the development of potent and selective binders for the TREKs and other membrane proteins, as they identify a viable workflow for identification of binders using biophysical methods.

Jit Hang Jackie Ang, Hilary 2017

Submitted in partial fulfilment of the requirements for the degree of Doctor of Philosophy.

Acknowledgements

This work would not have been possible without the help and support of many colleagues and friends. I would like to thank first of all my supervisors, Prof. Liz Carpenter, whose advice, support and understanding throughout this journey has been invaluable. I would also like to thank Prof. Stephen Tucker for his supervision, enthusiasm and help provided, especially with electrophysiology experiment planning and writing this thesis. My industrial supervisor, Dr. Darren Cawkill from Pfizer also contributed many ideas and gave very helpful advice which has been incorporated in this work. I am very blessed to have this team of supervisors helping me along in this long and at times, arduous journey of a DPhil.

I would next like to thank all my colleagues from the Integral Membrane Proteins group for their help, support and gossip provided over the last 3 years or so. Special thanks go to Dr. Andy Quigley and Dr. Yin Yao Dong, who first trained me in protein purification and the planning and execution of biophysical assays at the SGC. He also kept me out of trouble when I was new to the place. I would also like to thank Dr. Oleg Fedorov and his team at the Target Discovery Institute for the access to facilities, training and samples provided. For keeping the laboratory running as well as ensuring a constant supply of cells with which to purify protein from, I'd like to thank Dr. Nicola Burgess Brown and the Biotechnology group as well as Dr. Andy Quigley for co-ordinating all the efforts on this front. Dr. Manuel Arcangeletti has my gratitude for helping me in the functional assays and oocyte handling at the Department of Physics. For providing support in SPR assays and running the facility, I'd also like to thank Dr. David Staunton from the

Department of Biochemistry. Lastly, for providing test compounds and industrial themed advice, I'd like to thank Dr. David Pryde and Dr. Edward Stevens from Pfizer.

Finally, I would like to thank my friends, family and especially my wife, Wee Suan for supporting me throughout these years and my home country, Singapore for giving me this chance to expand my horizons in the United Kingdom.

My D.Phil. has been generously supported the Agency of Science, Technology and Research, Singapore and the Systems Approaches to Biological Science – Industrial Doctorate Centre, University of Oxford.

Table of Contents

Index of Figures

Index of Tables

Chapter 1: Introduction

1.1: Ion Channels

Cell membranes are barriers to the permeation of molecules and ions as they are amphipathic in nature. The hydrophobic interior of the cell membrane makes the permeation of hydrophilic molecules and ions energetically unfavourable. It also creates two separate environments between the inside and outside of cells[1]. Ion channels are proteins that allow for the passive movement of ions down an electrochemical gradient through the hydrophobic cell membrane. They are integral membrane proteins and as such, are embedded within the phospholipid bilayer of plasma membranes or within internal membranes of cells. There are at least 232 different ion channel genes found in humans[2] and much more structural and functional diversity from the formation of heteromultimers.

Ion channels contain pores that remain in an open state while conducting ions through membranes, which make them much more efficient in facilitating ion permeation when compared to transporters such as the Na^+/K^+ ATPase[3]. Another difference is that ion channels do not require adenosine triphosphate (ATP) in order to perform their function while active transporters require this as ion channels allow ions to flow down electrochemical gradients while active transporters or pumps transport ions against chemical gradients[3]. Secondary transporters and passive transporters do not require ATP and transport small molecules down a chemical gradient.

Ion channels can be switched between conductive and non-conductive states through a process known as gating. This involves conformational changes which open or close a transmembrane pathway between the extracellular and intracellular environments[4].

Gating of ion channels can be regulated by diverse stimuli, including changes in transmembrane potential[5], pH[6], mechanical stretching of membranes[7], temperature[8] and environmental light intensity[9]. In addition, they can be gated by binding to ligands[10] which can either open or close the channels.

Ion channels can be classified by their ion permeation properties. They can broadly be divided into those which selectively conduct a single ion, for example sodium, potassium, calcium or chloride ions, and less selective channels which conduct multiple ions[11, 12].

Ion channels are important drug targets, as almost every cell in the body has a transmembrane potential and is thus electrically active. Changes in ion concentrations within the cell underlie processes such as osmotic regulation[13], signal transduction[14] and cell migration[15]. Ion channels are also important for nerve cell function and maintenance of membrane potentials of cells, which underpin the ability of humans to respond to external stimuli. Loss of function of ion channels often leads to diseases known as channelopathies[16]. In addition, modulation of ion channels can lead to changes in cell function and are potential ways to treat other diseases. Many ion channels are the targets for currently available drugs[17] or are the sites of adverse off target effects. For example, lidocaine and other local anaesthetics target the voltage-gated sodium channels and nifedipine or verapamil target L-type calcium channels and are commonly used to treat cardiac diseases[18]. Novel discoveries of ion channel modulators, both in terms of novel drugs and novel methods to finding drugs would thus be very useful for the pharmaceutical industry.

1.2 Challenges in Ion Channel Drug Discovery

Ion channels are important therapeutic targets as they underpin many biological processes. About 13% of all known drugs are targeted at these channels[19] whereas they make up only about 1% of all human proteins[17]. Over 55 "channelopathies", diseases linked to the dysfunction of a single ion channel, have been identified and these diseases represent challenges for drug discovery[20].

However, there have been many challenges in ion channel discovery. There are many approaches to check for drug efficacy and many drugs that target ion channels today were discovered using classical tissue or animal based pharmacology techniques, without knowledge of their target of action. In this respect, ion channel drug discovery has lagged far behind other types of proteins, such as enzymes, where an assay involving catalysis with labelled substrates is often used in early stage drug discovery[20]. The 'gold standard' functional assay for ion channel drug discovery is the manual patch clamp. However, this depends on the successful overexpression of ion channels in a model cell type.

Ion channels are challenging to clone and express in a functional manner. They are integral membrane proteins, are often made up of multiple subunits and many are heteromultimers. This poses difficulty in the expression system for correct assembly and folding as well as the replication of the physiological distribution of human channels. In addition, overexpression of ion channels can also lead to toxicity and they are often poorly tolerated, leading to poor cell growth or viability.

Protein-only approaches are able to avoid all the problems associated with cell expression. This is a simplified system which allows direct interactions between proteins

and ligands to be explored without confounding factors such as cell signalling. However, ion channels are integral membrane proteins, which are challenging to purify and obtain in significant amounts as they have hydrophobic external surfaces due to the requirement to interact with hydrophobic cores of cell membranes. This makes them insoluble unless detergents or artificial membranes are used to solubilize them. Detergents may also stabilise different portions of the protein as compared to native cell membranes and cause misfolding or misassembly of the protein.

The Carpenter group at the Structural Genomics Consortium (SGC) is now able to express and purify a group of ion channels in sufficient quantities and the main aim of this thesis is to evaluate protein-only approaches to investigating protein-ligand interactions in ion channels. I also aim to develop a workflow for medium-throughput screening of ion channels which can be scaled up to higher throughput methods. The model channels that are used in this project are Tandem-Pore Domain potassium channels (K2Ps).

1.3: Potassium Channels

An important class of ion channels are those that selectively conduct potassium ions. There are over 70 different members within this family and they are found in every kingdom of life[22]. Potassium channels are mostly either tetrameric or dimeric but all share a common sequence which defines their K^+ selectivity[23].

Potassium channels perform important functions such as maintaining the resting membrane potential of excitable cells[23], maintaining electrolyte balances[23] and mediating the effect of GPCR signalling[24].

The Na^+-K^+ ATPase generates a large asymmetric gradient for sodium and potassium ions across the cell membrane. This results in a higher concentration of K^+ inside the cell compared to outside (20-30X). Thus, opening of potassium channels allows the efflux of K^+ ions down this electrochemical gradient which hyperpolarises the inside of the cell to produce a membrane potential of between -20 mV to -120 mV[23]. The ability to change the membrane potential allows the gating of potassium channels to be a control mechanism for the generation and transmission of action potentials[25], cell apoptosis[26] and the release of insulin and glucagon, important hormones that govern metabolism in humans[27].

There are three main classes of potassium channels and although they share a common overall architecture, they differ by the number of transmembrane helices they contain per subunit. The simplest potassium channels are those with two transmembrane helices connected by an intramembrane loop per subunit. These include the K_{ir} family of channels[28]. A second family of potassium channels is voltage-gated and have 6 transmembrane helices per subunit and contain a 4 transmembrane-helix voltage sensing domain[28]. A third family, the two-pore domain potassium channels (K2Ps) have 4 transmembrane helices per subunit and assemble as dimers to produce a pseudo-tetrameric pore. These channels have multiple modes of activation and are the subject of this thesis[28].

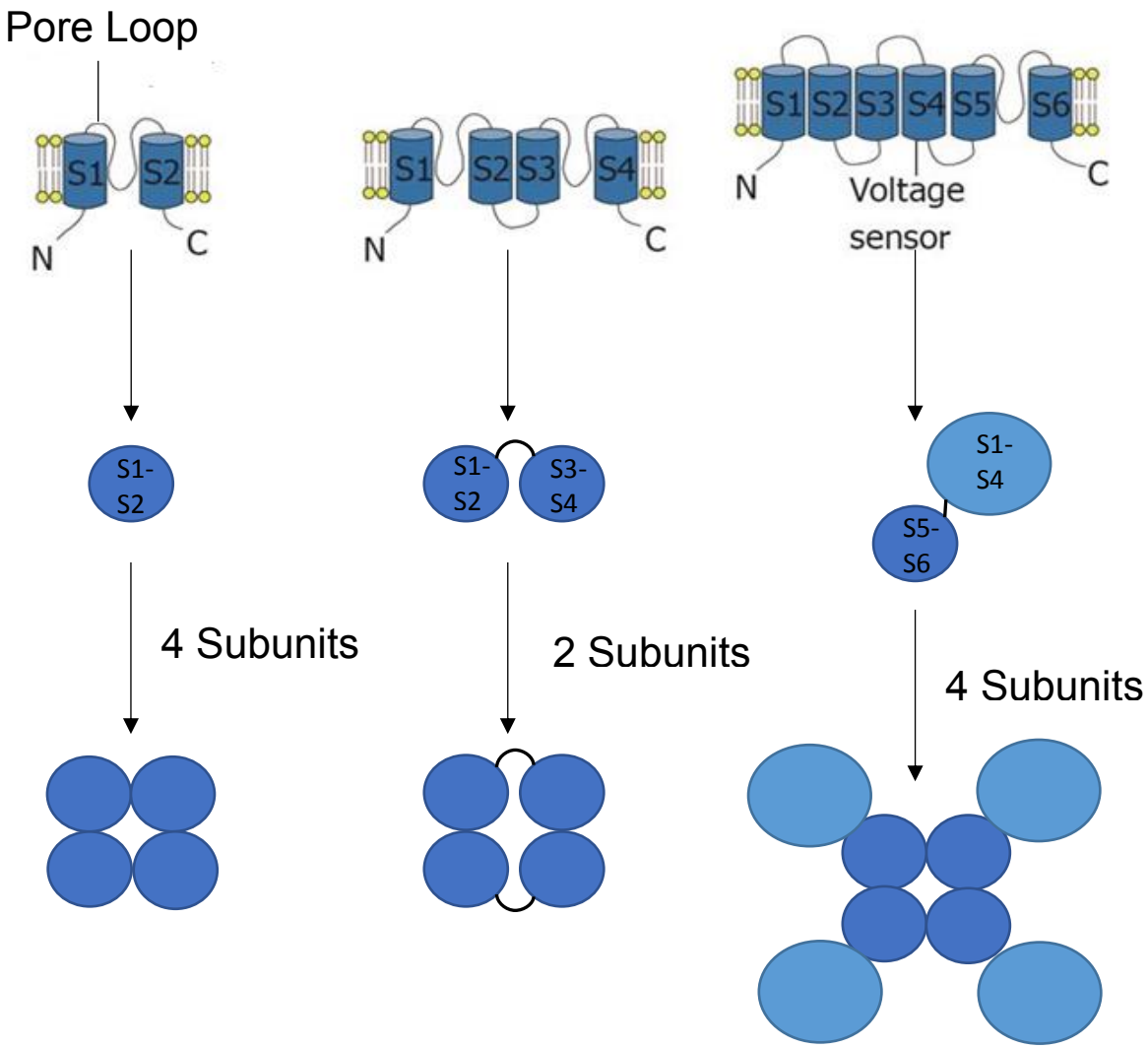

Figure 1.1: The 3 different families of potassium channels found in mammals: *The 3 main families of potassium channels found in mammals are those containing 2 transmembrane helices per subunit and assemble in a tetrameric form (K_{ir} channels, left), those containing 4 transmembrane subunits that assemble in a dimeric form (K_{2P} channels, middle) and those containing 6 transmembrane subunits that assemble in a tetrameric form (K_v channels, right).The top structures show the topology of each type of potassium channel. Each cylinder represents 1 transmembrane helix. The bottom figure shows the 2 or 4 fold symmetry that all potassium channels exhibit around the pore domain. Figure adapted from Zhou et al., 2012*[29].

1.4: Two Pore Domain Potassium Channels (K2Ps)

K2Ps are unique among potassium channels in that they form dimers instead of tetramers. This is because each monomer of a K2P channel contains two pore forming subunits instead of one, allowing for a dimer to form a functional channel with four pore forming subunits with a pseudotetrameric selectivity filter for potassium[30,31]. Potassium channels with two pore forming subunits per monomer were first discovered in yeast in 1995 via genome mining[32] and since then, many other such channels have been found in plants and animals[33,34].

K2Ps serve the function of maintaining the resting membrane potential in cells. They underpin the leak current[35] and modulate the excitability of cells[36]. Most K2Ps, when fully activated, are open rectifying channels which follow the Goldman-Hodgkin-Katz voltage equation[37, 38]. A sample IV graph is shown below in Figure 1.2.

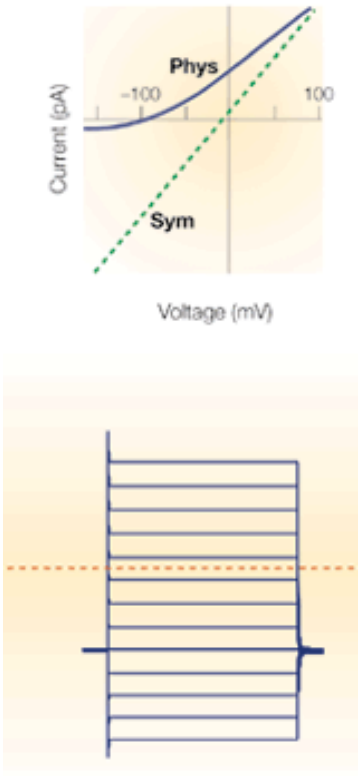

Figure 1.2: Current-Voltage Relationships for K2P channels. *The graph represents an ideal example of a K2P channel current-voltage relationship. Both symmetric and physiological K^+ concentrations have been shown. In the bottom panel, currents are drawn according to symmetric conditions from -80 to +60 mV. The IV graph shows the open rectifier nature of K2P channels[39]. Figure taken from Goldstein et al., 2001[39].*

There are 15 members of the K2P family found in humans[40]. They are broadly divided into 6 families based on their sequence identity and functional similarity[40]. The gene names for these proteins are given in brackets after the protein names. The **T**WIK related **A**cid **S**ensitive $\mathbf{K^+}$ channels, TASK1 (KCNK3), TASK3 (KCNK9) and TASK5 (KCNK15) are acid sensitive channels, which are inhibited by extracellular acidification[41, 42]. The **T**andem pore-forming domains in the **W**eakly **I**nwardly rectifying $\mathbf{K^+}$ channels TWIK1 (KCNK1) and TWIK2 (KCNK6) are weak inward rectifiers[43, 44] while the **T**WIK **Re**lated $\mathbf{K^+}$ channels TREK1 (KCNK2), TREK2 (KCNK10) and the TWIK-related arachidonic acid–activated K+ **channel**

TRAAK (KCNK4) are membrane stretch activated[45]. The **T**WIK- related **Al**kaline pH-activated K^+ channels TALK1 (KCNK16) and TALK2 (KCNK17), like the TASKs are pH sensitive but are instead gated open by extracellular high pH[46] and the **T**WIK **Re**lated **S**pinal chord K^+ channel TRESK (KCNK18) is an extracellular calcium activated channel[47]. The **T**andem pore domain **H**alothane-**I**nhibited K^+ channels THIK1 (KCNK13) and THIK2 (KCNK12) are inhibited by halothane[48]. This project focuses primarily on the TREK1 and TREK2 channels, with some studies on the TASK1 and TWIK1 channels. The relationship between the channels is shown in the phylogenetic tree in Figure 1.3.

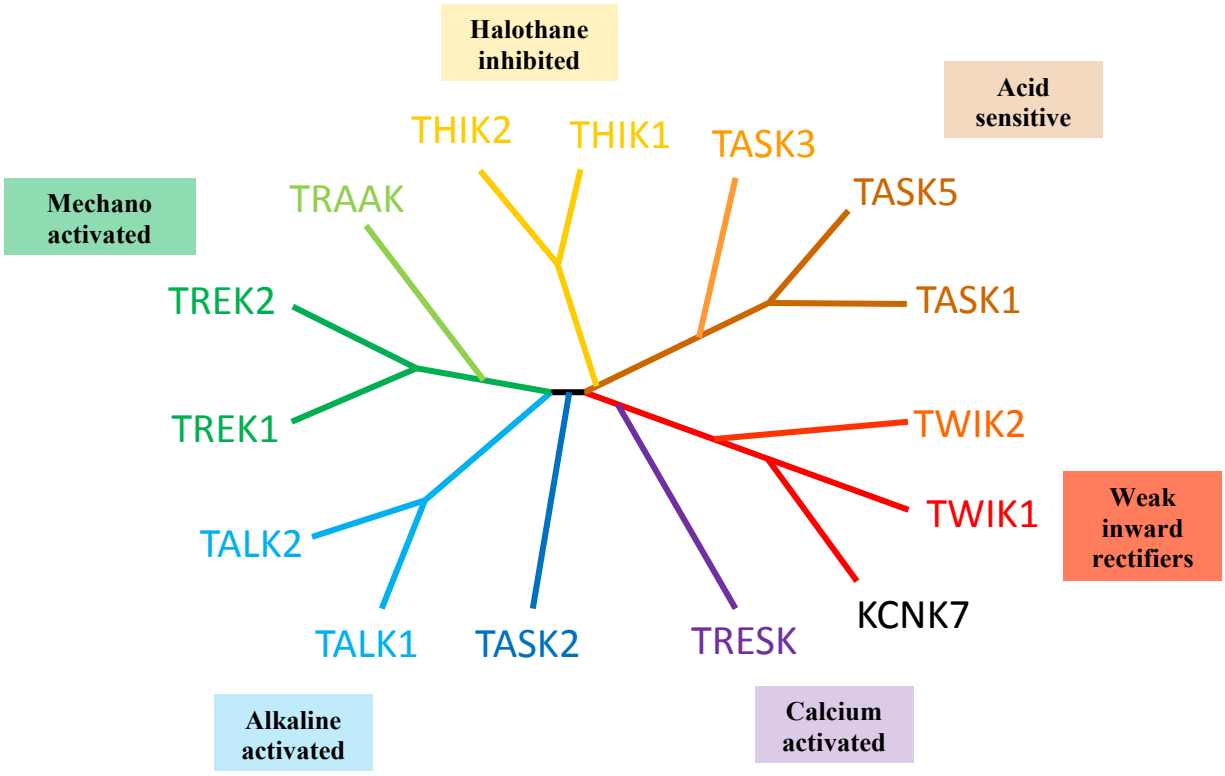

Figure 1.3: Phylogenetic Tree of K2P channels. *There are 15 members of the K2P family and where they stand in relation with one another is shown in this phylogenetic tree. Figure was taken and adapted from Dong Y., Carpenter group, SGC.*

Although the prevailing view is that most K2P channels assemble as homodimers and are studied as such, there is some evidence from co-localisation and co-expression that certain K2P channels can form functional heterodimers within subfamilies. Examples of such heterodimeric channels are TASK1/TASK3 and TREK/TRAAK[49,50]. In addition, there is some controversial evidence for the formation of TWIK1/TREK1[51]. Heterodimerization could increase the functional diversity of such channels. It is not known what proportion of K2P channels can form heterodimers in different tissues or cell types but this is important in further elucidating the function of these proteins.

1.5: Structure of K2P Channels

Structures of potassium channels were the first among all ion channel structures to be solved by X-ray crystallography[52]. The first ion channel structure solved was that of KcsA, a bacterial potassium channel and this was accomplished by Doyle *et al*. in 1998[53]. The monomer structure showed 2 transmembrane helices with a pore forming loop between them (Figure 1.4) and the overall tetrameric architecture of a potassium channel as shown by KcsA has been proven to be highly conserved in all other potassium channels.

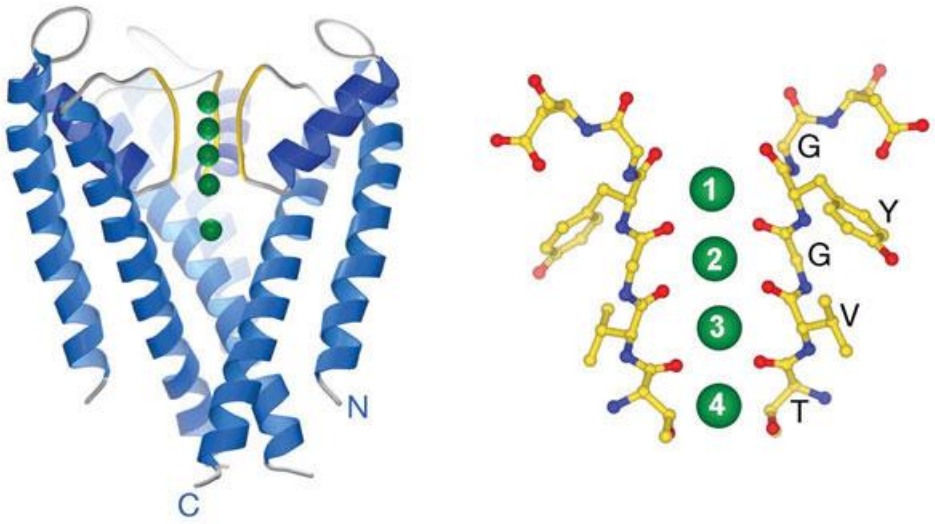

***Figure 1.4*: Structure of KcsA.** *Structure of KcsA (Left) showing the position of potassium ions, transmembrane helices and the selectivity filter pore (right) of KcsA. Three of the four chains are shown for clarity, the fourth is removed to reveal the selectivity filter. Residues that interact directly with potassium ions (TVGYG) are highly conserved in all K channels (Figure adapted from Morais-Cabral et al., 2001)[54].*

Examples of nearly all the major subfamilies of potassium channels have been solved by X-ray crystallography[55, 56, 57]. This includes 4 structures of K2P channels and differences seen between the solved K2P structures can be compared and linked to their functional

diversity. TWIK1 was elucidated by Miller and Long in 2012[30] and following that, structures were determined for TRAAK (PDB ID: 3UM7)[58], TREK2 (PDB ID: 4BW5)[59] and TREK1 (PDB ID: 4TWK), the latter two by the SGC in Oxford.

The main difference between the K2Ps and other potassium channels is that they are dimeric, not tetrameric. They also have an extracellular cap, which consists of 2 helices[30, 58, 59]. This extracellular cap is seen in all K2Ps and its function is unknown. A disulphide bond between cysteine residues connects the extracellular cap domains of the 2 monomers in all 3 published structures, but this connection is not a requirement for the folding of the protein[30, 58, 59].

***Figure 1.5**: **Sequence Alignment for crystal constructs of TREK1, TREK2, TRAAK and TWIK1.** This figure shows the BLAST amino acid sequence alignments for the 4 K2Ps with known structures. Transmembrane helical sections are highlighted in green, cysteine residues in blue or yellow. The cysteine residue highlighted in yellow is the residue which is located in the extracellular cap domain and forms a disulphide bond with the corresponding residue on the other monomer in the structure. The sections indicated with "h" represent helical secondary structure for these sections of the protein.*

Some published K2Ps structural conformations also exhibit a fenestration between the M2 and M4 helices, which allows the inner part of the channel to interact with the hydrophobic part of the cell membrane and is a possible site for ligand binding[30, 58, 59]. This is important in later work elucidating ligand binding to such channels and will be discussed further with TREK2 as a model.

1.6: Function of K2P Channels

In humans, the resting membrane potential, which is the voltage across a plasma membrane of a cell is about -70 mV. This is very close to the reversal potential of potassium ions, which indicates that the cell membrane must be highly permeable

towards potassium ions as derived from the Goldman-Hodgkin-Katz equation[1] (Equation 1.1) which is shown here:

$$E_m = \frac{RT}{F}\ln\left(\frac{P_{Na^+}[Na^+]_{out} + P_{K^+}[K^+]_{out} + P_{Cl^-}[Cl^-]_{out}}{P_{Na^+}[Na^+]_{in} + P_{K^+}[K^+]_{in} + P_{Cl^-}[Cl^-]_{in}}\right) \quad (1.1)$$

In this equation, Em is the membrane potential across any given membrane, R is the gas constant (8.314 J / mol. K.), T is the temperature in Kelvins, F is the Faraday constant (96485.33289 C/mol) and P is the permeability of the membrane towards a given ion (in siemens)[1].

This is the greatest single contribution to the resting cell membrane potential as the membrane is much less permeable to sodium and chloride ions[1]. The flow of potassium ions across the plasma membrane in the resting state is known as the "leak" current[35].

There are 2 types of potassium channels that facilitate the leak current in excitable cells the inward rectifying K_{ir} potassium channels, which have been extensively covered in other reviews[22, 61], and the K2P channels, which are the subject of this thesis.

K2P channel currents are described as time independent and non voltage-gated, but can be voltage dependent[62]. They are also regulated by a diverse range of stimuli as described in section 1.4. Their main function is thus to regulate cellular excitability in the presence of such stimuli.

1.7 K2Ps in human health and disease

As K2Ps modulate cellular excitability, they are linked to a range of diseases and are potentially interesting drug targets. Loss of function or gain of function mutations in members of the K2P family have been linked with cardiac and neural disorders. Two examples to highlight are a gain of function mutation in TASK4 (TALK2)[63] and a loss of function mutation in TRESK[64].

A single point mutation in TASK4 (G88R) is shown to slow down cardiac conduction and the upstroke beating of HL-1 cells in cardiac muscle. This is in conjunction to a splice mutation of SCN4A, a sodium channel and it has been proposed as a second hit mechanism for a severe cardiac conduction disorder[63]. In the case of TRESK, a frameshift mutation F139WfsX24 was shown to be associated with hereditary migraine with aura. This dominant negative mutation is passed down generations of the same family[64].

The roles in health and disease of many other K2P channels have been investigated via a variety of genetic approaches including rodent knockout studies, of which those of TREK1 and TREK2 will be discussed below in section 1.8.

1.8 Structure and Function of TREK1 and TREK2

The TREK family of K2P channels was first discovered in 1996[65] and contains 3 members, TREK1 which is encoded by the gene KCNK2[65], TREK2[66], encoded by the gene KCNK10 and TRAAK, which is encoded by the gene KCNK4[67]. Of these channels, TREK1 and TREK2 are very closely related, with 63% of amino acids being identical and 78% homologous in sequence[68]. TRAAK is more distantly related to both the other proteins (Sequence alignment in Figure 1.5). Both TREK1 and TREK2 are most highly expressed in the central

nervous system but also found in the peripheral nervous system, heart, pancreas and kidney[69, 70].

Both TREK1 and TREK2 also exhibit multiple splice variants[69] and N-terminal truncations due to weak Kozak sequences and the presence of internal start codons, which act as alternative start sites during translation[71, 72], thus increasing the potential functional diversity. Combined with the finding that the relative abundance of these splice variants is tissue-specific, it can be postulated that TREK channels perform diverse functions in different organs in the body[69].

In the published structures for TREK1 (PDB ID: 4TWK) and TREK2 (PDB ID: 4BW5), there is significant overlap in the structure of both proteins due to their sequence similarity (Figure 1.6). The extracellular cap domain and pore domains are almost identical, but the selectivity filter in the original TREK1 structure appeared to be distorted. The 4 classical selectivity filter sites however, have been seen in a more recent structure obtained by X-ray free electron laser (unpublished data).

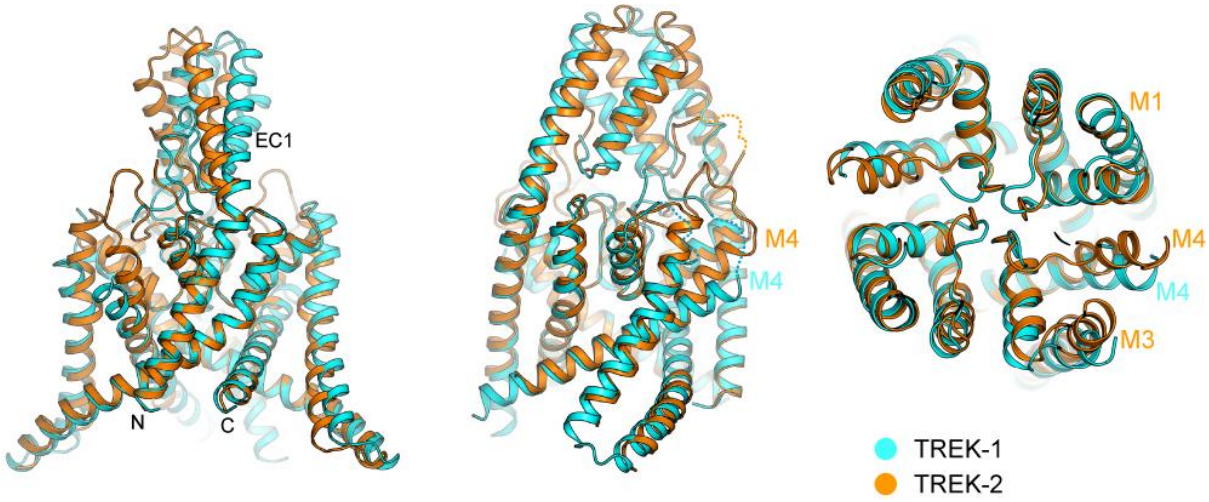

Figure 1.6: Comparison of Structures of TREK1 and TREK2. *The 2 channels are very similar in their structures. The main differences are the shifted extracellular cap, distortion of the TREK1 pore when compared to TREK2 and N-terminal shift of M4 helix (Pike A., unpublished work).The extracellular cap is indicated as EC1 on the figure, is also referenced in the sequence alignment in Figure 1.5.*

TREK1 and TREK2 respond to a wide range of stimuli. Other than the previously reported mechanical stretch, changes in the amount of heat, pH, membrane depolarisation and certain chemical stimuli such as phospholipids can cause channel opening or closure[36, 73]. This allows K2P channels to function as a signal integrator to regulate cellular excitability[36]. A C-terminal region, located just after the M4 helix of TREK1, of about 30 residues was found to be important in responding to these stimuli through mutagenesis and chimera studies[40]. This region extends from residues V298 to T322 in TREK1 and V324 to T348 in TREK2 and contains a highly charged region postulated to interact with phospholipid heads in cell membranes. Modifications to this region would change the conformation of the protein, leading to gating[40].

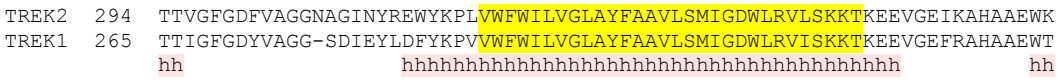

Figure 1.7: Sequence alignment for C-terminal sections of wild-type human TREK2 and TREK1. *The highly charged region which interacts with phospholipid heads in cell membranes is highly conserved and highlighted in yellow.*

The physiological functions of TREK1 and TREK2 have been predicted by mouse knockout studies. TREK1 knockout mice are very well studied and these mice are generally healthy, but have enhanced sensitivity to heat and painful mechanical stimuli, suggesting a role in pain sensation[74]. Knocking out TREK1 also leads to mice that are depression-resistant and more susceptible to ischaemia and epilepsy[75, 76]. TREK1 has also been linked to neuroprotection in knockout mice studies. The neuroprotective effect associated with TREK1 is mediated by polyunsaturated fatty acids, which are released during brain ischaemia and were shown to activate TREK channels[75, 77]. When TREK1 is knocked out, injection of polyunsaturated fatty acids was found to exhibit no effect. Specificity was shown by performing the same experiment with TRAAK knockout mice and no effect was seen[75]. Much less is known about TREK2 knockout mice but a recent study has shown the channels to be involved in sensing moderate heat as well as moderately cool conditions. TREK2 channels are also important in mechanical and osmotic pain sensation due to their mechanosensitive properties[78].

These studies into the physiological roles of TREK1 and TREK2 may not provide the complete picture of their physiological roles, but what is known does make them interesting potential pharmaceutical targets for the treatment of pain.

1.9 Pharmacology of TREKs

While the physiological activation of TREK channels has been discussed above, a wide range of chemical agents have also been seen to interact with TREK channels. Volatile anaesthetics such as isoflurane and lidocaine have been shown to inhibit TREK1, consistent with studies on TREK1 knockout mice being resistant to the effects of these drugs[79]. A putative binding site has recently been found for anaesthetics by modelling and site-directed mutagenesis studies[80].

Activators of TREKs include riluzole (EC_{50} > 100 µM on TREK1), a neuroprotective agent[81], DCPIB (EC_{50} = 10 µM on TREK1)[82], flufenamic acid (EC_{50} = 100 µM on TREK1)[83] and BL1249 (EC_{50} = 1.5 µM on TREK1)[84]. A physiological activator of TREK1 is arachidonic acid, which is released from membrane lipids during stretch. Arachidonic acid has a EC_{50} of about 100 µM[85].

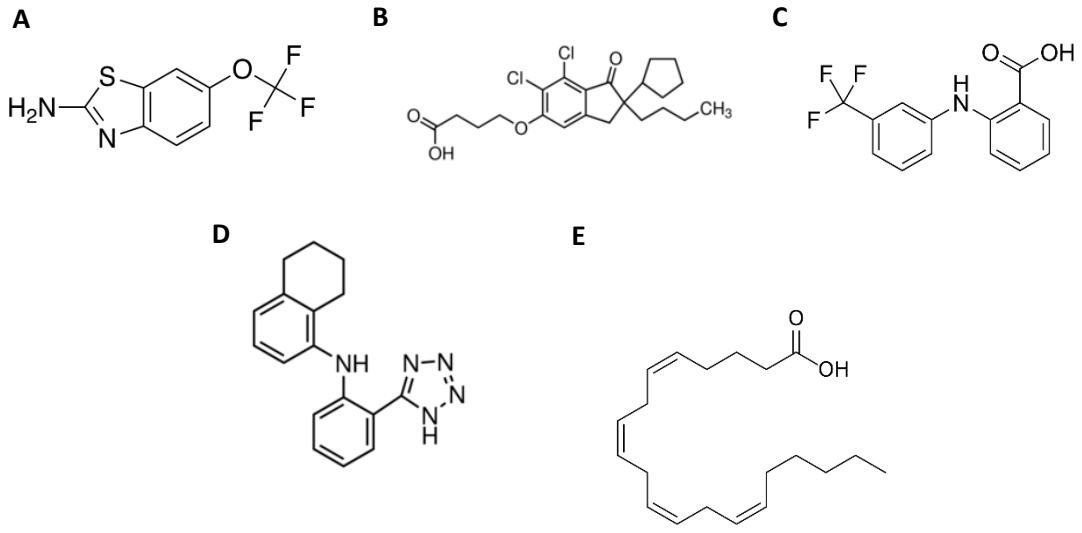

Figure 1.8: Known activators of TREKs. *Figure 1.8A shows riluzole, 1.8B shows DCPIB, 1.8C shows flufenamic acid, 1.8D shows BL1249 and 1.8E shows arachidonic acid.*

There are also many known inhibitors of TREKs. Other than channel pore blockers, small molecules that have been shown to inhibit TREK activity include pimozide (IC_{50} on TREK1

= 0.4 μM)[86], penfluridol (IC_{50} on TREK1 = 0.2 μM)[86], fluspirilene (IC_{50} on TREK1 = 0.2 μM)[86], L type calcium channel blockers such as amlodipine (IC_{50} on TREK1 = 0.4 μM)[87], volatile anaesthetics such as lidocaine (IC_{50} on TREK1 = 100 μM)[88] and the antidepressant drug fluoxetine (Prozac, IC_{50} on TREK1 = 18 μM and its metabolite norfluoxetine, IC_{50} on TREK1 = 9 μM)[89]. Norfluoxetine in particular has been co-crystallised by the Carpenter group with TREK2 and found to bind in the fenestration between the M2 and M4 transmembrane helices of TREK2[59].

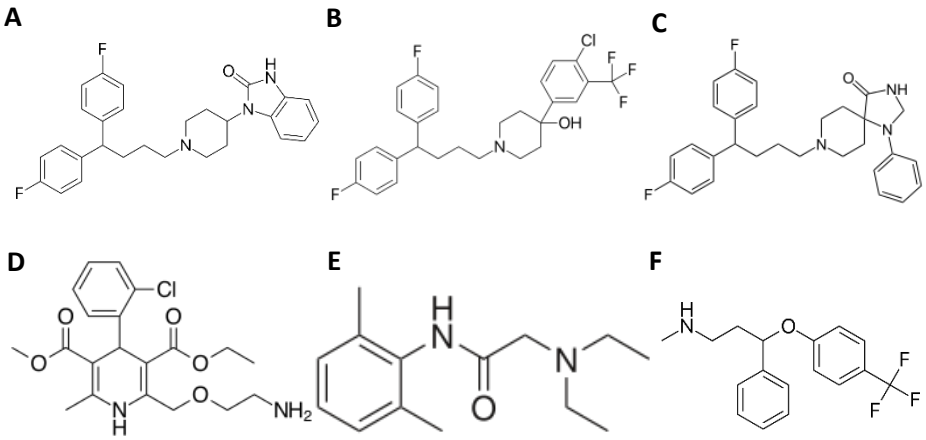

Figure 1.9: Known inhibitors of TREKs. *Figure 1.9A shows pimozide, 1.9B shows penfluridol, 1.9C shows fluspirilene, 1.9D shows amlodipine, 1.9E shows lidocaine and 1.9F shows fluoxetine. Refer to Chapter 3 for the chemical structure of norfluoxetine.*

While many binders for these channels are known, none of them are specific to a single protein and they are thus unsuitable for use as a drug against this family of targets.

1.10: The Pre-Clinical Drug Discovery Process

Drug discovery is a long and expensive process, with can take more than 15 years and over USD 1 billion for a single drug to go from initial target identification to launch[90]. A schematic of the drug discovery process is shown in Figure 1.10.

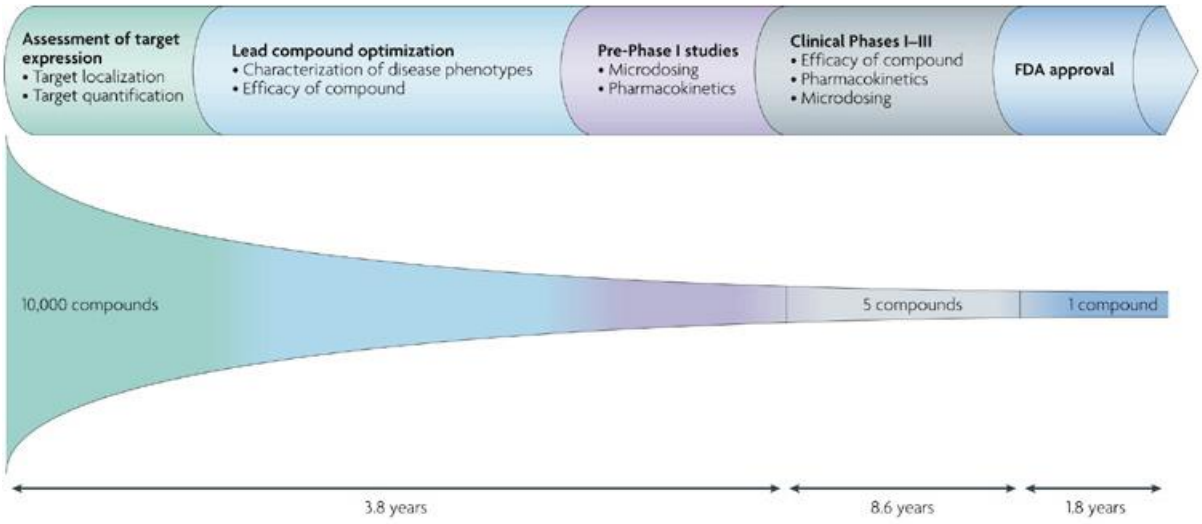

Figure 1.10: Drug Discovery Process Schematic. *The drug discovery process from target validation to FDA drug approval takes an average of 14.2 years and only 1 in every 10,000 compounds after primary high-throughput screening becomes an approved drug. Figure taken from Willmann et al., 2008*[91].

The optimisation of every stage of this process is thus of paramount importance to minimise the use of physical and human resources. Pipelines and workflows are thus developed to provide a standardised method to approach a particular stage of the overall process. In this work, we are most concerned with compound screening, which usually occurs after target validation. The overall goal of screening is to narrow down a library of compounds to a manageable number for further development[90]. Traditionally, libraries of 10000s to 1,000,000s of diverse compounds are screened, often with only one data point per compound, and from the long list of compounds a subset are identified that give a positive response on the initial screening assay. Most often, high-throughput screening assays are biochemical or cell-based with a fluorescent readout[92]. Compounds that gave a positive response are termed “hits” and after further triaging for drug-like properties, are taken forward to lead optimisation, where biophysical

assays among others are used to validate high-throughput assay results and related compounds are synthesised to determine structure-activity relationships.

A more recent approach is to use fragments instead of larger drug-like molecules for screening. These fragments are lower affinity binders and require more sensitive techniques but are able to survey a much larger amount of chemical space as compared to traditional screening of libraries[93].

Biophysical and functional techniques are widely used for the validation of traditional high-throughput screening and for primary compound and fragment screening. As each technique has a different set of requirements and false positives are possible, it is important to perform orthogonal assays and to develop a tiered system to screen larger numbers of compounds. A library of compounds would be put through a high-throughput primary screen and "hit" compounds from this screen put through a lower throughput secondary assays in order to determine which ones to take forward for optimization[94]. This screening cascade approach would allow the screening process to be much more efficient than if all compounds were screened twice, though some false negatives from the primary screen would be undetected and thus not taken forward.

Examples of such a process can be found in the pharmaceutical industry, where for example Astex Pharmaceuticals have established a process which involves initial thermal shift assay (DSF) screening followed by a secondary NMR spectroscopy screen and verification using ITC and X-ray crystallography[95]. Another cascade by Chen *et al.* uses Mass Spectrometry as the primary screening method, with SPR and ITC as secondary screening and hit validation methods[96].

With the method development and optimisation performed later in chapter3 and chapter 4, this work aims to bring together a workflow to screen a small library of known drugs and find alternative routes to identify binders for the TREK channels as well as TASK1. Verification of these compounds in functional assay will be described in chapter 6.

1.11: Alternative Methods in Ion Channel Drug Discovery

Other than direct electrophysiological methods such as two electrode voltage clamp (TEVC), manual patch clamp or high throughput patch clamp (eg. QPatch)[204], alternative cell-based techniques can be used for ion channel drug discovery. They measure channel function indirectly, through ion flux assays, where ion transport is measured. In such assays, ions which are radioisotopically labelled or have fluorescent dyes attached are used as markers and their transport across a membrane is measured in cells which overexpress a given channel[20]. Alternatively, ion sensitive fluorescent dyes are loaded into cells and the change in fluorescence after addition of a solution containing ions measured with a fluorescence plate reader[200]. The assumptions used are that the transport rate of these ions is similar to those of ions without labelling and that the overexpression of a given channel makes all other channels which transport the same ion inconsequential. Controls with the same type of cell but without the overexpression of the target ion channel are essential to determine if the process is selective.

All cell based techniques have the significant caveat that the function of ion channels can be affected by signalling pathways, so a compound which causes a change in channel function may not do so directly[97]. In addition, ion channel function can also be affected by changes in membrane composition or properties caused by the addition of the

compound. Methods which isolate the channel would avoid this problem, such as the use of artificial membranes where ion channels are purified and reconstituted into lipid bilayers and channel function then measured by patch clamp or ion flux assays[98, 99]. Another approach is to measure other properties of an ion channel to determine if ligand binding occurs, whether directly or indirectly, which will be discussed below.

While electrophysiology is the gold standard for ion channel drug discovery, both the two electrode voltage clamp (TEVC) and patch clamp methods are very low throughput and not suitable for screening of large numbers of compounds. While there are high-throughput techniques which measure ion channel function, such as ion flux assays and automated electrophysiology, they have the significant disadvantage of being cell based techniques, relying on the successful expression of channel in a model cell line and not being able to determine whether an effect is direct or indirect due to cell signalling[200]. Much early stage drug discovery is conducted with high-throughput screening and this would rely on an assay which is fast, cheap and reliable and can run many samples at once. Often, properties of an ion channel which are not directly related to its function such as its thermostability or light refraction properties are measured.

Biophysical methods have been developed for drug discovery to enable characterisation of protein-small molecule interactions based on changes to protein properties. These were first developed to improve the understanding of protein function. Methods may measure changes in thermal stability, light diffraction, fluorescence, nuclear magnetic resonance or mass of the protein or heat of reaction between protein and small molecule. All of them require purified protein and this has the advantage of measuring direct effects on proteins as compared to cell-based assays, where indirect effects

involving intracellular signalling may interfere with the readout. A more detailed review of each of the techniques used in this work will be provided in Chapters 3 and 4.

Technique	Property Measured
Mass Spectrometry (MS)	Changes in mass brought about by binding of small molecule to protein.
Nuclear Magnetic Resonance (NMR)	Chemical Shifts in the magnetic resonance of protein, to observe protein-ligand interactions, a thermal gradient is required.
Differential Scanning Fluorimetry (DSF)	Changes in intrinsic fluorescence or fluorescence from dyes bound to a protein and thus protein thermostability when protein is heated.
Differential Scanning Calorimetry (DSC)	Changes in protein thermostability based on energy required to denature protein.
Isothermal Titration Calorimetry (ITC)	Heat of reaction between protein and small molecule.
Surface Plasmon Resonance (SPR)	Changes in surface plasmon resonance angle of protein when bound to small molecule, where incident polarised light is absorbed.
Biolayer Interferometry (BLI)	Changes in light reflection profile of white light upon binding of small molecules to proteins.
Microscale Thermophoresis (MST)	Changes in diffusion coefficients of proteins and thus movement rate when bound to small molecules.

Table 1.1: Table of Biophysical Techniques Commonly Used in Drug Discovery[100, 101]

While all of the above methods are well characterised for drug discovery of soluble proteins, their record with integral membrane proteins and especially ion channels is a lot more uncertain. This is because membrane proteins are challenging to express and purify from any type of cell[102]. Membrane proteins must also be solubilised with detergents or lipids and these often interfere with biophysical assay measurements. Also, until very recently, it has not been possible to obtain enough protein from a single purification to conduct meaningful experiments over several types of assays and this is the most important reason for the relative lack of progress in this field. TREK1 and TREK2 were selected for use in this project as sufficient quantities of both proteins can be

purified and both proteins are stable over long periods of time when frozen, making them suitable for evaluating multiple biophysical techniques.

Biophysical approaches have become increasingly common for detecting protein-ligand interactions even for integral membrane proteins. For example, it has been shown that SPR can detect such interactions in a variety of G-protein coupled receptors (GPCRs)[103]. DSF has also been used for the same purpose on CXCR4, another GPCR[104]. However, Research in this field remains scarce and there is a need to characterise these assays and evaluate their use in ion channel drug discovery.

1.12: Aims and Purpose of this Thesis

The overall aim of this work is to use K2Ps to obtain a proof of principle that biophysical assays can find novel binders for ion channels and that it is a viable method for early stage drug discovery.

In chapter 3, I discuss the use of DSF with both a fluorescent labelling compound and a label free technique to measure protein thermostability, under various conditions and with several known ligands. I also evaluate their viability for use in screening large numbers of compounds using the Z' test, a widely-used statistical measure for assessing the quality of output from an assay in the pharmaceutical industry. I then compare the two techniques in their ability and reliability for high-throughput compound screening.

In chapter 4, I then discuss methods that measure protein-ligand using other physical properties and evaluate their effectiveness under various conditions with the TREK channels and known ligands. Following that, in chapter 5, I then devise a workflow that

allows us to screen hundreds of small molecules to arrive at compounds which interact with a target integral membrane protein.

In chapter 5, I also conduct a run of the proposed workflow, starting with a library of 1100 compounds and finding a few compounds which bind and affect the function of TREK1 or TREK2, as verified with electrophysiology experiments in chapter 6. Using the methods discussed in this thesis I was able to identify a compound that inhibited TREK2 and another that activated TREK1. These compounds were inactive on control channels such as TASK1, suggesting that the effects observed were specific to the target channels. These low micromolar binders had not previously been identified as K2P modulators and they provide new chemical scaffolds from which potent and selective K2P channel modulators can be designed.

Chapter 2: General Materials and Methods

2.1 Construct Design and Cloning of Proteins

All genes except TASK1 were purchased from the Mammalian Gene Collection (National Institutes of Health, USA). TASK1 was purchased from Origene (Rockville, MD, USA). The IMAGE IDs, MGC numbers and accession IDs are listed in Table 2.1.

Protein Name	IMAGE ID	MGC Number	Accession ID
TREK2	30915621	104160	BC075021
TREK1	8069199	162742	BC101693
TASK1	N/A	N/A	NM_002246
TWIK1	4817185	26384	BC018051
GLUT3	4396508	21198	BC039196

Table 2.1: Gene Information of Constructs Used in this Project.

Truncated constructs of TREK1, TREK2, TASK1, TWIK1 and GLUT3 were used at various stages of these project. All of the construct design, cloning, screening and purification optimisation were completed before I started this project. Construct design was performed by E. P. Carpenter, A. Quigley and Y. Y. Dong. Cloning was performed by the Biotechnology group of the SGC, led by Burgess-Brown N. Screening and purification optimisation was performed by the following people for these proteins: TREK1 and TREK2: Y. Y. Dong[59], TASK1 and GLUT3 by A. Quigley[105, 106]. TWIK1 was purified as described by the MacKinnon group in their structure determination paper [30]. GLUT3 is a glucose transporter which is used as a control protein for biophysical assay testing in this thesis.

Truncations were performed to remove disordered regions of protein that may hinder expression or purification. Truncations do not involve the transmembrane domains of the proteins. The proteins were also later tested for functionality if they express in

sufficient quantities. While these truncations were performed and designed by various members of the Carpenter group for mainly structural determination purposes, they are being used here for biophysical assays to correspond with possible crystallisation follow up experiments. In most cases, there was a truncation made to both the N and C termini of the proteins. A table of constructs referenced in later chapters is provided below (Table 2.2).

Protein Name	Start Residue	End Residue	Full Length of Protein (Residues)	Extinction Coefficient ($L.mol^{-1} \cdot cm^{-1}$)	Molecular Mass (Da)
TREK2	G67	E340	543	51910	31035.3
TREK1	P26	S300	426	50420	31209.7
TASK1	M1	E259	394	33350	30087.2
TWIK1	S9	Q290	336	48360	33388
GLUT3	M1	R474	496	42400	52483.8

Table 2.2: Protein Information of Constructs Used in this Project. The extinction coefficient is predicted based on the method developed by Pace *et al*.[107].

The truncated constructs above, with the exception of TWIK1 (untested) have been shown to be functional. TREK2[59] and TREK1 (unpublished data) were found by electrophysiology to be able to conduct currents. This construct of GLUT3 was shown to transport glucose[106]. The full truncated sequences as well as sequence alignment for the K2Ps are shown in Appendix 1.

All constructs contained a C-terminal purification tag with a tobacco etch virus (TEV) protease cleavage site, a 10 x His purification sequence and a FLAG tag, in the expression vector pFB-CT10HF-LIC (available from Addgene). The vector map is shown in Figure 2.1. Cloning was performed using standard Ligand-Independent Cloning techniques and was performed by the Biotechnology group of the SGC (Goubin, S., Shrestha, L., Burgess-Brown, N.)[108].

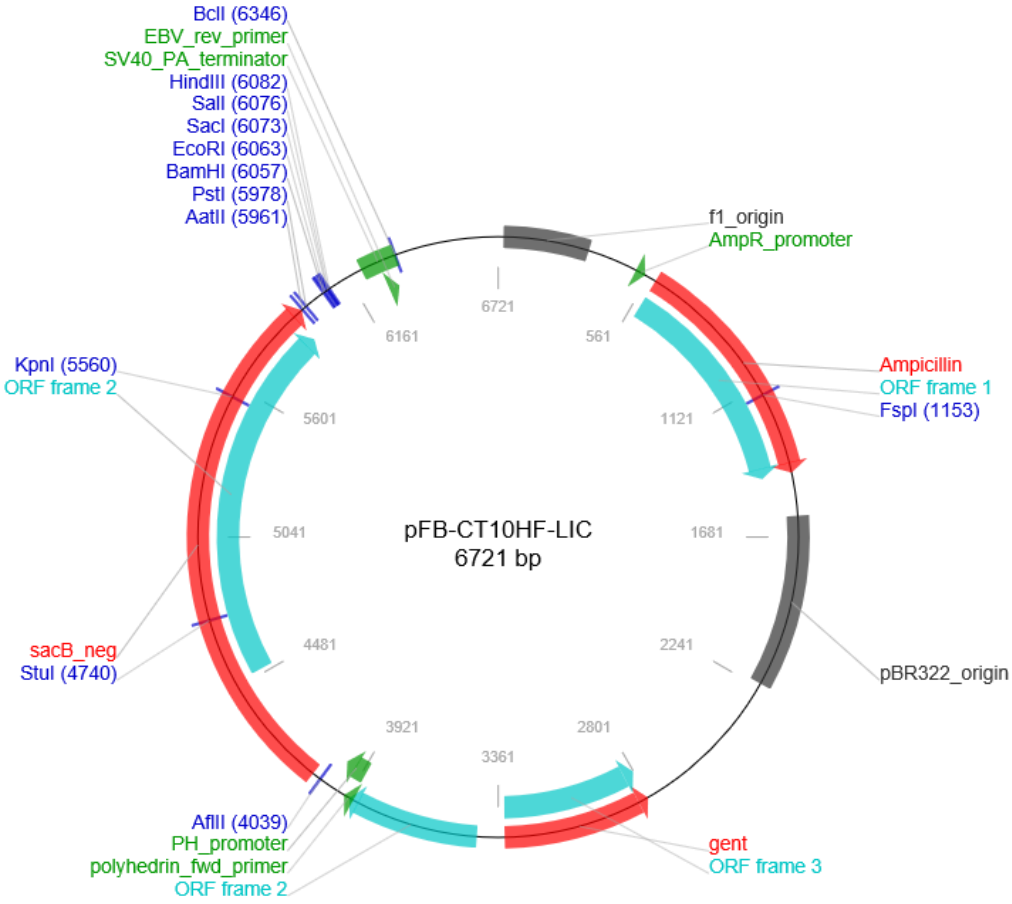

Figure 2.1: Vector map for pFB-CT10HF-LIC. *The ampicillin site is used for gene cloning in all cases for this project.*

2.2 Expression and Purification of Proteins

Bacmids containing the gene for the target protein were produced by transformation of DH10Bac cells and subsequent DNA extraction of recombinant bacmids from *E. Coli*. *Spodoptera frugiperda* (Sf9) insect cells in Sf-900 II SFM medium (Life Technologies, Thermo-Fisher, Waltham, MA, USA) were then transfected with bacmid DNA in order to create baculoviruses containing the target DNA. After 2 passages, previously cultured Sf9 cells were infected with recombinant baculovirus and incubated for 65 h at 27 °C in shaker flasks. Cells were then pelleted by centrifugation at 900g for 15 minutes, washed with phosphate buffered saline (Sigma, St. Louis, MO, USA) and flash-frozen in liquid nitrogen.

Cell pellets were thawed out and resuspended in 30 ml of extraction buffer per litre. The buffers used for extraction as well as for size exclusion chromatography are listed in Table 2.3.

Protein	Extraction Buffer	Size Exclusion Chromatography Buffer
TREK2	50 mM HEPES, pH7.5, 200 mM KCl, 5% glycerol, 5 mM imidazole, 1 Roche protease inhibitor cocktail tablet per litre of cells.	50 mM HEPES, pH7.5, 200 mM KCl
TREK1	50 mM HEPES, pH7.5, 200 mM KCl, 5% glycerol, 5 mM imidazole, 1 Roche protease inhibitor cocktail tablet per litre of cells.	50 mM HEPES, pH7.5, 200 mM KCl
TASK1	50 mM HEPES, pH7.5, 200 mM KCl, 5% glycerol, 5 mM imidazole, 1 Roche protease inhibitor cocktail tablet per litre of cells.	50 mM HEPES, pH7.5, 200 mM KCl
TWIK1	30 mM TRIS, pH8.5, 150 mM KCl, 5 mM imidazole, 1 Roche protease inhibitor cocktail tablet per litre of cells.	30 mM TRIS, pH8.5, 150 mM KCl
GLUT3	50 mM HEPES, pH7.5, 300 mM NaCl, 5% glycerol, 1 Roche protease inhibitor cocktail tablet per litre of cells.	50 mM HEPES, pH7.5, 300 mM NaCl

Table 2.3: Extraction and Size Exclusion Chromatrography (SEC) buffers for all proteins used. Protease inhibitor cocktail was obtained from Roche (Roche Holding AG, Basel, Switzerland).

In all cases the cells were lysed by two passes through an EmulsiFlex-C5 homogenizer (Avestin, Ottawa, Canada) at 4°C and between 5000 and 10,000 psi pressure. Protein was extracted from cell membranes by incubation of the crude lysate with the addition of 1% (w/v) extraction detergent (dependent on protein) for 1h at 4°C with agitation on a rotator. Cell debris and unlysed cells were removed by centrifugation at 35,000g for 1h and disposing of the cell pellet. Detergent-solubilized protein was purified by immobilized metal affinity chromatography by batch binding to 1 ml of 50% Co^{2+} charged TALON resin (pre-equilibrated with EXB without detergent) per litre of cells (Clontech, Takara Bio, Kusatsu, Shiga, Japan) at 4°C for 1h with agitation on a rotator. The resin was washed with 30 column volumes of wash buffer (same as extraction buffer except that

20 mM imidazole was added and the detergent concentration is lowered to 3 X critical micelle concentration (CMC)) and eluted with wash buffer supplemented with 250 mM imidazole. The CMC is defined as the concentration of detergent above which micelles form in an aqueous solution. The eluted protein was desalted using a PD10 column (GE healthcare, Little Chalfont, Buckinghamshire, UK) pre-equilibrated with extraction buffer containing 3 X CMC of the extraction detergent. Desalted protein was subsequently treated with 10:1 TEV protease and 20:1 PNGaseF (w:w, protein:enzyme) overnight at 4°C. If the His-tag on the protein is required for an assay, no TEV is added.

The TEV and PNGaseF treated protein was separated from the 6 x His-tagged enzymes and uncleaved protein by incubation for 1h with 1 ml of TALON resin at 4°C with agitation on a rotator. The resin was collected in a column and the flow-through was collected (the 2nd affinity chromatography step is skipped if no TEV was added). A further 1 ml of extraction buffer with 3 X CMC detergent was added and collected.

The protein was then concentrated using a 30 kDa cut-off polyethersulfone membrane concentrator (Vivaspin, Sartorius AG, Goettingen, Germany). The concentrated protein was further purified by size exclusion chromatography (SEC) using a Superose 6 10/300GL column or a Superose 6 Increase 10/300 GL column (GE Healthcare, Little Chalfont, Buckinghamshire, UK) equilibrated with 2 column volumes of SEC buffer (extraction buffer without glycerol or imidazole and with 2 x CMC of the detergent). 0.5 ml fractions were then collected, peak fractions were combined and the protein was analysed by SDS-PAGE and mass spectrometry to ensure the purification was successful.

2.3 Mass Spectrometry of Proteins

Mass Spectrometry for the quality control of proteins was conducted using an Agilent 6530 Quantitative-Time of Flight Liquid Chromatography/Mass Spectrometry system (Agilent Technologies, Santa Clara, CA, USA). 5 µl of protein in SEC buffer at 1 mg/ml was mixed with 55 µl of 1% formic acid and the mixture was loaded onto a Chromolith Rp18-e High Performance Liquid Chromatography column (Merck Millipore, Billerica, MA, USA) and data were collected and analysed using the Agilent Masshunter Qualitative Analysis 7.0 software (Agilent Technologies, Santa Clara, CA, USA). The protein was then frozen in 500 µl aliquots at -80°C for use in biophysical assays.

Detergent	**Abbreviation**	**CMC (% w/v)**	**Purification Conc. (% w/v)**
Octyl Glucose Neopentyl Glycol	OGNG	0.058	0.18
Octyl Glucose Neopentyl Glycol + cholesteryl hemi-succinate	OGNG/CHS	0.058	0.18 + 0.018 CHS
***n*-Dodecyl β-D-maltoside**	DDM	0.0087	0.030
***n*-Dodecyl β-D-maltoside + cholesteryl hemi-succinate**	DDM/CHS	0.0087	0.030 + 0.0030 CHS
n-Decyl-β-D-Maltopyranoside	DM	0.087	0.27
Lauryl Maltose Neopentyl Glycol + cholesteryl hemi-succinate	LMNG/CHS	0.0010	0.0030 + 0.00030 CHS
Decyl Maltose Neopentyl Glycol + cholesteryl hemi-succinate	DMNG/CHS	0.0034	0.010 + 0.0010 CHS

Table 2.4: Detergents and lipid combinations used in Purification of Proteins. The CMC and purification concentrations are given to 2 significant figures.

Chapter 3: Development of Differential Scanning Fluorimetry Methods for the detection of protein-ligand interactions.

3.1: Introduction

3.1.1: Differential Scanning Fluorimetry and its Applications

One of the most commonly-used biophysical methods for early stage drug discovery is Differential Scanning Fluorimetry (DSF). This method, which is also known as the Thermofluor assay, is a method of measurement of the change in thermostability of proteins when bound to small molecules[109]. A fluorescent dye which can be attached to a protein can be used and the difference between the signal of a folded protein and an unfolded protein is measured. There is also Label-free DSF which does not make use of a fluorescent dye. This is discussed in Section 3.1.3.

The stability of a protein is related to its Gibbs Free Energy of unfolding, a function of the temperature[110]. As temperature increases, protein stability decreases and there is an equilibrium temperature where the Gibbs Free Energy of unfolding is zero, at which the concentrations of folded and unfolded protein are equal. This temperature is defined as the melting temperature of the protein (T_m). The assumption is that the protein follows a two-state model during unfolding. DSF was developed initially as a method to investigate the thermodynamic properties of proteins, with fluorescent dyes that bind to certain parts or residues of proteins. It was first described in 1991 by Semisotnov *et al.*[111], and first adapted into a format which can be performed by a 96-well plate reader by Pantoliano *et al.*[112]. A population of protein molecules unfold according to the logistic equation and the resultant fluorescent signal can be plotted as

a Boltzmann sigmoidal function and the T_m of the protein is determined as the inflection point of the sigmoid[110].

The Boltzmann sigmoidal function is as follows:

$$S(t) = \frac{1}{1 + e^{-t}} \tag{3.1}$$

Where S(t) is the sigmoidal function and t is time.

A typical signal is shown in Figure 3.1 below:

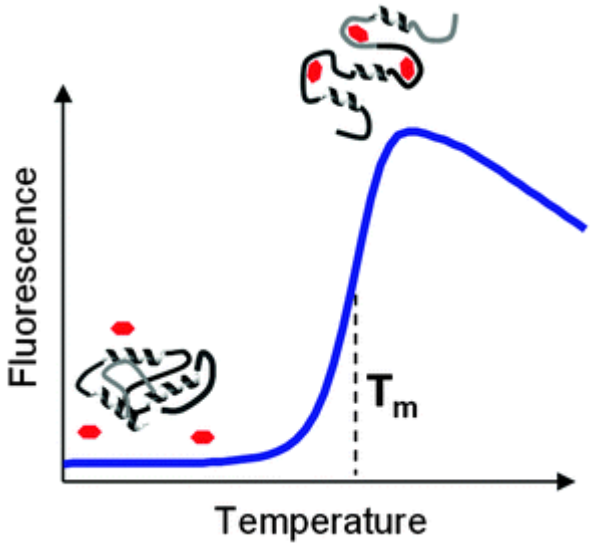

Figure 3.1: Sample DSF Curve. *Protein is folded completely at low temperatures and when it is gradually heated, it unfolds. The protein-labelling dyes used in DSF are not fluorescent in solution. However, once they bind to surfaces exposed by protein denaturation, they become fluorescent, causing an increase in fluorescence as the temperature increases. The fluorescence is measured at intervals and the data obtained is fitted to a Boltzmann sigmoid. The point of inflection obtained is taken as the T_m of the protein. Figure adapted from Rodrigues et al., 2011[113].*

Other than measuring the thermostability of proteins, another main use of DSF is to investigate protein-ligand interactions[117]. The binding between 2 or more molecules changes the thermodynamic properties and thus the Gibb's Free Energy of unfolding of

the protein and its T_m . This method is more commonly known as the T_m shift assay and has been developed to screen large numbers of possible protein binders in a high throughput format[117]. Its main advantages are firstly, only nanogram quantities of protein, dye and ligand are required. The assay can also be easily adapted to 96 or 384 well plate formats and up to 10,000s of small molecules can be screened in a single day in an industrial setting[118]. The equipment required for DSF analysis of protein-ligand interactions is also rather simple and ubiquitous in molecular biology laboratories, with only a Real Time-Polymerase Chain Reaction (RT-PCR) machine with the relevant light filter sets required. These advantages have led to our choice of DSF as the first technique to attempt optimisation for the analysis of ligand binding to the TREK channels.

Different dyes may be used based on the properties of the target protein. The main criteria for a dye would be that it is non-fluorescent in the initial conditions in which an assay is conducted but becomes fluorescent when bound to certain parts of a protein that are not exposed in solution unless the protein is denatured. A selection of available dyes and binding points is shown below in Table 3.1:

Dye	Binding Points on Protein	Peak Absorption Wavelength (nm)	Peak Emission Wavelength (nm)
8-Anilinonaphthalene-1-sulfonic acid (ANS)[111]	Hydrophobic Sections	380	545
SYPRO Orange[109]	Hydrophobic Sections	492	610
Nile Red[114]	Hydrophobic Sections	585	665
BODIPY FL-Cystine[115]	Cysteine Residues	443	530
7-diethylamino-3-(4'-maleimidylphenyl)-4-methylcoumarin (CPM)[116]	Cysteine Residues	385	470

Table 3.1: Fluorescent Compounds used for DSF Screening.

Most dyes that are currently in use either bind to hydrophobic sections of proteins or cysteine residues. Binding to hydrophobic sections is useful for tracking the unfolding of soluble proteins as they almost always contain a hydrophobic core which becomes exposed upon denaturation by heating. Soluble protein surfaces, if correctly folded are hydrophilic in order to interact with water molecules. Integral membrane proteins however, have a hydrophobic surface and are usually purified in detergents or lipids, which are amphipathic. Such dyes would not be suitable for DSF with these proteins.

3.1.2 The CPM Dye

As K2Ps are integral membrane proteins, the fluorescent dye used for this project is CPM, which is a maleimide based cysteine binder that was first described for this purpose by Alexandrov *et al.* in 2008[116]. The chemical structure of CPM and an illustration of how it binds to cysteine residues is shown in Figure 3.2.

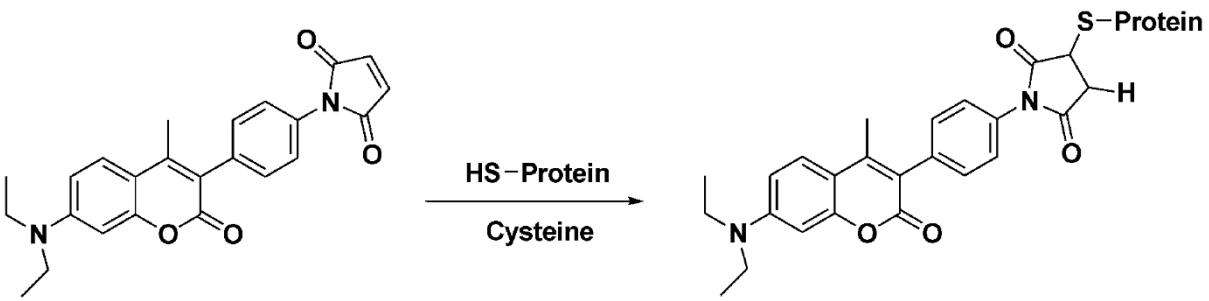

Figure 3.2: CPM (left) and its fluorescent cysteine adduct (right). *CPM undergoes nucleophilic attack by the sulfhydryl groups in cysteine residue sidechains via a Michael reaction to form its covalent adduct.*

CPM has since been used to investigate membrane protein thermostability in a multitude of conditions, from within detergent micelles[119], lipidic cubic phase[120] and within nanodiscs[121]. It has also been used to predict ease of crystallisation of membrane proteins[119]. Proteins investigated with this method include GPCRs[116], enzymes[122] and ion channels[123]. However, as far as I am aware, there have been no published papers on the use of CPM for screening large numbers of compounds with detergent purified human ion channels. This chapter describes the development of such an assay.

3.1.3 Label Free DSF

In addition to the dye-based DSF methods, there are also methods for label-free thermostability measurements using changes in the intrinsic fluorescence of proteins. Most proteins contain amino acids with aromatic sidechains, such as phenylalanine, tyrosine and in particular tryptophan, that absorb light at 280 nm and emits it at 330-350 nm[124]. This property has been used for the quantitation of proteins[125] where the extinction coefficient of the protein is calculated. Using these methods DSF can be

conducted on integral membrane proteins that do not have available sulfhydryl groups to react with CPM or another thiol binding dye.

The intensity of tryptophan fluorescence is very sensitive to changes in the conformation of the protein, which can cause a change in the peak wavelength and intensity of fluorescence[124]. This is usually measured as a red shift or blue shift in fluorescence. This property has been used in nano-DSF, which was developed by Nanotemper (Munich, Germany) to measure the thermal stability of proteins based on label free DSF[126]. While fluorescence spectroscopy isn't novel and has been used by many groups to measure protein stability[197], the mechanical setup to test up to 48 samples in parallel while heating the protein and measuring fluorescence emission at 330 nm and 350 nm wavelengths is new and was recently implemented by Nanotemper and other companies. There are no current publications reviewing the use of this technique with ion channels or the use of this method for quantifying interactions between membrane proteins and possible ligands using the Nanotemper developed device. This chapter also describes the characterisation of this assay for determining the effects of small molecules on TREK channel thermostability.

3.1.4: Statistical Tests for Assay Robustness

One of the key aspects of assay development for screening is that the assay is statistically relevant. This requires a measure of assay sensitivity and reproducibility across all wells. There are a few widely used statistical methods used for such purposes, such as the Student's t-test, simple calculations of signal to background ratios and a method making use of strictly standardised mean differences (SSMD)[128]. The Student's T-test is a statistical test used where normality is assumed within populations and is used to

compare two population means. In this case, it can be applied to the comparison of mean T_m shifts between the control and the test compound. The SSMD method is also robust and can handle multiple controls instead of just a single positive and negative control. However, it was developed for RNAi screening instead of small molecule screening techniques.

A statistical test commonly used in the pharmaceutical industry is the Z' factor. The Z' factor was first proposed by Zhang *et al.* in 1999[129] and was developed as a method to evaluate the suitability of a high-throughput screening assay and to compare different assays in terms of their sensitivity and reliability.

The Z' factor test relies on 4 values only, the mean and standard deviation of the positive and negative control measurements. The differences in the means between negative and positive controls and the individual standard deviations of the measurements are taken into consideration to obtain the equation below:

$$\text{Z-factor} = 1 - \frac{3(\sigma_p + \sigma_n)}{|\mu_p - \mu_n|}. \tag{3.2}$$

Where μ_p is the mean of the positive control measurements, μ_n is the mean of the negative control measurements and σ_p and σ_n are the standard deviations of the positive and negative control measurements respectively.

The Z' factor test effectively takes into consideration two main factors of an assay: the difference between the positive and negative control groups and the variation within each group of samples. The maximum possible Z-factor is 1, which represents a perfect assay but in general, a Z-factor of > 0.4 represents an assay suitable for high throughput screening use[129].

The Z' factor test continues to be widely used for small molecule screening and is the industrial standard. Hence, it is chosen as the statistical method to check for assay robustness. Our study aims to use the Z' factor test to determine the assay quality of DSF with the CPM dye.

3.2 Materials and Methods

3.2.1 CPM Assay

CPM (Thermo-Fisher Scientific, Waltham, MA, USA) was weighed out and dissolved in dimethyl sulfoxide (DMSO) at a 4 mg/ml concentration. This stock solution was then aliquoted into 50 µl portions and frozen at -20°C. Protein was diluted with SEC buffer (differs by protein, refer to Chapter 2) containing relevant amounts of compound to 0.1 mg/ml and aliquoted into a 96 well RT-PCR plate (Product Number: 4ti-0955, 4titude, Surrey, UK) with 20 µl per well (0.2 µg of protein per well). CPM stock was then diluted 100-fold to obtain a 40 µM concentration and 5 µl was added to each well using a multi-channel pipette.

The 96-well plate was then sealed and inserted into an Agilent Stratagene Mx3005P RT-qPCR system (Agilent Technologies, Santa Clara, CA, USA). The programme was set as a 1°C increase in temperature per minute starting at 25°C and terminating at 95°C, with recordings taken every minute (every 1°C increase). The fluorescence data is then analysed by fitting a Boltzmann sigmoidal curve on Graphpad Prism 6 (Graphpad, La Jolla, CA, USA) for every well and then reading off the V_{50} values to determine the T_m of the proteins.

For both CPM and label-free DSF screening, activator B was obtained from Pfizer (New York City, NY, USA), di-octanoyl PI(4,5)P_2 from Avanti Polar Lipids (Alabester, AL, USA), norfluoxetine from Tocris (Bristol, UK) and nifedipine, BL1249 and penfluridol from Sigma (St Louis, MO, USA).

3.2.2 Label Free DSF

Protein was diluted with SEC buffer containing the compound of interest to 0.1 mg/ml (about 3µM for all K2Ps) for Label Free DSF. 10 µl of protein was then aliquoted in 96 well Real-Time PCR plates per capillary and Nanotemper Prometheus NT.48 Series nanoDSF Grade Standard Capillaries (Nanotemper Technologies GmbH, Munich, Germany) were then inserted into the wells containing the protein-compound mix. The solution enters the capillary via capillary action and the capillaries were then inserted into the Nanotemper Prometheus NT.48 system (Nanotemper Technologies GmbH, Munich, Germany).

The capillaries containing the protein-compound mix were then heated from 25°C to 95°C at 2°C per minute and fluorescence data were collected at 330 nm and 350 nm. The 330 nm to 350 nm fluorescence ratio was also calculated. The 330/350 fluorescence ratio data was then fitted onto a Boltzmann Sigmoidal curve and analysed on Graphpad Prism 6 (Graphpad, La Jolla, CA, USA). A V_{50} was obtained and this was used as the T_m of the protein.

3.3 Results

3.3.1 Expression and Purification of TREK1 and TREK2

Both TREKs were expressed in baculovirus-infected insect cells and were purified using first immobilised metal affinity chromatrography (IMAC) with a Co^{2+} based TALON resin and then SEC as described in Chapter 2. TREK1 and TREK2 can be purified in both OGNG/CHS and DDM and sample SEC profiles and SDS-PAGE analysis of both proteins are shown in Figure 3.3.

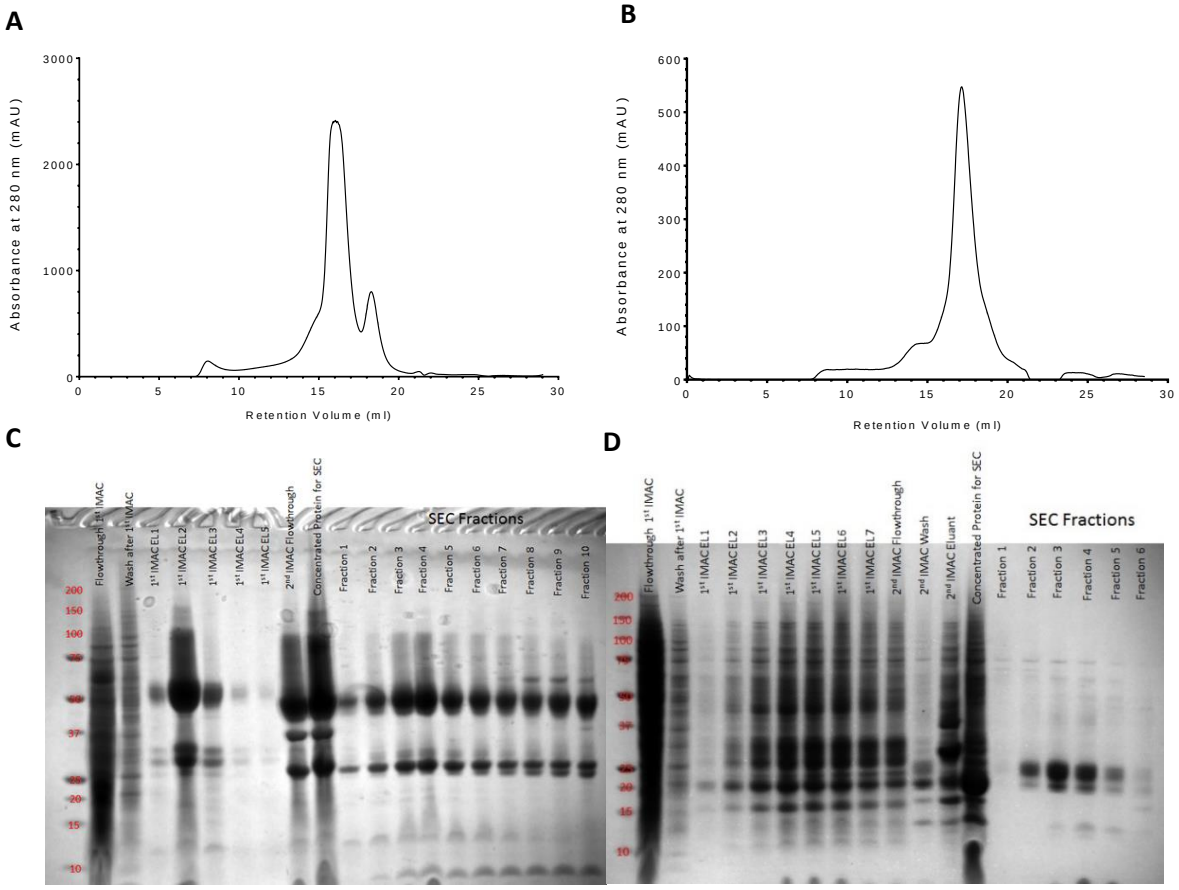

Figure 3.3: SEC Profile and SDS-PAGE of TREK2 (A and C) and TREK1 (B and D). *The rounded peak on the TREK2 profile is the result of the amount of protein exceeding the effective detection limit. The lower molecular weight peak in Figure 3.3A is shown in Fractions 9 and 10 in Figure 3.3C. In the SDS-PAGE, TREK2 has 2 distinct bands, which correspond to the monomer (Lower MW) and dimer (Higher MW) of the protein. TREK1 has 1 main band and 1 slightly smaller band, which correspond to the monomer and a truncated form of the protein. Lanes labelled IMAC refer to 1 ml fractions taken after affinity chromatography.*

Different detergents form micelles of various sizes, which changes their extraction and purification efficiency and leads to different protein yields. Typical protein yields of TREK1 and TREK2 purified in a range of detergents are shown below in Table 3.2.

Protein	Detergent	Yield (mg/L of culture)
TREK2	OGNG/CHS	1.2 ± 0.1
TREK2	OGNG	0.7 ± 0.1
TREK2	DDM/CHS	1.2 ± 0.1
TREK2	DDM	1.5
TREK2	DMNG/CHS	1.2
TREK1	OGNG/CHS	0.3 ± 0.1
TREK1	DDM	0.2

Table 3.2: Examples of purified protein yields in various protein-detergent combinations. Results are expressed as (Mean ± SEM if 3 or more purifications performed in these conditions).

3.3.2 Effects of protein detergent, concentration and DMSO on DSF of TREK2

The thermostability of a protein could be affected by many factors, including the concentration of the protein. Higher protein concentrations could lead to lower thermostability due to an increased likelihood of association and aggregation[130]. This trend is borne out with the CPM-based DSF assay, with TREK2 exhibiting decreased thermostability at higher concentrations (Figure 3.5). It is therefore important that the protein concentration is kept constant when comparing changes in thermostability caused by protein-ligand interactions.

Different purification detergents also affect the thermostability of TREK2. Indeed, thermostability has been used as a parameter for the optimisation of protein purification and crystallisation[131]. While earlier detergent screens conducted by Y. Y. Dong from the Carpenter group, SGC Oxford have shown that TREK2 can be purified in a multitude of detergents, the resulting protein is of differing thermostability. This may be due to the differing micelle sizes due to different detergent properties. Micelle size

relates to protein stability by affecting the amount of protein surface exposed to the solution[132]. The chemical structures of the detergents used in this test are shown below:

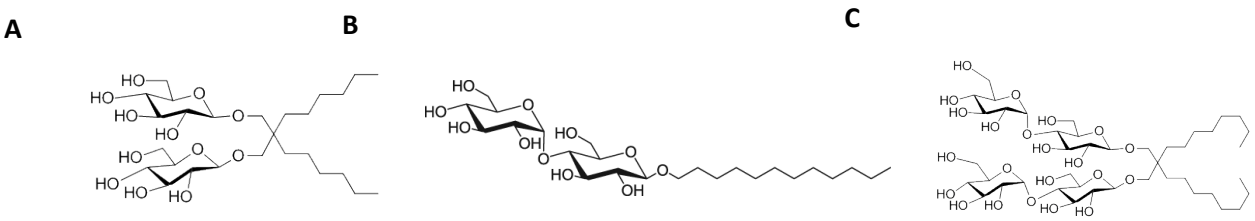

Figure 3.4: Chemical Structures of a) OGNG, b) DDM and c) DMNG. *All these detergents belong to the glucoside or maltoside families, with the sugar headgroups and length of alkyl chains differing between the detergents.*

The alkyl chain lengths and headgroup sizes of detergents are different, leading to formation of differently sized micelles. The addition of CHS also stabilises protein-micelle complexes by reducing movement of detergent molecules and acting as a replacement for cholesterol in natural membranes. Figure 3.5A shows the data obtained from the DSF of TREK2 purified in different detergents. Figure 3.5B shows the dependence of TREK2 thermostability on its concentration as well as purification detergent and CHS.

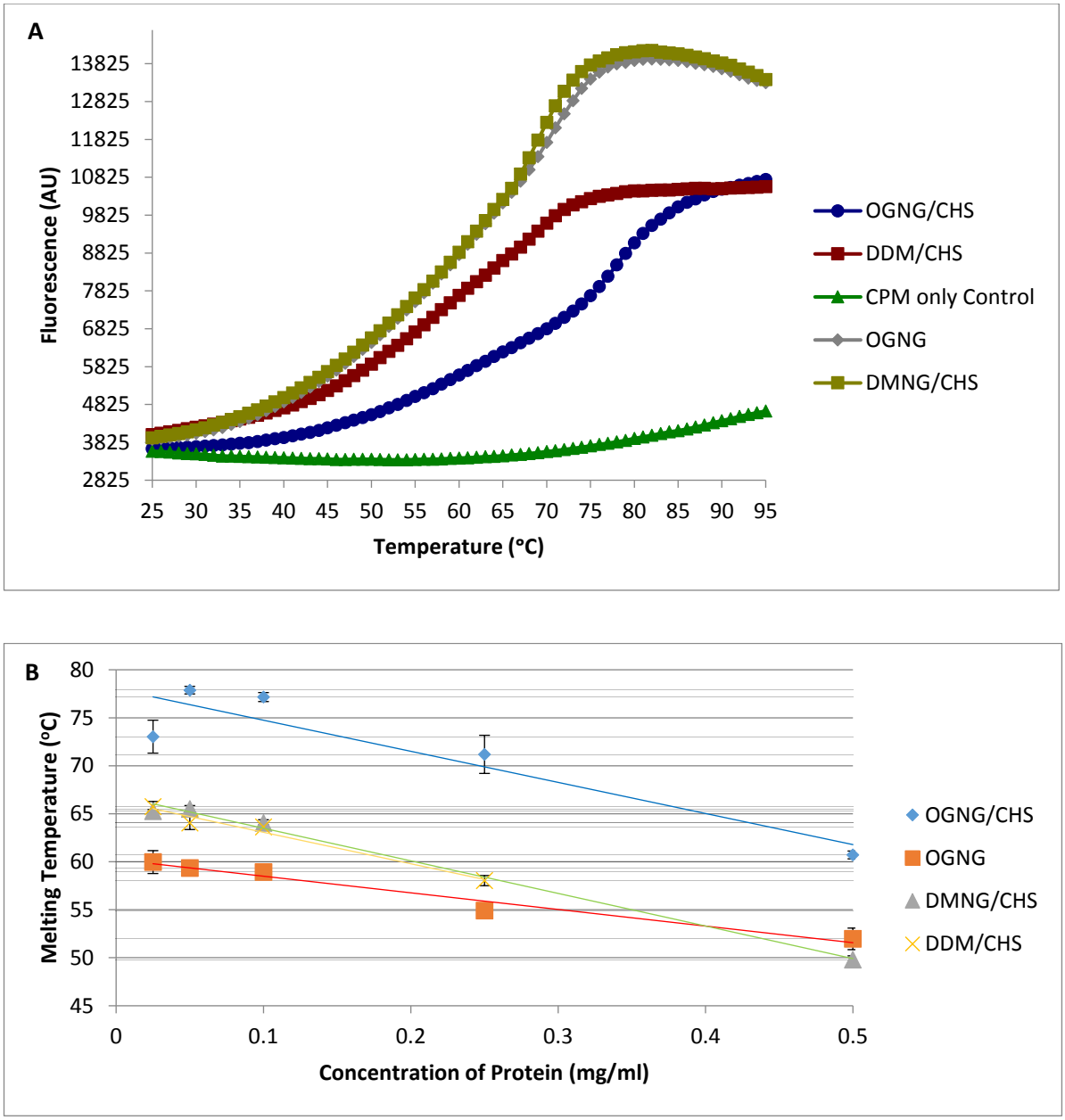

Figure 3.5: Concentration-dependent thermostability of TREK2 in different detergent conditions (n = 4 technical replicates per detergent). *Figure 3.5A shows the raw data obtained from the DSF assay. This data is plotted and fitted onto a Boltzmann sigmoidal curve, a V_{50} obtained and this temperature is taken as the melting temperature of the protein. Figure 3.5B shows the concentration and detergent dependence of the thermostability of TREK2. The detergent concentration in all cases is 3 X CMC. Trendlines are fitted and shown in the same colour as the points for the detergent used.*

In all cases, increased concentration of protein decreases protein thermostability. Also, the addition of CHS increases TREK2 thermostability. The protein is clearly most stable in OGNG/CHS as compared to all other detergents and most other later assays, unless otherwise stated are performed with protein purified in OGNG/CHS as it has the highest stability and gives the greatest yield. TREK2 has a melting point of about 74°C and TREK1 of 72°C when purified in OGNG/CHS.

Another factor which influences protein thermostability in DSF assays is the presence of DMSO. DMSO, being a universal solvent, is used to dissolve most compounds to create stock solutions. It significantly changes buffer properties and may disrupt detergent micelles, causing the destabilisation of proteins. We show that DMSO has a negligible effect on both TREK2 and TREK1 thermostability up to a 1% volume by volume concentration (Figure 3.6). All future experiments are thus carried out at DMSO concentrations below 1%. Water was used as a control for DMSO and showed no significant effect at any concentration added. There was also no signal when DMSO is incubated with the dye alone.

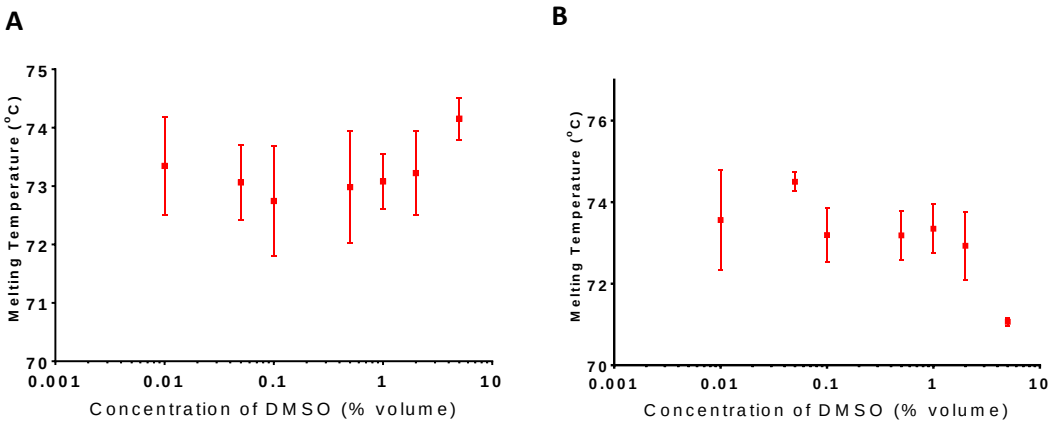

Figure 3.6: Logarithmic Plot of Thermostability of TREKs with DMSO. *TREK2 (Figure 3.6A) and TREK1 (Figure 3.6B) were purified in OGNG/CHS and 2 µg of protein per well (about 3 µM concentration) was used for this DMSO tolerance test. Differing percentages of DMSO were added to SEC buffer and 5 µl of CPM dye was added to the protein-DMSO mixture (total 25 µl). The assay was performed three times with 4 wells per concentration of DMSO. The concentrations of DMSO used were 0.01%, 0.05%, 0.1%, 0.5%, 1%, 2% and 5%. Error bars were calculated from the SD of 12 wells (3 protein preparations, 4 duplicate wells per preparation).*

3.3.3: Z' Factor with DSF assay using CPM dye

The next test was to then determine if the DSF assay using CPM dye is suitable for high throughput screening. This was done by performing Z' factor determination on two known ligands of TREK2 and TREK1. To determine the Z' factor in a 96 well plate setup, I divided the plate into 4 quadrants, 2 of which contain protein only and the other 2 containing protein and a known ligand. This allows me to check for variation between T_m readings from different parts of the 96 well plate, which may be due to uneven heating or other edge effects from the RT-PCR machine. The ligands chosen for this analysis were penfluridol and BL1249, which are an inhibitor and activator of TREKs respectively. BL1249 and penfluridol were shown to stabilise and destabilise both TREKs in Section 3.3.5. The plate layout for this test is shown in Figure 3.7.

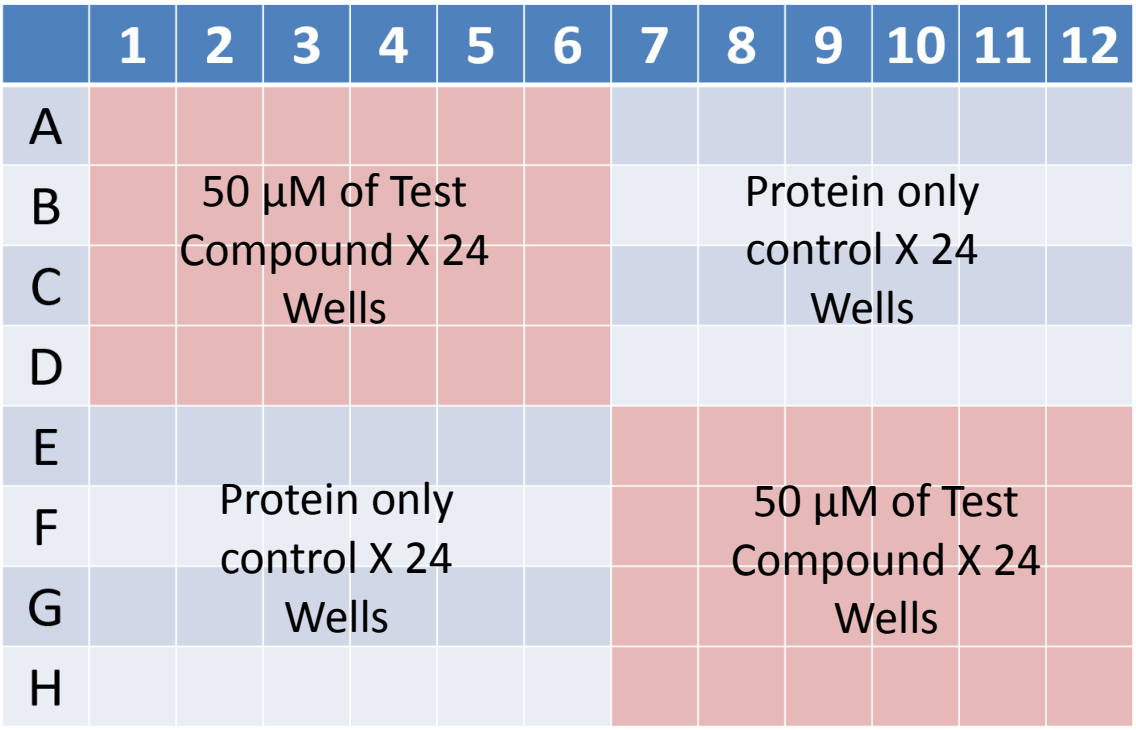

Figure 3.7: Z' factor plate layout. *There are 48 wells of both protein and protein + test compound at 50 µM.*

The assay was carried out once using the protocol described in Section 3.2.1 with each protein-ligand combination and the results are as shown below in Table 3.3:

Protein	Ligand	T_m Shift	SD T_m Shift	Z' Factor
TREK1	Penfluridol	-5.61	0.13	0.831
TREK1	BL1249	4.83	0.09	0.888
TREK2	Penfluridol	-2.01	0.14	0.657
TREK2	BL1249	2.04	0.06	0.839

Table 3.3: Full Plate Z' Factor Test Data for TREK1 and TREK2 with Penfluridol and BL1249.

As can be seen in Table 3.3, the Z' Factor values for a full plate assay of TREK1 and TREK2 with a known activator or inhibitor at a concentration far in excess of their EC_{50} or IC_{50} are between 0.658 and 0.888. This indicates that the CPM assay should be of sufficient quality for single point screening as the minimum cutoff required is a value of 0.5.

In comparison, a Student's t-test was also performed on the same sets of data as the Z test and the results summarised below.

Protein	Ligand	T_m Shift	Variance	T-value	P-value
TREK1	Penfluridol	-5.61	0.01778	170.56	<0.001
TREK1	BL1249	4.83	0.00798	261.08	<0.001
TREK2	Penfluridol	-2.01	0.01976	83.75	<0.001
TREK2	BL1249	2.04	0.00388	204	<0.001

Table 3.4: Full Plate Student's T-Test Data for TREK1 and TREK2 with Penfluridol and BL1249

In the analysis above, the number of degrees of freedom in all cases was 94 and the critical T-value for p = 0.001 is 3.19. Both norfluoxetine and penfluridol are shown to significantly affect the melting temperature of the proteins TREK1 and TREK2. This corroborates with the results of the Z' test above in that both agree that there is ample signal-noise ratio in this assay.

3.3.4 Purification of two control proteins: TASK1 and GLUT3

TASK1 is a K2P channel described in Chapter 1. GLUT3 however, is a glucose transporter unrelated to any ion channel family. Its main function is to transport glucose across cell membranes in the central nervous system[108]. In this thesis, GLUT3 is used as a control protein as it is unrelated to any of the K2Ps and thus has a completely different sequence and structure. It is also purified in the same detergent as TREK1 and TREK2, OGNG with CHS, which eliminates any variation due to changes in detergent micelle size and structure. This makes it a good negative protein control for determining the effects of small molecules on TREK1 and TREK2.

TASK1 and GLUT3 were purified as described in Section 2.2. TASK1 was purified in LMNG/CHS while GLUT3 was purified in OGNG/CHS. SEC profiles and SDS-PAGE of both proteins are shown in Figure 3.8. The thermostability of TASK1 and GLUT3 were also tested with DSF and their melting temperatures were found to be 48 ± 2°C (Mean ± SEM) and 54 ± 2°C (Mean ± SEM) when purified in LMNG/CHS and OGNG/CHS respectively.

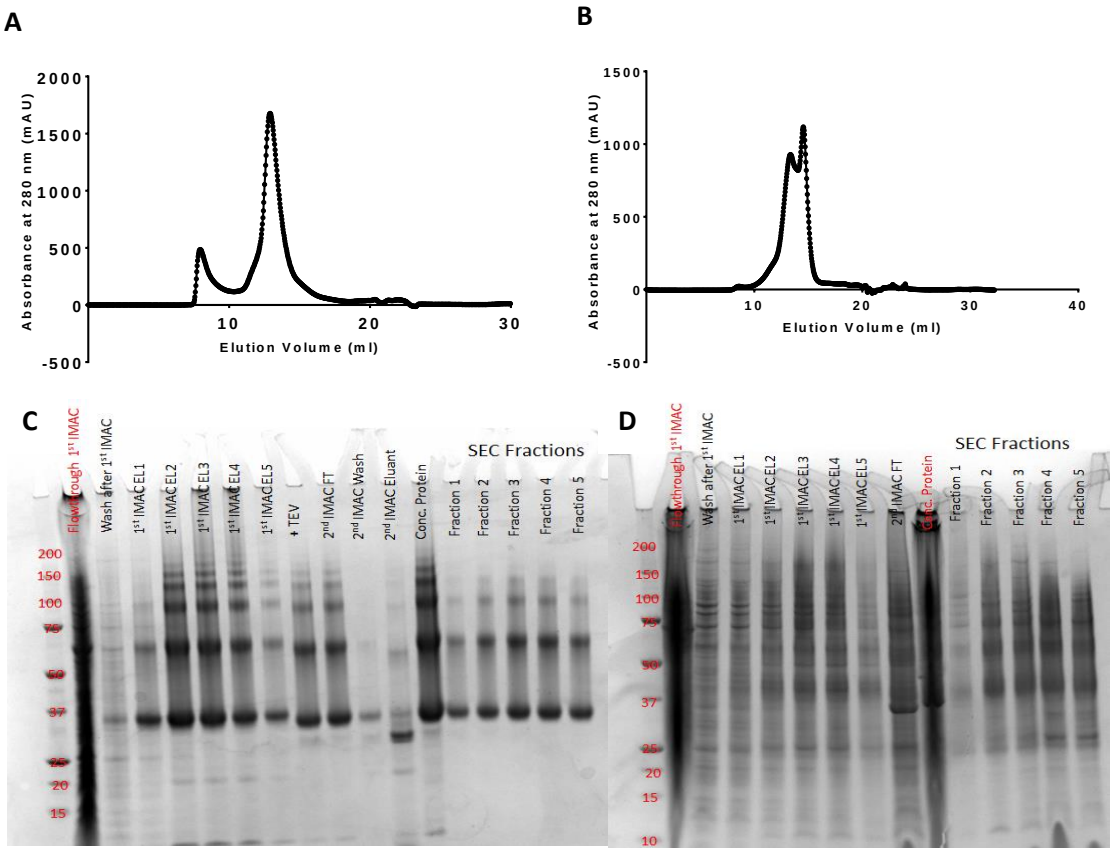

Figure 3.8: SEC Profile and SDS-PAGE of GLUT3 (A and C) and TASK1 (B and D). *GLUT3 is monodisperse while TASK1 has 2 distinct peaks and both the higher MW and lower MW peak are the same protein as shown by SDS-PAGE. The higher MW peak is an aggregate of TASK1 (Fractions 1 and 2 of SEC from Figure 3.8D). In the SDS-PAGE, GLUT3 and TASK1 have distinct bands, which correspond to the monomer (Lowest MW) and multimer aggregates of the protein. Lanes labelled IMAC (Immobilised Metal Affinity Chromatography) refer to 1 ml fractions taken after affinity chromatography.*

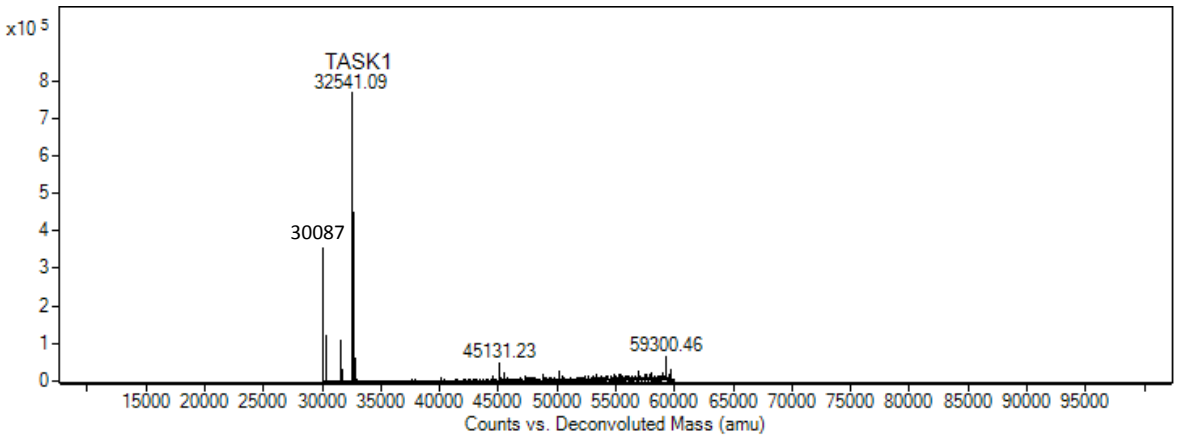

Figure 3.9: Mass Spectrometry of TASK1. *The TASK1 construct used has an expected mass of 32,541 Daltons (inclusive of the His Tag). The smaller peak of 30,087 Daltons is the protein monomer without the Histidine Tag.*

3.3.5 DSF of TREK1, TREK2, TASK1 and GLUT3 with known Ligands

Both TREK1 and TREK2 are activated or inhibited by a large range of compounds as discussed in Chapter 1, and the next aim is to determine whether the CPM assay is able to detect changes in thermostability in a panel of known ligands to these proteins.

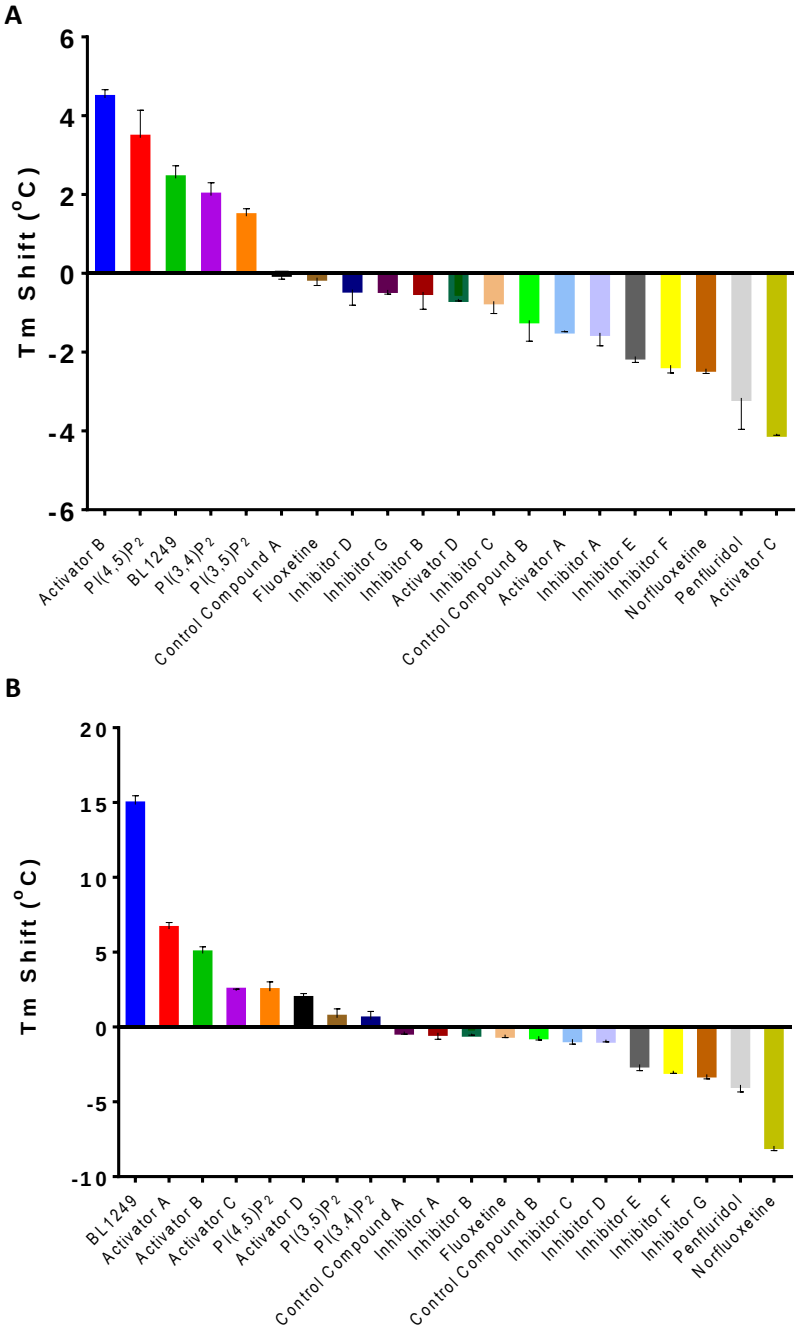

Figure 3.10: Screening of TREK2 (A) and TREK1 (B) against known activators and inhibitors using DSF with CPM dye. *All compounds were screened at 50 µM concentration as this is above the K_d in all cases where known, either literature or measured. The unknown compounds are labelled as activators, controls or inhibitors based on their effect on either or both TREKs in ion flux assays. The unknown compounds were provided in powder form by Pfizer and stocks of 10 mM were made up in DMSO and later diluted to 50 µM. For the known ligands of TREK1 or TREK2, their K_d values can be found in Chapter 1.*

There is a general trend of activators stabilising and inhibitors destabilising the TREKs, but this is not true in all cases.

Dose response assays were also conducted with all the compounds above, but only a selected range that have published structures are shown here. We consider the activators B, BL1249, and $PI(4,5)P_2$[133] and the inhibitors norfluoxetine, penfluridol and nifedipine. The structures of $PI(4,5)P_2$ and nifedipine are shown below in Figure 3.11:

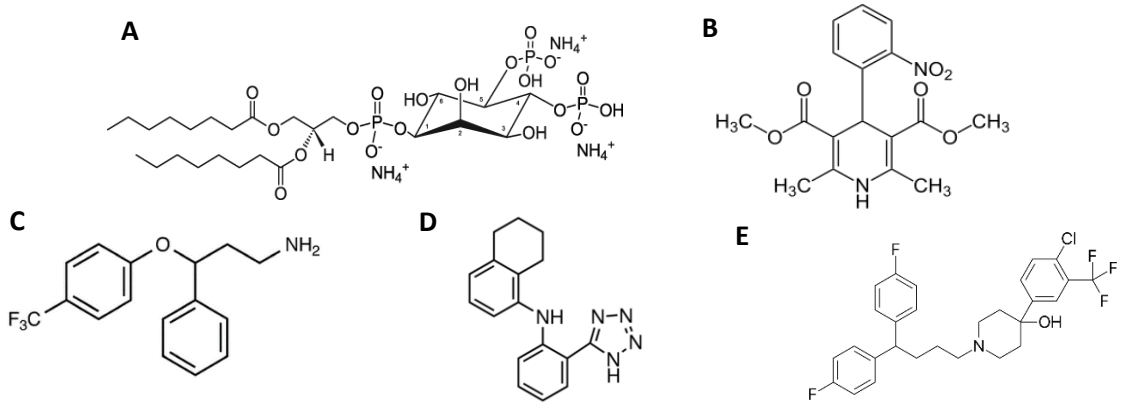

Figure 3.11: Chemical Structures of di-octanoyl $PI(4,5)P_2$ (A), nifedipine (B), norfluoxetine (C), penfluridol (D) and BL1249 (E).

The compounds were screened at concentrations of 1, 2, 5, 10, 20, 50 and 100 µM against the K2Ps TREK1, TREK2, TASK1 and the control protein GLUT3. Each protein-compound combination at a given concentration was screened with 3 preparations of the same protein. 4 technical replicates were performed with each protein-compound combination so 12 T_m values were obtained. Graphs of the data obtained are shown below in Figure 3.12, together with a comparison of T_m shifts at 10 and 50 µM compound concentrations (Tables 3.5 and 3.6).

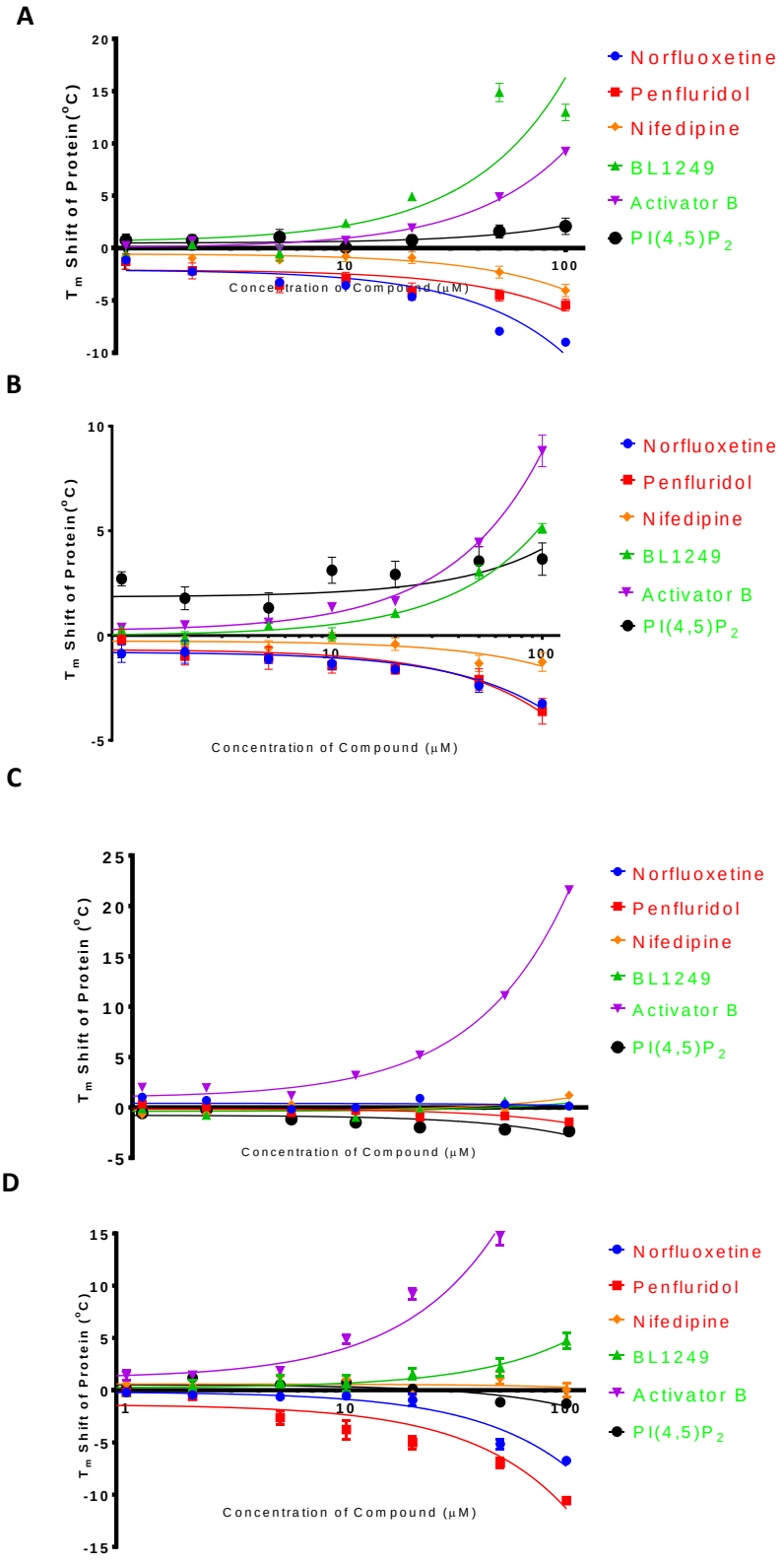

Figure 3.12: Dose Response Curves for known TREK activators (BL1249, PI(4,5)P2 and Activator B) and known TREK inhibitors (Norfluoxetine, Penfluridol and Nifedipine) against a selection of proteins using DSF with CPM fluorescent dye. *Activators are shown in green text in the legend and inhibitors in red. Figure 3.12A is for TREK2, Figure 3.12B for TREK1, Figure 3.12C for GLUT3 and Figure 3.12D is for TASK1. Graphs are all plotted on Log 10 scale with nonlinear regression fitting.*

Protein	Tm Shift for Norfluoxetine (°C ± SEM)	Tm Shift for Penfluridol (°C ± SEM)	Tm Shift for BL1249 (°C ± SEM)	Tm Shift for Activator B (°C ± SEM)	Tm Shift for $PI(4,5)P_2$ (°C ± SEM)	Tm Shift for Nifedipine (°C ± SEM)
TREK2	-1.35 ± 0.29	-1.43 ± 0.36	0.06 ± 0.31	1.36 ± 0.12	3.12 ± 0.62	-0.07 ± 0.22
TREK1	-3.55 ± 0.30	-2.94 ± 0.62	2.36 ± 0.21	0.74 ± 0.25	0.05 ± 0.38	-0.79 ± 0.51
GLUT3	-0.02 ± 0.21	-0.31 ± 0.12	-0.99 ± 0.24	3.21 ± 0.11	-1.48 ± 0.07	-0.08 ± 0.09
TASK1	-0.55 ± 0.29	-3.77 ± 0.90	0.68 ± 0.74	4.89 ± 0.43	0.76 ± 0.30	1.04 ± 0.30

Table 3.5: Table of Compound Response Data from DSF for TREK1, TREK2, GLUT3 and TASK1 at 10 µM compound concentration. Compounds which stabilised the target protein are coloured in green, those that destabilised the target protein are coloured in red.

Protein	Tm Shift for Norfluoxetine (°C ± SEM)	Tm Shift for Penfluridol (°C ± SEM)	Tm Shift for BL1249 (°C ± SEM)	Tm Shift for Activator B (°C ± SEM)	Tm Shift for $PI(4,5)P_2$ (°C ± SEM)	Tm Shift for Nifedipine (°C ± SEM)
TREK2	-2.40 ± 0.31	-2.11 ± 0.52	3.04 ± 0.32	4.45 ± 0.21	3.55 ± 0.70	1.04 ± 0.30
TREK1	-7.95 ± 0.16	-4.52 ± 0.53	14.87 ± 0.87	4.91 ± 0.14	1.59 ± 0.62	-2.30 ± 0.57
GLUT3	0.31 ± 0.09	-0.84 ± 0.26	0.62 ± 0.16	11.12 ± 0.30	-2.18 ± 0.08	-0.20 ± 0.13
TASK1	-5.15 ± 0.47	-6.98 ± 0.45	2.18 ± 0.84	14.80 ± 0.90	-1.15 ± 0.24	1.19 ± 0.58

Table 3.6: Table of Compound Response Data from DSF for TREK1, TREK2, GLUT3 and TASK1 at 50 µM compound concentration. Compounds which stabilised the target protein are coloured in green, those that destabilised the target protein are coloured in red.

The data above shows that norfluoxetine and penfluridol destabilise all 3 K2Ps appreciably when tested at 20 µM or higher concentrations. The 2 compounds also have no effect on the control protein GLUT3. Penfluridol was also screened at a single concentration against other control proteins in Chapter 5.

BL1249 stabilises all 3 K2Ps at a concentration of 50 µM and has a greater effect on TREK1 than on TREK2 and TASK1. It also has no stabilising effect on the control protein

GLUT3. Activator B seems to have the same effect regardless of the protein, and indeed it affects the control protein more than the TREKs, so we concluded that either it interferes with the assay, or it is a nonspecific stabilizer. Nifedipine only destabilises TREK1 at 50 µM or above. $PI(4,5)P_2$ stabilises both TREKs considerably at 50 µM, with a much greater effect on TREK2 than on TREK1. $PI(4,5)P_2$ is also more specific towards TREK2 than towards TREK1, with the stabilising effect seen at lower concentrations. $PI(4,5)P_2$ does not interact with TASK1 and has a slight destabilising effect on GLUT3.

3.3.6 The Effects of Divalent Cations on TREK Channel Thermostability

The DSF assay using CPM was conducted on both TREK1 and TREK2 with differing concentrations of potassium, calcium and magnesium ions (Figure 3.13). While K2Ps selectively conduct potassium ions, it has been reported that both magnesium and calcium inhibit the activity of TREK1[134,135]. This is of relevance as the structure of TREK1 solved by the Carpenter Group at the SGC (PDB ID: 4TWK) contains Mg^{2+} ions due to the conditions in which the crystals were grown. Some compounds also contain counterions, which may affect the thermostability of the protein. It is thus important to elucidate the effects ions may have on the protein.

The physiological extracellular concentration of calcium and magnesium are about 1.2 mM[136, 138] and 1.3 mM[137, 139] respectively. The localisation of both divalent cations are highly regulated as they are involved in many physiological processes, including cell signalling and enzyme-catalysed reactions[136, 137]. Localised levels of both cations can reach up to 10 - 20 mM within a given organelle or in parts of the cytoplasm and would cause changes in cell metabolism[136, 137]. Changes in the thermostability of K2Ps attributed to the presence of divalent ions would possibly indicate a direct rather than indirect physiological effect on these channels.

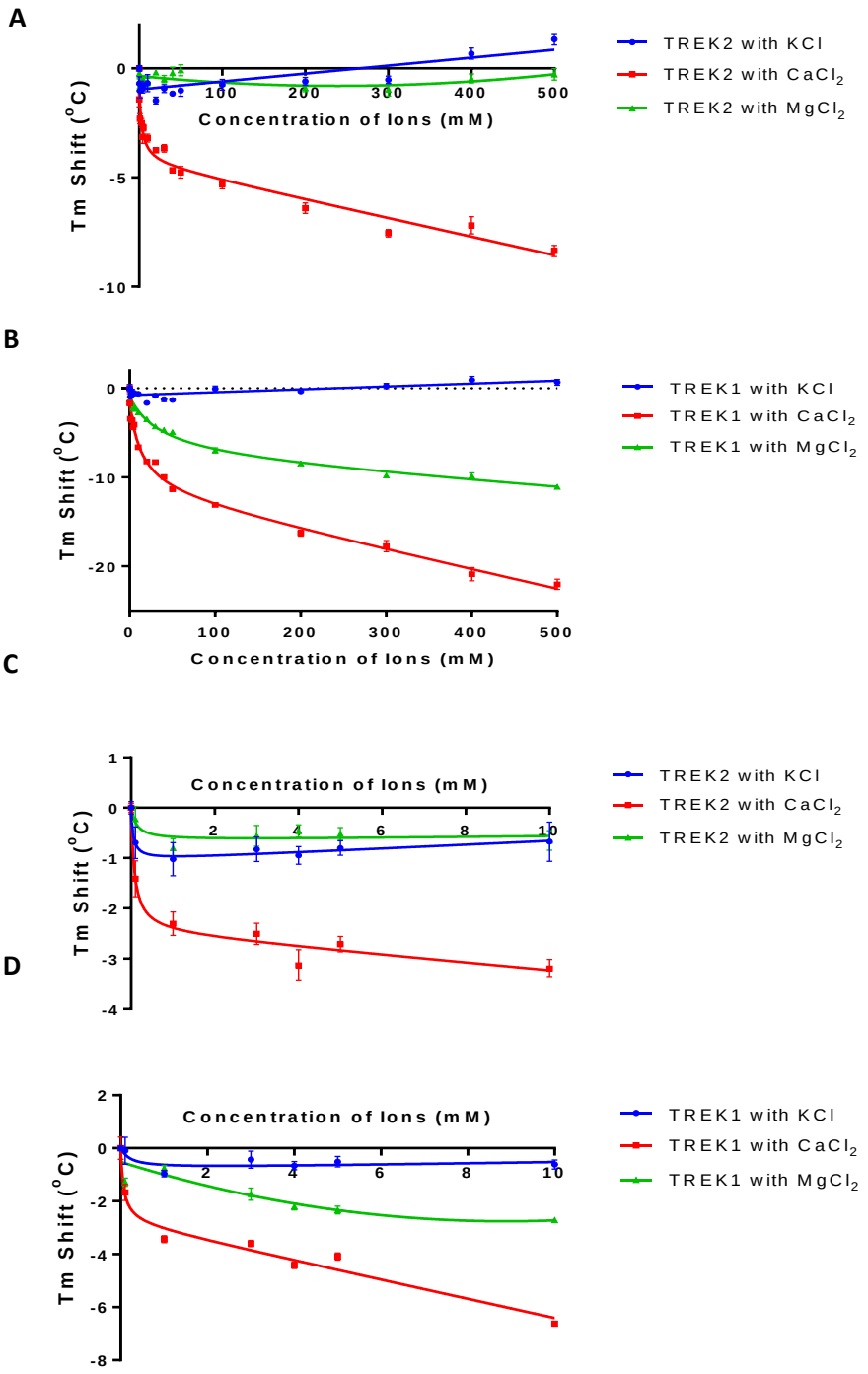

Figure 3.13: Effects of divalent cations on the thermostability of TREK2 and TREK1. *Calcium and magnesium chloride were added in different concentrations to TREK1 and TREK2 in SEC buffer and OGNG/CHS. Each well contained 2 µg of protein and the assay was performed with 2 biological replicates and 4 technical replicates per plate (n = 8). Error bars are the SEM of each data point. Figures 3.13A and 3.13B demonstrate the effect of divalent cations over the full concentration range used on TREK1 and TREK2 respectively while Figures 3.13C and 3.13D focus on physiological concentrations of these ions which are up to 10 mM. Concentrations measured are 0.1, 1, 3, 4, 5, 10, 20, 30, 40, 50, 100, 200, 300, 400 and 500 mM of divalent cations.*

Calcium was shown to reduce the thermal stability of both TREK1 and TREK2, with TREK1 (-11.2°C at 50 mM $CaCl_2$) showing a much greater magnitude of thermostability decrease than TREK2 (-4.76°C at 50 mM $CaCl_2$). Magnesium, however only destabilises TREK1 (-4.94°C at 50 mM $MgCl_2$), having no effect on TREK2 (-0.07°C at 50 mM $MgCl_2$). The destabilisation of TREK1 is significant at physiological concentrations.

3.3.7 Label Free DSF of TREK1, TREK2, GLUT3 and TASK1

Label free DSF was carried out with all 4 test proteins used for the CPM assay and the reference compounds from Section 3.3.5. The aim of this experiment was to confirm or refute the findings from previous assays as well as to verify if this assay is useful in detecting changes in protein stability caused by known ligands of TREKs. This is especially important due to the high incidence of false positives from the DSF assay with CPM, as will be shown in Chapter 5. The proteins were first measured alone for their initial melting temperatures. Dose responses at the concentrations of 5, 10, 20, 50 and 100 µM of compounds used in Section 3.3.5 were carried out with 3 technical replicates and 2 biological replicates (n = 3 X 2) for each protein. The melting points as determined by label-free DSF for the 4 proteins were 72-74 °C for TREK2, 70-72 °C for TREK1, 53-55°C for GLUT3 and 46-48°C for TASK1, which were in broad agreement with those measured by the CPM assay. Subsequently the stabilities of the four proteins were tested in the presence of known activators and inhibitors of the TREKs. BL1249 was not included in these experiments as it interferes with the experiment. The results of these thermostability assays are summarised in Figure 3.14 and Tables 3.7 and 3.8 below:

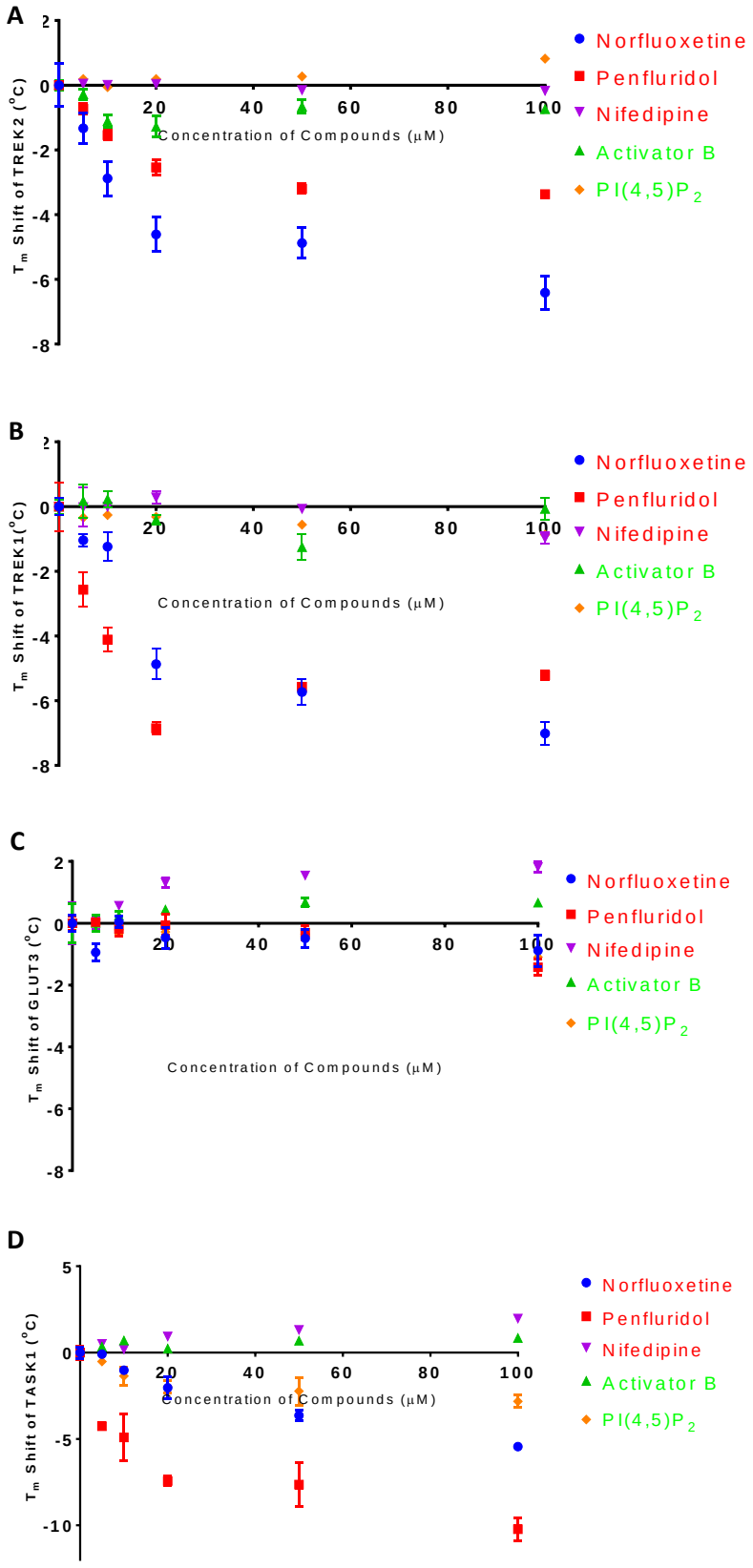

Figure 3.14: Dose Response Curves for known TREK activators (PI(4,5)P2 and Activator B) and known TREK inhibitors (Norfluoxetine, Penfluridol and Nifedipine) against TREK2 (A), TREK1 (B), GLUT3 (C) and TASK1 (D) using Label-Free DSF.

BL1249 was found to absorb at 280 nm wavelength and no usable spectrum was obtained with any protein when BL1249 was added to the mixture at high concentrations (> 20 µM). The results with the other 5 compounds at 10 and 50 µM compound concentrations are shown in Tables 3.7 and 3.8.

Protein	Tm Shift for Norfluoxetine (°C ± SEM)	Tm Shift for Penfluridol (°C ± SEM)	Tm Shift for Activator B (°C ± SEM)	Tm Shift for $PI(4,5)P_2$ (°C ± SEM)	Tm Shift for Nifedipine (°C ± SEM)
TREK2	-2.88 ± 0.53	-1.54 ± 0.15	-1.11 ± 0.08	0.01 ± 0.07	-0.06 ± 0.09
TREK1	-1.24 ± 0.45	-4.11 ± 0.36	0.23 ± 0.25	-0.26 ± 0.12	-0.01 ± 0.03
GLUT3	0.04 ± 0.19	-0.19 ± 0.24	0.25 ± 0.14	-0.21 ± 0.17	0.57 ± 0.13
TASK1	-1.02 ± 0.09	-4.91 ± 1.36	0.70 ± 0.14	0.19 ± 0.18	-1.36 ± 0.54

Table 3.7: Table of Compound Response Data for Label-Free DSF for TREK1, TREK2, GLUT3 and TASK1 at 10 µM compound concentration. Compounds that destabilised the target protein are coloured in red.

Protein	Tm Shift for Norfluoxetine (°C ± SEM)	Tm Shift for Penfluridol (°C ± SEM)	Tm Shift for Activator B (°C ± SEM)	Tm Shift for $PI(4,5)P_2$ (°C ± SEM)	Tm Shift for Nifedipine (°C ± SEM)
TREK2	-4.88 ± 0.47	-3.20 ± 0.15	-0.66 ± 0.20	0.27 ± 0.08	-0.15 ± 0.07
TREK1	-5.73 ± 0.41	-5.57 ± 0.13	-1.25 ± 0.41	-0.56 ± 0.11	-0.07 ± 0.02
GLUT3	-0.49 ± 0.30	-0.30 ± 0.23	0.68 ± 0.15	-0.35 ± 0.16	1.55 ± 0.13
TASK1	-3.64 ± 0.28	-7.64 ± 1.27	0.69 ± 0.10	1.31 ± 0.21	-2.23 ± 0.80

Table 3.8: Table of Compound Response Data for Label-Free DSF for TREK1, TREK2, GLUT3 and TASK1 at 50 µM compound concentration. Compounds which stabilised the target protein are coloured in green, those that destabilised the target protein are coloured in red.

As with the CPM assay, Label free DSF is able to detect the destabilisation of TREK2, TREK1 and TASK1 by norfluoxetine and penfluridol if the cutoff is taken to be a T_m shift

of 1.5°C. This is because the variance observed between samples is in almost all cases much lower than 1.5°C. Both norfluoxetine and penfluridol also have no effect on GLUT3 thermostability. This effect is however of differing magnitudes to those measured using the CPM assay. Activator B exhibits no significant effect on any protein, unlike in the CPM assay where it appeared to have an effect of all proteins, which suggests that it interferes with the assay, possibly by reacting with the maleimide dye rather than on the protein-detergent complex.

$PI(4,5)P_2$ also had no significant effect on any of the 4 proteins at concentrations below 50 μM, which does not correspond to the CPM assay result of it being a stabiliser of TREKs and a destabiliser of GLUT3. Nifedipine is seen to stabilise GLUT3 and destabilise TASK1 at high concentrations (> 50 μM), which also does not agree with what is shown by the DSF assay using CPM in that it only destabilises TREK1 in that assay. This effect may be due to non-specificity of the effect of nifedipine or an artefact which occurs at high compound concentrations.

3.4 Discussion

3.4.1: Assessment of Suitability of DSF for Compound Screens

The use of DSF for measuring the thermostability of proteins is well known, as is its use for high throughput screening of compounds with the dye Sypro Orange, which is widely used for soluble proteins[112]. This work attempts to evaluate the use of DSF using the CPM dye, as well as the use of Label-Free DSF, for compound screening against ion channel proteins. K2Ps were used as model proteins due to their ease of purification and stability.

In order to evaluate the techniques described above, the melting points of 4 proteins were obtained in their most favourable buffer conditions as determined by previous detergent screens conducted by other members of the Carpenter group, at the SGC. The effects of purification detergent and DMSO on protein thermostability were then analysed with TREK1 and TREK2. The CPM assay was found to be compatible with DDM, OGNG, both with and without the addition of CHS and up to 1% DMSO, making it possible to screen any compound that is soluble up to a concentration of 50 µM in 1% DMSO, which encompasses a vast quantity of chemical space.

TREK2 was shown to have different melting temperatures when purified in different detergents, making the choice of detergent an important factor in protein-detergent complex stability. This has consequences in both structure determination and compound screening, as detergents would affect the experimental setup and results.

Following this, a pharmaceutical industry standard Z' test was performed to determine the statistical power of the CPM assay. The Z' test showed that the CPM assay has a high signal-noise ratio and a low variance and is thus suitable for compound screening in 96 well plates. This establishes it as a useful alternative to currently existing cell-based or biochemical assays as a method to triage a large number of compounds.

It is possible to upscale the CPM assay to 384 or even 1536 well plates if suitable fluorescent detectors are available. I was limited by the availability of equipment to 96 well plate readers and it would be useful to repeat the Z' test on larger setups to determine the effectiveness of this assay on even lower amounts of material and thus its sensitivity.

I then determined the ability of the CPM assay as well as the label free DSF to detect changes in thermostability with a small panel of 5 known activators or inhibitors of

TREKs as well as the specificity of these compound-induced interactions with the unrelated control protein GLUT3 and the related K2P channel TASK1. Both assays showed that the inhibitors norfluoxetine and penfluridol were destabilisers of TREK1, TREK2 and TASK1 but had no effect on GLUT3 at concentrations close to their reported IC_{50} values. The results with the other compounds were much less conclusive, with $PI(4,5)P_2$ and Activator B exhibiting effects with the CPM assay which are not seen with label free DSF. This difference in effect can be due to a few possible factors, as described below:

Firstly, it is possible for a compound to bind to a protein and not cause a change in its thermostability as the binding can cause certain parts of the protein to become less stable while stabilising some others by holding it in a different conformation from the apo-protein. Binding of a ligand causes a protein to adopt the most energetically favourable conformation of the protein-ligand complex, which may not be more thermostable than the conformation of the apo-protein. This phenomenon also explains why some ligands can destabilise the protein, an observation not previously reported in soluble proteins[140].

Secondly, a small molecule may interact directly with the detergent or the fluorescent dyes, which causes a false positive effect to occur. Activator B appears to stabilise all proteins including the negative control GLUT3 in the CPM assay but has no effect on any of the proteins when tested with Label Free DSF. This is likely due to the compound binding directly to the dye or otherwise interfering with the ability of the dye to bind to exposed cysteine residues in the protein, thus causing this apparent T_m shift. However, when Activator B was combined with CPM in the absence of the protein there was no fluorescence signal change, so the effect of Activator B on the assay is not simply due to

a reaction of CPM with the Activator B. It is therefore unclear exactly how Activator B interferes with the assay.

Thirdly, a compound may absorb at the same wavelength as the fluorescent dye or the tryptophan residue. The effect of BL1249 was not measurable with Label-Free DSF as the compound absorbs at the same wavelength as tryptophan, causing a high background signal. However, later experiments not described in this thesis using light scattering with the Nanotemper Prometheus showed BL1249 to be a stabiliser of TREK1, TREK2 and TASK1 but not GLUT3.

3.4.2: Comparison of CPM assay and Label Free DSF

As highlighted in section 3.4.1, there are advantages and disadvantages to both of these methods as well as limitations to their use. Both methods are applicable to a large range of other classes of membrane proteins as well as soluble proteins.

Both thermostability assays described above allow for medium scale compound screening with high signal to noise ratio when optimised. They are simple and fast to use with results shown in an easily analysable form. They also require relatively easy to obtain equipment. However, both techniques are not able to measure protein-protein interactions as these would cause multiple signals to be obtained.

The CPM assay is higher throughput and is scalable to larger numbers of protein-compound concentrations, up to 10,000s of compounds could in theory be screened in a day in a single point assay. However, label-free DSF, with technology available at the time of testing can only screen 48 samples at a time, giving 2 orders of magnitude less throughput with a single machine, though higher throughput label-free DSF technology is now available.

The CPM assay also requires much less protein per sample than label-free DSF, up to 1 order of magnitude less per single data point (10^{-7} g against 10^{-6} g). This is important as even large scale purification of most membrane proteins does not yield more than 10^{-3} grams of proteins and it is time-consuming and very costly to produce larger amounts of protein for screening purposes.

However, label free DSF does not require a dye and thus eliminates any possibility of interaction between the dye and the protein or the compound. This removes an important confounding factor in the analysis and makes the results obtained potentially more relevant than those obtained from the CPM assay.

The main limitations of both of these techniques is firstly, they must be performed on protein samples which are highly purified as any contaminants would give an extra signal which would make the data difficult to analyse. Secondly, the detergent and all other buffer components used must not interact with the CPM dye or fluoresce at 330 or 350 nm for the Label Free DSF. In addition, they also cannot fluoresce at 470 nm wavelength, which is the emission wavelength of CPM.

Thirdly, the protein must contain interior cysteine residues for the CPM assay to be effective or aromatic residues for Label-free DSF to be used. The signal intensity is proportional to the number of such residues in the test solution, which requires that different amounts of different proteins be used when screening is performed due to variation in signal intensity and hence the signal-noise ratio. The amount of protein required for sufficient statistical power in the assay must be optimised and calculated before screening begins.

Fourthly, the protein-detergent complex must be thermostable to at least 30°C for any meaningful signal to be obtained as otherwise the protein will be partially denatured

even before the experiment starts, giving an unstable initial reading, making it impossible to fit a simple sigmoid curve to the data. Optimising purification conditions such as buffer, detergent, pH and lipids is thus crucial before these methods are used with most membrane proteins.

3.4.3: Possible Structural Implications on TREKs from DSF Results.

The results above show that norfluoxetine destabilises TREK1, TREK2 and TASK1, and BL1249 is a stabiliser of the same 3 proteins. The binding between norfluoxetine and BL1249 and TREK2 has been verified using X-ray crystallography[59] (MacKenzie, A., unpublished data) as well as by electrophysiology[86, 91].

TREK2 has been visualised in multiple states in X-ray crystallography[59] and a ligand could lock the protein into a single conformation. In the case of norfluoxetine, the compound binds within the fenestrations of TREK2 and stabilises what was putatively thought to be a closed channel state, leading to inhibition. However, the precise mechanism of inhibition remains unknown [141].

Different states of a single protein have different thermostability and one possible explanation for a change in melting temperature upon compound binding is the locking of protein into a single state which may be more or less stable than the initial state or composition of different states. It has been suggested that for soluble proteins, if a small molecule reduces the thermostability, it may cause unfolding of the protein. In the case of the TREK channels we see small changes in thermostability, a few degrees, with an overall stability of changing from over 70°C, to 60 – 65°C. These small changes are unlikely to be caused by denaturing of the protein and it is more likely that they represent a shift to a state with a slightly lower stability. Further structural studies can

be performed to explore the relationship between ligand binding and the changes in conformation of proteins as well as their function.

3.5 Conclusion

The data above shows that both DSF using the CPM dye and label free DSF are able to effectively measure the thermostability of the K2P ion channels tested and the melting points found were in broad agreement between these techniques. They are also able to detect the effects of selected inhibitors on TREK2 and TREK1. The activators tested were more problematic as one appears to interfere with the CPM assay, the other interfered with the label free TRP fluorescence assay and the third gave moderate effects only in one assay. This shows the value of using both methods, to assess the validity of the other method. The CPM assay in particular has been shown using the Z' test to have enough statistical power for use in medium to large scale screening of compounds. We thus conclude that initial screening of a compound library with the aim of finding novel TREK binders could be conducted using the CPM assay, with subsequent validation of the results using label free DSF.

Chapter 4: Using Biophysical Methods which Measure Properties other than Fluorescence to Characterise the Binding of Ligands to TREKs

4.1 Introduction

4.1.1: Isothermal Titration Calorimetry and its Applications in Membrane Protein Drug Discovery.

Chapter 3 discussed the use of fluorescence methods to measure membrane protein thermostability and the use of changes in thermostability to assess ligand binding. In this chapter, the use of a range of other biophysical methods to determine ligand binding with K2P ion channels are discussed.

Ligand binding to protein can be determined using biophysical means through a multitude of parameters, including the measurement of reaction enthalpy, changes in light refraction or diffraction properties of the protein, mass of the complex or magnetic resonance[101]. Mass spectrometry and nuclear magnetic resonance of protein-ligand complexes are major research subjects that are beyond the scope of this thesis[142, 143, 144].

This chapter discusses the use of isothermal titration calorimetry (ITC), surface plasmon resonance (SPR) and biolayer interferometry (BLI) for detection of binding interactions between membrane proteins solubilised in detergent and small molecules which interact with the proteins.

ITC can measure the enthalpy of a reaction between a protein and either a ligand or another protein [145, 146, 147]. It was first described in 1965 by Christensen *et al.* for use with inorganic systems[148]. The method was later applied to biological systems[146, 147]. During an ITC experiment, fixed volumes of one of the interacting pair is titrated against a

constant amount of its partner. The temperature of the mixture is kept constant compared to that of a reference cell using a heating or cooling element and constant, rapid stirring. High sensitivity thermocouple circuits are used to detect the changes in the temperature of the sample cell during the titration process. The energy required to keep the temperature of the solution constant is recorded using a feedback loop between the 2 cells, measuring the amount of power needed. The enthalpy of the reaction can then be derived from the change in power over a period of time. Power is related to current, voltage and energy by the equation below:

$$P = IV = W/t \tag{4.1}$$

Where P is the power in Watts, I is current in Amperes (A), V is voltage in Volts (V), W is work done in Joules (J) and t is time in seconds (s). The enthalpy of a reaction can be obtained by summing up the total change in power in the feedback circuit over a course of the reaction. This can be done by obtaining the total area under the curve (or baseline) in a graph with power in the feedback circuit plotted against time. An example of such a graph can be seen in Figure 4.5.

Stepwise titration allows us to track the total enthalpy as well as the stoichiometry and association constant of the reaction through the determination of a half-life of decay in enthalpy generated. This can be obtained through the plotting of a graph between enthalpy of reaction per titration step against the number of moles of the injectant (or the molar ratio between the injectant and the molecule in the sample cell). The graph obtained is then fitted to the Wiseman isotherm if one set of binding sites is assumed[149] or other more complex models otherwise.

From this, the Gibb's Free Energy and the entropy of the reaction can be derived using the equation:

$$\Delta G = RT \ln K = \Delta H - T\Delta S \quad (4.2)$$

Where ΔG is the Gibb's free Energy of a reaction in kJ/mol, R is the gas constant (8.314 J/mol K), T is the temperature at which the reaction takes place in Kelvins, K is the association constant of the compound in moles, ΔH is the enthalpy of the reaction in J/mol and ΔS is the entropy of the reaction in J/mol K.

The ability to check these thermodynamic quantities quickly allows us to determine the effect of optimisation of compounds from an initial hit of a screening process. It also allows the prediction of effects and concentrations of compound to be used on cell-based assays and physiological studies in downstream drug discovery. It is thus widely used in the pharmaceutical industry and is considered the 'gold standard' assay for determining ligand binding to a protein[150]. In this work, ITC was tested with a known ligand of TREK2 determined by electrophysiology, so as to ascertain its viability in ion channel work.

Figure 4.1 illustrates the use of this technique.

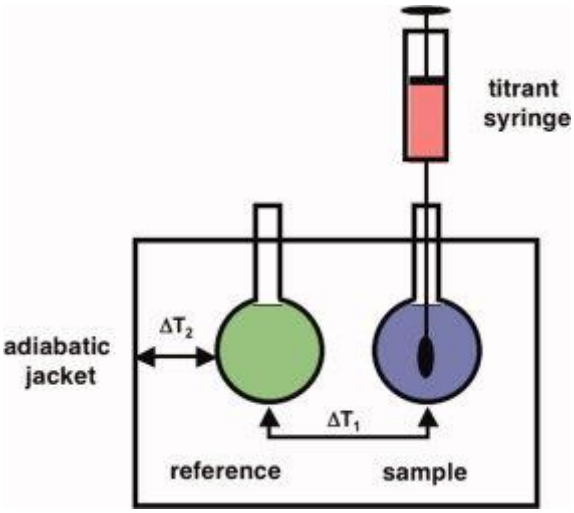

Figure 4.1: Isothermal Titration Calorimetry. *A reference and sample compartment within an adiabatic jacket are kept at a constant temperature ($\Delta T_1 = \Delta T_2 = 0$). Prior to titration, this power is maintained by a constant reference power applied to the reference cell, which activates a heater on the sample cell via a feedback loop. As a titrant is added into the sample cell with stirring, the reaction enthalpy is measured by recording the amount of power required to keep ΔT_1 at 0 using the feedback loop, which decreases in an exothermic reaction and increases in an endothermic reaction. Figure taken from Feig, 2007*[151].

However, the use of ITC has a few requirements and limitations. Firstly, the protein and compound of interest must be purified to a high standard in order to minimise non-specific interactions. Next, before the experiment is conducted, a Wiseman 'c' value must be estimated if a Wiseman isotherm was to be fitted on the result graph. The 'c' value is dependent on both the protein concentration and the ligand dissociation constant as shown below:

$$c = nP/K_d \tag{4.3}$$

Where n is the number of binding sites in the protein for the ligand, P is the protein concentration in moles and K_d is the dissociation constant for the ligand in moles.

The c value determines the shape of the Wiseman binding isotherm between the protein and ligand, and only if the c value is between 5 and 100 can a good estimate of the dissociation constant be obtained through curve fitting. If the c value is below 5, no thermodynamic parameters can be calculated. If the c value is too high it is not possible to calculate the binding dissociation constant, although enthalpy and stoichiometry can still be obtained[152]. An illustration of the binding isotherms obtained with different c values can be seen in Figure 4.2.

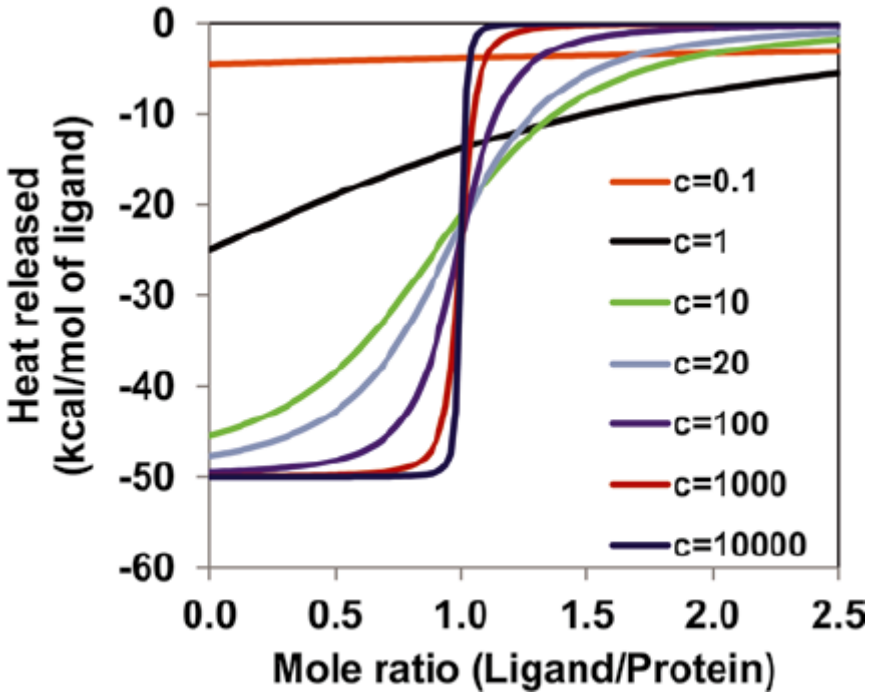

Figure 4.2: Examples of binding isotherms obtained from different c values during an ITC experiment. *Figure taken from Dutta et al., 2015[152]. Data derived from Wiseman et al., 1989[149].*

In addition, the buffers in which the protein and ligand are dissolved must be exactly matched. This is especially difficult for membrane proteins as they are purified in detergent micelles and exact determination of detergent concentration is challenging[153]. Detergents also provide another confounding factor as the ligand may interact with the detergent micelle, either directly with the detergent or through the uptake or release of detergent molecules from the micelle, which also produces

enthalpy change and this may obscure any effect the ligand has on the protein even if a suitable control is performed[154].

Despite these challenges, there have been studies where ITC was used to quantify the binding parameters of ligands to membrane proteins, especially with GPCRs[155,156]. A separate study found the binding properties of strychnine and glycine with the glycine receptor, which is a homopentameric ion channel[157].

Other limitations of ITC are that it requires large amounts of protein (milligram quantities with a 10^{-4} M binder, stronger binders need proportionally less protein), it can only run one protein-ligand combination at a time and multiple control experiments per combination. It is thus very low throughput and cannot be used for screening compound libraries.

4.1.2: Surface Plasmon Resonance and its applications in Membrane Protein Drug Discovery.

Another method that is widely used to detect and quantify binding of ligands to proteins is Surface Plasmon Resonance (SPR). This method, which was first described in 1991 for use in drug discovery[158], makes use of changes in surface plasmon resonance angle or wavelength caused by the change in particle size and refractive index. Surface plasmons refer to the natural oscillation of conductive electrons at the interface between two materials of which one has a positive real dielectric constant and the other has a negative real dielectric constant. Examples of such interfaces are metal/air and metal/water interfaces. A schematic of how SPR works is shown in Figure 4.3:

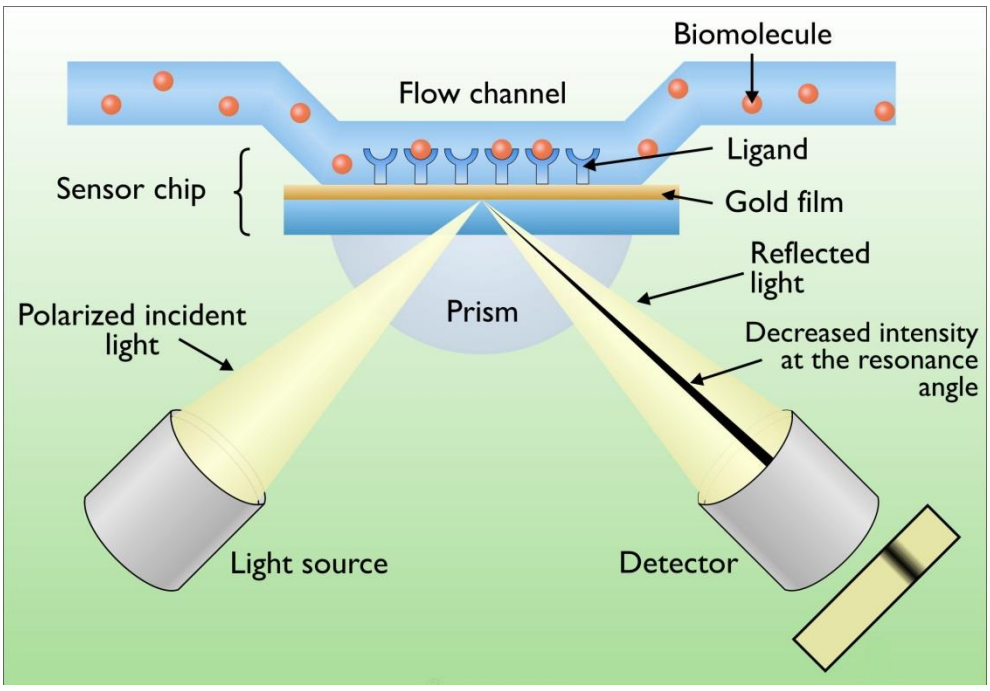

Figure 4.3: A Schematic of SPR. *The SPR schematic above has a setup that contains two media with different refractive indexes. The prism has a much higher refractive index than the fluid medium above, so when a polarised incident light beam hits a gold film situated between the two media, total internal reflection occurs when the incident angle is greater than the critical angle[159]. An evanescent wave is created at the interface between the metal film and the solution in the flow channel, which excites the surface plasmons on the gold film and causes a phenomenon known as SPR. The surface plasmon resonance is an oscillation of electrons which creates electromagnetic wave which propagates only along the surface of the gold film[162]. Light at the resonance angle is absorbed and is detected as a decreased intensity by a detector placed at the total internal reflection angle. Figure taken from Heygi et al., 2013[160].*

SPR is very sensitive to changes in the amount of substance on the gold film surface and this property is the principle behind measurement of biomolecular interactions. While it is possible to construct one's own SPR setup[159], the most common equipment used is the Biacore series (GE Healthcare Life Sciences, Little Chalfont, Buckinghamshire, UK), which makes use of gold film microchips coated with a substance which binds the protein of interest. The mostly commonly used substance to coat the chip is a dextran

matrix that can bind proteins via amine, carboxyl, thiol or aldehyde groups[161]. The drawback with this method is that the binding would not be specific to a single protein and mixtures cannot be loaded onto the chip. To overcome this, an antibody or streptavidin can be loaded onto the chip using the dextran matrix before the protein is loaded as a secondary binder. This method is known as indirect capture and is able to provide much more specificity to the assay as only the target protein would then be attached in significant amounts to the chip[161]. Alternatively, gold foil chips coated with streptavidin or Ni-NTA are commercially available for the binding of proteins tagged with biotin or His respectively.

After the target protein is loaded onto the chip, the possible interacting partners are then passed over a chip in a flow channel. The interaction between the small molecule introduced in this way and the protein immobilised on the chip changes the resonance wavelength of the surface plasmon wave and thus the resonance angle at which light is absorbed. This change in resonance angle is directly proportional to the mass of molecules bound to the chip[162]. This property is important in the use of SPR in investigating protein-ligand interactions as it allows researchers to elucidate both the binding affinity and kinetics of the reaction. A representation of an SPR measurement is shown in Figure 4.4:

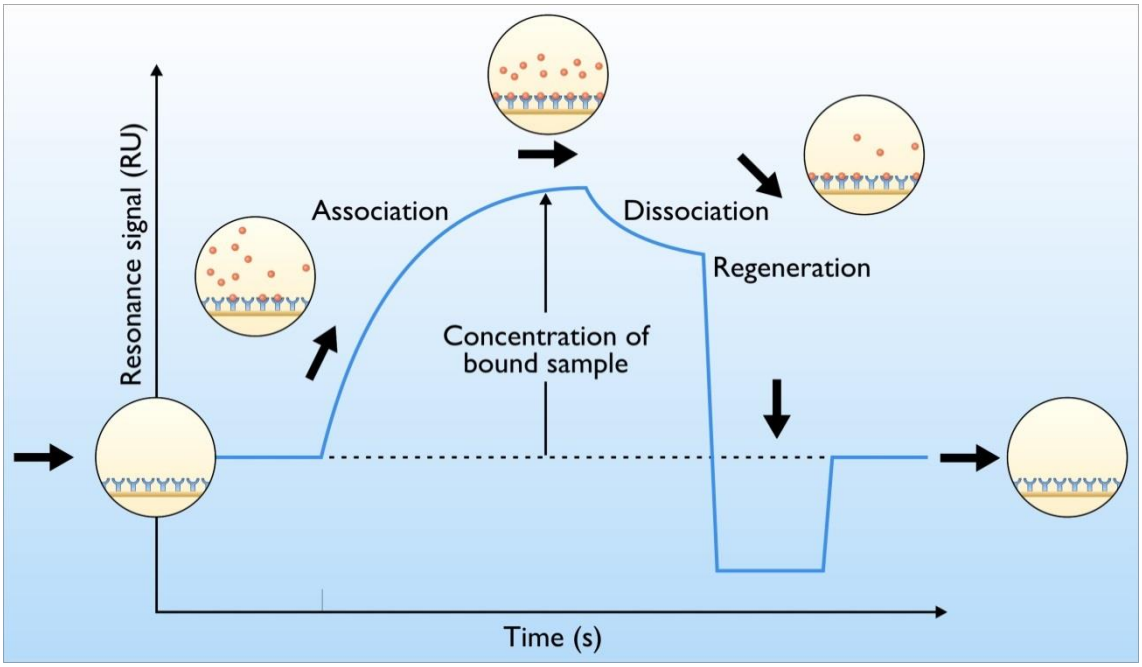

Figure 4.4: Process of a SPR Experiment. *As a ligand within a flow cell is passed over an immobilised protein on a chip, the protein-ligand interaction can be measured as an association curve which follows a first-order decay equation. The chip is then perfused with ligand-free buffer to measure dissociation kinetics. The K_d of the ligand can be derived from the association and dissociation kinetics*[160]*. The chip surface can then be regenerated by perfusion of an acidic or basic solution which removes the ligand but leaves the protein intact. The chip with immobilised protein can then be reused for the next potential ligand. Figure taken from Heygi et al., 2013*[160]*.*

In recent years, SPR has been widely used to quantify binding parameters on a range of target proteins, including the interactions between GPCRs, their ligands or their accessory proteins[163, 164]. IMPs pose a number of challenges when this technique is used. As membrane proteins are generally purified in detergent micelles, the part of the protein that binds to the gold chip must be exposed for immobilisation to occur. The detergent micelle must also not interact directly with any part of the ligand or buffer or it would result in a false positive signal. Relevant controls with different proteins and negative ligand controls should also be performed to verify the data.

This work aims to develop, optimise and demonstrate the use of SPR to quantify binding between TREKs and their known ligands. It also aims to evaluate the usefulness of SPR as an assay for compound screening.

4.1.3 Biolayer Interferometry and its Application in Membrane Protein Drug Discovery.

Biolayer Interfometry (BLI) uses changes in refractive index when small molecule ligands bind to proteins to detect these interactions[165]. In this technique, a biomolecule is bound to a sensor coated with a substance which interacts with a portion of the target. A white light is then passed through the biosensor and the light is reflected by two interfaces: the surface between the glass fibre of the sensor and the biocompatible optical reference layer as well as the surface between the optical reference layer and the solution. When a biomolecule is bound to the sensor, the interference pattern of white light after reflection in the first surface is unchanged, but that of the second layer changes[165]. This change in interference pattern is recorded and magnitude of this change is proportional to the mass of molecules bound to the biosensor[166].

In a BLI experiment, one of the interacting partners is immobilised onto a biosensor which has either Ni-NTA, Anti-GST or streptavidin attached to the sensor. The target protein has a His-tag, GST or biotin tag attached to it. The sensors are then dipped into a solution containing the other interacting partner, causing the change in interference pattern seen with binding between the 2 molecules.

BLI can measure both the binding affinity and the kinetics of an interaction and is sensitive enough to pick up interactions between proteins and small molecules[167, 168]. BLI is compatible with most detergents and standard buffers. In the case of membrane proteins, it has been used to investigate protein-protein interactions in ATPase in a

nanodisc environment[169]. This is because the groups bound to the sensor surface ensure specificity of binding to proteins. One main challenge with BLI and small molecule screening is that with micromolar binders and a size of about 300-500 Da, the interaction is at the threshold of detection with current systems and the signal-noise ratio is an issue[167, 170]. Small molecules may also interact with the sensors, causing false positive signals. The protein may also come off the chip with time, leading to reduced signals. In this work, an attempt was made to use BLI to check for the binding between the TREK channels and known binders to evaluate its potential for use in screening or verifying the screening results of larger numbers of compounds.

4.2: Materials and Methods

4.2.1: Sample Preparation

Protein was prepared according to the methods described in Chapter 2. For ITC, protein was frozen at -80°C in 2 mg/ml aliquots. For SPR, 1 mg/ml aliquots were produced instead.

4.2.2: Isothermal Titration Calorimetry

ITC was conducted with the MicroCal VP-ITC system (Malvern Instruments, Malvern, Worcestershire, UK) which has a cell volume of 1.4 ml and a total injection volume of 300 µl.

Before the experiment was conducted, the amount of protein and compound required for a C-value of 10 was determined based on the literature EC_{50} or IC_{50} for the compound against the protein or its close analogue. The protein was concentrated in a 30 kDa cutoff concentrator as described in Chapter 2 if required. The detergent concentration of the protein was then determined using size exclusion chromatrography with standards as

described by Slotboom et al., 2008[171]. Small molecule binders were then dissolved at the concentration determined in the SEC buffer for the protein with the detergent concentration added as measured earlier. The concentrated protein was in all cases then inserted into the cell as its concentration was always much lower than the small molecule. The small molecule was loaded into the injection syringe and injected in aliquots. The experimental setup was as follows:

No. of injections: 20

Volume per injection: 15 µl

Time between injections: 240 seconds

Temperature: 15°C

Spinning speed of stirrer: 286 revolutions per minute

After the initial protein-compound interaction experiment, a heat of dilution control was performed. In a heat of dilution control experiment, instead of injecting small molecule containing solution into a protein-containing solution, the small molecule containing solution is injected into SEC buffer containing the same amount of detergent as measured earlier. The result obtained from the heat of dilution experiment is then subtracted from that of the protein-compound interaction experiment. The data obtained was then recorded using the Origin 7.0 software (Malvern Instruments, Malvern, Worcestershire, UK) which is linked with the VP-ITC setup and thermodynamic parameters (Enthalpy, Entropy, Gibb's Free Energy, K_d) and stoichiometry of reaction obtained using the method described in section 4.1.1.

4.2.3: Surface Plasmon Resonance

SPR was performed using the Biacore T200 instrument (GE Healthcare Life Sciences, Little Chalfont, Buckinghamshire, UK) located in the Department of Biochemistry, University of Oxford. The gold foil chip used for all experiments is the CM5 Chip (GE Healthcare Life Sciences, Little Chalfont, Buckinghamshire, UK). Protein is attached to the chip via direct amine coupling within a pH 5 buffer which contains the SEC buffer of the protein and acetate. The pH was adjusted with dropwise titration of sodium acetate pH 4.0 into an appropriate amount of SEC buffer with constant stirring. Detergent at 2 X CMC was added afterwards. In order to achieve direct amine coupling, 1-Ethyl-3-(3-dimethylaminopropyl)carbodiimide (EDC) is mixed with N-hydroxysuccinimide (NHS) and then added over 7 minutes at 10 µl per minute to the dextran-coated chip surface to form a highly reactive activated acid intermediate which couples directly with amine groups of proteins. The protein was then added and flowed through the chip at 10 µl per minute for 7 minutes. Unreacted succinimide groups were then quenched with ethanolamine at the same flow rate and with the same amount of time as the protein. The ligand was then passed over the sensor chip surface at a rate of 60 µl per minute for 10 minutes at a concentration of up to 32 µM. Sensorgrams were recorded and the peak response of each sensorgram is taken and analysed after blank subtraction. The chip surface was then regenerated by passing 0.7 ml of Glycine-HCl pH 1.5 through the flow cells at 60 µl per minute. SEC was then passed over the chip surface at a rate of 100 µl per minute for 30 minutes to wash away the regeneration solution.

For each protein-ligand combination analysed by SPR, a blank with ligand flowing through a sensor chip that does not contain protein bound is also used. The blank sensorgrams are then subtracted from the protein-ligand sensorgrams to obtain a blank-

subtracted signal, which is analysed with the Biacore T200 Software (GE Healthcare Life Sciences, Little Chalfont, Buckinghamshire, UK). Maximal signals are then read off and plotted as a dose response curve for known ligands.

4.2.4: Biolayer Interferometry

Biolayer Interferometry was performed using the Fortebio Octet QK384 system (Pall Fortebio, Menlo Park, CA, USA) located in the Target Discovery Institute, University of Oxford. Ni-NTA sensors were used for all experiments (Pall Fortebio, Menlo Park, CA, USA) as all proteins involved had a 10-His tag attached to the C-terminus. For immobilisation, a protein solution containing 200 µl of 0.01 mg/ml protein in SEC buffer was prepared in a 96 well plate and Ni-NTA biosensors were dipped into the solution for a 120 second equilibration phase followed by a 600 second immobilisation phase and a 120 second dissociation phase. The interferometry signal was recorded with the Fortebio Octet Software Version 7.0 (Pall Fortebio, Menlo Park, CA, USA).

Following immobilisation, a 96 well plate was prepared with test compounds dissolved in SEC buffer (Sample plate layout in Section 4.3.4) and protein-containing sensors were inserted into the wells containing compound in left to right order. The protocol for testing compound binding was as follows:

Step 1: Equilibration step of 120 seconds where the sensor is in a well containing only SEC buffer.

Step 2: Association step of 240 seconds where sensor is in a well containing test compound.

Step 3: Dissociation step of 240 seconds where sensor is in well containing only SEC buffer.

The interferometry traces were recorded and a dissociation constant determined if there is saturation of signal. Otherwise dose response curves were plotted using maximal responses at each concentration of known ligand.

4.2.5 Nanobody Expression and Purification

TREK2 specific Nanobodies were manufactured in *Camelidae* and obtained from Structural Biology Brussels (Brussels, Belgium) in plasmid form (pMESy4). Nanobodies are heavy-chain only antibodies which are monomeric and much smaller than conventional antibodies, having a molecular weight of approximately 15 kDa.

The nanobody sequences are as follows:

Nanobody 1

QVQLVESGGGLVQAGGSLRLSCAASGRTSSTYAMSWFRQPPGKEREFVARIRWSGSNTYYADSV
KGRFTISGDNAKNTVYLQMNSLKAEDTAVYYCAAVIDPYSSAYEYWGQGTQVTVSSHHHHHHEP
EA

Nanobody 2

QVQLVESGGGLVQAGGSLRLSCAASGRTFSTYAMSWFRQAPGKEREFVARIRWSGTSTAYADSV
KGRFFISGDNAKNTVYLQMNSLKPEDTAVYYCAAVINPYSSAYEYWGQGTQVTVSSHHHHHHEP
EA

Nanobody 3

QVQLVESGGGLVQAGGSLRLSCAASGRTFSTYAMSWFRQAPGKEREFVARIRWSTTRTSSTYYAD
SVKGRFTISGDNAKNTVYLQMDSLKPEDTAVYYCAAVINPYSSAYEYWGQGTQVTVSSHHHHHH
EPEA

Nanobody 4

QVQLVESGGGLVQAGGSLRLSCAASGLTFSRYNMGWFRQAPGKEREFVAAINRYGGTMYATDS

VKGRFTISRDNVKSTVDLQMNRLKPEDTAVYYCAADQQYMSRLEADFGSWGQGTQVTVSSHHH
HHHEPEA

The plasmids were transformed into WK6 competent *E. coli* cells by heat shock and subsequently cultured overnight at 37°C in LB agar-containing petri dishes with 1:1000 ampicillin (100 mg per L).

A colony was then picked out and cultured in 5 ml of LB containing 100 µg/ml ampicillin overnight at 37°C. The culture was then added to 1L of fresh LB containing 100 µg/ml ampicillin and shaken at 37°C and at 180 rpm with monitoring of the OD600. When the OD600 reaches 0.8, 1 mM IPTG was added to induce the expression of the nanobody. The culture was then left overnight shaking at 180 rpm at 26°C.

The cells were harvested by centrifugation at 4000 rpm for 20 minutes and the pellets were lysed with a buffer containing 0.2 M TRIS pH 8.0, 0.5 mM EDTA, 0.5 M sucrose and 1% Triton X-100. The cell debris was then removed by centrifugation at 35,000g for 45 minutes and the supernatant was then taken and 1 ml of 50% Co^{2+} charged TALON resin was added per litre of cells used (Clontech, Takara Bio, Kusatsu, Shiga, Japan) and the mixture rotated at 4°C for 1h in an IMAC step. The resin was washed with 30 column volumes of wash buffer (50 mM sodium phosphate, 1M NaCl, pH 6 and eluted with wash buffer supplemented with 300 mM imidazole. The protein was then desalted with a PD10 column preequilibrated with wash buffer. The protein obtained was then flash frozen and stored at -80°C in 3 mg/ml, 1 ml aliquots for future use.

4.3 Results

4.3.1 Protein Purification

TREK1, TREK2 and SLC2A3 were purified using the methods described in Section 2.1. SEC profiles and SDS-PAGE of these proteins can be found in Sections 3.3.1 and 3.3.5. Multiple purifications were performed for all proteins and all protein was stored at -80°C prior to use. The His-tag was cleaved for ITC but not for SPR or BLI.

4.3.2: Isothermal Titration Calorimetry Shows Binding of Norfluoxetine to TREK2.

As the IC_{50} for the inhibition of TREK1 by norfluoxetine is known (9 µM) and there is structural evidence for the binding of norfluoxetine and TREK2, which is absent for all other known ligands of TREK2, norfluoxetine was selected as the tool compound with which to attempt optimisation of ITC with TREK2.

Prior to the experiment being conducted, a c-value of 10 was calculated to determine the amount of TREK2 and norfluoxetine to be used. Assuming the K_d of norfluoxetine to TREK 2 = IC_{50} of norfluoxetine on TREK1 and one binding site per monomer of TREK2, a protein concentration of 90 µM of TREK2 monomer was required. This corresponds to 1.41 ml of protein at a concentration of 3.0 mg/ml for a total of 4.25 mg of protein per experiment. In order to set the molar ratio of compound to protein at 2:1, norfluoxetine was injected at a concentration of 423 µM. The results of both the ITC experiment and the heat of dilution control can be seen in Figure 4.5 and 4.6.

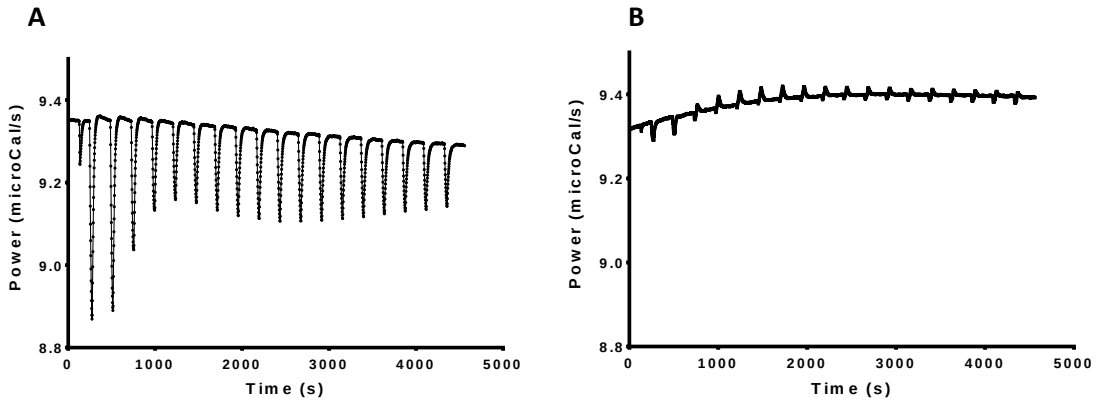

Figure 4.5: ITC of Norfluoxetine on TREK2 (A) and Heat of Dilution (B). *Norfluoxetine was added stepwise to a solution containing TREK2 protein and the resultant change in heat required to keep the cell at a constant temperature was measured and shown in Figure 4.5A. Heat of dilution ITC obtained by adding norfluoxetine stepwise to SEC buffer without added protein.*

The very low heat of dilution shows that the solutions are closely matched for detergent and salt concentrations. The heat of dilution is then subtracted from the ITC plot and curve fit was then attempted with partial results from Figure 4.5 and this is shown in Figure 4.6.

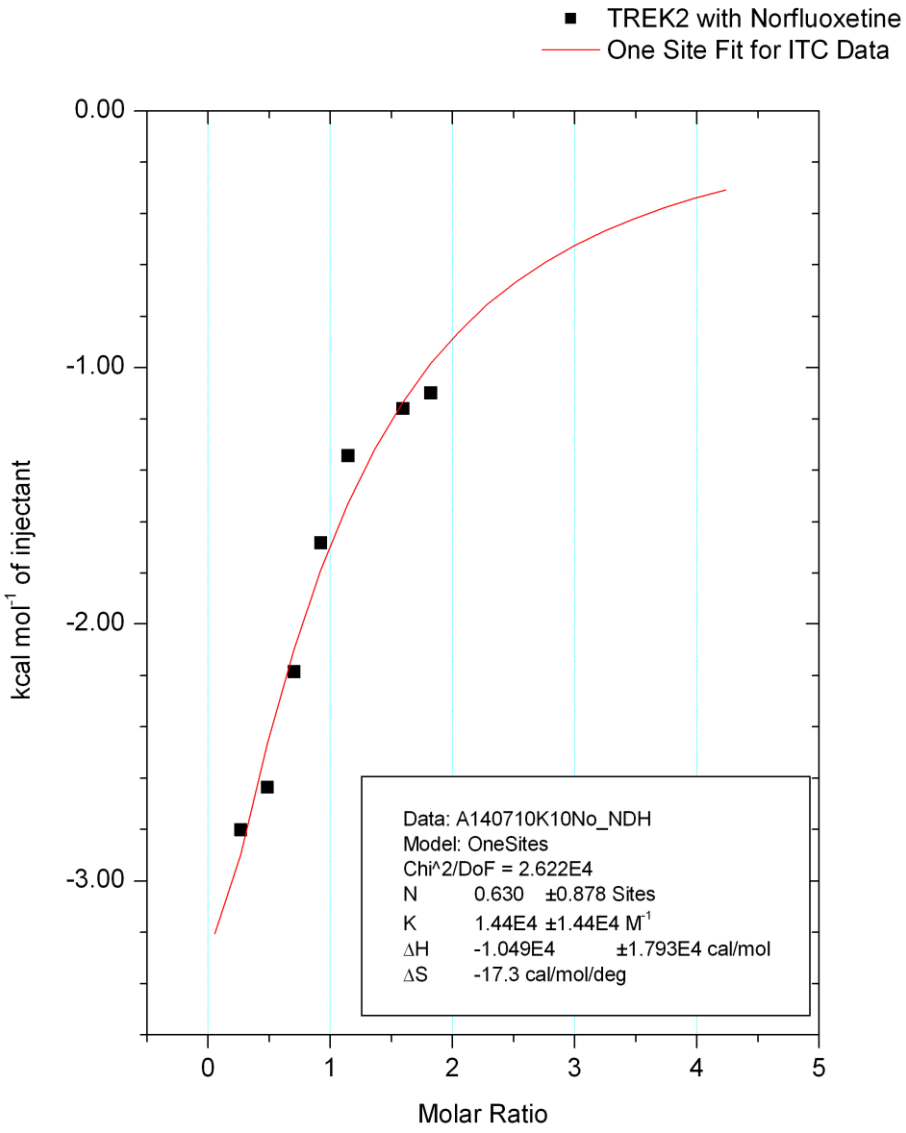

Figure 4.6: Curve fit attempt of ITC between TREK2 and Norfluoxetine. *A one site curve fit was attempted with the experiment described in Figure 4.5 with the exclusion of all points after stabilisation of response. The binding parameters obtained were shown in the figure and do not appear to be in the expected order of magnitude when compared to literature IC_{50} values. The values obtained also have very large errors and thus should not be used for analysis.*

However, as the binding does not appear to be saturated even at a molar ratio of 2:1 between norfluoxetine and TREK2 monomer, a binding curve could not be obtained and binding parameters could not be calculated for this interaction.The experiment was repeated twice with different purifications of TREK2 with similar results, with repeated

inability to obtain a binding curve despite clear evidence of binding between the protein and norfluoxetine. A further experiment was tried with double the concentration of norfluoxetine and TREK2 in an attempt to increase the c-value of the experiment to 20 but it was found that the heat of dilution was much larger in that set of conditions. Further optimisation with TREK2 and norfluoxetine or any other ligand was not carried out due to the experiment requiring too much protein and ligand to be economical. Other ligands also had solubility problems at the concentrations required even if their EC_{50} or IC_{50} were lower, such as penfluridol and BL1249. We thus decided to shelve the optimisation of ITC and focus on other techniques.

4.3.3: Effects of known ligands on TREK2 and GLUT3 as shown by SPR.

SPR was performed on purified TREK2 as well as GLUT3 as a control protein. Both proteins were immobilised using direct amine coupling to the surface dextran matrix of the CM5 chip. Immobilisation data is shown in Figure 4.7.

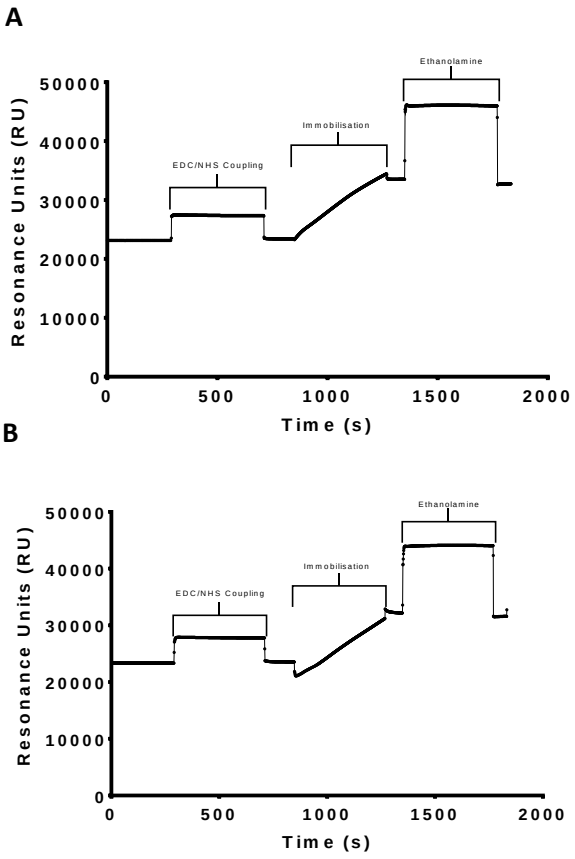

Figure 4.7: Immobilisation of the integral membrane proteins TREK2 and GLUT3 to a CM5 chip using direct amine coupling. *The final immobilisation responses were in the region of 8,000-11,000 RUs. Figure 4.7A shows the immobilisation graph for TREK2 while Figure 4.7B shows the immobilisation graph for GLUT3.*

Following immobilisation, compounds are passed through the chip at the concentrations of 1, 2, 4, 8, 16 and 32 µM in a dose response experiment. The compounds used were the known binders norfluoxetine, fluoxetine, BL1249 and penfluridol as well as the non-binder fenchol, which is a binder to TRPA1[172]. Sensorgrams of the experiments can be seen in Appendices 2 (for TREK2) and 3 (for GLUT3).

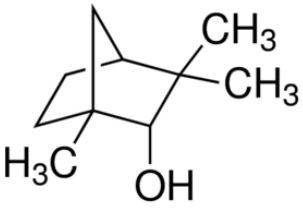

Figure 4.8: Chemical structure of fenchol, an activator of TRPA1 channels.

The remainder of the compounds were shown in Section 3.3.5.

The compounds were passed over the immobilised protein in ascending concentrations and washed after each flowthrough. The responses recorded with TREK2 are shown in Figure 4.9.

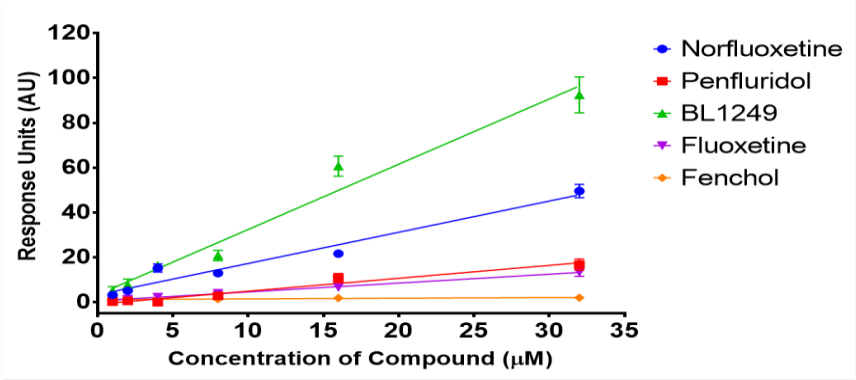

Figure 4.9: SPR dose response data of TREK2 with known binders and the non-binder fenchol. *All 4 known binders give a response which is dose sensitive with TREK2 immobilised on the CM5 chip, while there is no response with fenchol. All experiments were repeated with 2 replicates from 2 separate purifications of protein. Error bars represent the SEM of the measurements.*

The experiment was repeated with GLUT3 as the immobilised protein and the comparison between TREK2 and GLUT3 can be seen in Figure 4.10.

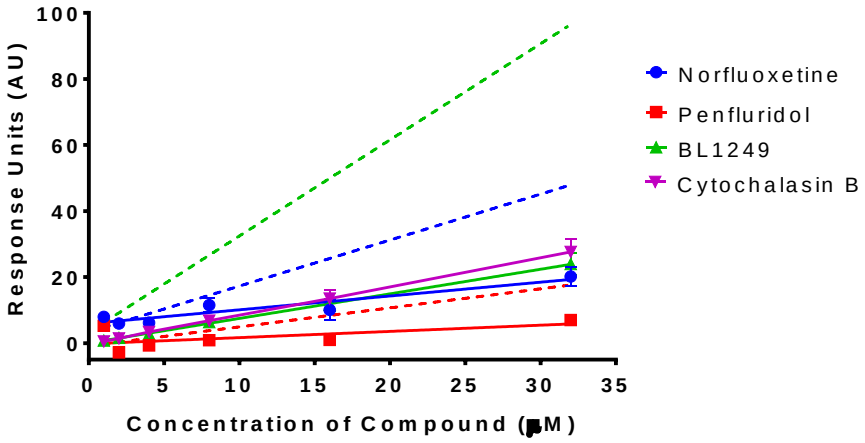

Figure 4.10: Comparison of dose-response data of TREK binders to TREK2 and GLUT3. *Concentrations of 1, 2, 4, 8, 16 and 32 µM compound were shown. Data for GLUT3 is in solid lines after fitting to best fit and TREK2 data, which was shown in Figure 4.8, is shown here as dotted lines. Error bars are shown as the SEM of the measurements. 2 biological replicates with different preparations of GLUT3 were tested.*

In all three cases, there is a much greater response of TREK binders to TREK2 than GLUT3 across most concentrations of compound. This is more apparent at higher concentrations as all three compounds are micromolar binders to TREKs and concentrations below 8 µM would be below their IC_{50} or EC_{50} in some cases.

In addition, a known binder of GLUT3 was also flowed through a chip, which contained immobilised GLUT3 as a positive control. The binder was cytochalasin B, a cell-permeable mycotoxin that also inhibits glucose transport through all GLUT transporters[173]. The dose response curve for this is shown in Figure 4.10.

Cytochalasin B has a dose dependent response on the SPR with GLUT3 immobilised on the chip. This effect did not saturate even at 64 µM and there was no significant binding to a chip which did not contain any protein.

4.3.4: Known Ligand Effects on TREK2 and TREK1 as Shown by BLI

We next investigated the use of biolayer interferometry with the known binders norfluoxetine and penfluridol on TREK1 and TREK2. Concentrations of 1, 2, 5, 10, 20 and 50 µM of both compounds were used with TREK1 and TREK2 immobilised on a Ni-NTA sensor. immobilisation data is shown in Figure 4.11.

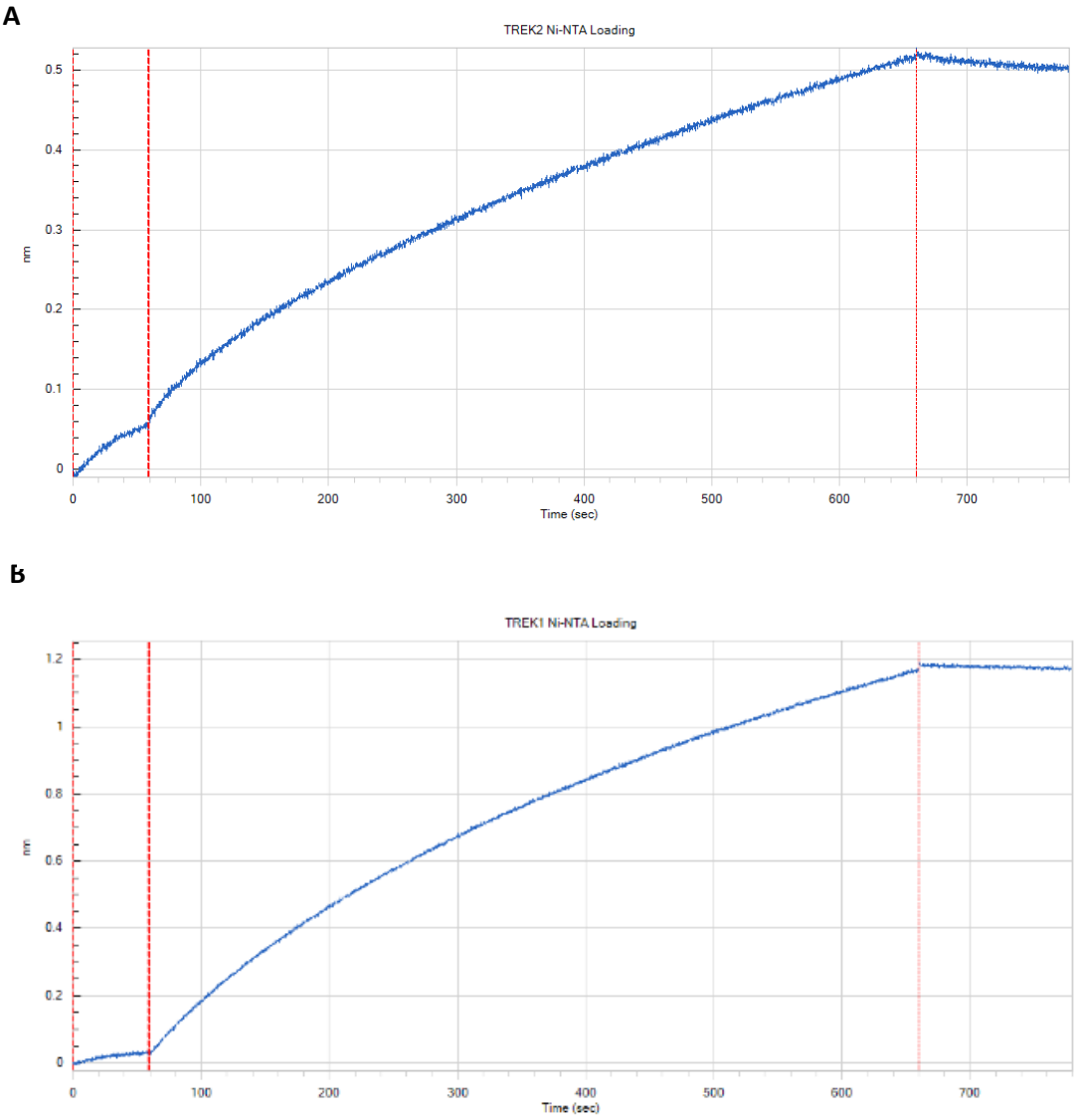

Figure 4.11: Immobilisation onto Ni-NTA sensor of TREK2 (A) and TREK1 (B).

Both proteins immobilised successfully onto biosensors coated with Ni-NTA.

Figures 4.12 and 4.13 shows the sample plate layout and the dose response data for the interaction of norfluoxetine and penfluridol with the TREK proteins.

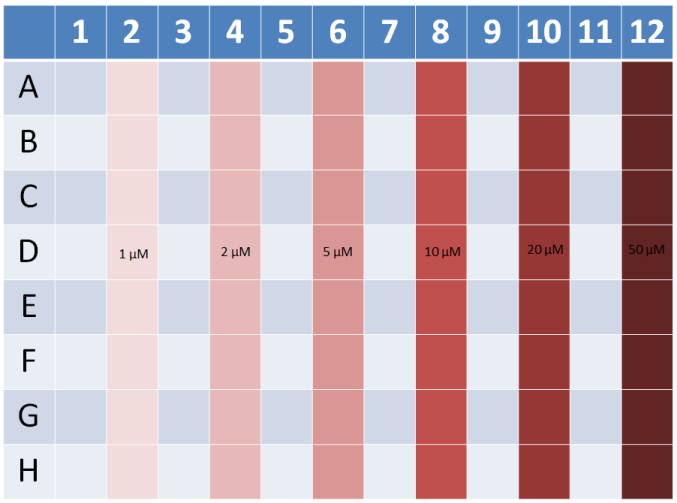

Figure 4.12: Sample Plate Layout for Biolayer Interferometry. *The concentration shown were those of the target compound while blue wells represent SEC buffer without any compound.*

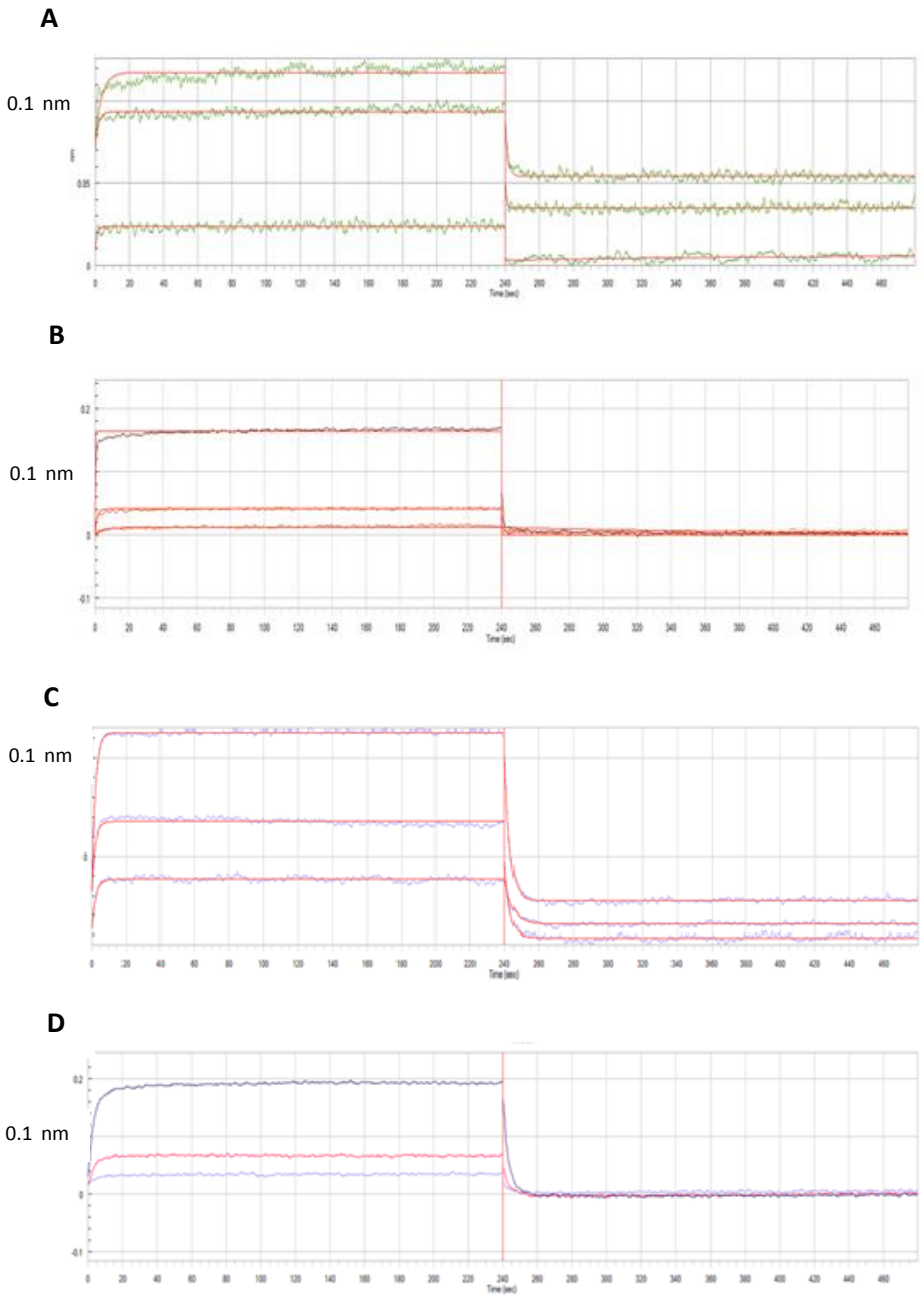

Figure 4.13: Biolayer Interferometry of TREK-2 and TREK-1 with norfluoxetine and penfluridol. A: TREK-2 with Norfluoxetine. B: TREK-1 with Norfluoxetine. C: TREK-2 with Penfluridol. D: TREK-1 with Penfluridol. *Sensors with bound His-tagged TREK-1 or TREK-2 were dipped into solutions containing differing concentrations of norfluoxetine or penfluridol for 4 minutes, then into buffer solutions without compound for a further 4 minutes and the change in absorption wavelength of the complex measured. The graphs represents the change in light absorption wavelength of the complex (nm) against time. The 3 traces on each graph represent the signal produced from 50 µM, 20 µM and 10 µM of compound interaction with protein immobilised on a Ni-NTA sensor (in all cases from top to bottom).*

There is a dose response correlation between the amount of change in absorption wavelength and the amount of compound bound to the sensor. However, when the experiments were performed without protein bound to the sensor, it was found that norfluoxetine and penfluridol also bound directly to the sensor, as seen on Figure 4.14.

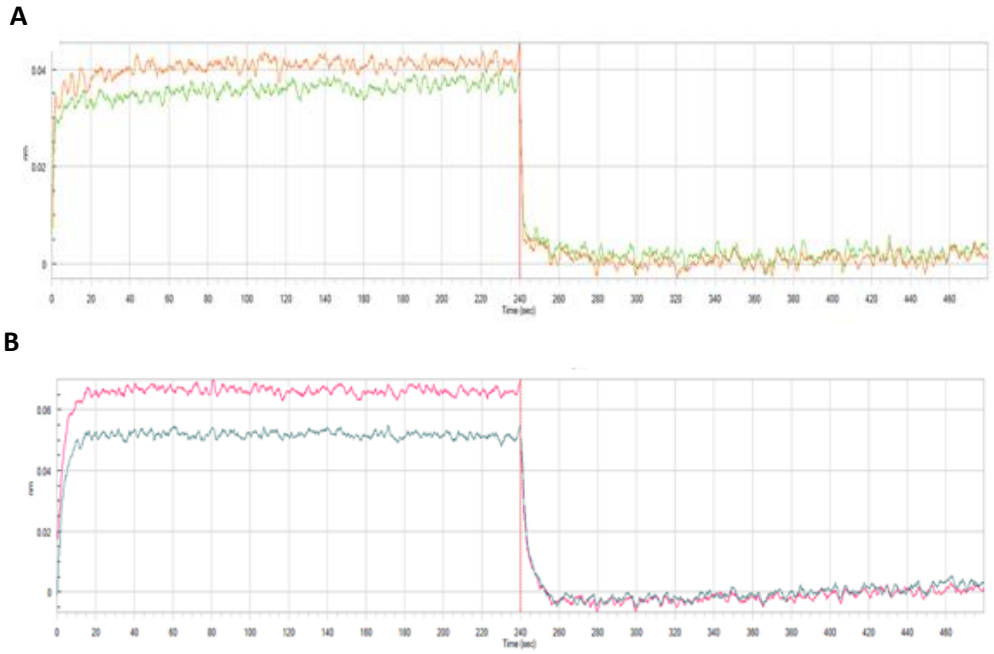

Figure 4.14: Compound-only Control Traces with BLI. *Sensors bound to His-tagged TREK-1 and without bound protein were dipped into solutions containing 20 µM norfluoxetine (Figure 4.14A) or 20 µM penfluridol (Figure 4.14B) for 4 minutes, then into buffer solutions without compound for a further 4 minutes and the change in absorption wavelength of the complex measured. The y-axis represents the change in light scattering wavelength (nm). The 2 graphs represent the signal produced from 20µM norfluoxetine with TREK-1 immobilised on a Ni-NTA sensor and the experiment repeated without protein as a control on the same plate from top to bottom.*

With the interference caused by the compounds, the signal caused by this needs to be subtracted from the signal obtained from compound binding to protein and this reduces the response obtained greatly and compromises the usefulness of this method in detecting protein-compound interactions. This technique was therefore not useful for working with either of these known ligands. BLI is however known to be useful for detecting interactions between proteins, so we next tested the use of BLI for this purpose.

4.3.5 Nanobody Purification and the use of Biolayer Interferometry to detect Protein-Protein Interactions with TREK2

In addition to testing BLI as a method for detecting small molecule binding to TREK2, we also tried to use it as a method to detect protein-protein interactions.

Four nanobodies specific to TREK2 were purified with IMAC. The nanobodies were run through a SEC column to check for monodispersity and the gel filtration profile can be seen in Figure 4.15.

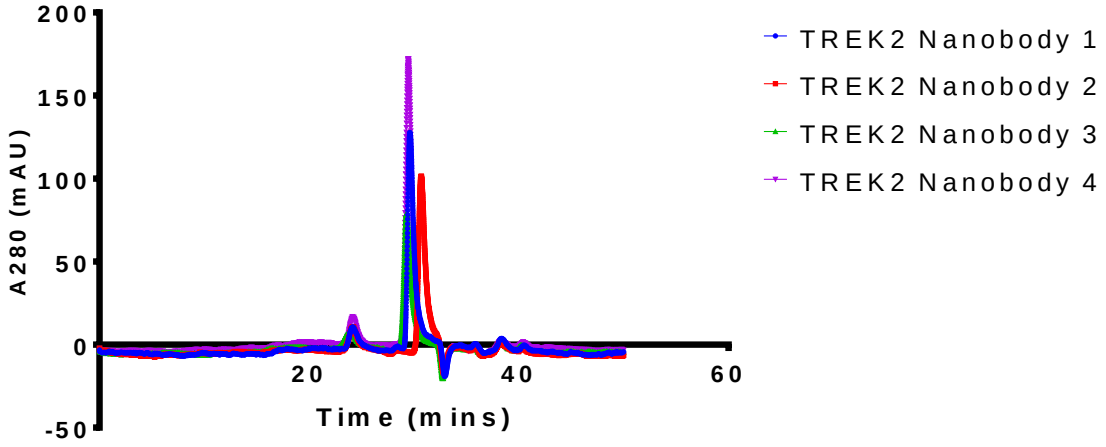

Figure 4.15: SEC profile of all TREK2 nanobodies. *Purified nanobodies were loaded onto a Superose 6 5/150 column and the A280 recorded. All 4 nanobodies purified were monodisperse.*

In order to check for binding with the target protein TREK2, the nanobodies were then bound to the Ni-NTA sensors with their His-tag. The loading profile of the 4 nanobodies is shown in Figure 4.16.

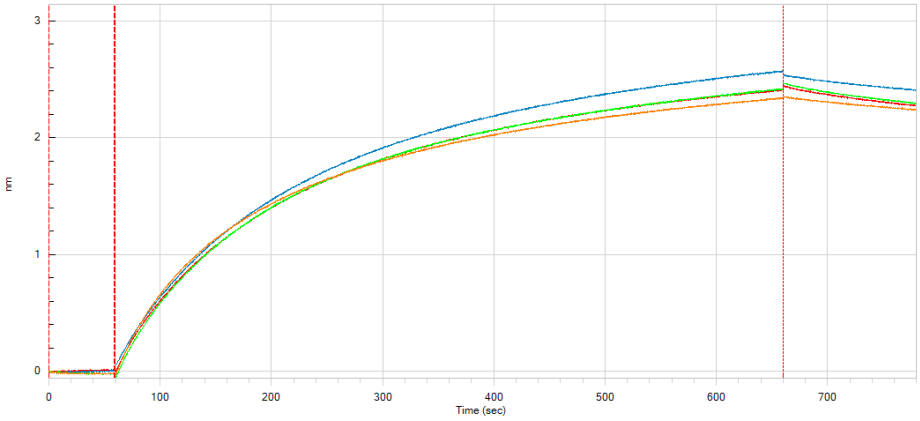

Figure 4.16: Immobilisation of TREK2 Nanobodies. *Nanobodies were immobilised to Ni-NTA sensors over 600 seconds. The 4 graphs represent the 4 different TREK2 nanobodies which were immobilised. (Blue: Nanobody 1, Red: Nanobody 2, Cyan: Nanobody 3, Orange: Nanobody 4).*

Following loading of the nanobodies, they were dipped into solutions containing 0.1 mg/ml (3 µM) of protein. Figure 4.17 shows the binding of the nanobodies to TREK2 and TREK1.

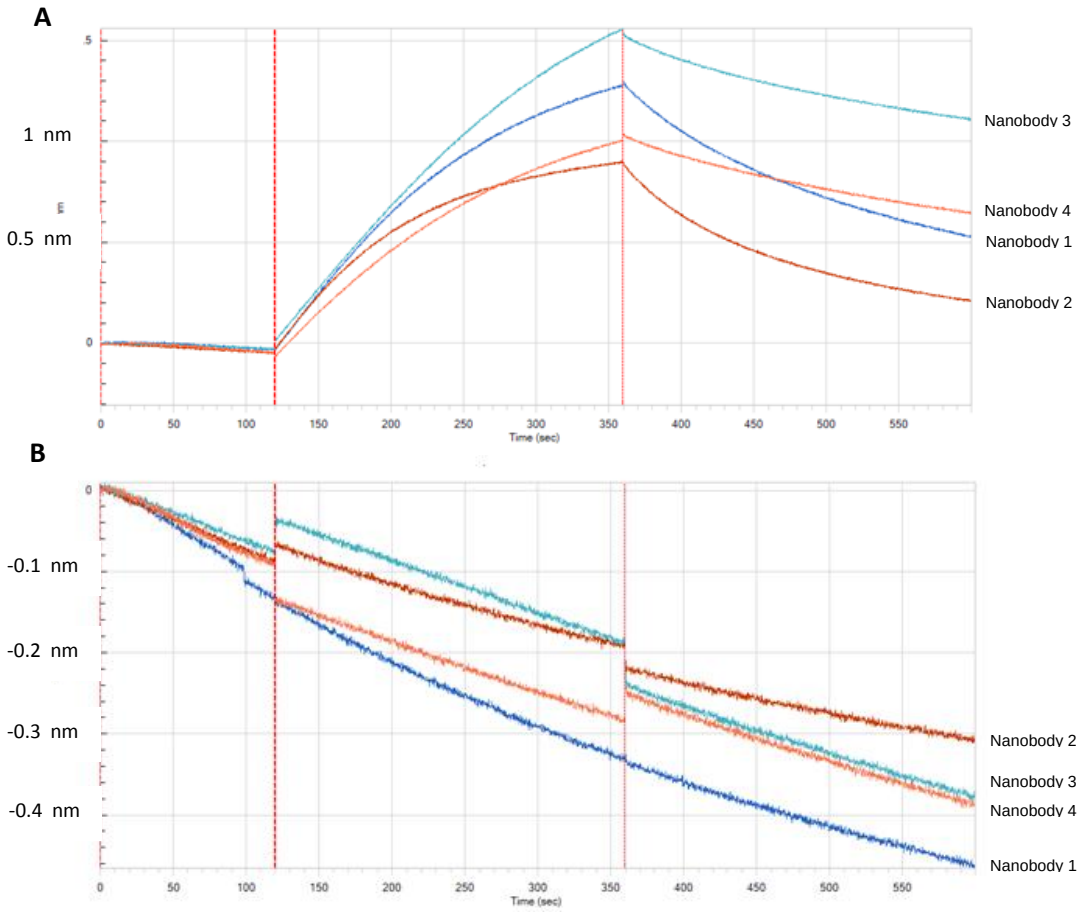

Figure 4.17: Nanobody binding to TREK2 and TREK1. *Sensors with bound His-tagged nanobodies and without bound protein were dipped into solutions containing 3 µM TREK2 (Figure 4.17A) or 3 µM TREK1 (Figure 4.17B) for 4 minutes, then into buffer solutions without compound for a further 4 minutes and the change in absorption wavelength of the complex measured. The y-axis represents the change in light scattering wavelength (nm). The 4 graphs represent sensors immobilised with 4 different nanobodies (Blue: Nanobody 1, Red: Nanobody 2, Cyan: Nanobody 3, Orange: Nanobody 4).*

The nanobodies are shown to bind to TREK2 by biolayer interferometry and are specific to this protein, with no binding observed when TREK1 was used instead. This experiment was repeated with a different purification of TREK1 and TREK2 with the same conditions and similar results were observed.

4.4 Discussion

4.4.1: Suitability of ITC for Analysis of Ligand Interactions with TREKs and Implications of Results.

The use of ITC and SPR to detect protein-ligand interactions in soluble proteins and some classes of membrane proteins is well-known. This work attempts to evaluate the use of these methods with the TREK2 potassium channel.

The challenges of using ITC with membrane proteins are the result of the lack of purified protein and complications arising from the inaccuracies in the determination of detergent concentration. This is because ITC is very sensitive to differences in buffer between the two solutions in the test and control chambers. We were unable to completely eliminate the buffer mismatch, but did minimise it enough to see an indication of binding between TREK2 and norfluoxetine. Further experiments were not performed due to two reasons:

1. The lack of stronger binders to TREKs. The amount of protein required to maintain a given C-value in an ITC experiment is directly proportional to K_d of the ligand. As the strongest binders we currently have are only micromolar in affinity, the experiments would require very large amounts of protein to perform and are it is thus very costly and time consuming to prepare the protein samples for this usage. Solubility of compounds in SEC buffer is also an issue if high concentrations of compound is required.
2. Buffer mismatch problems: Even though this was minimised, it was not completely eliminated and for future experiments to be more accurate and a K_d to be determined, this problem has to be solved. Further optimisation would be very costly in time and resources and was thus not attempted.

A possible improvement to this set of experiments would be to attempt to miniaturise the assay, using the Nano-ITC which uses only 200 µl of solution in the cell instead of 1.4 ml for the VP-ITC. This method is however even more sensitive to buffer mismatch and extensive optimisation would have to be carried out before accurate results could be obtained.

As ITC is a definitive method to assess binding between proteins and ligands which can be both quantitative and qualitative, it should still be used even with some buffer mismatch as an orthogonal assay to complement the fluorescent assays discussed in Chapter 3. However, as it is low-throughput and uses very large amounts of protein, it should be used late in the workflow and only on compounds which were shown by other methods to be strong potential binders. Functional assays could also be performed with the compound before ITC is used.

4.4.2: Suitability of SPR and BLI for Analysis of Ligand Interactions with TREKs and Implications of the Results.

SPR and BLI have been used as medium-throughput methods for the detection of protein-ligand binding through changes in the refraction of light. In this work, SPR has been shown to be able to detect binding between TREK2 and a range of known binders and this effect was shown to be specific at least to some extent as the compounds do not give a large response with GLUT3, an unrelated protein. A positive control with cytochalasin, a GLUT3 binder was also performed and that gave a much larger response at similar concentrations to all the TREK binders.

BLI was shown to be not definitively able to detect binding between TREK2 and the known binders norfluoxetine and penfluridol as the 2 compounds also gave a signal

without the protein being bound to the sensor. This implies that there is insufficient signal to noise ratio for this technique with either small molecule.

BLI however, was able to detect the binding between TREK2 and nanobodies specific to this protein, also showing them to be specific against the closely related TREK1 protein. This is because of the much larger change in mass caused by the protein binding to the nanobody attached to the sensor, as compared to small molecule binding. Protein binding therefore gives a much larger signal.

The main challenge with these methods is that small molecules are at or near the limit of sensitivity for SPR and BLI. The signals caused by the binding of small molecules to proteins are minuscule compared to those caused by protein-protein interactions, which both techniques were originally designed to detect. Both techniques are also not high-throughput, making them unsuitable for initial screening of compounds. Also, biolayer interferometry requires one of the interacting partners to be tagged so it can be immobilised onto a sensor and this labelling may cause binding sites to be occluded, leading to possible false negatives.

There were also two large caveats to the results for SPR. Firstly, the signal with SPR did not saturate even at 32 μM of compound for any compound, making the determination of K_d not possible and thus incomplete characterisation of binding was obtained in these experiments. The other problem is that the signal produced by the binding of BL1249 to norfluoxetine is higher than the calculated theoretical maximal signal of about 57 RUs at the highest concentration tested. This suggests non-specific binding or interactions between the compound and the chip surface, which is a large confounding factor in the assay. The non-saturation of signal with other compounds also suggests non-specific binding, which is directly proportional to the amount of protein and compound and does

not fit a one-phase binding curve. Higher concentrations of compounds were not used due to their effect on the pH of the running buffer and noise caused by compound binding to the dextran matrix on the gold foil chip. In these experiments BLI was also not able to provide a K_d for any compound due to the noise issues of compounds interacting directly with sensors.

Compared with ITC, both methods use much less protein and compound and are thus much more economical to perform. Both methods can also be improved to be carried out at higher throughput, with the Fortebio Octet being able to be configured for use with 384 well plates and the Biacore T200 as well as other competitor setups now being able to run multiple SPR experiments in parallel.

4.5 Conclusion

The above work shows that although SPR and ITC were able to detect binding of known ligands to their target proteins, they each have major drawbacks and are much lower throughput than DSF and label free DSF. One caveat with this work is that the ligands tested have relatively low affinity as they are in the micromolar range. It would be valuable to test a series of nanomolar binders for the TREKs once such ligands are available. SPR and BLI should thus only be considered as orthogonal verification assays, perhaps only for ligands with high affinity, to confirm and further characterise binding between protein and potential ligands found through DSF.

Chapter 5: Screening of a Small Compound Library to Identify Novel Binders for K2P Potassium Channels.

5.1 Introduction

5.1.1: Proposed Workflow for the Screening of K2Ps against Unknown Compounds to Identify Potential Binders

The proposed cascade for the screening of TREKs against a library of compounds starts from the highest throughput biophysical method and uses lower throughput methods as validation assays. In Chapter 3 of this work, I demonstrated that the CPM thermal shift assay is robust and reliable, with a high Z' factor and can be used as a primary screen. Following that, label-free DSF was used as an orthogonal validation assay as it targets a different residue within the protein and does not use the fluorescent dye, which is a potential source of interference. In order to validate the hits obtained in this assay a small set of compounds were tested for their effects on the function of TREK1 and TREK2 using electrophysiology, as described in chapter 6. The proposed screening cascade is thus as follows:

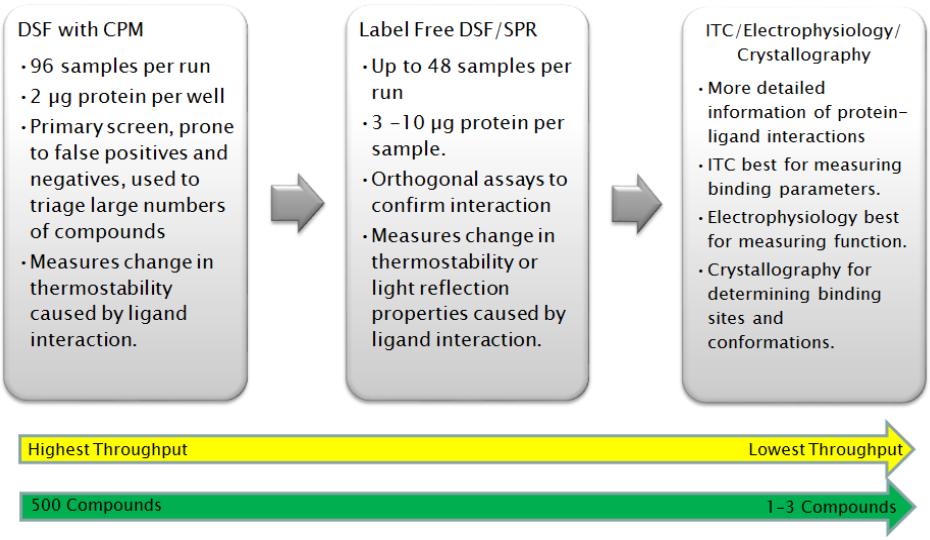

***Figure 5.1: Proposed Screening Cascade**. This screening cascade uses thermostability methods with highest throughput as primary and secondary screens. Lower throughput methods that can measure function or direct binding were used for validation of earlier hit compounds.*

In this work, a commercial library of FDA-approved compounds from Selleck Chemicals, (Houston, TX, USA) was taken as the starting point for compounds and a representative subset of 351 compounds were selected based on their diversity of chemical structures, lack of free sulphur residues and solubility in SEC buffer. These compounds are then screened with the CPM assay (DSF) and prospective hits validated with Label-free DSF. Five membrane proteins were screened in total, including the two TREKs (TREK1 and TREK2), two other members of the K2P family (TWIK1, TASK1) and an unrelated solute carrier, the sugar transporter GLUT3.

5.2 Materials and Methods

5.2.1 DSF Compound Screening

The Selleck Chemical FDA-approved Drug library was available at the SGC, stored at -20°C, dissolved in DMSO at a concentration of 10 mM. The selected compounds were transferred to four 96-well Corning plates (Sigma-Aldrich, Darmstadt, Germany. A Labcyte ECHO 550 liquid handler (Labcyte, Sunnyvale, CA, USA) was used to transfer a volume of 40 nl of each compound to the 96 well plates. The final concentration of each compound in the assay was 20 µM. Controls are manually pipetted in at the relevant concentrations dissolved in the SEC buffer of the target protein as shown in Section 5.3.2.

Protein was then added at a final concentration of 1 µM and volume of 20 µl directly to the plates containing the compounds. The protein-compound mix was then incubated for 1 hour and then 5 µl of 0.04 mg/ml CPM was added. The plate was then put into a RT-PCR machine and a heating protocol was run described in Section 3.2.1.

The results were analysed by fitting to a Boltzmann sigmoidal curve as described in Chapter 3 using Graphpad Prism 6.0. Melting points of the proteins were determined as the y-value of the inflection point of the fitted Boltzmann sigmoidal curve (V_{50} value), which fits the logistic equation described in Section 3.1.1.

5.2.2 Label Free DSF

The compounds that were identified as potential hits, and a range of control compounds, were purchased from various suppliers as described in Section 5.3.5 and dissolved in DMSO at a concentration of 10 mM. The stock was then diluted to 100 µM with the relevant SEC buffer to create a secondary stock solution. This stock solution

was then added to diluted protein solution to create a solution with a final concentration of 0.1 mg/ml protein (approximately 3 μM for all K2Ps, 2 μM for GLUT3) and 20 μM compound. The protein-compound mixtures were then incubated for 1 hour. Capillaries were then filled and inserted into the Nanotemper Prometheus instrument by dipping them into the solution and allowing for capillary action. The protocol for the label-free DSF run was as described in Section 3.2.2.

The data obtained was analysed by taking the inflection point of the first derivative of the 330 nm wavelength response and averaging this melting point of the protein across 2 or 3 biological replicates. A T_m shift value was then calculated.

5.3 Results

5.3.1 Protein purification

TREK2, TREK1, TASK1 and GLUT3 purification was discussed in Chapter 3. TWIK1 is a member of the K2P family and its structure and function have been covered briefly in Chapter 1. TWIK1 was purified in LMNG/CHS and the purification method can be found in Section 2.2.

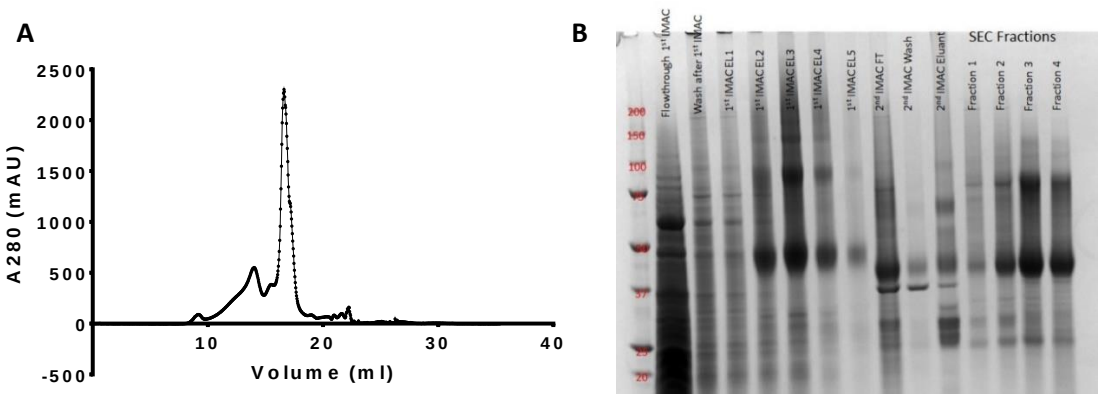

Figure 5.2: SEC profile(A) and SDS-PAGE(B) for the purification of TWIK1. *The SEC profile of TWIK1 contained 1 main peak which was collected for all future experiments. In the SDS-PAGE, TWIK1 has 2 distinct bands, which correspond to the monomer (Lower MW) and dimer (Higher MW) of the protein. Lanes labelled IMAC refer to 1 ml fractions eluted after affinity chromatography.*

The thermostability of TWIK1 was measured using the CPM assay and it was found to have a melting point of 39-42°C.

5.3.2 DSF Screening of TREKs with 351 Compounds from the Selleck FDA-Approved Drug Library

All proteins were screened against the Selleck FDA-approved drug library available from the Target Discovery Institute. The screen was available as a 10 mM stock solution of all compounds and contained 1119 compounds. 351 compounds were selected for initial screening against a range of proteins. This is to ensure the entire subset fits into 4 X 96 well plates with 8 control wells on each plate. The breakdown of both the full screen and the 351 selected compounds is shown in Table 5.1:

Target or Pharmaceutical Usage	No. of Compounds in Full Screen	No. of Compounds in Selected Subset
Kinase Inhibitor	30	5
Steroid Analogue	74	11
Antibiotic	148	23
Antifungal	24	8
Antihelmintic/Antiparasitic	23	4
Anticancer	50	20
Nucleic Acid Analogue	45	6
Antiviral	35	10
Calcium Channel Blocker	19	9
Other ion channel blocker/activator	22	17
Antipsychotic	23	13
Antidepressant	23	14
Dopaminergic Transmission	16	8
5HT Receptor Agonist/Antagonist	17	8
Cholinergic Transmission	45	14
Adrenoceptor Agonist/Antagonist	61	25
Non-steroidal anti-inflammatory drug	68	16
Folate Analogue	5	2
Antioxidant	7	4
Immunosuppressant	17	7
Platelet Inhibitor/Anticoagulant	16	8
Anti-allergic	9	2
Anti-diabetic	25	12
Anti-hypertensive	35	8
Anaesthetic	18	5
Phosphodiesterase Inhibitor	14	7
Renin-Angiotensin system	15	3
Anti-histamine	25	8
Others	210	74

Table 5.1: Breakdown of Selleck FDA-Approved Drug screen by compound function, both with the full screen and subset selected for DSF testing with K2Ps.

To determine the 351 compounds picked, the following 4 criteria were applied:

1. Compounds with sulfhydryl groups (-SH) were excluded due to their potential interaction with the CPM dye.
2. Structural repetition was avoided where possible. e.g. only 1 estrogen analogue and one taxol derivative was picked for screening. This was performed by visual

analysis of the compounds. The structures of the compounds can be seen in Appendix 6.

3. Compounds which were too difficult to further develop as improved binders were avoided, such as talcum powder and others containing heavy metals. Such compounds are very unlikely to be useful for targeting the TREK channels in physiological conditions.
4. Given the known binders and tissue distribution for TREKs, a greater proportion of ion channel binders and neuroactive compounds were selected.

A flowchart of the triaging process is shown in Figure 5.3 below. The triaging was performed manually.

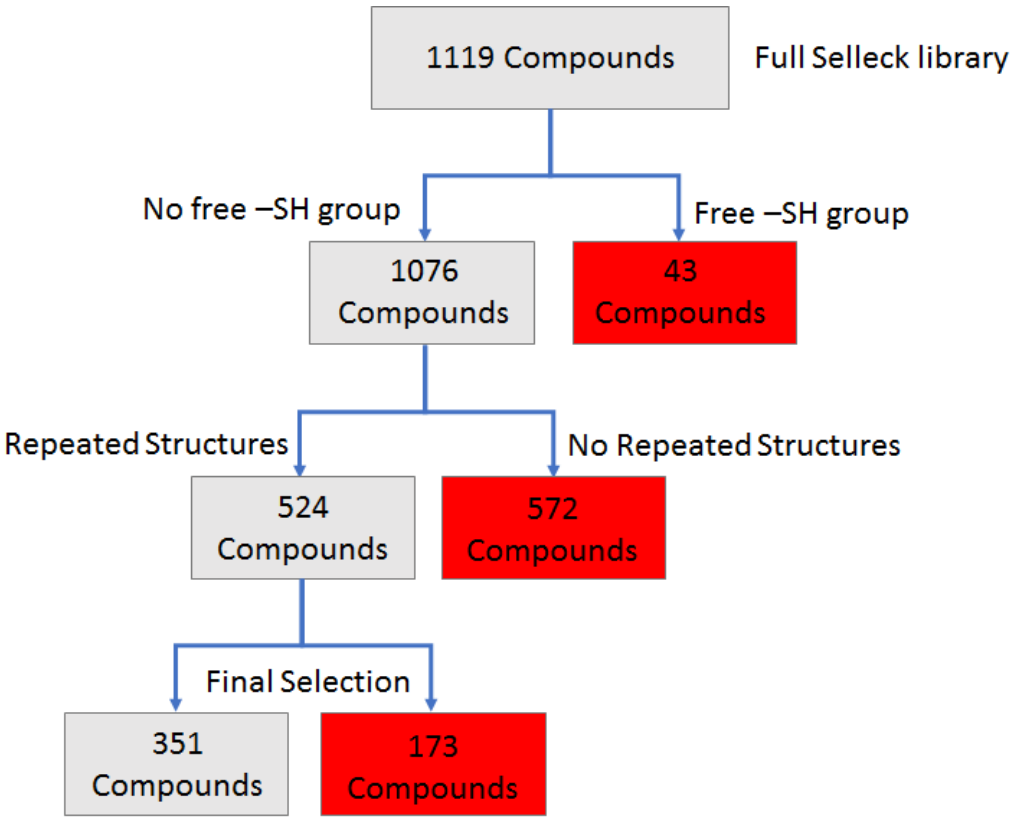

Figure 5.3: Flowchart of compound triaging to create mini-library for screening of FDA-approved drug library. *Compounds were triaged based on the criteria described above. The final selection is based on compound properties such as solubility, drug-like characteristics and also an overall skewing of the remaining compounds towards those which target neurological or ion channel targets.*

The 351 compounds were then laid out in a predetermined order based on their original plate locations in four 96-well plates. The plate layout is shown in Figure 5.4:

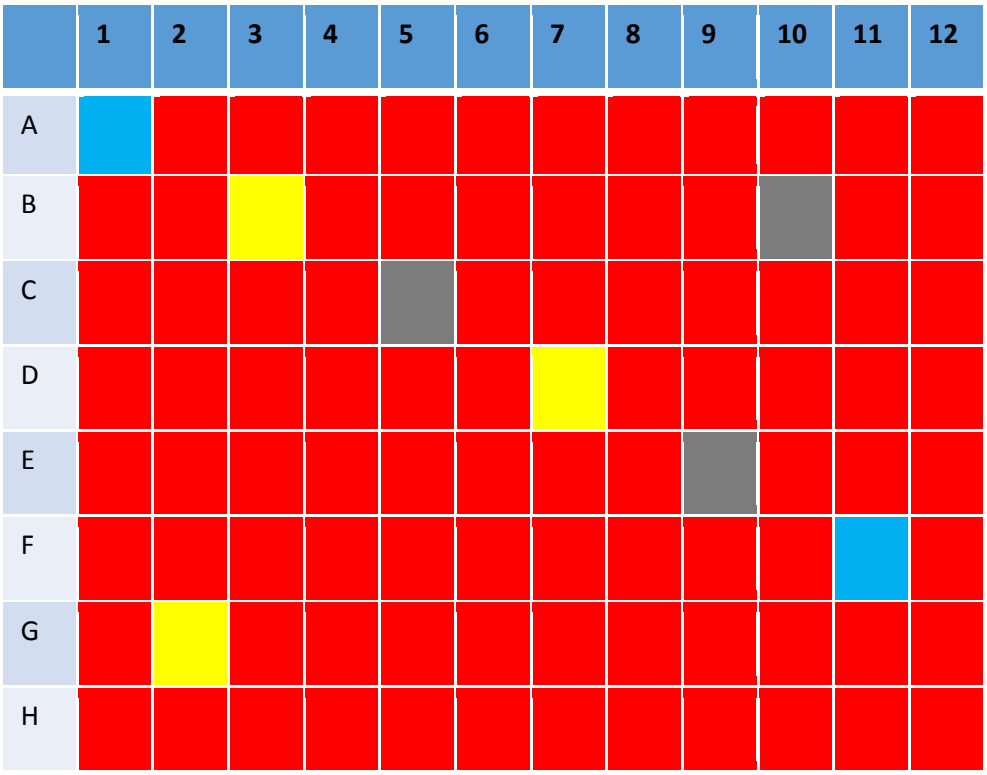

Figure 5.4: Selleck FDA Approved Drug Screening Plate Layout for CPM assay. *All compounds are screened at 20 µM and are placed in wells coloured red. Blue wells are for DMSO Control (1% DMSO in SEC buffer of the protein to be screened), yellow wells for a stabiliser control (BL1249 for TREKs and TASK1, 1% DMSO control for GLUT3 and TWIK1 as no suitable stabilisers were available for use) and grey wells for a destabiliser control (Penfluridol for TREKs and TASK1, 1% DMSO control for GLUT3 and TWIK1 as no suitable destabilisers were available for use).*

The controls chosen were penfluridol and BL1249 for TREKs in accordance to that from the Z' factor test, discussed in Section 3.3.3. Eight buffer controls were used instead for the non-TREK proteins as these were not the focus of this work and the ligands for these proteins were not previously extensively tested for thermostability effects. The positive and negative controls worked as expected, with 20 µM BL1249 stabilising TREK2 and TREK1 by 3.07 ± 0.52°C and 2.00 ± 0.23°C respectively. 20 µM penfluridol destabilised TREK2 and TREK1 by 1.93 ± 0.11°C and 2.36 ± 0.36°C respectively.

In total, 3 repeats of the screen were carried out with both TREK1 and TREK2 with different preparations of the same protein constructs. In both cases, the protein was purified in the presence of DDM and the construct used was the crystallisation construct defined in Chapter 2. The cutoff for a compound to be identified as a stabiliser or a

destabiliser is a T_m shift of ±1.5°C. This T_m shift is an arbitrary cutoff positioned at about 3 standard deviations from a repeated measurement of thermostability (See Section 3.3.5). This would ensure a 99.7% probability that the change in thermostability did not occur by random chance. The statistics for the screening of TREKs are shown in Table 5.2:

Action of Compound	Results for TREK2	Results for TREK1
No Effect	274 (78.1%)	276 (78.6%)
Stabiliser in 1 Screen	36 (10.3%)	21 (6.0%)
Stabiliser in 2 Screens	3 (0.9%)	6 (1.7%)
Stabiliser in 3 Screens	5 (1.4%)	9 (2.6%)
Destabiliser in 1 Screen	19 (5.4%)	29 (8.3%)
Destabiliser in 2 Screens	8 (2.3%)	5 (1.4%)
Destabiliser in 3 Screens	6 (1.7%)	5 (1.4%)

Table 5.2: Summary of Screening Results for TREKs. Significant numbers of compounds had a stabilising or destabilising effect on both TREK1 and TREK2. However, only a small number of compounds had consistent effects on multiple preparations of both proteins.

Following the screening, the number and identity of stabilisers and destabilisers that have an effect on at least 2 out of the 3 preparations of protein were determined. Figures 5.5 and 5.6 show the degree of overlap between compounds that appear to stabilise or destabilise TREK1 or TREK2 as well as their identities.

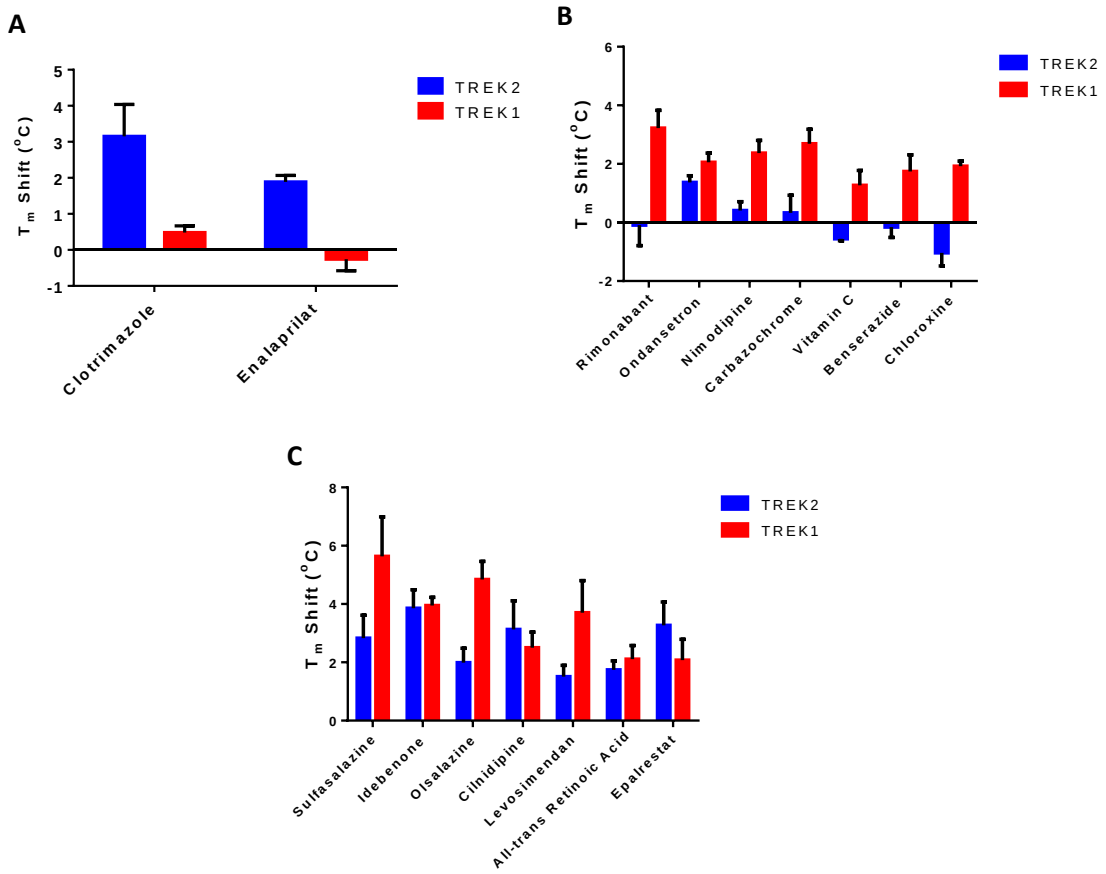

Figure 5.5: Stabilisers of TREKs as detected by screening of the Selleck FDA-approved Drugs Library. *There are 7 compounds which appear to stabilise both TREKs and an additional 9 which stabilise either TREK1 or TREK2. Figure 5.5A shows compounds which stabilise TREK2 but not TREK1, figure 5.5B shows compounds which stabilise TREK1 but not TREK2 and figure 5.5C shows compounds which stabilise both TREKs. Only compounds which stabilise the protein in at least 2 out of 3 screens are shown. Error bars show the SEM for each compound.*

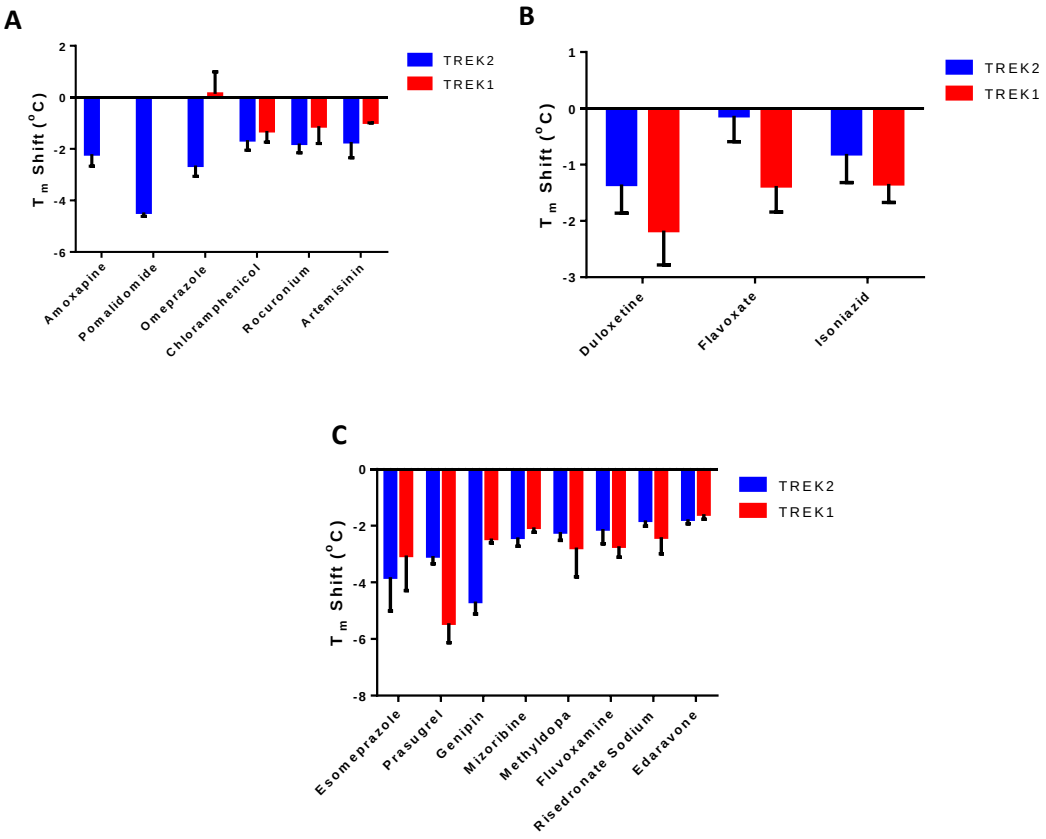

Figure 5.6: Destabilisers of TREKs as detected by screening of the Selleck FDA-approved Drug library. *There are 8 compounds that appear to destabilise both TREKs and an additional 9 that destabilise either TREK1 or TREK2. Figure 5.6A shows compounds which stabilise TREK2 but not TREK1, figure 5.6B shows compounds which stabilise TREK1 but not TREK2 and figure 5.6C shows compounds which stabilise both TREKs. Only compounds which stabilise the protein in at least 2 out of 3 screens are shown.*

From the results shown, there is significant but not complete overlap in compounds that appear to affect the thermostability of TREK1 and TREK2. However, this may not be due to the sequence and structure similarity between the proteins, but instead be due to compound interaction with the dye or other components of the assay. The sequence alignment for the constructs tested can be seen in Appendix 1. Notably, all 4 transmembrane helices are highly conserved between these 2 proteins. Given the known binding site of norfluoxetine is between the M2 and M4 helices of TREK2, it is highly likely that that binding pocket is highly conserved between the 2 proteins. In order to further

explore the specificity of the interactions between compounds and the 2 proteins, screening was performed with the related K2P channels TWIK1 and TASK1, and the unrelated solute carrier GLUT3.

5.3.3 DSF screening of GLUT3 with Compounds from the Selleck FDA-Approved Drug Library

GLUT3 is a solute carrier protein which is unrelated to the K2P ion channels. Its function has been discussed in Chapter 3. It was chosen as a control protein for this screening as the optimal SEC buffer for the purification of this protein also contains the detergent OGNG with CHS. This minimises the effect of changing the detergent on the assay and would eliminate compound-detergent interaction changes due to switching detergents.

The plate layout and screening protocol for GLUT3 was identical to that of the K2Ps, except that only two biological replicates were performed instead of 3 with the TREKs. The results are summarised in Table 5.3.

Action of Compound	Results for GLUT3
No Effect	339 (96.6%)
Stabiliser in 1 Screen	7 (2.0%)
Stabiliser in 2 Screens	3 (0.9%)
Destabiliser in 1 Screen	2 (0.6%)
Destabiliser in 2 Screens	0 (0%)

Table 5.3: Summary of Screening Results for GLUT3. Overall, there is a much smaller number of compounds that stabilise or destabilise GLUT3 when compared to TREK1 or TREK2. Notably, there are no destabilisers which have effects on both preparations of GLUT3.

As there are very few compounds that change the thermostability of GLUT3, all 12 compounds that either stabilised or destabilised GLUT3 on the DSF assay are shown in Table 5.4, which details the overlap between these compounds and those that stabilise or destabilise TREK1 or TREK2.

GLUT3-only Stabilisers	GLUT3-only Destabilisers	GLUT3 and TREK1/2 Stabilisers	GLUT3 and TREK1/2 Destabilisers
Ipratropium	Oxalaidin	Sulfasalazine	Duloxetine
Bentiromide		Olsalazine	
Tolperisone		Idebenone	
Azaperone		Levosimendan	
		Epalrestat	
		All-trans Retinoic Acid	

Table 5.4: Stabilisers and Destabilisers of GLUT3 and overlap with those that interact with TREKs. There is some overlap between the compounds that appear to change the thermostability of TREKs and GLUT3 in the CPM assay. Compounds that stabilise in both screens of GLUT3 are highlighted in red. All GLUT3-only stabilisers and destabilisers appear to exert their effects on only 1 out of the 2 preparations of GLUT3.

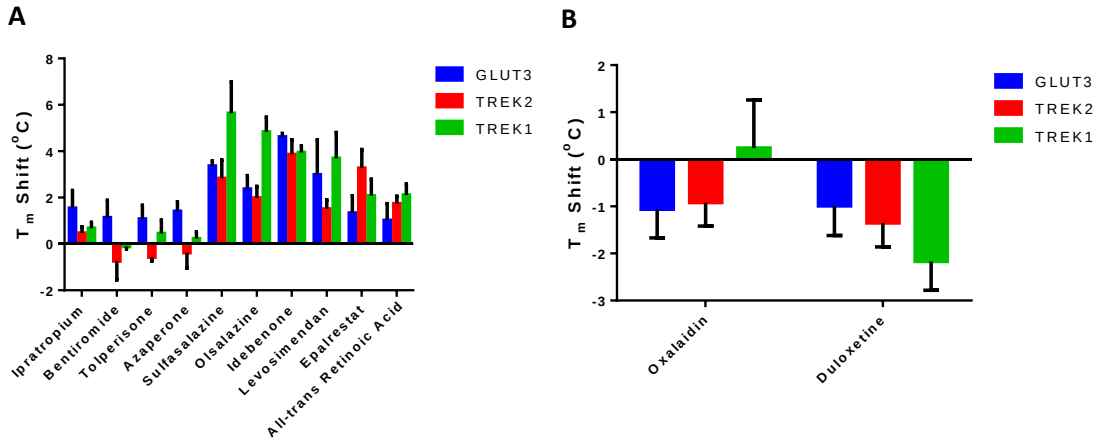

Figure 5.7: Compounds that appear to Stabilise or Destabilise GLUT3 as detected by Selleck FDA-approved Drug library screening. *The overlap of these compounds with those which affect TREK thermostability has been discussed in Table 5.4. Figure 5.7A shows compounds which stabilise GLUT3 while Figure 5.7B shows those that destabilise GLUT3.*

As shown in table 5.4, compounds such as sulfasalazine and idebenone appear to thermostabilise both TREKs and GLUT3. Such compounds are more likely than those specific to one protein to be interacting with the fluorescent dye or the detergent as the proteins are not related and would likely have very different binding pockets. Sulfasalazine, idebenone and pomalidomide were later tested in a control experiment without protein on DSF and found to fluoresce when interacted with CPM at high

temperatures, proving that the compounds were interfering with the assay (See Section 5.3.6 for the data).

5.3.4 DSF screening of TASK1 and TWIK1 with Selleck FDA-Approved Drug Library and Comparison with TREKs

After screening with the unrelated protein GLUT3, I screened other K2P channels, to find out more about the specificity of the interactions between the compounds and TREKs. I thus screened the 351 compound library against two other members of the K2P family, TASK1 and TWIK1.

For TASK1 and TWIK1, there are differences in the buffer used for purification compared to the buffers used for TREK1 and TREK2, details of which can be found in Chapter 2. Notably, the detergents used for purification are different from those of the TREKs, where OGNG with CHS was the preferred detergent/lipid combination. The summary of results for the screening of these 2 proteins can be seen in Table 5.5.

Action of Compound	Results for TASK1	Results for TWIK1
No Effect	314 (89.5%)	322 (91.7%)
Stabiliser in 1 Screen	8 (2.3%)	11 (3.1%)
Stabiliser in 2 Screens	2 (0.6%)	3 (0.9%)
Destabiliser in 1 Screen	11 (3.1%)	7 (2.0%)
Destabiliser in 2 Screens	6 (1.7%)	8 (2.3%)

Table 5.5: Summary of Screening Results for TWIK1 and TASK1. 28 and 29 compounds stabilise or destabilise TASK1 and TWIK1 respectively.

Considerably lower numbers of compounds were found to stabilise or destabilise TWIK1 or TASK1 as compared to the TREKs (8 and 11 as compared to 22 and 25 seen in at least 2 screens). Their overlap with the compounds that interact with TREK1 or TREK2 is shown in Tables 5.6 and 5.7 as well as figures 5.8 and 5.9.

TASK1-only Destabilisers	TASK1 and TREK1/2 Destabilisers
Cinacalcet	Omeprazole
Entacapone	
Lomerizine	
Dronedarone	

Table 5.6: Stabilisers and Destabilisers of TASK1 as well as overlap with those that interact with TREKs. There is a considerable amount of overlap (4 out of 8) between the compounds which affect the thermostability of TASK1 and those that do so for TREK1 and TREK2. Only compounds that stabilised or destabilised TASK1 in both screens are shown here. Compounds which appeared to stabilise or destabilise GLUT3 and both TREKs were not included as they were likely to be false positives.

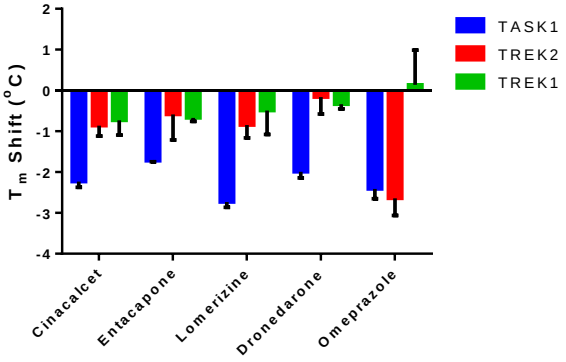

Figure 5.8: Stabilisers and Destabilisers of TASK1 as detected by screening of the Selleck FDA-approved Drug library. *The overlap of these compounds with those which affect TREK thermostability has been discussed in Table 5.6.*

TWIK1-only Stabilisers	TWIK1-only Destabilisers	TWIK1 and TREK1/2 Destabilisers
Bromhexine	Benserazide	Prasugrel
		Genipin
		Omeprazole
		Mizoribine
		Methyldopa
		Amoxapine

Table 5.7: Stabilisers and Destabilisers of TWIK1 as well as overlap with those that interact with TREKs. There is a very high degree of overlap (8 out of 10) between the compounds that affect the thermostability of TWIK1 and those that do so for TREK1 and TREK2. Only compounds that stabilised or destabilised TWIK1 in both screens are shown here.

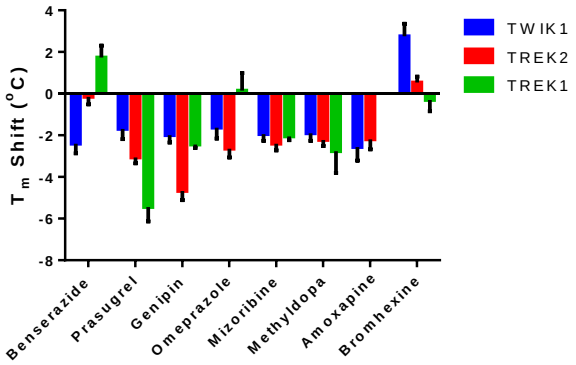

Figure 5.9: Stabilisers and Destabilisers of TWIK1 as detected by Selleck FDA-approved Drug library screening. *The overlap of these compounds with those which affect TREK thermostability has been discussed in Table 5.7.*

From the tables and figures above, there are many compounds which cause a thermostability change in multiple proteins. These effects may be due to interaction between the protein and compound, but can also be due to other factors, such as interaction between the compound and dye or with detergent micelles. However, the use of multiple targets and negative controls allowed me to narrow down the number of compounds to focus on to those that affect the target of interest.

It is required to use an orthogonal assay to confirm the findings. As discussed earlier in this chapter, label-free DSF was proposed as this orthogonal assay.

5.3.5 Selection of Compounds to Take Forward to Label-Free DSF

As label-free DSF is lower throughput and requires significantly larger amounts of compound than the initial screening by CPM, compounds must be acquired from commercial sources. We thus only selected 20 compounds to proceed with label-free DSF screening. The criteria applied for the selection of compounds were to focus on those that changed the thermostability of TREK1 or TREK2, either together or singly, and include some negative controls. These compounds, along with their DSF data for TREK1, TREK2, GLUT3, TASK1 and TWIK1 are shown in Table 5.8. The summary of compound effects on DSF with TREK2, TREK1 and GLUT3 are shown in Table 5.9 Their medical functions and pharmacological mechanism of action are shown in Table 5.10. The raw data for the DSF screen for selected compounds against TREK2 and TREK1 can be found in the Appendix chapter, along with the data for penfluridol and BL1249.

Name of Compound	T_m Shift with TREK2	T_m Shift with TREK1	T_m Shift with TASK1	T_m Shift with TWIK1	T_m Shift with GLUT3
Sulfasalazine	2.83 ± 0.78	5.65 ± 1.36	2.29 ± 0.23	1.77 ± 0.43	3.36 ± 0.21
Idebenone	3.86 ± 0.63	3.94 ± 0.28	2.00 ± 0.25	-0.08 ± 0.26	4.62 ± 0.14
Cilnidipine	3.14 ± 0.58	2.50 ± 0.54	-0.97 ± 0.45	0.81 ± 0.22	0.99 ± 0.16
Rimonabant	-0.09 ± 0.72	3.22 ± 0.62	-0.32 ± 0.31	-0.26 ± 0.30	-0.38 ± 0.24
Ondansetron	1.37 ± 0.43	2.05 ± 0.31	0.18 ± 0.32	-0.33 ± 0.21	0.39 ± 0.18
Cetirizine	1.08 ± 0.62	0.06 ± 0.82	0.13 ± 0.63	0.80 ± 0.35	-0.84 ± 0.87
Mesalamine	1.71 ± 0.58	1.00 ± 0.55	0.08 ± 0.22	1.00 ± 0.25	0.54 ± 0.33
Tolperisone	-0.57 ± 0.17	0.45 ± 0.55	1.61 ± 0.95	0.44 ± 0.31	1.08 ± 0.58
Resveratrol	-0.45 ± 0.29	-0.20 ± 0.45	0.24 ± 0.25	0.13 ± 0.18	0.34 ± 0.47
Argatroban	-0.20 ± 0.40	-0.12 ± 0.53	0.45 ± 0.21	-0.24 ± 0.21	-0.30 ± 0.10
Prasugrel	-3.06 ± 0.27	-5.44 ± 0.69	-0.78 ± 0.55	-1.70 ± 0.35	-0.75 ± 0.34
Genipin	-4.69 ± 0.44	-2.45 ± 0.15	-1.03 ± 0.47	-2.00 ± 0.52	-0.20 ± 0.16
Mizoribine	-2.41 ± 0.31	-2.06 ± 0.17	-0.12 ± 0.58	-1.96 ± 0.35	0.23 ± 0.11
Methyldopa	-2.22 ± 0.30	-2.77 ± 1.03	-0.09 ± 0.65	-1.91 ± 0.60	0.32 ± 0.44
Amoxapine	-2.20 ± 0.47	-1.90 ± 0.28	-0.16 ± 0.64	-2.57 ± 0.48	0.41 ± 0.11
Pomalidomide	-4.46 ± 0.16	-1.21 ± 0.20	-1.01 ± 0.35	0.60 ± 0.25	-0.68 ± 0.33
Duloxetine	-1.35 ± 0.51	-2.18 ± 0.61	-2.13 ± 0.09	0.25 ± 0.32	-0.99 ± 0.63
Flavoxate	-0.14 ± 0.46	-1.38 ± 0.46	-0.32 ± 0.30	0.00 ± 0.20	0.59 ± 0.56
Isoniazid	-0.81 ± 0.51	-1.34 ± 0.33	0.41 ± 0.08	-0.30 ± 0.36	-0.11 ± 0.41
Ticlopidine	0.34 ± 0.41	0.43 ± 0.48	-0.54 ± 0.25	0.50 ± 0.24	0.44 ± 0.69

Table 5.8: Table of T_m shifts using CPM assay for compounds selected for Label-free DSF analysis with target proteins. In each screen of the library, compounds that either stabilise or destabilise the target protein by more than 1.5°C are considered to elicit a positive response. Compounds that stabilised TREK2 or TREK1 in all 3 screens and other proteins in both screens are shaded in green. Those that stabilised in 2 out of 3 screens for TREKs or 1 out of 2 screens for other proteins are shaded in blue. Compounds which destabilise TREK1 or TREK2 in all 3 screens and other proteins in both screens are shaded in red. Those which destabilise in 2 out of 3 screens for TREKs or 1 out of 2 screens for other proteins are shaded in yellow. All values were expressed as (Mean ± SD °C).

Name of Compound	TREK2 Screen Result	TREK1 Screen Result	GLUT3 Screen Result
Sulfasalazine	Stabiliser: 3 Screens	Stabiliser: 3 Screens	Stabiliser: 2 Screens
Idebenone	Stabiliser: 3 Screens	Stabiliser: 3 Screens	Stabiliser: 2 Screens
Cilnidipine	Stabiliser: 3 Screens	Stabiliser: 2 Screens	No Effect
Rimonabant	No Effect	Stabiliser: 3 Screens	No Effect
Ondansetron	No Effect	Stabiliser: 3 Screens	No Effect
Cetirizine	Stabiliser: 1 Screen	Stabiliser: 1 Screen	No Effect
Mesalamine	Stabiliser: 1 Screen	Stabiliser: 1 Screen	No Effect
Tolperisone	No Effect	No Effect	Stabiliser: 1 Screen
Resveratrol	No Effect	No Effect	No Effect
Argatroban	No Effect	No Effect	No Effect
Ticlopidine	No Effect	No Effect	No Effect
Prasugrel	Destabiliser: 3 Screens	Destabiliser: 3 Screens	No Effect
Genipin	Destabiliser: 3 Screens	Destabiliser: 3 Screens	No Effect
Mizoribine	Destabiliser: 3 Screens	Destabiliser: 3 Screens	No Effect
Methyldopa	Destabiliser: 3 Screens	Destabiliser: 2 Screens	No Effect
Amoxapine	Destabiliser: 3 Screens	No Effect	No Effect
Pomalidomide	Destabiliser: 3 Screens	No Effect	No Effect
Duloxetine	Destabiliser: 1 Screen	Destabiliser: 3 Screens	Destabiliser: 1 screen
Flavoxate	No Effect	Destabiliser: 2 Screens	No Effect
Isoniazid	No Effect	Destabiliser: 2 Screens	No Effect

Table 5.9: Summary of effects of 20 selected compounds on TREK2, TREK1 and GLUT3 using the DSF with CPM method. Compounds were colour coded and grouped into 6 groups: TREK2, TREK1 and GLUT3 stabilisers, TREK1-only stabilisers, control compounds, TREK2-only destabilisers, TREK1-only destabilisers and TREK2, TREK1 and GLUT3 destabilisers.

Name of Compound	Medical Function/Mechanism of Action
Sulfasalazine	Treatment for rheumatoid arthritis, inhibits NF-κB, prevents synthesis of immunomodulatory molecules[174].
Idebenone	Treatment for Alzheimer's disease, nootropic[175]. Acts as a quinone analogue, an intermediate in electron transport in mitochondria.
Cilnidipine	Dihydropyridine analogue, antihypertensive drug[176]. L and N-type calcium channel blocker.
Rimonabant	Antiobesity drug. Endocannabinoid receptor inverse agonist, μ-opioid receptor antagonist[177, 178].
Ondansetron	Antiemetic drug. $5HT_3$ receptor antagonist[179].
Cetirizine	2^{nd} generation antihistamine for treatment of allergies, selective H_1 receptor antagonist[180].
Mesalamine	Aminosalicylate anti-inflammatory drug, used for treatment of inflammatory bowel disease. Activator of PPAR-γ in colon[181].
Tolperisone	Centrally acting muscle relaxant. Blocks voltage gated sodium and calcium channels[182].
Resveratrol	Stilbenoid antioxidant naturally occurring in many fruits. Unclear mechanism of action, suggested to activate sirtuin enzymes (SIRT1)[183].
Argatroban	Anticoagulant, used for treatment of thrombosis. Direct thrombin inhibitor[184].
Prasugrel	Platelet inhibitor, prevents formation of blood clots. Binds to $P2Y_{12}$ receptors, preventing adenosine diphosphate induced platelet aggregation[185].
Genipin	Aglycone naturally occurring in plants, crosslinking agent for pericardial tissues and UCP2 blocker[186, 187].
Mizoribine	Immunosuppresive drug, nucleoside analogue that blocks guanine synthesis. Arrests DNA synthesis in S phase[188].
Methyldopa	Dopamine analogue used for treatment of hypertension, inhibits DOPA decarboxylase and thus production of adrenaline and noradrenaline, which cause elevated blood pressure[189].
Amoxapine	Tetracyclic antidepressant. Binds to a range of receptors found in neurones, as well as being a potent noradrenaline and serotonin reuptake inhibitor[190, 191].
Pomalidomide	Thalidomide derivative, anti-angiogenic, used to treat myeloma. Mechanism of action not clear[192].
Duloxetine	Serotonin and noradrenaline reuptake inhibitor (SNRI) antidepressant[193].
Flavoxate	Anticholinergic muscle relaxant. Mechanism of action possibly as phosphodiesterase inhibitor or as local anaesthetic[194].
Isoniazid	Antibiotic used for tuberculosis treatment[195]. Combines with NADH to form an adduct which inhibits the action of bacterial enoyl-acyl carrier protein reductase, interfering with fatty acid synthesis.
Ticlopidine	Antiplatelet agent, blocks ADP receptor on platelets, preventing them from sticking to each other[196].

Table 5.10: Table of Compounds taken forward to Label-free DSF as well as their medical uses and mechanism of action. The 20 compounds chosen have a variety of medical uses and target a range of different receptors, enzymes and channels. Binding to K2Ps is considered a novel function for any of these compounds as there is no literature regarding this.

Roughly equal numbers of stabilisers and destabilisers were selected among the 20 compounds taken forward. Also, both compounds that had a broad spectrum of effect as well as those which seem more specific to TREKs were selected. I hypothesized that:

1. Compounds which have an effect on all proteins tested such as sulfasalazine and idebenone are likely to be interacting with the dye directly or fluorescing at the emission wavelength and are therefore much less likely to give any effect when measured without the dye and at a different wavelength. Possible dye interaction was investigated and results shown in Table 5.11.
2. Compounds which are specific to K2Ps or even to a single protein are likely to retain specificity in a label-free DSF analysis.
3. Compounds that cause the stabilisation or destabilisation of proteins in both methods are more likely to be binding directly to the surface of the protein. This is because the methods measure the effect on different residues at different areas of the protein.

5.3.6 Label free DSF of TREK2, TREK1, GLUT3, TWIK1 and TASK1 with Shortlisted Compounds

All 20 compounds selected in Section 5.3.5 were diluted to 100 µM in the respective SEC buffers of the proteins listed. They were then made up with 0.1 mg/ml of protein (about 3 µM of protein in the case of K2Ps) at 20 µM compound concentration for use in label free DSF. 3 biological replicates of this screen were performed with TREK2 and TREK1. 2 biological replicates were performed with all other proteins. The T_m shifts observed using the inflection point of the 330 nm fluorescence signal are shown in Table 5.11.

Name of Compound	T_m Shift with TREK2	T_m Shift with TREK1	T_m Shift with TASK1	T_m Shift with TWIK1	T_m Shift with GLUT3
Sulfasalazine	-0.44 ± 0.05	0.71 ± 0.55	-0.15 ± 0.45	0.97 ± 0.35	0.35 ± 0.17
Idebenone	-0.46 ± 0.14	-1.07 ± 0.05	-0.79 ± 0.02	-0.94 ± 0.07	0.85 ± 0.26
Cilnidipine	1.70 ± 0.58	-0.06 ± 0.47	-0.44 ± 0.06	-0.43 ± 0.25	0.20 ± 0.35
Rimonabant	0.29 ± 0.27	-2.13 ± 0.18	-0.59 ± 0.08	0.29 ± 0.17	-0.43 ± 0.25
Ondansetron	0.42 ± 0.23	-0.64 ± 0.45	-0.20 ± 0.07	-0.03 ± 0.42	0.36 ± 0.30
Cetirizine	-0.42 ± 0.27	-1.07 ± 0.52	-0.32 ± 0.02	-0.17 ± 0.14	-0.52 ± 0.21
Mesalamine	0.35 ± 0.24	-0.88 ± 0.29	-0.37 ± 0.04	0.11 ± 0.18	0.24 ± 0.34
Tolperisone	0.34 ± 0.32	-0.63 ± 0.57	-0.37 ± 0.07	-0.18 ± 0.28	0.35 ± 0.15
Resveratrol	No Signal	No Signal	No Signal	No Signal	No Signal
Argatroban	-0.04 ± 0.39	-1.07 ± 0.22	-0.11 ± 0.31	0.55 ± 0.25	1.30 ± 0.29
Prasugrel	2.08 ± 0.63	3.08 ± 0.98	-0.17 ± 0.10	0.33 ± 0.14	0.70 ± 0.68
Genipin	3.42 ± 0.41	3.30 ± 0.04	-0.18 ± 0.06	0.75 ± 0.06	0.83 ± 0.17
Mizoribine	0.95 ± 0.31	1.80 ± 0.17	-0.23 ± 0.36	-0.01 ± 0.16	0.95 ± 0.47
Methyldopa	1.06 ± 0.14	-1.59 ± 0.52	-0.16 ± 0.05	0.25 ± 0.24	0.13 ± 0.35
Amoxapine	0.17 ± 0.42	-1.14 ± 0.61	-1.32 ± 0.16	-0.92 ± 0.47	-0.30 ± 0.16
Pomalidomide	0.11 ± 0.26	-0.67 ± 0.15	-0.45 ± 0.14	-0.32 ± 0.13	-0.42 ± 0.15
Duloxetine	-0.26 ± 0.35	-1.86 ± 0.84	-2.31 ± 0.11	-2.11 ± 0.20	-0.70 ± 0.52
Flavoxate	-1.03 ± 0.13	-1.55 ± 0.47	-0.68 ± 0.08	-0.32 ± 0.25	0.92 ± 0.25
Isoniazid	-0.16 ± 0.12	-2.11 ± 0.49	-0.28 ± 0.03	-0.23 ± 0.14	-0.83 ± 0.31
Ticlopidine	-0.38 ± 0.37	-1.08 ± 0.52	-0.46 ± 0.23	-0.29 ± 0.31	0.40 ± 0.26

Table 5.11: Table of T_m shifts using Label-free DSF for selected compounds with target proteins. In each screen of the library, compounds which either stabilise or destabilise the target protein by more than 1.5°C are considered to elicit a positive response. Compounds which stabilise TREK2 or TREK1 in all 3 screens, and other proteins in both screens, are shaded in green. Those that stabilise in 2 out of 3 screens for TREKs are shaded in blue. Compounds that destabilise TREK1 or TREK2 in all 3 screens, and other proteins in both screens, are shaded in red. Those that destabilise in 2 out of 3 screens for TREKs are shaded in yellow. Data is expressed as (Mean ± SD) °C.

With label free DSF, the number of compounds that affect the thermostability of the target proteins was much lower than with the assay using the CPM dye. There was however, significant overlap in the compounds that caused thermostability changes. None of the negative controls tolperisone, argatroban or ticlopidine caused a T_m shift in the TREKs.

The stabilisers sulfasalazine, idebenone and the destabiliser pomalidomide also had no effect on either TREK in the label-free DSF. They were found to be the only 3 coloured compounds in the shortlist of 20 and may have affected the fluorescence in the CPM

assay by also absorbing or emitting light at that wavelength when heated. A table of fluorescent signals with the 3 coloured compounds at 25, 60 and 95°C, along with that of protein-only and buffer only controls is provided in Table 5.12.

Temperature (°C)	Sulfasalazine Fluorescence (AU)	Idebenone Fluorescence (AU)	Pomalidomide Fluorescence (AU)	TREK2 Fluorescence (AU)	Buffer only Fluorescence (AU)
25	2853	3013	8757	4839	2408
60	3594	3554	15,792	14,380	2221
95	9220	9900	19,369	51,907	2162

Table 5.12: CPM fluorescence raw data for the coloured compounds sulfasalazine, idebenone and pomalidomide with those of TREK2 only and SEC buffer only. All 3 coloured compounds have significant fluorescence when the DSF assay protocol with the CPM dye was run with no protein. This fluorescence would affect the signal obtained when protein was in the mixture as well and change the apparent T_m.

Among the other compounds, prasugrel and genipin stabilised both TREKs and were previously destabilisers in the CPM assay. Mizoribine did the same but was specific to TREK1 only and rimonabant destabilised TREK1 in this assay when it was a stabiliser in the CPM assay. Possible reasons for these changes will be considered in section 5.4. Methyldopa, amoxapine and duloxetine were found to have no significant effect on TREK2 but still caused destabilisation of TREK1 and in the case of duloxetine, also TASK1 and TWIK1. Ondansetron, cetirizine and mesalamine also had no effect on the thermostability of any protein tested with label-free DSF despite being TREK stabilisers in the CPM assay.

Overall, the label-free DSF results do not corroborate those from the CPM assay to a large extent as the amount of change in stability as well as the direction of change of thermostability in some cases differ. Most of the compounds however, do affect the thermostability of the test proteins in both assays. The compounds which were shown to change the thermostability of TREKs in both assays in any direction therefore represented good candidates to be taken forward to examine any possible effects on the function of these channels.

5.4 Discussion

In chapter 3, I established both the CPM assay and label-free DSF as reliable and fast methods that can be used to determine the changes in thermostability in proteins caused by ligand binding. In this chapter, I applied both methods to screen and follow up on a medium-sized library of known pharmaceutical agents, compared the hits between both techniques, and later in chapter 6, attempt to validate these results using a functional assay.

351 compounds were chosen with a bias towards those targeted at ion channels from the original library. While it would be more relevant to obtain an ion channel or pain-focused library, this was not possible despite original offers from my sponsors at Neusentis (Pfizer) that one would be made available (the unit was closed before the project was completed). The FDA-approved drug library was the most suitable library readily available in a catalogued form and was thus chosen for this work.

The caveat with using a FDA-approved drug library is that the chemical space covered by existing pharmaceutical agents is limited. This would not offer the same level of coverage as fragment screening or even a set of random molecules of drug-like nature. However, the main advantage is that any hits obtained would already have been tested for a different medical use, which makes the process of getting approval from regulatory bodies much easier. Also, the pharmacokinetics of these compounds would be well known, making their further development for targeting certain organs easier to carry out.

The CPM assay is clearly prone to giving a large number of false positives. Despite a score of 0.65 to 0.88 in the Z' test, a single point assay proved to give an excessively high it rate, with about 10% of compounds giving a positive readout on any given screen.

Duplicate and triplicate repeats of this assay were necessary to narrow down the number of hits. The hit-rate for TREKs was still high even with replicates, with 6.1 to 7.2% of compounds causing a stabilisation or destabilisation effect on either TREK1 or TREK2 in at least 2 out of the 3 screens performed with both proteins.It was much lower for the other proteins, ranging from 0.9% for GLUT3 to 2.2% with TASK1 and 3.1% for TWIK1. These hit rates are much higher than the reported hit rate with a random selection of small molecules of 0.1 to 0.5%[197]. However, the selection of compounds is more comparable to a library of known drugs, where a hit rate of 3.2% was seen in a screen for inhibitors of *C. Albicans* biofilms[198]. Target focused libraries can exhibit even higher hit rates, with 0.7-20% reported in a range of experiments[199].

The high hit rate requires the assay to be repeated in order to narrow down the number of possible hits to take forward. Repeating the assay also makes the follow up steps more manageable in terms of the number of compounds to be tested. However, this is not ideal for a high throughput screen with hundreds of thousands of compounds.

There was significant overlap between compounds that appeared to change the thermostability of TREK1 and TREK2 and to a lesser extent, TWIK1. There was also much less overlap between the compounds that changed the thermostability of the TREKs and TASK1 or GLUT3. This could be due to similarity in structure between these proteins, especially between TREK1 and TREK2. Specificity is very important in drug development and though we did take forward some compounds that were not specific to a single protein to label free DSF, care was taken to include all the compounds which may be specific to one protein.

The 20 selected compounds for label-free DSF do not encompass all hits from the initial screening and this is due to the cost of obtaining the compounds in significant amounts

for both the label-free DSF and follow-up electrophysiology experiments in Chapter 6. When choosing the compounds to purchase I opted for diversity in their chemical structure, including the negative controls.

The label free DSF results show that a significant proportion of compounds that affect the thermostability of TREKs on the CPM assay also do so on the label-free DSF. This result is expected as the ease of unfolding a protein should be the same when a given compound is bound regardless of assay used. However, the results differ for many compounds. The lack of response on label-free DSF for coloured compounds has been discussed in Section 5.3.6, but for the remainder, the most likely explanation is that the compounds interact locally with a domain of the protein containing cysteine but not tryptophan. The locations and domains of the cysteine and tryptophan residues for TREK1 and TREK2 are shown in Table 5.13. Only cysteines and tryptophan residues located within the range which is covered by the constructs used for analysis are listed below.

Cysteines in TREK2	Cysteines in TREK1	Tryptophans in TREK2	Tryptophans in TREK1
C123 (extracellular cap)	C93 (extracellular cap)	W74 (N-term cytoplasmic)	W44 (N-term cytoplasmic)
C189 (TM helix 2)	C159 (TM helix 2)	W157 (extracellular)	W127(extracellular)
C249 (TM helix 3)	C219 (TM helix 3)	W266 (interior, near pore forming domain)	W199 (cytoplasmic)
		W300 (TM helix 4)	W236 (interior, near pore forming domain)
		W306 (TM helix 4)	W275 (TM helix 4)
		W308 (TM helix 4)	W277 (TM helix 4)
		W326 (C-term cytoplasmic)	W295 (C-term cytoplasmic)

Table 5.13: Locations of cysteine and tryptophans in TREK1 and TREK2. As the 2 proteins are highly similar in sequence and structure, they have the same numbers of cysteines and tryptophans in almost the same locations and domains. Both proteins have 3 cysteines and 7 tryptophans within the part of the sequence used for these assays. The cysteine and tryptophan residues of the 2 proteins are located in different domains from each other, which makes local distortions caused by ligand binding causing T_m shifts in 1 assay but not in the other possible.

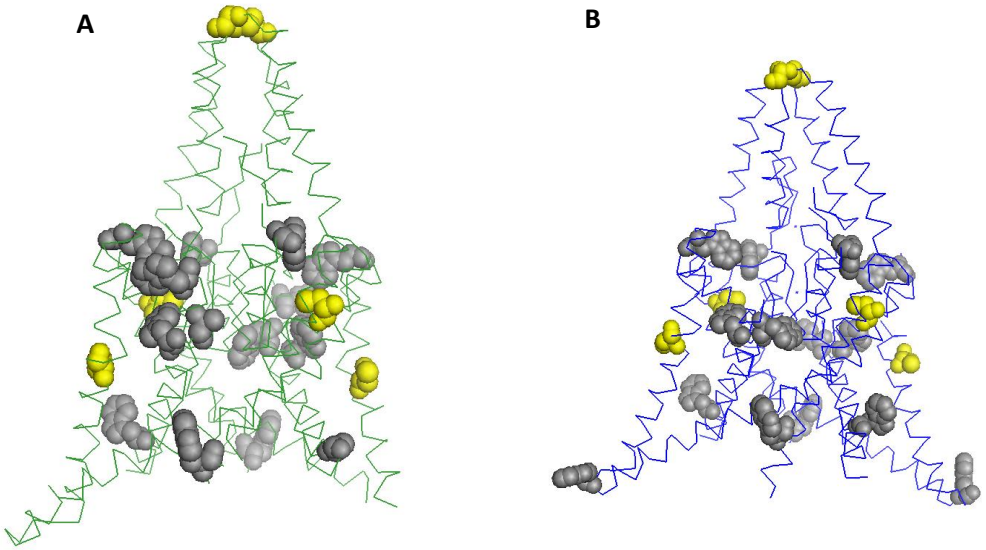

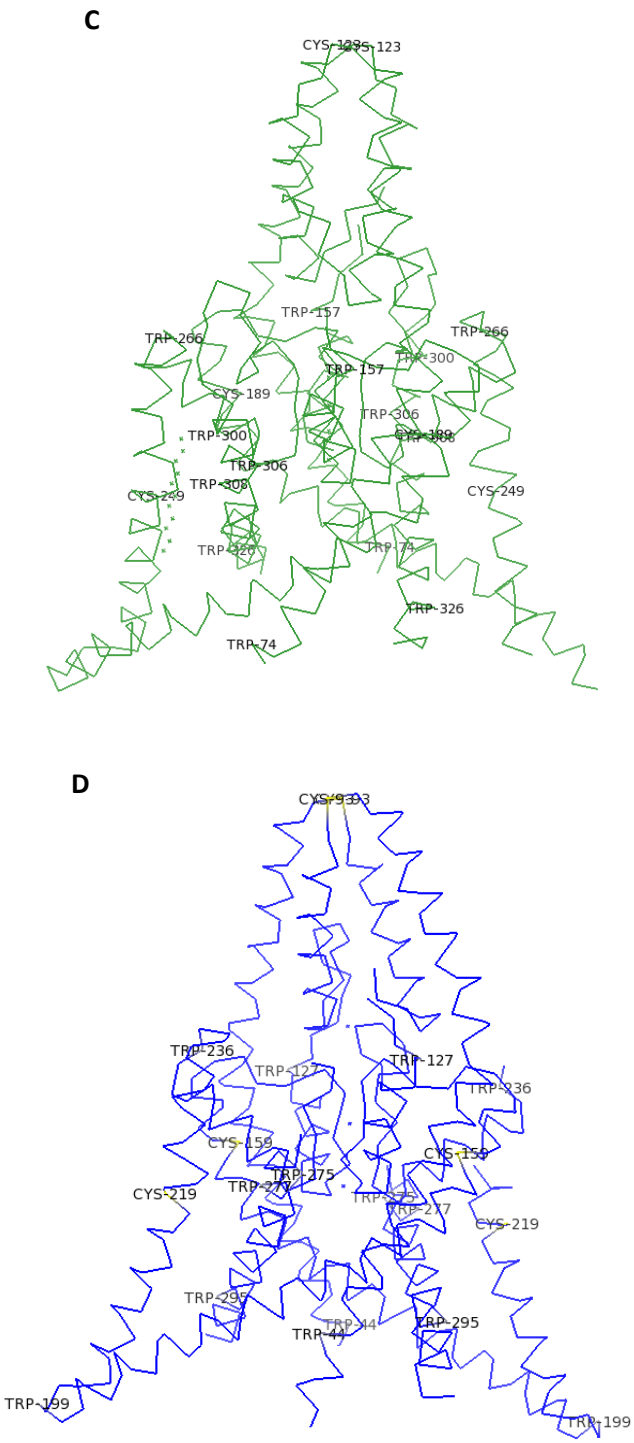

Figure 5.10: Annotated figures of TREK2 and TREK1 with labelled cysteines and tryptophans. *Figures 5.10A and 5.10B are ribbon diagrams of TREK2 and TREK1 respectively. The cysteine residues are shown in yellow and the tryptophan residues are shown in grey. Figures 5.10C and 5.10D are ribbon diagrams of TREK2 and TREK1 respectively with the locations of cysteine and tryptophan residues labelled.*

The binding site of norfluoxetine was shown by Dong *et al.* with crystallography to be in the fenestration near the M2 and M4 helices[59] and it is conceivable that some compounds might bind to that fenestration, causing localised conformational change in that area and thus a T_m shift that is different between the 2 assays.

False negatives are a problem with both assays as it is possible for a compound to bind to a protein without changing the thermostability by either measure. This effect is difficult to quantify as the relevant compounds are not identified. However, for the purposes of this thesis we do not need to check for false negatives as there are enough compounds to take forward to functional assays.

A recent study published after the completion of this work used thallium flux assays as a functional high throughput screen for TREK2, followed up by manual patch clamp electrophysiology for validation[209]. This represents an alternative approach to screening ion channels and such an assay should be considered along with protein-only approaches as described in this work as possible ways to characterise protein-small molecule interactions with K2Ps.

5.5 Conclusion

In this chapter, I screened a 351 compound subset of a FDA-approved drug library and found a significant number of stabilisers and destabilisers of TREK1 and TREK2. 20 compounds were selected based on their effect of the thermostability of the test proteins and also screened against the same proteins using label-free DSF. While the results show some agreement between the methods, they are not definitive. Therefore, direct binding assays and functional approaches are required to confirm whether they are of interest.

In Chapter 6, we take forward all 20 selected compounds to study their effects on the functional activity on these channels using direct electrophysiological methods.

Chapter 6: Functional Assay of Compounds which Affect K2P Protein Thermostability.

6.1 Introduction

6.1.1 Functional Assays for Ion Channels

The industry standard method to test for effects of a compound on a protein linked to a disease is to use a functional assay. Such assays can make use of purified protein in vitro, or a protein expressed in cells. Both approaches have advantages and disadvantages, as discussed below:

Interactions with other cell components: Proteins interact with other components of the cell to perform their function. In a system with only purified protein, these interactions are lost unless the other partners are introduced. Hence, if a cell based system is used, it is not possible to tell if the effect of the compound is on the target protein or indirect through its interaction partners.

Phenotypic Effects: Cell-based assays allow us to visualise the effects of a compound phenotypically, which makes the link to the treatment of a disease clearer than with a protein-only approach.

In the case of ion channels, a natural or artificial membrane is also required for functional assays as the transport of ions can only be quantified if there are 2 separate environments[200]. Such assays can be conducted either with the expression of a target ion channel in a cellular environment or with the reconstitution of purified ion channel proteins in an artificial membrane[201]. The gold standard functional assay for ion channels is manual electrophysiology.

6.1.2. Manual Electrophysiology Techniques

Should an ion channel be stably overexpressed in a cell line or in *Xenopus laevis* oocytes, the most frequently used method to study their function and thus response to drugs is through classical electrophysiology, the measurement of electrical currents across a membrane.

In this study I have used the *Xenopus* oocyte expression system to study the functional properties of recombinantly expressed K2P channels. *Xenopus* oocytes are ideal as they readily express microinjected mRNA and their relative lack of endogenous ion channels make them an ideal expression system for the K2P channels[201]. They are also easy to handle due to their large size and are also easy to maintain, making them good for electrophysiological studies.

TEVC is a technique where the membrane potential of a cell is artificially controlled through a voltage electrode which senses the membrane potential and a current electrode which introduces electrical current to balance control this potential[202] (Figure 6.1). If functional and open channels are present in the membrane then ions will flow through them and these currents can be detected and recorded. The main assumption taken here is that the cell involved overexpresses the target channel to such an extent that other channels' share of current is inconsequential to the total current recorded.

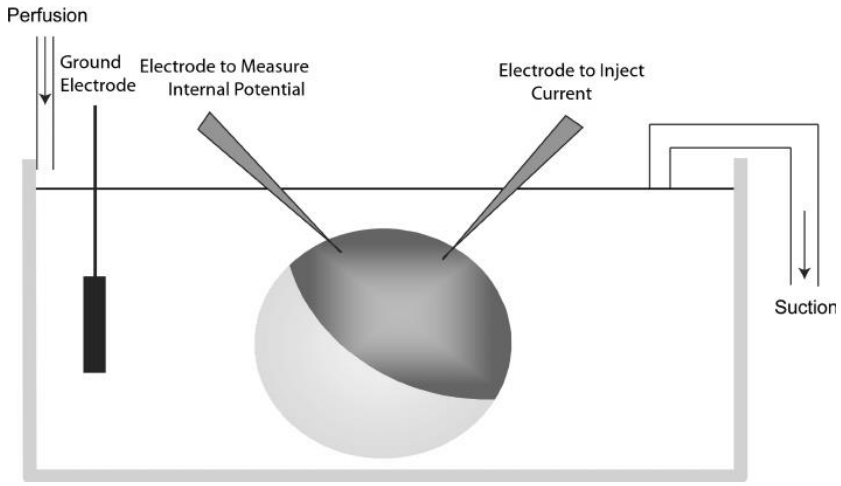

Figure 6.1: Schematic of Two Electrode Voltage Clamp. *2 electrodes, 1 measuring membrane voltage and 1 to apply a current to maintain a certain clamping voltage are inserted into an oocyte and the resultant ion channel current is measured after a current to voltage conversion*[210]*.*

Whereas TEVC records whole cell currents, the patch clamping technique records the activity of channels in a smaller patch of membrane. A glass electrode is placed against the cell membrane and suction applied to create a gigaohm resistance seal[21]. The voltage is kept constant by passing current into the system and the response of the channels involved are recorded. Patch clamping has developed enormously since it was first used introduced in the 1970s and there are now several automated methods which can make high-throughput screening more efficient[203, 204].

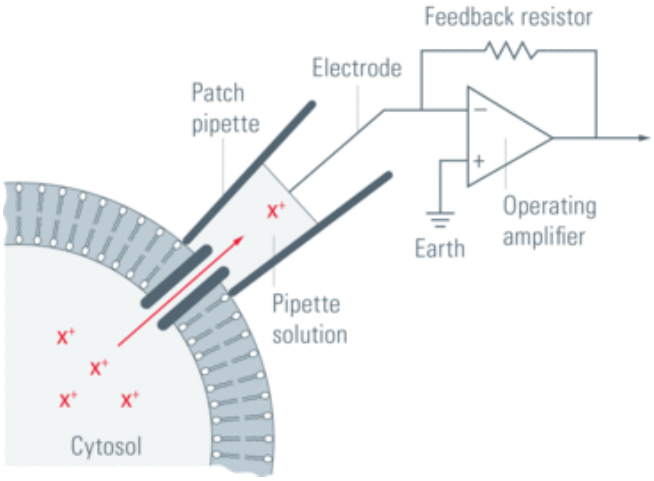

Figure 6.2: Schematic of a patch clamp setup. *A single or multiple channel conductance can be measured by the use of a patch pipette which creates a very high resistance seal with the cell membrane. This setup shown represents the cell-attached patch clamp configuration. There are several other configurations including those with excised patches of membrane. (Veitinger, 2011)*[205].

Traditional manual patch clamping is challenging and requires significant training whilst automated patch clamping requires specialised equipment. Hence, the first approach chosen for analysing the hit compounds from chapter 5 was the TEVC method.

6.2 Materials and Methods

6.2.1 Preparation of mRNA

Wild type TREK1 (Accession Number: NP_001017424), TREK2 (Accession Number: NP_612191) and TASK1 (Accession Number: NP_002237) genes were obtained from Source Bioscience (Source Biosciences, Nottingham, UK). They were then subcloned into a plasmid vector (pBF) (Origene, Rockville, MD, USA), suitable for in vitro transcription and expression in Xenopus oocytes and based on pUC. The subcloning was performed by members of the Tucker group, Department of Physics, University of Oxford. The pBF vector incorporates 3' and 5' untranslated regions of the *Xenopus* β–globin gene to

boost expression, as well as a 5' GCCGCCACC Kozak sequence preceding the start codon[206]. It also contains an SP6 promoter and an MluI restriction enzyme site.

The pBF plasmid containing the gene of interest was then cut with the restriction enzyme MluI (Promega, Madison, WI, USA) and the DNA linearised for mRNA transcription. The DNA linearization reaction was carried out for 1 hour at 37°C. Qiaquick columns were then used to purify the product (Qiagen, Hilden, Germany).

In vitro transcription was carried out using the SP6 RNA polymerase and the AmpliCap SP6 High Yield Message Maker kit (CellScript, Madison, WI, USA). mRNA was then cleaned using a RNAeasy Mini kit (Qiagen, Hilden, Germany). mRNA was quantified using a Nanodrop 1000 spectrophotometer (Nanodrop, Wilmington, DE, USA) and mRNA integrity was assessed by agarose gel electrophoresis (1% agarose) (Sigma Aldrich, St. Louis, MO, USA). The mRNA was then frozen at -20°C. In all 3 cases, 40-60 ng of mRNA was obtained, dissolved in RNA-ase free water for use in electrophysiology experiments.

6.2.2 Preparation and Injection of Oocytes

Xenopus Laevis oocytes were removed from female frogs (Nasco, Fort Atkinson, WI, USA) and were prepared for injection of mRNA by collagenase digestion followed by manual defolliculation and stored in ND96 solution, which contained 96 mM NaCl, 2 mM KCl, 1.8 mM $CaCl_2$, 1 mM $MgCl_2$, and 10 mM HEPES, pH 7.4, and was supplemented with 2.5 mM sodium pyruvate, 50 µg/ml gentamycin, 50 µg/ml tetracycline, 50 µg/ml ciprofloxacin, and 100 µg/ml amikacin. All salts were obtained from Sigma-Aldrich and antibiotics from Apollo Scientific (Storage was at 17°C for 12-24 hours. pH of buffer was adjusted with HCl or NaOH when required.

Oocytes were then injected with 50 nl of 80 ng/µl mRNA (4 ng per cell) and left to incubate at 17°C for 12-24 hours in ND96 solution before electrophysiology experiments were performed.

6.2.3 Two Electrode Voltage Clamp Electrophysiology

For two-electrode voltage-clamp recordings, electrodes were pulled from thick-walled borosilicate glass (Harvard Apparatus, Cambridge, Cambs, UK) and filled with 3 M KCl. ND96 bath solution was used for all recordings and cells were placed in a holder of about 350 µl capacity. Oocytes were perfused with solution through a peristaltic pump perfusion system (Ismatec, Wertheim, Germany). Currents were recorded using a Geneclamp 500 amplifier (Molecular Devices, Sunnyvale, CA, USA) and digitised with a Digidata 1322A (Molecular Devices, Sunnyvale, CA, USA). Unless otherwise stated, currents were recorded using 300 ms voltage steps from a holding potential of -80 mV delivered in 10 mV increments between -120 mV and +80 mV. A diagram of the overall two-electrode voltage clamp is shown in Figure 6.3. Data was visualised and analysed using pClamp Clampex 9.0 and Clampfit 9.0 (Molecular Devices, Sunnyvale, CA, USA).

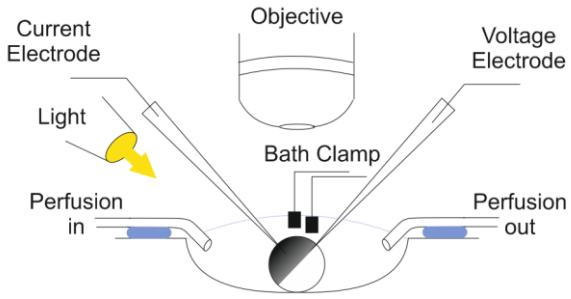

Figure 6.3: The Two-Electrode Voltage Clamp Experimental Set Up. *Oocytes are submerged in a recording chamber and impaled by two glass microelectrodes (connected to Gene Clamp 500 amplifier and Digidata 1322A digitiser) to record membrane voltage (voltage electrode) and inject current to maintain voltage clamp (current electrode). The transmembrane voltage is recorded with reference to the 0 mV bath voltage maintained by the bath clamp. Perfusion inflow and outflow was controlled by a peristaltic pump.*

6.3 Results

6.3.1 Native Currents of TREK2 and TREK1

Xenopus oocytes were prepared as described in Section 6.2.2 and injected with mRNA of the target gene. After 12-24 hours of incubation at 17°C, the oocytes are placed in a two electrode voltage clamp setup as shown in Section 6.2.3. Native currents of TREK1 and TREK2 were recorded and shown in Figure 6.4.

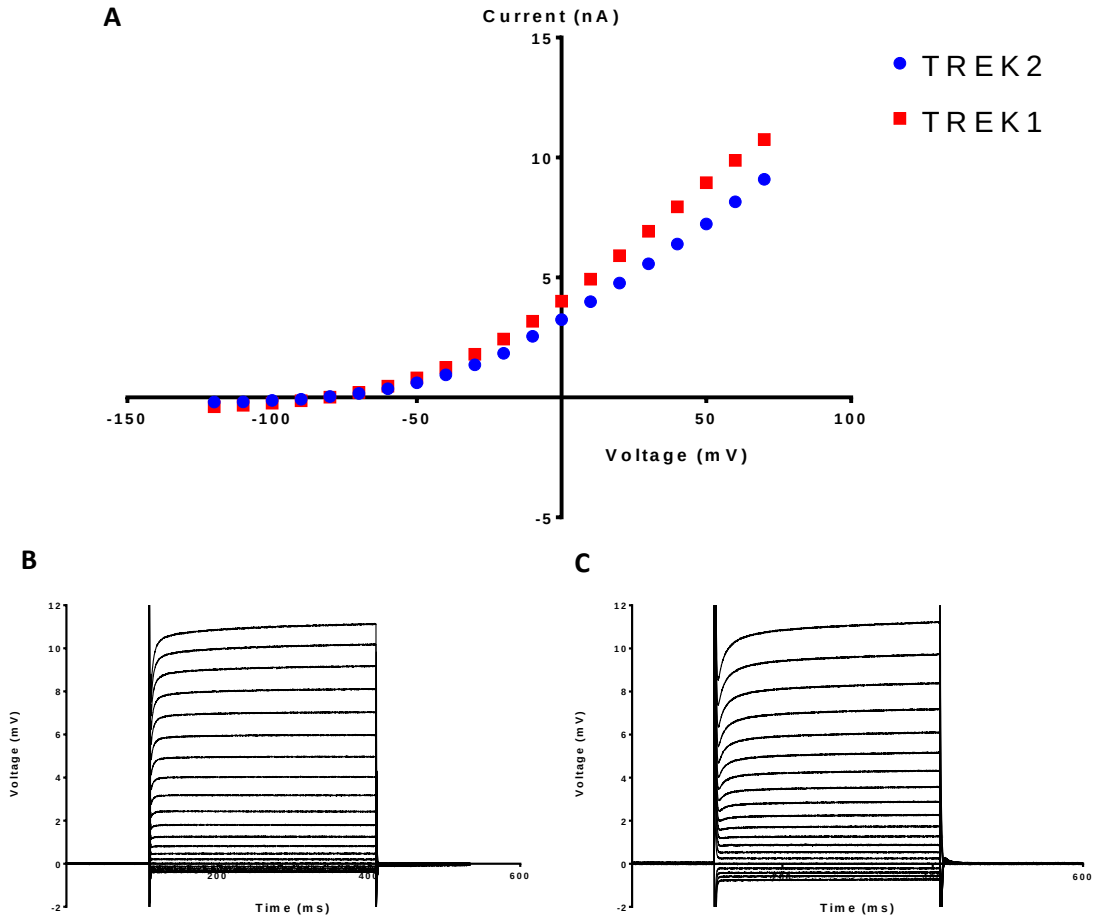

Figure 6.4: Currents recorded from Wild-type TREK1 and TREK2. *Currents were recorded with the step protocol described in Section 6.2.3. Both TREK1 and TREK2 are open rectifiers with a reversal potential of about -80 mV. Figure 6.4A shows the IV relationship of the currents recorded while Figure 6.4B shows the currents generated by TREK2 in 10 mV steps. Figure 6.4C shows TREK1 currents.*

6.3.2 Effects of the Inhibitor Norfluoxetine and the Activator BL1249 on TREK2 and TREK1

Norfluoxetine has previously been shown be an inhibitor of TREK channels whilst BL1249 is known to be an activator[84, 89, 207]. They are first used as control compounds here to see changes in function of TREK channels expressed in oocytes. The effects of norfluoxetine and BL1249 on TREK currents are shown in Figures 6.5 and 6.6.

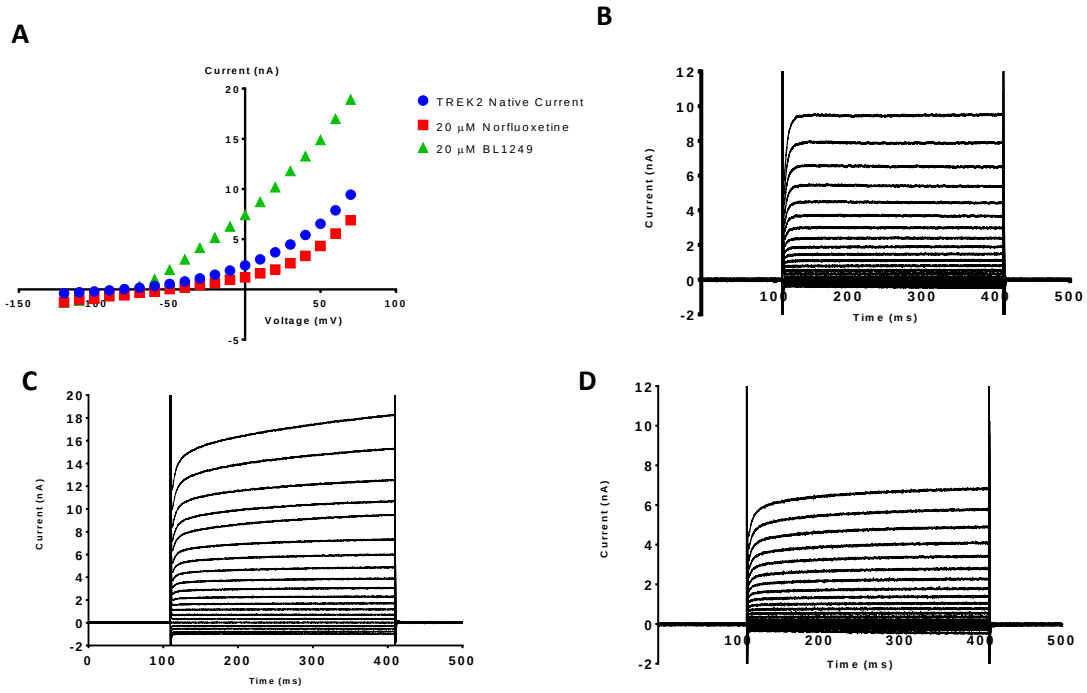

Figure 6.5: Norfluoxetine and BL1249 effects on currents from oocytes expressing TREK2. *Oocytes expressing TREK2 were perfused with 20 µM Norfluoxetine (a known TREK inhibitor) or BL1249 (a known TREK activator) for 3 minutes and then further incubated for 2 minutes. Currents were then measured. The IV relationship of the TREK2 expressing oocytes is shown in Figure 6.5A, with native TREK2 current shown in Figure 6.5B, the result after perfusion of BL1249 in Figure 6.5C and the result after perfusion of norfluoxetine in Figure 6.5D.*

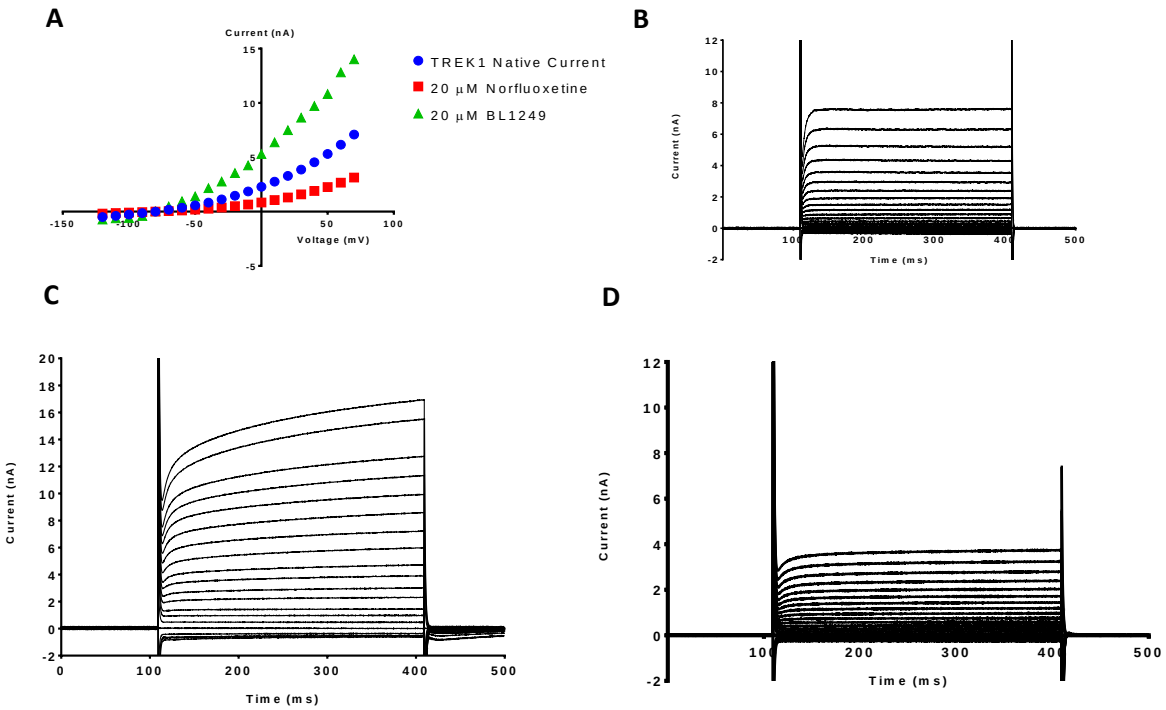

Figure 6.6: Norfluoxetine and BL1249 effects on currents from oocytes expressing TREK1. *Oocytes expressing TREK1 were perfused with 20 µM Norfluoxetine (a known TREK inhibitor) or BL1249 (a known TREK activator) for 3 minutes and then further incubated for 2 minutes. Currents were then measured. The IV relationship of the TREK1 expressing oocytes is shown in Figure 6.6A, with native TREK1 current shown in Figure 6.6B, the result after perfusion of BL1249 in Figure 6.6C and the result after perfusion of norfluoxetine in Figure 6.6D.*

The above data shows that the *Xenopus* oocytes injected with TREK1 or TREK2 mRNA and expressing these ion channels were able to respond to both activation and inhibition by known ligands. This also further confirms that the channels are functional when expressed in the oocytes.

6.3.3 Screening of Selected Compounds against TREK2 and TREK1

Having now demonstrated the ability to activate and inhibit TREK channel currents, we next examined the functional effect of the compounds identified in Chapter 5. These 20 compounds were selected based on their effect on the thermostability of TREK1 and TREK2 with the DSF assay using the CPM dye and were further screened with label-free DSF to validate these effects. The compounds were then tested here for their functional effects on *Xenopus* oocytes expressing TREK1 or TREK2. All compounds were perfused at 20 µM for 3 minutes with 2-minute-long incubation with the oocyte after perfusion. Currents were then measured and normalised against the control current from the oocyte without any perfused compound.

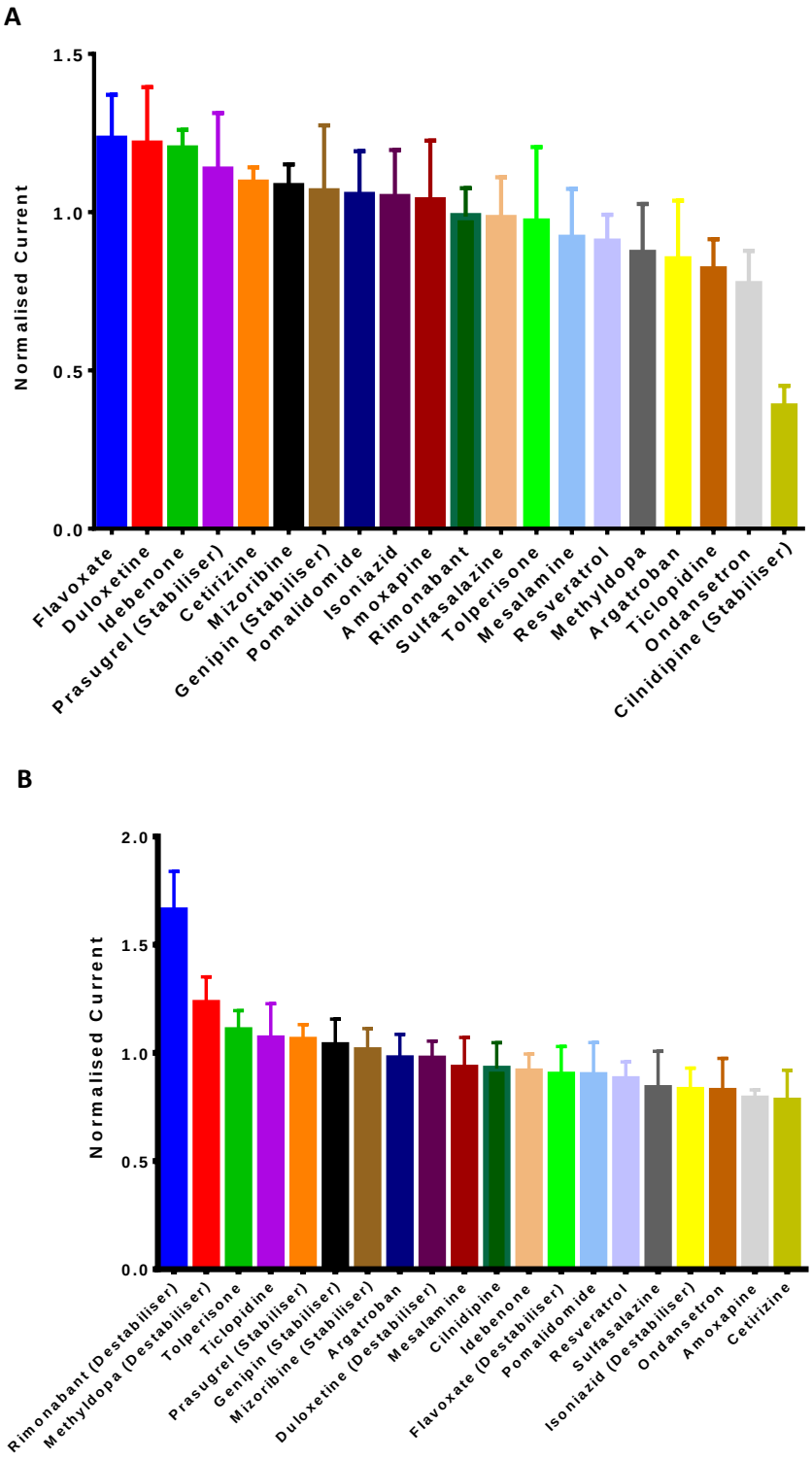

Figure 6.7: Compound Screening using Electrophysiology. *20 compounds were dissolved in ND96 buffer at 20 µM and perfused onto oocytes which express TREK2 (Figure 6.7A) or TREK1 (Figure 6.7B). The current change after drug application was measured +80 mV and normalised to current levels before application (Native current = 1.0).*

The single point compound screen was conducted twice and the error bars in figure 6.7 are the SD of the 2 measurements. The current was normalised to allow the comparison between different oocytes, which have differing initial current levels. The cutoff for a significant effect on channel function was set at a 25% increase or decrease in current. This is because the SDs for compound effects lie between 3 and 20% of the native current. With this cutoff in mind, only cilnidipine appeared to function as an inhibitor of TREK-2, whilst only rimonabant appeared to activate TREK1.

6.3.4 Dose Response Data of Cilnidipine and Rimonabant in TREK Expressing Oocytes

As a follow on to the experiments conducted in Section 6.3.3, dose response data was collected for cilnidipine in oocytes expressing TREK2 and rimonabant in oocytes expressing TREK1. Oocytes were perfused with increasing concentrations of compound (in order, 1, 5, 10, 20 and 50 μM) dissolved in ND96 buffer. The perfusion protocol is the same as that described in section 6.3.2 and 6.3.3. The dose response data is shown in Figure 6.8 below:

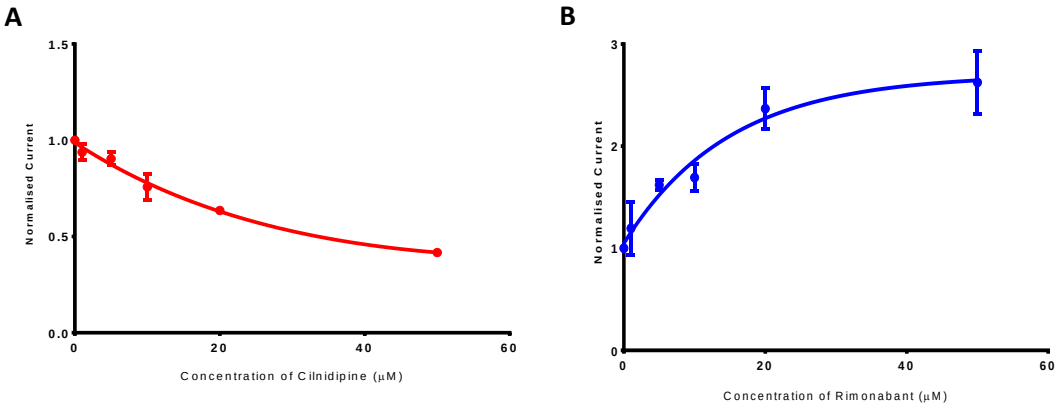

Figure 6.8: Dose response of cilnidipine with TREK2 expressing oocytes (Figure 6.8A) and rimonabant with TREK1 expressing oocytes (Figure 6.8B). *Oocytes were perfused with increasing concentrations of compound and their current reading at +70 mV was collected using a steps protocol and compared to the native current of the TREK expressing oocytes (Native Current = 1.0). Each experiment was conducted in triplicate and data is expressed as normalised current Mean ± SEM. A single exponential decay curve is fitted onto both graphs in order to attempt to find a EC_{50} or IC_{50} for the compounds.*

Both cilnidipine and rimonabant exhibit dose-dependent effects on channel function. The effects fit those on a single-phase decay curve, which allows for an EC_{50} or IC_{50} to be determined. The IC_{50} of cilnidipine on TREK2 was determined to be 18.4 µM while the EC_{50} of rimonabant on TREK1 was determined to be 10.6 µM. Both compounds were earlier found in the single point assay to not have effect on the channel function of the other TREK channel TREK1.

6.3.5 Cilnidipine and Rimonabant Effects on TASK1

In order to better determine the specificity of this response, I examined the effect of these compounds on an unrelated K2P channel. TASK1 was expressed in *Xenopus* oocytes as described in Section 6.3.1. The ND96 buffer for current measurement of TASK1 was adjusted to pH 7.4 instead of pH 7 in order to ensure significant current readings for this pH-sensitive channel. The recorded currents and IV relationship for TASK1 are shown in Figure 6.9.

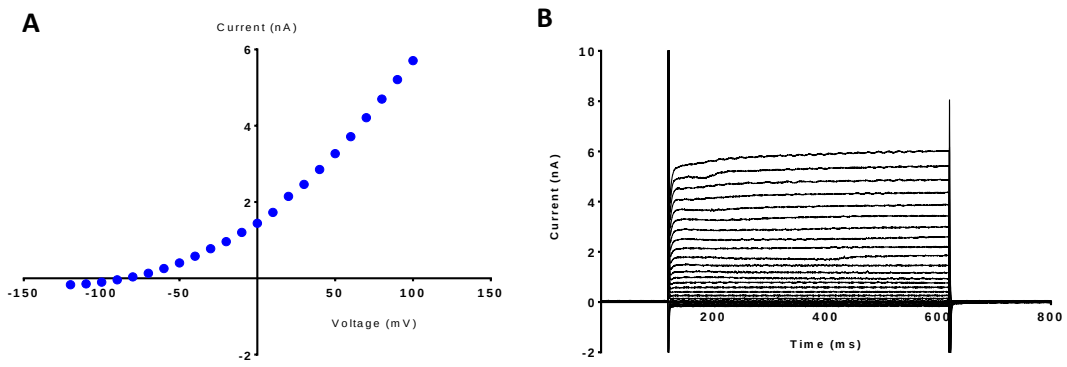

Figure 6.9: Wild-type TASK1 currents. *Currents were collected using the protocol described in Section 6.2.3. Figure 6.9A shows the IV relationship of TASK1 while Figure 6.9B is data collected using the step protocol described in Section 6.2.3 and 6.3.1.*

While it would be ideal to examine a greater panel of different K2P channels, showing the compounds' preference for TREKs over TASK1 would give some indication of specificity as both compounds exhibited no significant effect on the thermostability of TASK1 when tested via the DSF assay with CPM or the label-free DSF.

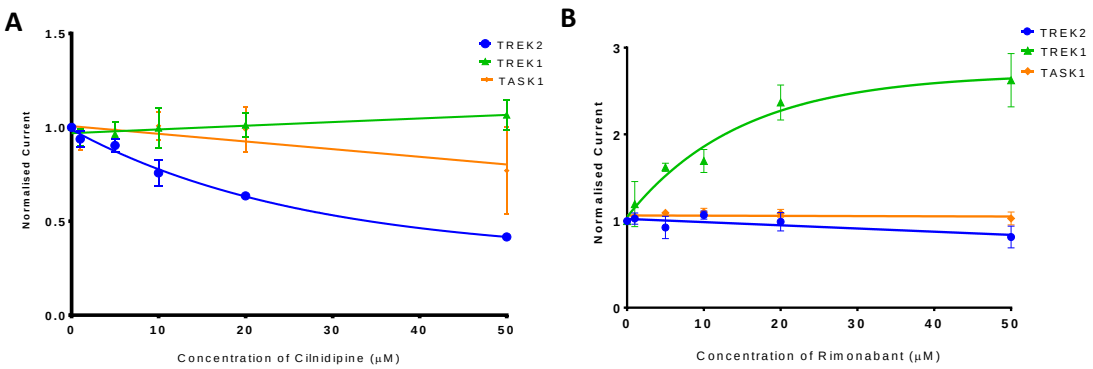

Figure 6.10: Cilnidipine and Rimonabant effects on TREK and TASK-expressing oocytes. *Oocytes were perfused with increasing concentrations of compound and their current reading at +70 mV was collected using a steps protocol and compared to the native current of the TREK expressing oocytes. Each experiment was conducted in triplicate and data is expressed as normalised current Mean ± SEM. A one-phase decay curve was fitted for the TREK data but linear regression was used for the TASK data. Cilnidipine data is shown in Figure 6.10A while rimonabant data is shown in Figure 6.10B.*

It is seen from Figure 6.10 that neither cilnidipine nor rimonabant exhibit any significant effect on TASK1 function.

6.3.6 Cilnidipine Effects on TREK2 Function in Excised Patches

Cilnidipine effects on TREK2 function were next investigated in excised patches by manual patch clamping. The experiments were performed by Dr. M. Arcangeletti. of the Tucker group at the Department of Physics and constitute a follow-up to the two electrode voltage clamp experiments conducted earlier as part of this thesis. It was shown in Figure 6.11 that cilnidipine exhibits a dose-dependent inhibition on TREK2 in excised patches (IC_{50} = 1 µM). The effect of cilnidipine is also shown to be reversible in Figure 6.12.

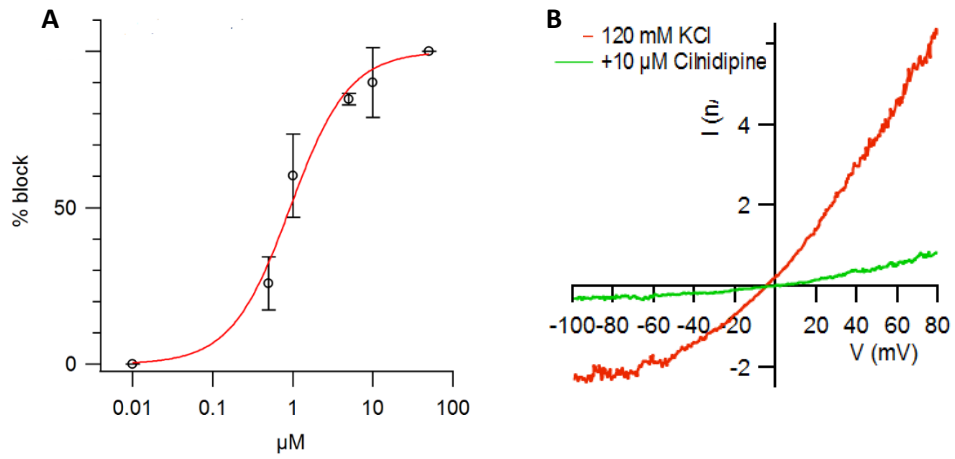

Figure 6.11: Cilnidipine effects on TREK2 as measured in excised patches from Xenopus oocytes. *Figure 6.11A shows the dose response inhibition effect of cilnidipine on TREK2 function in excised patches. Figure 6.11B shows the IV relationship of currents recorded in excised patches (Data and figure courtesy of M. Arcangeletti).*

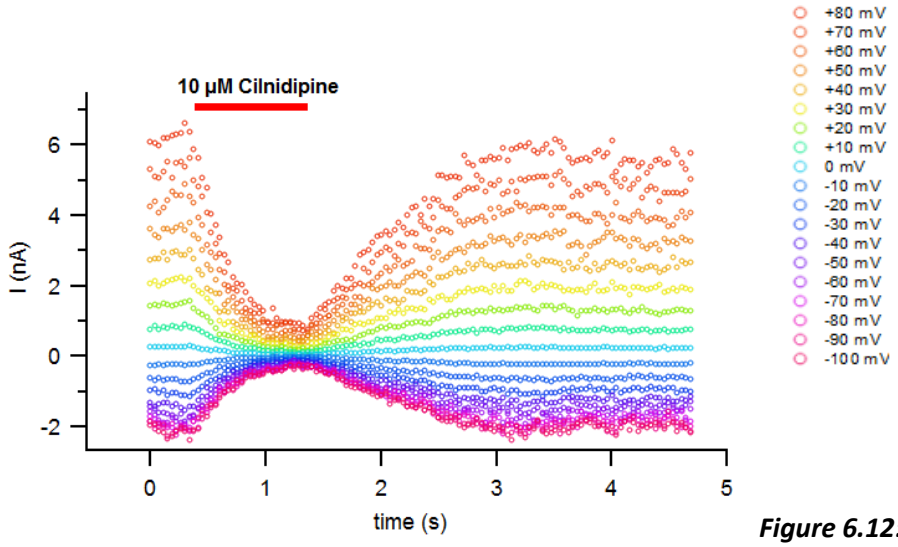

Figure 6.12: Cilnidipine effects on TREK2 as measured in excised patches from Xenopus oocytes using a step protocol. *The action of cilnidipine on TREK2 in excised patches is reversible when the compound is washed out with buffer after a steps protocol. (Data and figure courtesy of M. Arcangeletti).*

The effects of rimonabant on TREK1 in excised patches have also been investigated, but there is not enough evidence to suggest a direct effect of the compound on the channel.

6.4 Discussion

In chapter 5, we obtained a subset of 20 compounds consisting of compounds which changed the thermostability of either TREK1 or TREK2 along with some controls. These compounds were taken forward to be tested on their functional effects on the channels described in this chapter.

A single point screen at 20 µM was first performed in order to replicate the concentration of compound used in both the biophysical assays. However, many of the compounds found to affect the stability of purified TREK proteins did not appear to affect the functional activity of TREK1 or TREK2. There are a few possible explanations for this phenomenon, which are discussed below:

1. Detergent Effects – As TREKs are purified in detergent micelles, the compounds may interact with the detergent to cause the apparent shift in thermostability in both assays. The protein within the detergent micelle may also be in a slightly different conformation to that within the cell membrane, which can change the binding properties of a compound. Permeability to small molecules of the detergent micelle and cell membrane is also different, which can change the ability of a compound to access its binding site in the ion channel.
2. Signalling Pathways – The cell system is much more complex than a protein only system, with signalling pathways also involved in regulating the function of the ion channel. A compound could be interacting with other parts of a signalling system which affects K2P function, augmenting or mitigating its direct effect and leading to the presence or absence of phenotypical changes. This often leads to false positive results seen in TEVC but not in excised patches.

3. Buffer Conditions – The pH and salt conditions are somewhat different between the biophysical and electrophysiology tests. This can affect the function of an ion channel and lead to differences in data. The conditions in which the electrophysiology experiments were conducted are much closer to physiological conditions within which cells are present.
4. Temperature – Both the DSF assays involve heating of the protein and measure the ability of a compound to change thermostability, which can only be accurately determined close to the melting point of the proteins. At such high temperatures, proteins may adopt slightly different conformations than those found in a constant lower temperature present in cells. This may also change the ability of the K2Ps to bind to some small molecules.
5. Construct – The biophysical assays were conducted with truncated protein constructs while the electrophysiology was conducted with full length protein. The extra parts of the protein which were present in the electrophysiology assays may have prevented binding of small molecules which were seen to interact with truncated protein constructs.

Nevertheless, despite these negative results, 2 compounds were identified which changed the thermostability of the proteins and affected their functional activity. These were cilnidipine for TREK2 and rimonabant for TREK1.

The dose response experiments showed that the effects of both cilnidipine and rimonabant were dose dependent and fit on a 1-phase decay curve, suggesting an effect which can be saturated at high concentrations. The EC_{50} and IC_{50} of both compounds with TREK2 and TREK1 respectively were determined and both found to exhibit effects in the 10^{-5}M range. This is in line with most other known binders of both proteins such

as norfluoxetine, BL1249 and penfluridol, but not potent enough to be considered as molecules with therapeutic potential. Cilnidipine shares the same dihydropyridine chemical skeleton which other reported inhibitors of TREK1 such as nifedipine and amlodipine have (IC_{50} < 1 μM on TREK1)[87]. Cilnidipine was also shown to inhibit TREK2 function in excised patches at a much higher potency. The IC_{50} of cilnidipine at 1 μM represents one of the most potent intracellular blockers of this protein. Cilnidipine has an IC_{50} of 10 nM against L-type Ca channels[208].

It is interesting that cilnidipine only seems to have an effect on TREK2 as detected in both the thermostability and electrophysiology assays. Structural-activity relationships should be determined with compounds with similar scaffold with the aim of improving potency as well as better understanding selectivity of the compounds within the K2P family of proteins. Follow-up experiments using a range of commercially available analogues of cilnidipine and rimonabant have been planned and will be carried out in the near future by other members of the group.

Both cilnidipine and rimonabant were then tested against TASK1 to elucidate any possible off-target effects with a related protein. TASK1 was chosen as this protein was also used as a control for thermostability assays in Chapter 5 and both purified protein as well as mRNA were available for use. Both compounds were found to have no significant functional effect on TASK1, which corroborates with the data obtained in the thermostability assay. If any compound developed shows potential as a potent modulator of TREK1 or TREK2, then its selectivity will need to be tested against a larger panel of K2P channels as well as representatives from other unrelated ion channel families. This process would be similar to selectivity panels in use for other assays in the pharmaceutical industry.

The TEVC technique has obvious limitations, chief of which being that it does not isolate the ion channel and any effect observed may be due to non-specific interactions. However, the effect of cilnidipine in excised patches suggests that this is a direct effect. Unfortunately, not enough data was available for rimonabant at the time of writing this thesis.

Other than biophysical and electrophysiological experiments, in order to further characterise the interaction between protein and compound, it is possible that structural studies can be carried out. For example, co-crystallisation with both TREK2 and TREK1 is a very possible strategy. Structural information would be very helpful to rational drug design and would make the process of drug discovery much more efficient.

6.5 Conclusion

Overall this work has found 2 novel ligands for TREK2 and TREK1 starting from a small library of compounds which are already used as drugs for different targets. While significant follow up tests must be performed before further investment should be considered, the studies in this chapter appear to validate this overall biophysical assay for drug-screening against ion channels and may provide a blueprint for future projects.

Chapter 7: Overall Discussion and Broader Perspectives

7.1 Overall Discussion of Biophysical Methods in Ion Channel Drug Discovery

As discussed in this work, biophysical methods represent a viable alternative to existing cell-based techniques in drug discovery for ion channels. They can be used for initial screening, secondary screening and for hit to lead optimisation. The pros and cons of such an approach are as follows:

Simplicity of System: Biophysical methods make use of protein-ligand only systems, which make any interaction detected this way much more likely to be directly on the protein and not through any signalling system.

Membrane Environments: While efforts have been made to mimic the cell membrane by using cholesterol hemisuccinate in combination with detergents in this work, detergent micelles represent a vastly different environment for ion channel proteins as compared to cell membranes. This is always a potential confounding factor for any biophysical measurement that relies on protein purified in detergent.

Data Obtained: Electrophysiology gives only a functional readout, while biophysical techniques can give binding data and can provide insights into the mode and strength of binding between a protein and ligand, allowing for further drug development through the investigation of structure-activity relationships.

Ease and Cost of Usage: Many biophysical measurements can be carried out at a much lower cost in terms of protein, compound usage and time as compared to traditional electrophysiology. Much of the equipment used for biophysical measurements are also significantly easier to use and less costly than those used for high-throughput electrophysiology. For example, thermal shift assays only require a RT-PCR machine with

the correct fluorescent detection light filters, and this machine is very commonly found in molecular biology laboratories and thus this method would not require large amounts of investment in equipment.

The determination of whether to use biophysical techniques to investigate protein-ligand interactions is determined by the ease and cost of protein purification, compound availability and solubility, the cost of equipment acquisition and maintenance and ultimately, a cost-benefit analysis per data point obtained, especially for drug screening.

The range of biophysical techniques suitable for ion channel drug discovery was discussed in Chapter 1 and they have vastly different requirements and usage. The main similarity is the requirement for solubilised and purified protein as well as soluble target compounds. The amount of protein required, tagging of protein, ability to measure binding parameters (K_d, kinetics etc.) and amount of throughput is shown in Table 7.1 below:

Technique	Amount of Protein Required per Sample (g)	Tagging Requirement	Ability to Measure Binding Parameters	Throughput (Assuming 1 machine, per day)
Differential Scanning Fluorimetry	10^{-6}	None	No	10^4 samples
Label-Free DSF	10^{-6}	None	No	10^3 samples
Isothermal Titration Calorimetry	10^{-4} to 10^{-3}	None	Yes, K_d, stoichiometry, binding energetics.	10^0 samples
Surface Plasmon Resonance	10^{-8} to 10^{-6}	None required, but possible for indirect capture techniques.	Yes, K_d, binding kinetics.	10^0 to 10^4 samples
Microscale Thermophoresis	10^{-6}	Fluorescent tag required.	Yes, K_d, stoichiometry.	10^1 to 10^2 samples
Biolayer Interferometry	10^{-8} to 10^{-7}	His, GST or Strepavidin tag required.	Yes, K_d, stoichiometry, binding kinetics.	10^3 samples
Intact Mass Spectrometry	10^{-6} to 10^{-5}	None	Yes, stoichiometry only.	10^2 samples
Nuclear Magnetic Resonance	10^{-4} to 10^{-3}	None, but isotopic NMR possible.	Yes, stoichiometry only.	10^1 samples

Table 7.1: Table of Comparison between Biophysical Techniques used to investigate protein-ligand interactions.

The methods above also have other specific requirements for proteins and ligands. These are discussed below:

Differential Scanning Fluorimetry: For integral membrane proteins, it is not suitable to use a hydrophobic region-binding dye as this would result in very high background signals due to the conformation of such proteins. If a cysteine binding dye was used, the number of internal cysteines that the protein contains will affect the amount of protein used per sample. The presence of reducing agents within the buffer must also be taken into consideration as this would break disulphide bonds and cause increased

background signals if there are exposed disulphide bonds. In addition, the target compound should not fluoresce at the wavelength where the dye is either excited or absorbed at as this would cause a change in signal intensity.

Label Free DSF: The signal obtained is dependent on internal aromatic residues, particularly tryptophan. Thus, the amount of sample required is inversely related to the number of internal tryptophan residues.

Isothermal Titration Calorimetry: This method is very sensitive to buffer inequalities between the solution containing protein and that containing ligand. If detergents were used in purification process for the protein, they must be exactly matched and this is difficult as detergent molecules form micelles around proteins, making total detergent concentration within the sample higher than the free detergent concentration. Much optimisation must be performed to minimise buffer mismatch. Also, 'C' value restrictions require high concentrations of both protein and ligand to be used and thus very high amounts of protein are required to perform meaningful measurements. If a high concentration of protein is required, buffer mismatch is more likely. Ligand must also be soluble at the concentration desired.

Surface Plasmon Resonance: Protein must be stable at immobilisation pH (pH 4 - 5) as this is much lower than physiological pH. If chip is to be reused, protein must be able to remain in functional state after regeneration of surface which occurs in either highly acidic or alkaline conditions.

Nuclear Magnetic Resonance: Protein must be relatively small (<30 kDa) for interpretable signal to be obtained.

While the above requirements must be taken into consideration when planning for biophysical assays, the throughput of the assay and nature of the screening process are also very important. Higher throughput methods such as DSF would provide less information on protein-ligand interactions and have much higher false positive and negative rates than lower throughput methods such as ITC. Some assays are more suitable for primary screening and others for hit validation and profiling. These differences are illustrated in Figure 7.1.

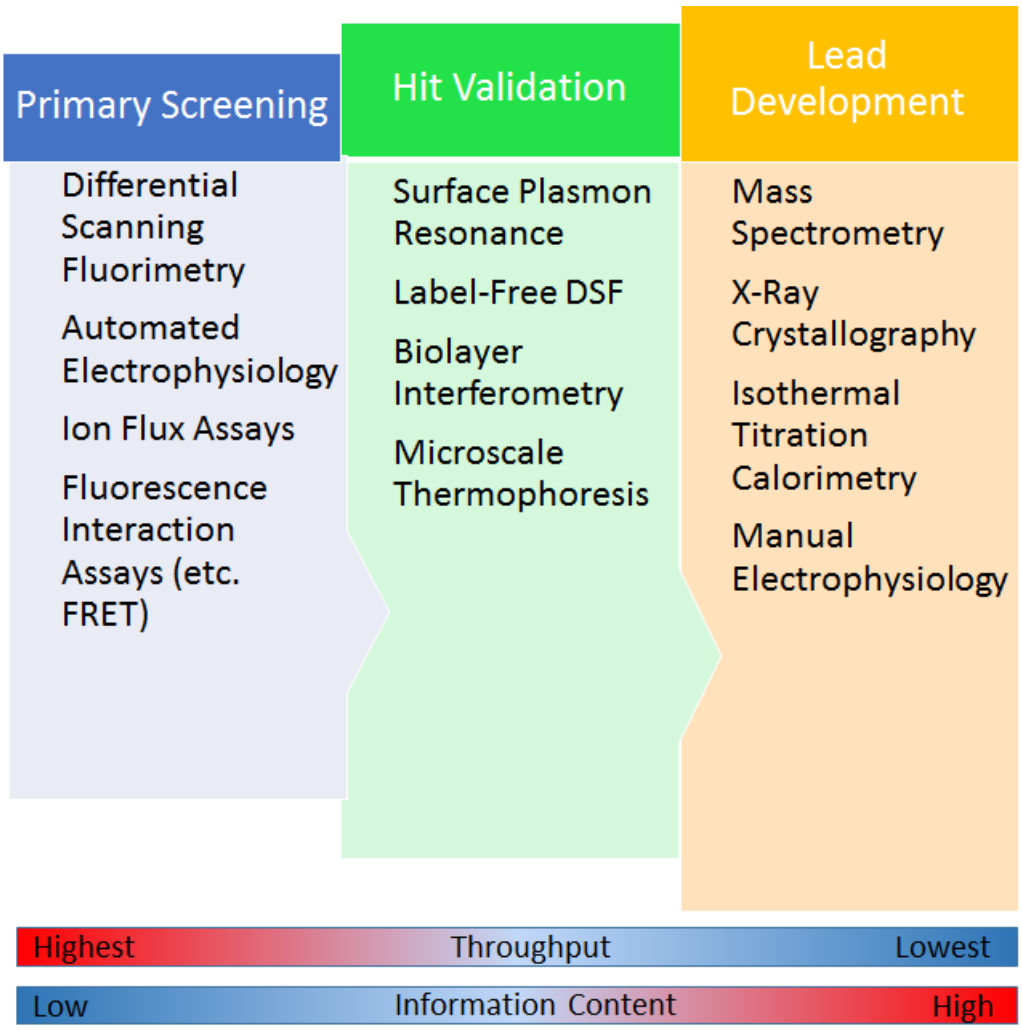

Figure 7.1: Biophysical and functional methods and their usage in the drug discovery process for ion channels. Highest throughput methods are used for primary screening while lower throughput methods that provide more information are mainly used only at the lead development phase. Cell based functional approaches are included in this figure for comparison purposes.

In order to properly utilise such biophysical methods in drug discovery, due consideration of the weaknesses and limitations of such methods should also be performed. The most important weakness of protein-ligand only methods lies in the environments which the proteins have been purified in.

Proteins which are purified within artificial membranes, liposomes or detergent micelles may fold and function differently to those within physiological cell membranes. Effects seen with such methods must thus be treated with this caveat in mind. Proving the functionality of the protein in purification conditions through functional assay is thus

essential. This issue is even more pertinent with a membrane stretch activated ion channel such as TREK2 or TREK1, where it is not clear if the detergent micelle environment these proteins are purified in change their activity from those in native cell membranes.

The detergent micelle environment may also interfere with assay output. This may be due to direct interaction between compound and detergent micelle. This may also be due to the detergent micelle environment allowing for the exposure of parts of the protein which would be not accessible in a native cell membrane, leading to compound interaction being seen that would not be possible otherwise. The reverse may also be true, with the detergent micelle obscuring and causing inaccessibility to compounds certain parts of a protein which may be otherwise targeted by compounds. A possible approach would be to investigate such interactions with methods using different protein stabilisation materials (liposomes, artificial membranes or cell-based approaches in addition to detergent micelles).

The strengths and limitations of each technique used in this thesis have been discussed in the relevant chapters. However, they are also summarised in Table 7.2 below:

Technique	Strengths	Weaknesses
DSF with Fluorescent Dye	Efficient and gives consistent data. Requires minimal equipment investment and training. Moderate amount of protein usage.	Thermodynamic measurement, not direct measure of binding. No measurement of binding parameters. Possible compound interference with fluorescent dye. Measurement at non-physiological temperatures. High false positive and false negative rate.
Label-Free DSF	Efficient and gives consistent data. Moderate amount of protein usage. Protein aggregation can be measured simultaneously via backreflection optics.	Thermodynamic measurement, not direct measure of binding. No measurement of binding parameters Measurement at non-physiological temperatures. Possible binding of protein-detergent micelles to capillary well may affect signal. Low throughput, cannot be used for primary screening.
Isothermal Titration Calorimetry	High information content, binding parameters can be determined. Can use competition assays to determine possible binding sites.	Very high sample usage. Low throughput. Needs extensive optimisation to minimise buffer mismatch.
Surface Plasmon Resonance	High information content. Low amount of protein usage. Can use competition assays to determine possible binding sites.	Requires immobilisation of protein, may lead to false negatives. Needs extensive optimisation for immobilisation, time consuming. Low to medium throughput depending on setup. Prone to artefacts due to compound aggregation or other non-specific effects.
Biolayer Interferometry	High information content. Low amount of protein usage. Can use competition assays to determine possible binding sites. Protein is always captured in same position due to tagging requirement.	Requires immobilisation of protein, may lead to false negatives. Low sensitivity for protein-ligand interaction analysis, much more suited to protein-protein interactions. Requires tagging of protein.

Table 7.2: Strengths and Weaknesses of Biophysical Techniques used in this Work.

In addition to the inherent strengths and weaknesses of the individual techniques, thought should also be given to how proteomics can be integrated into these assays to obtain more information about protein-ligand interactions. For example, site directed mutagenesis can be performed for a putative binding site to verify if binding occurs at that region of the protein. Competition assays with known ligands would also provide further information on binding, especially if the binding site of the known ligand is known through structural methods.

7.2 Summary of Findings in this Thesis and Evaluation of Methods Used.

This work has shown, for a group of ion channels, it is possible to conduct medium throughput screening to find novel compounds that interact with the protein and modulate their function. This is done by performing an initial DSF screen on 351 compounds, then selecting a set of 20 compounds which have differing effects on the protein and testing them using an orthogonal biophysical method (Label-free DSF) and a cell based method (TEVC). The overall result of discovering 1 novel inhibitor of TREK2 and 1 novel activator of TREK1 is remarkable given the small number of compounds screened and is proof of concept that such an approach is workable.

However, there are many shortcomings for the data presented. Some of these flaws are discussed in Chapters 3 and 4 as well as Section 7.1. In chapter 4, I was not able to obtain binding curves for both ITC and SPR. While this may be explained by the presence of detergent or other confounding factors, an important consideration was also the lack of time and resources to further optimise these techniques. SPR with indirect capture using an antibody which bound to the chip could certainly have been attempted even though initial trials using this method showed no immobilisation of TREK2 when an anti-His monoclonal antibody was used (Data not shown). Another limitation of SPR is the lack

of knowledge of protein conformation at the immobilisation pH, which is significantly lower than that of protein purification and physiological conditions. This should be verified through functional means with purified protein if possible.

The data as presented also only shows that the proteins and compounds are interacting in a manner that changes its function. More information about the nature of the interaction can be gained through a few means. For example, the binding pocket for norfluoxetine and TREK2 is known through crystallography. A competition assay can be set up using norfluoxetine and the target compound using a functional method. If there is a competition effect, we can deduce that the binding pocket for the compound near or the same as that for norfluoxetine. Another method to gain insight on the nature of binding is to use nanobodies or site directed mutagenesis on a purported binding site obtained through experimental means or modelling. If the binding interaction is stopped by such interference, it would be definitive proof of the site involving the mutated or blocked residues. Competition assays would not be possible with either form of DSF but mutagenesis or nanobody based assays would be as the competing ligand would also trigger a T_m shift and this would not be quantifiable when a new ligand is added.

While each of the methods shown in Table 7.2 have been tested on a range of proteins which the Carpenter group works on (Integral Membrane Proteins), progress on the characterisation of such methods on other integral membrane proteins is slow due to the lack of protein sample available. It is imperative to reduce the cost of production of integral membrane protein samples for such methods to be in direct competition with high-throughput cell based methods for primary screening.

In conclusion, biophysical approaches should be considered for hit validation with smaller numbers of compounds as they can provide information which cell-based assays

are not able to, such as changes in protein stability or binding parameters. They are also able to remove any confounding factors based on cell signalling, which may provide false positive results in cell based assays. They can also be used for lead development, where structure-activity relationships are investigated to find more potent or selective compounds. Overall, these approaches provide quality data to complement traditional high throughput screening methods and can greatly improve our understanding of protein-ligand interactions at a lower material cost than structural approaches.

References

1. Alberts, B *et al.*, *Molecular Biology of the Cell 5th Edition* (Garland Science, 2008).

2. Jegla, T. J. *et al.*, Evolution of the human ion channel set. *Comb Chem High Throughput Screen.* **12(1)**, 2-23 (2009).

3. Gadsby, D. C., Ion channels versus ion pumps: the principal difference, in principle. *Nat Rev Mol Cell Biol.* **10,** 344–52 (2009).

4. Doyle, D. A., Structural changes during ion channel gating. *Trends Neurosci*. **27(6)**, 298-302 (2004).

5. Catterall, W. A., Ion channel voltage sensors: structure, function, and pathophysiology. *Neuron* **67,** 915–28 (2010).

6. Sherwood, T. W. *et al.*, Structure and activity of the acid-sensing ion channels. *Am J Physiol Cell Physiol.* **303,** C699–710 (2012).

7. Haswell, E. S. *et al.*, Mechanosensitive channels: what can they do and how do they do it? *Structure* **19,** 1356–69 (2011).

8. Cao, E. *et al.*, TRPV1 channels are intrinsically heat sensitive and negatively regulated by phosphoinositide lipids. *Neuron* **77,** 667–79 (2013).

9. Nagel, G. *et al.,* Channelrhodopsin-2, a directly light-gated cation-selective membrane channel. *Proc Natl Acad Sci.* **100,** 13940–13945 (2003).

10. Goto M. et al., Properties of ligand-gated potassium channels in neurons of rat dorsolateral septal nucleus. *Kurume Med J.* **44(2)**, 125-133 (1997).

11. Venkatachalam K. and Montell C., TRP channels. *Annu Rev Biochem.* **76**, 387-417 (2007).

12. Owsianik, G. *et al*., Permeation and selectivity of TRP channels. *Annu Rev Physiol.* **68,** 685–717 (2006).

13. Schroeder, J. I. & Hedrich, R. Involvement of ion channels and active transport in osmoregulation and signaling of higher plant cells. *Trends Biochem Sci.* **14,** 187–92 (1989).

14. Mowrey, D. *et al.* Signal transduction pathways in the pentameric ligand-gated ion channels. *PLoS One* **8,** e64326 (2013).

15. Schwab, A. *et al.*, Role of ion channels and transporters in cell migration. *Physiol Rev.* **92,** 1865–913 (2012).

16. Kim, J., Channelopathies. *Korean J Pediatr.* **57(1)**, 1-18 (2014).

17. Bagal S. K. et al., Ion channels as therapeutic targets: a drug discovery perspective. *J Med Chem.* **56(3)**, 593-624 (2013).

18. Katz A. M., Pharmacology and mechanisms of action of calcium-channel blockers. *J Clin Hypertens.* **2(3 Suppl.)**, 28S-37S (1986).

19. Overington J. P. *et al.*, How many drug targets are there? *Nat Rev Drug Discov.* **5(12)**, 993-6 (2006).

20. Clare, J. J., Targeting ion channels for drug discovery. *Discov Med.* **9(46)**, 253-60 (2010).

21. Sakmann, B. and Neher, E., Patch clamp techniques for studying ionic channels in excitable membranes. *Annu Rev Physiol.* **46**, 455-72 (1984).

22. Miller, C., An overview of the potassium channel family. *Genome Biol.* **1(4)**, reviews0004.1–reviews0004.5 (2000).

23. Starace, D. M. and Bezanilla, F., Histidine scanning mutagenesis of basic residues of the S4 segment of the shaker K^+ channel. *J Gen Physiol.* **117(5)**, 469-490 (2001).

24. David, M. *et al.*, Interactions between GABA-B1 receptors and Kir 3 inwardly rectifying potassium channels. *Cell Signal.* **18(12)**, 2172-81 (2006).

25. Liu, P. W. and Bean, B. P., Kv2 channel regulation of action potential repolarization and firing patterns in superior cervical ganglion neurons and hippocampal CA1 pyramidal neurons. *J Neurosci.* **34,** 4991–5002 (2014).

26. McFerrin, M. B. *et al*., Differential role of IK and BK potassium channels as mediators of intrinsic and extrinsic apoptotic cell death. *Am J Physiol Cell Physiol.* **303,** C1070–8 (2012).

27. Iwanir, S. and Reuveny, E., Adrenaline-induced hyperpolarization of mouse pancreatic islet cells is mediated by G protein-gated inwardly rectifying potassium (GIRK) channels. *Pflügers Arch* **456***,* 1097–1108 (2008).

28. Choe, S., Potassium channel structures. *Nat Rev Neurosci.* **3(2)**, 115-21 (2002).

29. Zhou, C. *et al.*, General anaesthesia mediated by effects on ion channels. *World J Crit Care Med*. **1(3)**, 80-93 (2012).

30. Miller, A. N. and Long, S. B., Crystal structure of the human two-pore domain potassium channel K2P1. *Science* **335,** 432–6 (2012).

31. Brohawn, S. G., del Marmol, J. & MacKinnon, R. Crystal Structure of the Human K2P TRAAK, a Lipid- and Mechano-Sensitive K^+ Ion Channel. *Science* **335,** 436–441 (2012).

32. Ketchum, K. A. *et al.*, A new family of outwardly rectifying potassium channel proteins with two pore domains in tandem. *Nature* **376(6542),** 690-5 (1995).

33. Czempinski, K. *et al.*, New structure and function in plant K^+ channels: KCO1, an outward rectifier with a steep Ca2+ dependency. *EMBO J.* **16,** 2565–75 (1997).

34. Lesage, F. *et al.* TWIK-1, a ubiquitous human weakly inward rectifying K^+ channel with a novel structure. *EMBO J.* **15,** 1004–11 (1996).

35. Hodgkin, A. L. and Huxley A. F., Potassium leakage from an active nerve fibre. *J Physiol.* **106**, 341 (1947).

36. Honoré, E., The neuronal background K2P channels: focus on TREK1. *Nat Rev Neurosci.* **8,** 251–61 (2007).

37. Chen, H. *et al.*, Classification of 2-pore domain potassium channels based on rectification under quasi-physiological ionic conditions. *Channels (Austin)* **8(6)**, 503-8 (2014).

38. Hodgkin, A. L. and Huxley, A. F., A quantitative description of membrane current and its application to conduction and excitation in nerve. *J Physiol.* **117**, 500 (1952).

39. Goldstein, S. A. M. *et. al.*, Potassium leak channels and the KCNK family of two-p-domain subunits. *Nature Rev Neurosci.* **2**, 175-184 (2001).

40. Enyedi, P. & Czirják, G. Molecular background of leak K^+ currents: two-pore domain potassium channels. *Physiol Rev.* **90,** 559–605 (2010).

41. Ma, L. *et al.*, Acid-sensitive TWIK and TASK two-pore domain potassium channels change ion selectivity and become permeable to sodium in extracellular acidification. *J Biol Chem.* **287 (44)**, 37145-53 (2012).

42. Rajan, S. *et al.*, TASK-3, a novel tandem pore domain acid-sensitive K^+ channel. An extracellular histiding as pH sensor. *J Biol Chem.* **275 (22),** 16650-7 (2000).

43. Patel, A. J. *et al.*, TWIK-2, an inactivating 2P domain K^+ channel. *J Biol Chem.* **275 (37),** 28722-30 (2000).

44. Chatelain, F. C. *et al.*, TWIK1, a unique background channel with variable ion selectivity. *Proc Natl Acad Sci.* **109(14)**, 5499-504 (2012).

45. Brohawn, S. G., How ion channels sense mechanical force: insights from mechanosensitive K2P channels TRAAK, TREK1, and TREK2. *Ann N Y Acad Sci.* **1352**, 20-32 (2015).

46. Kang, D. and Kim, D., Single-channel properties and pH sensitivity of two-pore domain K^+ channels of the TALK family. *Biochem Biophys Res Commun.* **315(4),** 836-44 (2004).

47. Czirják, G. *et al.*, The two-pore domain K^+ channel, TRESK, is activated by the cytoplasmic calcium signal through calcineurin. *J Biol Chem.* **279(18),** 18550-8 (2004).

48. Wischmeyer, E. *et al.*, THIK-1 and THIK-2, a novel subfamily of tandem pore domain K^+ channels. *J Biol Chem.* **276(10)**, 7302-11 (2001).

49. Czirják, G. and Enyedi, P., Formation of functional heterodimers between the TASK-1 and TASK-3 two-pore domain potassium channel subunits. *J Biol Chem.* **277**, 5426–32 (2002).

50. Blin, S. *et al.*, Mixing and matching TREK/TRAAK subunits generate heterodimeric K_{2P} channels with unique properties. *Proc Natl Acad Sci.* **113(15)**, 4200-5 (2016).

51. Hwang, E. M. *et al.*, A disulphide-linked heterodimer of TWIK-1 and TREK-1 mediates passive conductance in astrocytes. *Nat Commun.* **5**, 3227 (2014).

52. Rees, D. C. *et al.*, Crystallographic analyses of ion channels: lessons and challenges. *J Biol Chem.* **275(2),** 713-6 (2000).

53. Doyle, D. A. *et al.* The structure of the potassium channel: molecular basis of K^+ conduction and selectivity. *Science* **280,** 69–77 (1998).

54. Morais-Cabral, J. H. *et al.*, Energetic optimization of ion conduction rate by the K^+ selectivity filter. *Nature* **414(6859)**, 37-42 (2001).

55. Long, S. B. *et al.*, Crystal structure of a mammalian voltage-dependent Shaker family K^+ channel. *Science* **309(5736)**, 897-903 (2005).

56. Hansen, S. B. *et al.*, Structural basis of PIP2 activation of the classical inward rectifier K^+ channel Kir2.2. *Nature* **477(7365)**, 495-8 (2011).

57. Jiang, Y. *et al.*, Crystal structure and mechanism of a calcium-gated potassium channel. *Nature* **417(6888)**, 515-22 (2002).

58. Brohawn, S. G. *et al.*, Crystal Structure of the Human K2P TRAAK, a Lipid- and Mechano-Sensitive K^+ Ion Channel. *Science* **335,** 436–441 (2012).

59. Dong, Y. Y. *et al.*, K2P channel gating mechanisms revealed by structures of TREK-2 and a complex with Prozac. *Science* **347,** 1256-1259 (2015).

60. Poulsen, H. and Nissen, P., Structural biology. The inner workings of a dynamic duo. *Science* **335(6067)**, 416-7 (2012).

61. Hibino, H. *et al.*, Inwardly rectifying potassium channels: their structure, function, and physiological roles. *Physiol Rev.* **90(1)**, 291-366 (2010).

62. Schewe, M. *et al.*, A Non-canonical Voltage-Sensing Mechanism Controls Gating in K2P K(+) Channels. *Cell* **164(5)**, 937-49 (2016).

63. Friedrich, C. *et al.*, Gain-of-function mutation in TASK-4 channels and severe cardiac conduction disorder. *EMBO Mol Med.* **6(7)**, 937-51 (2014).

64. Lafrenière, R. G. *et al.*, A dominant-negative mutation in the TRESK potassium channel is linked to familial migraine with aura. *Nat Med.* **16(10)**, 1157-60 (2010).

65. Fink, M. *et al.,* Cloning, functional expression and brain localization of a novel unconventional outward rectifier K^+ channel. *EMBO J.* **15,** 6854–62 (1996).

66. Bang, H. *et al.*, TREK-2, a new member of the mechanosensitive tandem-pore K^+ channel family. *J Biol Chem.* **275,** 17412–9 (2000).

67. Fink, M. *et al.*, A neuronal two P domain K^+ channel stimulated by arachidonic acid and polyunsaturated fatty acids. *EMBO J.* **17(12)**, 3297-308 (1998).

68. Noël, J. *et al.*, Molecular regulations governing TREK and TRAAK channel functions. *Channels (Austin).* **5,** 402–9 (2011).

69. Gu, W. *et al.*, Expression pattern and functional characteristics of two novel splice variants of the two-pore-domain potassium channel TREK-2. *J Physiol.* **539**, 657-668 (2002).

70. Veale, E. L. *et al.*, Dominant negative effects of a non-conducting TREK1 splice variant expressed in brain. *J Biol Chem.* **285(38),** 29295-304 (2010).

71. Thomas, D. *et al.*, Alternative translation initiation in rat brain yields K2P2.1 potassium channels permeable to sodium. *Neuron* **58,** 859–70 (2008).

72. Simkin, D. *et al.*, Control of the single channel conductance of K2P10.1 (TREK-2) by the amino-terminus: role of alternative translation initiation. *J Physiol.* **586,** 5651–63 (2008).

73. Chemin, J. *et al.*, Regulation of the mechano-gated K2P channel TREK-1 by membrane phospholipids. *Current Topics in Membranes* **59(7)**, 155-170 (2007).

74. Alloui, A. *et al.*, TREK-1, a K^+ channel involved in polymodal pain perception. *EMBO J.* **25(11)**, 2368-76 (2006).

75. Heurteaux, C. *et al.*, TREK-1, a K^+ channel involved in neuroprotection and general anesthesia. *EMBO J.* **23(13),** 2684-95 (2004).

76. Heurteaux, C. *et al.*, Deletion of the background potassium channel TREK-1 results in a depression-resistant phenotype. *Nat Neurosci.* **9(9)**, 1134-41 (2006).

77. Franks, N. P. and Honoré, E., The TREK K2P channels and their role in general anaesthesia and neuroprotection. *Trends Pharmacol Sci.* **25(11)**, 601-8 (2004).

78. Pereira, V. *et al.*, Role of the TREK2 potassium channel in cold and warm thermosensation and in pain perception. *Pain* **155(12)**, 2534-44 (2014).

79. Patel, A. J. *et al.*, Inhalational anesthetics activate two-pore-domain background K^+ channels. *Nat Neurosci.* **2(5),** 422-426 (1999).

80. Bertaccini, E. J. *et al.*, Molecular modeling of a tandem two pore domain potassium channel reveals a putative binding site for general anesthetics. *ACS Chem Neurosci.* **5(12)***,* 1246-1252 (2014).

81. Duprat, F. *et al.*, The neuroprotective agent riluzole activates the two P domain K(+) channels TREK-1 and TRAAK. *Mol Pharmacol.* **57(5)**, 906-912 (2000).

82. Minieri, L. *et al.* The inhibitor of volume-regulated anion channels DCPIB activates TREK potassium channels in cultured astrocytes. *Br J Pharmacol.* **168,** 1240–54 (2013).

83. Takahira, M. *et al.*, Fenamates and diltiazem modulate lipid-sensitive mechano-gated 2P domain K(+) channels. *Pflugers Arch.* **451,** 474–8 (2005).

84. Tertyshnikova, S. *et al.*, BL-1249 [(5,6,7,8-tetrahydro-naphthalen-1-yl)-[2-(1H-tetrazol-5-yl)-phenyl]-amine]: a putative potassium channel opener with bladder-relaxant properties. *J Pharmacol Exp Ther.* **313(1)**, 250-9 (2005).

85. Saeki, Y. *et al.*, The presence of arachidonic acid-activated K^+ channel, TREK-1, in human periodontal ligament fibroblasts. *Drug Metab Rev.* **39(2-3)**, 457-65 (2007).

88. Gomora, J. C. and Enyeart, J. J., Dual pharmacological properties of a cyclic AMP-sensitive potassium channel. *J Pharmacol Exp Ther.* **290(1)**, 266-75 (1999).

87. Liu, H. *et al.*, Potent inhibition of native TREK-1 K^+ channels by selected dihydropyridine Ca2+ channel antagonists. *J Pharmacol Exp Ther.* **323(1),** 39-48 (2007).

88. Nayak, T. K. *et al.*, Inhibition of human two-pore domain K^+ channel TREK1 by local anesthetic lidocaine: negative cooperativity and half-of-sites saturation kinetics. *Mol Pharmacol.* **76(4),** 903-17 (2009).

89. Kennard, L. E. *et al.*, Inhibition of the human two-pore domain potassium channel, TREK-1, by fluoxetine and its metabolite norfluoxetine. *Br J Pharmacol.* **144(6)**, 821-9 (2005).

90. Hughes, J. P. *et al.*, Principles of Early Drug Discovery. *Br J Pharmacol.* **162(6)**, 1239-49 (2011).

91. Willmann, J. K. *et al.*, Molecular Imaging in Drug Development. *Nat Rev Drug Discovery* **7**, 591-607 (2008).

92. Pereira, D. A. and Williams J. A., Origin and evolution of high throughput screening. *Br J Pharmacol.* **152(1)**, 53-61 (2007).

93. Leach, A. R. *et al.*, Fragment Screening: an Introduction. *Mol Biosyst.* **2(9)**, 430-46 (2006).

94. Ciulli, A., Biophysical screening for the discovery of small-molecule ligands. *Methods Mol Biol.* **1008**, 357-88 (2013).

95. Silvestre, H. L. *et al.*, Integrated biophysical approach to fragment screening and validation for fragment-based lead discovery. *Proc Natl Acad Sci.* **110(32)**, 12984-9 (2013).

96. Chen, X. *et al.*, A ligand-observed mass spectrometry approach integrated into the fragment based lead discovery pipeline. *Sci Rep.* **10(5)**, 8361 (2015).

97. Zakharian, E., Recording of ion channel activity in planar lipid bilayer experiments. *Methods Mol Biol.* **998**, 109-18 (2013).

98. Coronado, R. and Latorre, R., Phospholipid bilayers made from monolayers on patch-clamp pipettes. *Biophys J.* **43**, 231–236 (1983).

99. Nimigean, C. M., A radioactive uptake assay to measure ion transport across ion channel-containing liposomes. *Nat Protoc.* **1(3)**, 1207-12 (2006).

100. Holdgate, G. *et al.*, Biophysical methods in drug discovery from small molecule to pharmaceutical. *Methods Mol Biol.* **1008**, 327-55 (2013).

101. Renaud, J. P. *et al.*, Biophysics in drug discovery: impact, challenges and opportunities. *Nat Rev Drug Discov.* **15(10)**, 679-98 (2016).

102. Carpenter, E. P. *et al.*, Overcoming the challenges of membrane protein crystallography. *Curr Opin Struct Biol.* **18(5)**, 581-6 (2008).

103. Patching, S. G., Surface plasmon resonance spectroscopy for characterisation of membrane protein-ligand interactions and its potential for drug discovery. *Biochim Biophys Acta.* **1828(1 Pt A)**, 43-55 (2014).

104. Bergsdorf, C. *et al.*, An Alternative Thiol-Reactive Dye to Analyze Ligand Interactions with the Chemokine Receptor CXCR2 Using a New Thermal Shift Assay Format. *J Biomol Screen.* **21(3)**, 243-51 (2016).

105. Quigley, A. *et al.*, The structural basis of ZMPSTE24-dependent laminopathies. *Science* **339(6127)**, 1604-7 (2013).

106. Hresko, R. C. *et al.*, Mammalian Glucose Transporter Activity Is Dependent upon Anionic and Conical Phospholipids. *J Biol Chem.* **291(33)**, 17271-82 (2016).

107. Pace, C. N. *et al.*, How to measure and predict the molar absorption coefficient of a protein. *Protein Sci.* **4(11)**, 2411-23 (1995).

108. Savitsky, P. *et al.*, High-throughput production of human proteins for crystallization: the SGC experience. *J Struct Biol.* **172(1)**, 3-13 (2010).

109. Niesen, F. H. *et al.*, The use of differential scanning fluorimetry to detect ligand interactions that promote protein stability. *Nat Protoc.* **2(9)**, 2212-21 (2007).

110. Schellman, J. A., Temperature, stability, and the hydrophobic interaction. *Biophys J.* **73(6)**, 2960-4 (1997).

111. Semisotnov, G. V. *et al.*, Study of the "molten globule" intermediate state in protein folding by a hydrophobic fluorescent probe. *Biopolymers* **31(1)**, 119-28 (1991).

112. Pantoliano, M. W. *et al.*, High-density miniaturized thermal shift assays as a general strategy for drug discovery. *J Biomol Screen.* **6(6)**, 429-40 (2001).

113. Rodrigues, J. V. *et al.*, Protein stability in an ionic liquid milieu: on the use of differential scanning fluorimetry. *Phys Chem Chem Phys* **13(30)**, 13614-16 (2011).

114. Hawe, A. *et al.*, Extrinsic fluorescent dyes as tools for protein characterization. *Pharm Res.* **25(7)**, 1487-99 (2008).

115. Niu, L. *et al.*, BODIPY-based fluorescent probe for the simultaneous detection of glutathione and cysteine/homocysteine at different excitation wavelengths. *RSC Adv.* **5**, 3959-3964 (2015).

116. Alexandrov, A. I. *et al.*, Microscale fluorescent thermal stability assay for membrane proteins. *Structure* **16(3)**, 351-9 (2008).

117. Vivoli, M. *et al.*, Determination of Protein-ligand Interactions Using Differential Scanning Fluorimetry. *J Vis Exp*. **(91)**, e51809 (2014).

118. Lo, M. C. *et al.*, Evaluation of fluorescence-based thermal shift assays for hit identification in drug discovery. *Anal Biochem.* **332**, 153-9 (2004).

119. Sonoda, Y. *et al.*, Benchmarking membrane protein detergent stability for improving throughput of high-resolution X-ray structures. *Structure* **19(1)**, 17-25 (2011).

120. Liu, W. *et al.*, LCP-Tm: an assay to measure and understand stability of membrane proteins in a membrane environment. *Biophys J.* **98(8)**, 1539-48 (2010).

121. Ashok, Y. and Jaakola, V. P., Nanodisc-Tm: Rapid functional assessment of nanodisc reconstituted membrane proteins by CPM assay. *MethodsX* **14(3)**, 212-8 (2016).

122. Chung, C. C. *et al.*, A fluorescence-based thiol quantification assay for ultra-high-throughput screening for inhibitors of coenzyme A production. *Assay Drug Dev Technol.* **6(3)**, 361-74 (2008).

123. Tol, M. B. *et al.*, Thermal unfolding of a mammalian pentameric ligand-gated ion channel proceeds at consecutive, distinct steps. *J Biol Chem.* **288(8)**, 5756-69 (2013).

124. Vivian J. T. and Callis P. R., Mechanisms of tryptophan fluorescence shifts in proteins. *Biophys J.* **80(5)**, 2093-109 (2001).

125. Desjardins, P. *et al.*, Microvolume protein concentration determination using the NanoDrop 2000c spectrophotometer. *J Vis Exp.* **33**, 1610 (2009).

126. Martin, L. *et al.*, Analyzing Thermal Unfolding of Proteins: The Prometheus NT.48. *Nanotemper Application Note*, NT-PR-001 (2014).

127. Eftink, M. R., The use of fluorescence methods to monitor unfolding transitions in proteins. *Biophys J.* **66(2 Pt. 1)**, 482-501 (1994).

128. Zhang, X. D., A new method with flexible and balanced control of false negatives and false positives for hit selection in RNA interference high-throughput screening assays. *J Biomol Screen.* **12(5)**, 645-55 (2007).

129. Zhang, J. H. *et al.*, A Simple Statistical Parameter for Use in Evaluation and Validation of High Throughput Screening Assays. *J Biomol Screen.* **4(2)**, 67-73 (1999).

130. Wang, W. *et al.*, Protein aggregation--pathways and influencing factors. *Int J Pharm*. **390(2)**, 89-99 (2010).

131. Mancusso, R. *et al.*, Simple screening method for improving membrane protein thermostability. *Methods* **55(4)**, 324-9 (2011).

132. Kunji, E. R. *et al.*, Determination of the molecular mass and dimensions of membrane proteins by size exclusion chromatography. *Methods* **46(2)**, 62-72 (2008).

133. Lopes, C. M. *et al.*, PIP2 hydrolysis underlies agonist-induced inhibition and regulates voltage gating of two-pore domain K^+ channels. *J Physiol.* **564(Pt 1)**, 117-29 (2005).

134. Maingret, F. *et al.*, Molecular basis of the voltage-dependent gating of TREK-1, a mechano-sensitive K(+) channel. *Biochem Biophys Res Commun.* **292(2)**, 339-46 (2002).

135. Enyeart, J. H. *et al.*, Calcium-dependent inhibition of adrenal TREK-1 channels by angiotensin II and ionomycin. *Am J Physiol Cell Physiol.* **301(3)**, C619-29 (2011).

136. Dvorak, M. M. *et al.*, Physiological changes in extracellular calcium concentration directly control osteoblast function in the absence of calciotropic hormones. *Proc Natl Acad Sci.* **101(14)**, 5140-5 (2004).

137. Romani, A. M., Cellular magnesium homeostasis. *Arch Biochem Biophys.* **512(1)**, 1-23 (2011).

138. Lu, B. *et al.*, Extracellular calcium controls background current and neuronal excitability via an UNC79-UNC80-NALCN cation channel complex. *Neuron* **68(3)**, 488-99 (2010).

139. Swaminathan, R., Magnesium metabolism and its disorders. *Clin. Biochem. Rev.* **24(2)**, 47-66 (2003).

140. Ericsson, U. B. *et al.*, Thermofluor-based high-throughput stability optimization of proteins for structural studies. *Anal Biochem.* **357(2)**, 289-98 (2006).

141. McClenaghan, C. *et al.*, Polymodal activation of the TREK-2 K2P channel produces structurally distinct open states. *J Gen Physiol.* **147(6)**, 497-505 (2016).

142. Gault, J. *et al.*, High-resolution mass spectrometry of small molecules bound to membrane proteins. *Nat Methods* **13(4)**, 333-6 (2016).

143. Barrera, N. P. and Robinson, C. V., Advances in the mass spectrometry of membrane proteins: from individual proteins to intact complexes. *Annu Rev Biochem.* **80**, 247-71 (2011).

144. Kaptein, R. and Wagner, G., NMR studies of membrane proteins. *J Biomol NMR.* **61(3-4)**, 181-4 (2015).

145. Friere, E. *et al.*, Isothermal titration calorimetry. *Anal Chem.* **62(18)**, 950A-959A (1990).

146. Pierce, M. M. *et al.*, Isothermal titration calorimetry of protein-protein interactions. *Methods* **19(2)**, 213-21 (1999).

147. Duff, M. R. Jr. *et al.*, Isothermal titration calorimetry for measuring macromolecule-ligand affinity. *J Vis Exp.* **55**, 2796 (2011).

148. Christensen, J. J. *et al.*, Thermodynamics of metal cyanide coordination. V. Log K, ΔHo, and ΔS values for the Hg2 + -cn-system. *Inorg Chem.* **4**, 1278-80 (1965).

149. Wiseman, T. *et al.*, Rapid measurement of binding constants and heats of binding using a new titration calorimeter. *Anal Biochem.* **179**, 131-37 (1989).

150. Freyer, M. W. and Lewis E. A., Isothermal titration calorimetry: experimental design, data analysis, and probing macromolecule/ligand binding and kinetic interactions. *Methods Cell Biol.* **84**, 79-113 (2008).

151. Feig, A. L., Applications of Isothermal Titration Calorimetry in RNA Biochemistry and Biophysics. *Biopolymers* **87(5-6)**, 293-301 (2007).

152. Dutta, A. K. et al., Using isothermal titration calorimetry to determine thermodynamic parameters of protein-glycosaminoglycan interactions. *Methods Mol Biol.* **1229**, 315-24 (2015).

153. Prince, C. C. and Jia, Z., Detergent quantification in membrane protein samples and its application to crystallization experiments. *Amino Acids* **45(6)**, 1293-302 (2013).

154. Rajarathnam, K. and Rosgen, J. Isothermal titration calorimetry of membrane proteins - progress and challenges. *Biochim Biophys Acta.* **1838(1 Pt A)**, 69-77 (2014).

155. Nisius, L. *et al.*, Large-scale expression and purification of the major HIV-1 coreceptor CCR5 and characterization of its interaction with RANTES. *Protein Expr Purif.* **61**, 155-162 (2008).

156. Sikora, C. W. and Turner R. J., Investigation of ligand binding to the multidrug resistance protein EmrE by isothermal titration calorimetry. *Biophys J.* **88**, 475-82 (2005).

157. Wöhri, A. B. *et al.*, Thermodynamic studies of ligand binding to the human homopentameric glycine receptor using isothermal titration calorimetry. *Mol Membr Biol.* **30**, 169-83 (2013).

158. Karlsson, R. *et al.*, Kinetic analysis of monoclonal antibody-antigen interactions with a new biosensor based analytical system. *J Immunol Methods.* **145(1-2)**, 229-40 (1991).

159. Tang, Y. *et al.*, Surface Plasmon Resonance: An Introduction to a Surface Spectroscopy Technique. *J Chem Educ.* **87(7)**, 742-746 (2010).

160. Heygi, G. *et al.*, Introduction to Practical Biochemistry, Section 8.7 *Eötvös Loránd University*, (2013).

161. Zhao, H. *et al.*, A comparison of binding surfaces for SPR biosensing using an antibody-antigen system and affinity distribution analysis. *Methods* **59(3)**, 328-35 (2013).

162. Patching, S. G., Surface plasmon resonance spectroscopy for characterisation of membrane protein-ligand interactions and its potential for drug discovery. *Biochim Biophys Acta.* **1838(1 Pt A)**, 43-55 (2014).

163. Salamon, Z. *et al.*, Surface plasmon resonance spectroscopy studies of membrane proteins: transducin binding and activation by rhodopsin monitored in thin membrane films. *Biophys J.* **71**, 283-294 (1996).

164. Hüttenrauch, F. *et al.*, Beta-arrestin binding to CC chemokine receptor 5 requires multiple C-terminal receptor phosphorylation sites and involves a conserved Asp-Arg-Tyr sequence motif. *J Biol Chem.* **277**, 30769-30777 (2002).

165. Rich, R. L. *et al.*, Higher-throughput, label-free, real-time molecular interaction analysis. *Anal Biochem*. **361**, 1-6 (2007).

166. Fang, Y. Label-free Optical Biosensors in Drug Discovery. *Trends in Biopharm Indus.* **3**, 34-38 (2007).

167. Abdiche, T. N. *et al.*, Determining Kinetics and Affinities of Protein Interactions Using a Parallel Real-time Label-free Biosensor, the Octet. *Anal Biochem.* **377(2)**, 209-217 (2008).

168. Ma, L. *et al.*, Design, Synthesis, and Structure-Activity Relationship of Novel LSD1 Inhibitors Based on Pyrimidine-Thiourea Hybrids as Potent, Orally Active Antitumor Agents. *J Med Chem.* **58(4)**, 1705-16 (2015).

169. Sharma, S. and Wilkens, S., Biolayer Interferometry of Lipid Nanodisc-Reconstituted Yeast Vacuolar H+ -ATPase. *Protein Sci.* **3143**, pro.3143 (2017).

170. Heym, R. *et al.*, Label-Free Detection of Small-Molecule Binding to a GPCR in the Membrane Environment. *Biochim Biophys Acta.* **1854(8)**, 979-86 (2015).

171. Slotboom, D. J. *et al.*, Static light scattering to characterize membrane proteins in detergent solution. *Methods* **46(2)**, 73-82 (2008).

172. Takaishi, M *et al.*, Inhibitory effects of monoterpenes on human TRPA1 and the structural basis of their activity. *J Physiol Sci.* **64(1)**, 47-57 (2014).

173. Ryder, J. W. *et al.*, In vitro analysis of the glucose-transport system in GLUT4-null skeletal muscle. *Biochem J.* **342(2)**, 321-8 (1999).

174. Weber, C. K. *et al.*, Suppression of NF-kappaB activity by sulfasalazine is mediated by direct inhibition of IkappaB kinases alpha and beta. *Gastroenterology* **119(5)**, 1209-18 (2000).

175. Gutzmann, H. *et al.*, Safety and efficacy of idebenone versus tacrine in patients with Alzheimer's disease: results of a randomized, double-blind, parallel-group multicenter study. *Pharmacopsychiatry* **35(1)**, 12-8 (2002).

176. Chandra, K. S. and Ramesh, G., The fourth-generation Calcium channel blocker: cilnidipine. *Indian Heart J.* **65(6)**, 691-5 (2013).

177. Fong, T. M. and Heymsfield S. B., Cannabinoid-1 receptor inverse agonists: current understanding of mechanism of action and unanswered questions. *Int J Obes (Lond).* **33(9)**, 947-55 (2009).

178. Seely, K. A. *et al.*, AM-251 and rimonabant act as direct antagonists at mu-opioid receptors: implications for opioid/cannabinoid interaction studies. *Neuropharmacology* **63**, 905-15 (2012).

179. Tyers, M. B. and Freeman, A. J., Mechanism of the anti-emetic activity of 5-HT3 receptor antagonists. *Oncology* **49(4)**, 263-8 (1992).

180. Sheffer, A. L. and Samuels L. L., Cetirizine: antiallergic therapy beyond traditional H1 antihistamines. *J Allergy Clin Immunol.* **86(6 Pt. 2)**, 1040-6 (1990).

181. Iacucci, M. *et al.*, Mesalazine in inflammatory bowel disease: a trendy topic once again? *Can J Gastroenterol.* **24(2)**, 127-33 (2010).

182. Kocsis, P. *et al.*, Tolperisone-type drugs inhibit spinal reflexes via blockade of voltage-gated sodium and calcium channels. *J Pharm Exp Ther.* **315(3)**, 1237-46 (2005).

183. Kaeberlein, M. *et al.*, Substrate-specific activation of sirtuins by resveratrol. *J Biol Chem.* **280**, 17038–17045 (2005).

184. Di Nisio, M. *et al.*, Direct thrombin inhibitors. *N Engl J Med*. **353**, 1028-40 (2005).

185. Baker, W. L. and White, C. M., Role of prasugrel, a novel P2Y(12) receptor antagonist, in the management of acute coronary syndromes. *Am J Cardio Drugs.* **9(4)**, 213-29 (2009).

186. Yoo, J. S. *et al.*, Study on genipin: a new alternative natural crosslinking agent for fixing heterograft tissue. *Korean J Thorac Cardiovasc Surg.* **44(3)**, 197-207 (2011).

187. Zhang, C. Y. *et al.*, Genipin inhibits UCP2-mediated proton leak and acutely reverses obesity- and high glucose-induced beta cell dysfunction in isolated pancreatic islets. *Cell Metabolism.* **3(6)**, 417-27 (2006).

188. Yokota, S., Mizoribine: mode of action and effects in clinical use. *Pediatr Int.* **44(2)**, 196-8 (2002).

189. Imaizumi, R. *et al.*, Mechanism of the Antihypertensive Effect of alpha-Methyldopa. *Nature* **203(4948)**, 982 (1964).

190. Tatsumi, M. *et al.*, Pharmacological profile of antidepressants and related compounds at human monoamine transporters. *Eur J Pharm.* **340(2-3)**, 249-58 (1997).

191. Richelson, E. and Nelson, A., Antagonism by antidepressants of neurotransmitter receptors of normal human brain in vitro. *J Pharm Exp Ther.* **230(1)**, 94-102 (1984).

192. McCurdy, A. R. and Lacy, M. Q., Pomalidomide and its clinical potential for relapsed or refractory multiple myeloma: an update for the hematologist. *Ther Adv Hematol.* **4(3)**, 211-6 (2013).

193. Bymaster, F. P. and Knadler, L., The dual transporter inhibitor duloxetine: a review of its preclinical pharmacology, pharmacokinetic profile, and clinical results in depression. *Curr Pharm Des.* **11(12)**, 1475-93 (2005).

194. Cazzulani, P. *et al.*, Pharmacological studies on the mode of action of flavoxate. *Arch Int Pharmacodyn Ther.* **268(2)**, 301-12 (1984).

195. Timmins, G. S. and Deretic, V., Mechanisms of action of isoniazid. *Mol Microbiol.* **62(5)**, 1220-7 (2006).

196. Bruno, J. J., The mechanisms of action of ticlopidine. *Thromb Res Suppl.* **4**, 59-67 (1983).

197. Dove, A., Drug screening—beyond the bottleneck. *Nature Biotechnology*. **17**, 859-63 (1999).

198. Siles, S. A. *et al.*, High-Throughput Screening of a Collection of Known Pharmacologically Active Small Compounds for Identification of *Candida albicans* Biofilm Inhibitors. *Antimicrob Agents Chemother.* **57(8)**, 3681-7 (2013).

199. Mercier, K. A. and Powers R., Determining the optimal size of small molecule mixtures for high throughput NMR screening. *J Biomol NMR.* **31(3)**, 243-58 (2005).

200. Yu, H. *et al.*, High throughput screening technologies for ion channels. *Acta Pharmacol Sin.* **37(1)**, 34-43 (2016).

201. Laub, K. R. *et al.*, Comparing ion conductance recordings of synthetic lipid bilayers with cell membranes containing TRP channels. *Biochim Biophys Acta.* **1818(5)**, 1123-34 (2012).

202. Guan, B. *et al.*, Two-electrode voltage clamp. *Methods Mol Biol.* **998**, 79-89 (2013).

203. Farre, C. *et al.*, Port-a-patch and patchliner: high fidelity electrophysiology for secondary screening and safety pharmacology. *Comb Chem High Throughput Screen.* **12(1)**, 24-37 (2009).

204. Jones, K. A. *et al.*, Automated patch clamping using the QPatch. *Methods Mol Biol.* **565**, 209-23 (2009).

205. Veitinger, S., The Patch Clamp Technique, An Introduction. Leica Science Lab, http://www.leica-microsystems.com/science-lab/the-patch-clamp-technique/ (2011).

206. Krieg, P. A. and Melton, D. A., Functional messenger RNAs are produced by SP6 in vitro transcription of cloned cDNAs. *Nucleic Acids Res.* **12(18)**, 7057-70 (1984).

207. Veale, E. L. *et al.*, Influence of the N-terminus on the Biophysical Properties and Pharmacology of TREK1 Potassium Channels. *Mol Pharm.* **85**, 671-81 (2014).

208. Löhn, M. *et al.*, Cilnidipine is a novel slow-acting blocker of vascular L-type calcium channels that does not target protein kinase C. *J. Hypertens*. **20(5)**, 885-93 (2002).

209. Prasanna, K. D. *et al.*, Selective Small Molecule Activators of TREK-2 Channels Stimulate Dorsal Root Ganglion c-Fiber Nociceptor Two-Pore-Domain Potassium Channel Currents and Limit Calcium Influx. *ACS Chem. Neurosci.* **8(3)**, 558-68 (2017).

210. Goldin, A. L., Expression of Ion Channels in *Xenopus* Oocytes. *Expression and Analysis of Recombinant Ion Channels: From Structural Studies to Pharmacological Screening,* 1-25 (2006).

Abbreviations

ADP	Adenosine Diphosphate
ATP	Adenosine Triphosphate
BLI	Biolayer Interferometry
CHS	Cholesterol Hemisuccinate
CMC	Critical Micelle Concentration
CPM	7-diethylamino-3-(4'-maleimidylphenyl)-4-methylcoumarin
DCPIB	4-(2-Butyl-6,7-dichloro-2-cyclopentyl-indan-1-on-5-yl) oxobutyric acid
DDM	*n*-Dodecyl β-D-maltoside
DM	n-Decyl-β-D-Maltopyranoside
DMNG	Decyl Maltose Neopentyl Glycol
DMSO	Dimethyl Sulfoxide
DSC	Differential Scanning Calorimetry
DSF	Differential Scanning Fluorimetry
EC_{50}	Half Maximal Effective Concentration
EDC	1-Ethyl-3-(3-dimethylaminopropyl)carbodiimide
EDTA	Ethylenediaminetetraacetic Acid
FDA	Food and Drug Administration (USA)
GPCR	G-Protein Coupled Receptor

HEPES	4-(2-hydroxyethyl)-1-piperazineethanesulfonic acid
I	Current (Electric)
IC_{50}	Half Maximal Inhibitory Concentration
IMAC	Immobilised Metal Affinity Chromatography
IMP	Integral Membrane Protein
IPTG	Isopropyl β-D-1-thiogalactopyranoside
ITC	Isothermal Titration Calorimetry
K2P	Tandem Pore Domain Potassium Channel
K_d	Dissociation Constant
K_{ir}	Inward Rectifying Potassium Channel
K_v	Voltage Gated Potassium Channel
LB	Luria-Bertani (Broth or Agar)
LMNG	Lauryl Maltose Neopentyl Glycol
MGC	Mammalian Gene Collection
MS	Mass Spectrometry
MST	Microscale Thermophoresis
MW	Molecular Weight
NADH	Nicotinamide Adenine Dinucleotide (+ Hydrogen)
NHS	N-hydroxysuccinimide
NMR	Nuclear Magnetic Resonance

OD	Optical Density
OGNG	Octyl Glucose Neopentyl Glycol
RNAi	RNA Interference
RT-PCR	Real Time – Polymerase Chain Reaction
SD	Standard Deviation
SDS-PAGE	Sodium Dodecyl Sulphate – Polyacrylamide Gel Electrophoresis
SEC	Size Exclusion Chromatography
SEM	Standard Error of the Mean
SGC	Structural Genomics Consortium
SPR	Surface Plasmon Resonance
SSMD	Strictly Standardised Mean Differences
TEV	Tobacco Etch Virus
TEVC	Two Electrode Voltage Clamp
T_m	Melting Temperature of Protein
TM	Transmembrane
TRIS	Tris(hydroxymethyl)aminomethane
UDM	*n*-Undecyl β-D-maltoside
UV	Ultraviolet
V	Voltage (Electric)

Appendix 1

```
TWIK1   ML--------Q-------------------------------------SLAGSSC-------------VR
TASK1   ------------------------------------------------------------------------
TREK2   MKFPIETPRKQVNWDPKVAVPAAAPVCQPKSATNGQPPAPAPTPTPRLSISSRATVVA-RMEGTSQGGLQ
TREK1   M--------------------AAPDLLDPKSA--------AQNSKPRLSFSTKPTVLASRVESDTT---I

TWIK1   LVERHRSAWCFGFLVLGYLLYLVFGAVVFSSVELPYEDLLRQELRKLKRRFLEEHECLSEQQLEQFLGRV
TASK1   --MKRQNVR-TLALIVCTFTYLLVGAAVFDALESEPELIERQRLELRQ-QELRARYNLSQGGYEELERVV
TREK2   TVMKWKTV---VAIFVVVVVYLVTGGLVFRALEQPFESSQKNTIALEKAEFLRDHVCVSPQELETLIQHA
TREK1   NVMKWKTV---STIFLVVVLYLIIGATVFKALEQPHEISQRTTIVIQKQTFISQHSCVNSTELDELIQQI

TWIK1   LEASNYGVSVLSNA-SGNWNWDFTSALFFASTVLSTTGYGHTVPLSDGGKAFCIIYSVIGIPFTLLFLTA
TASK1   LRLKPHK---------AGVQWRFAGSFYFAITVITTIGYGHAAPSTDGGKVFCMFYALLGIPLTLVMFQS
TREK2   LDADNAGVSPIGNSSNNSSHWDLGSAFFFAGTVITTIGYGNIAPSTEGGKIFCILYAIFGIPLFGFLLAG
TREK1   VAAINAGIIPLGNTSNQISHWDLGSSFFFAGTVITTIGFGNISPRTEGGKIFCIIYALLGIPLFGFLLAG

TWIK1   VVQRITVHVTRRPVLYFHIRWGFSK-QVVAIVHAVLLGFVTVSCFFFIPAAVFSVLEDDWNFLESFYFCF
TASK1   LGERINTLVRYLLHRAKKGLGMR---RADVSMANMVLIGFFSCISTLCIGAAAFSHYEHWTFFQAYYYCF
TREK2   IGDQLGTIFGKSIARVEKVFRKKQVSQTKIRVISTILFILAGCIVFVTIPAVIFKYIEGWTALESIYFVV
TREK1   VGDQLGTIFGKGIAKVEDTFIKWNVSQTKIRIISTIIFILFGCVLFVALPAIIFKHIEGWSALDAIYFVV

TWIK1   ISLSTIGLGDYVPGEGY-NQKFRELYKIGITCYLLLGLIAMLVVLETFCELHELKKFRKMFYVKKDKDED
TASK1   ITLTTIGFGDYVALQKDQALQTQPQYVAFSFVYILTGLTVIGAFLNLVVLRFMT----MNAEDEKR----
TREK2   VTLTTVGFGDFVAGGNA-GINYREWYKPLVWFWILVGLAYFAAVLSMIGDWLRV----LSKKTKEEVGEI
TREK1   ITLTTIGFGDYVAGGS--DIEYLDFYKPVVWFWILVGLAYFAAVLSMIGDWLRV----ISKKTKEEVGEF

TWIK1   QVHIIEH-------------------------------------------------------------
TASK1   -----------DAEHRALLTRNGQAGGGGGGGSAHTTDTASSTAAAGGGGFRNVYAEVLHFQSMCSCLWY
TREK2   KAHAAEWKANVTAEFRETRRRLSVE-------------------------------IHDKLQRAATIRSM
TREK1   RAHAAEWTANVTAEFKETRRRLSVE-------------------------------IYDKFQRATSI---

TWIK1   ------------------------------------DQLSFSSITDQA------AGMKEDQKQNEPFVA
TASK1   KSREKLQYSIP----------------------MIIPRDLSTSDTCVEQ------SHS--SPGGGGRYSD
TREK2   ERRRLGLDQRAHSLDMLSPEKRSVFAALDTGRFKASSQESINNRPNNLRLKGPEQLN-------------
TREK1   -KRKLSAELAGNHNQELTPCRRTL-----------------------------------------------

TWIK1   TQSSACVDGPANH-----------------------------------------------------------
TASK1   TPSRRCLCSGAPRSAISS--VSTGLHSLSTFRGLMKRRSSV-----------------------------
TREK2   ----------KHGQGASEDNI---INKFGSTSRLTKRKNKDLKKTLPEDVQKIYKTFRNYSLDEEKKEEE
TREK1   ----------------------------SVNHLTSERD-----VLP----PLLKTESIY----------

TWIK1   -------------------------------------------------
TASK1   -------------------------------------------------
TREK2   TEKMCNSDNSSTAMLTDCIQQHAELENGMIPTDTKDREPENNSLLEDRN
TREK1   -------------------------LNGLTPHCAG----EEIAVIENIK
```

Figure 9.1: Sequence Alignments for full length TREK1, TREK2, TASK1 and TWIK1. *Truncated constructs referenced in section 2.1 are highlighted in yellow.*

Appendix 2

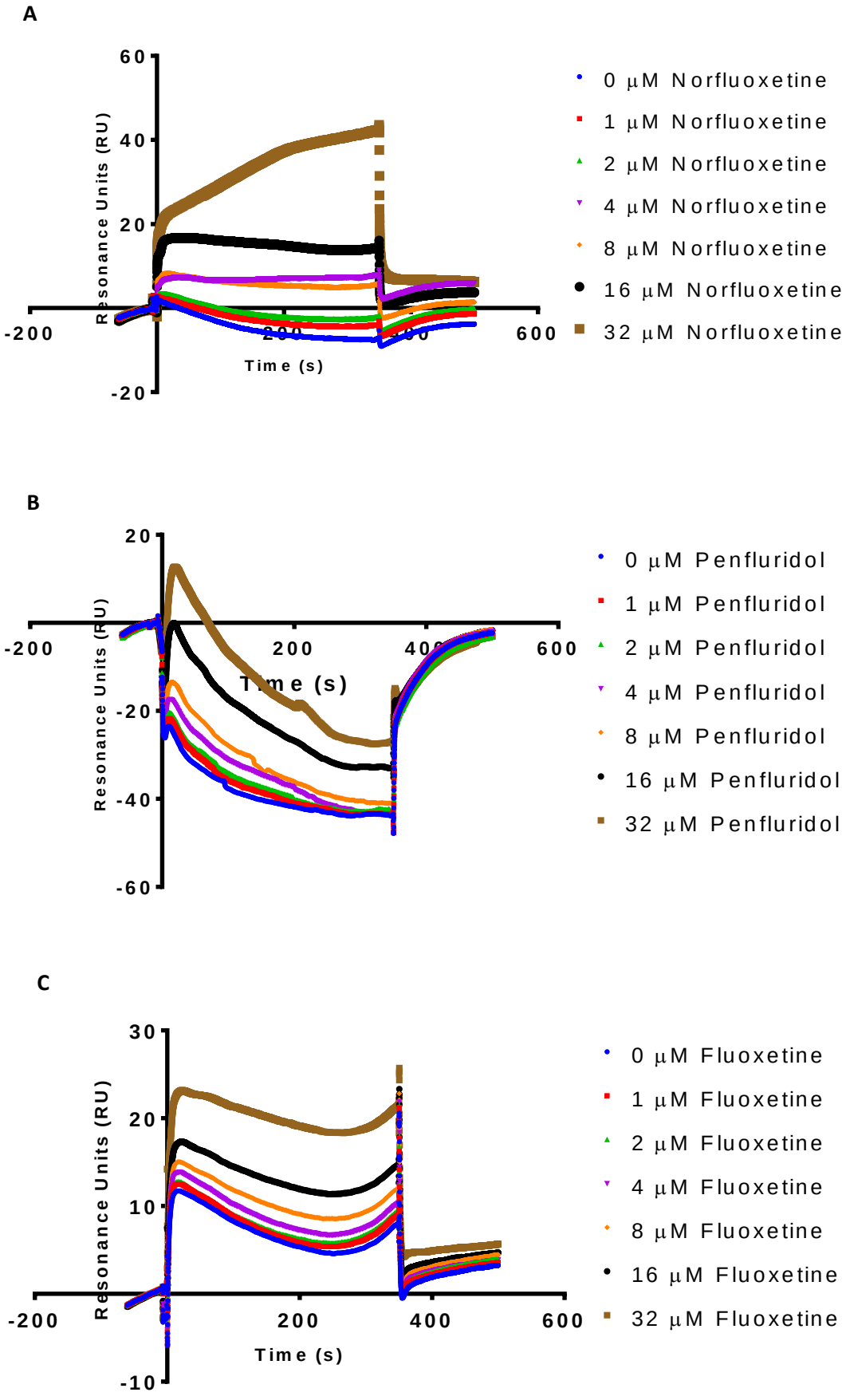
A
60
40
20
-20
-200
200
600
Resonance Units (RU)
Time (s)
0 µM Norfluoxetine
1 µM Norfluoxetine
2 µM Norfluoxetine
4 µM Norfluoxetine
8 µM Norfluoxetine
16 µM Norfluoxetine
32 µM Norfluoxetine
B
20
-20
-40
-60
-200
200
600
Resonance Units (RU)
Time (s)
0 µM Penfluridol
1 µM Penfluridol
2 µM Penfluridol
4 µM Penfluridol
8 µM Penfluridol
16 µM Penfluridol
32 µM Penfluridol
C
30
20
10
-10
-200
200
400
600
Resonance Units (RU)
Time (s)
0 µM Fluoxetine
1 µM Fluoxetine
2 µM Fluoxetine
4 µM Fluoxetine
8 µM Fluoxetine
16 µM Fluoxetine
32 µM Fluoxetine

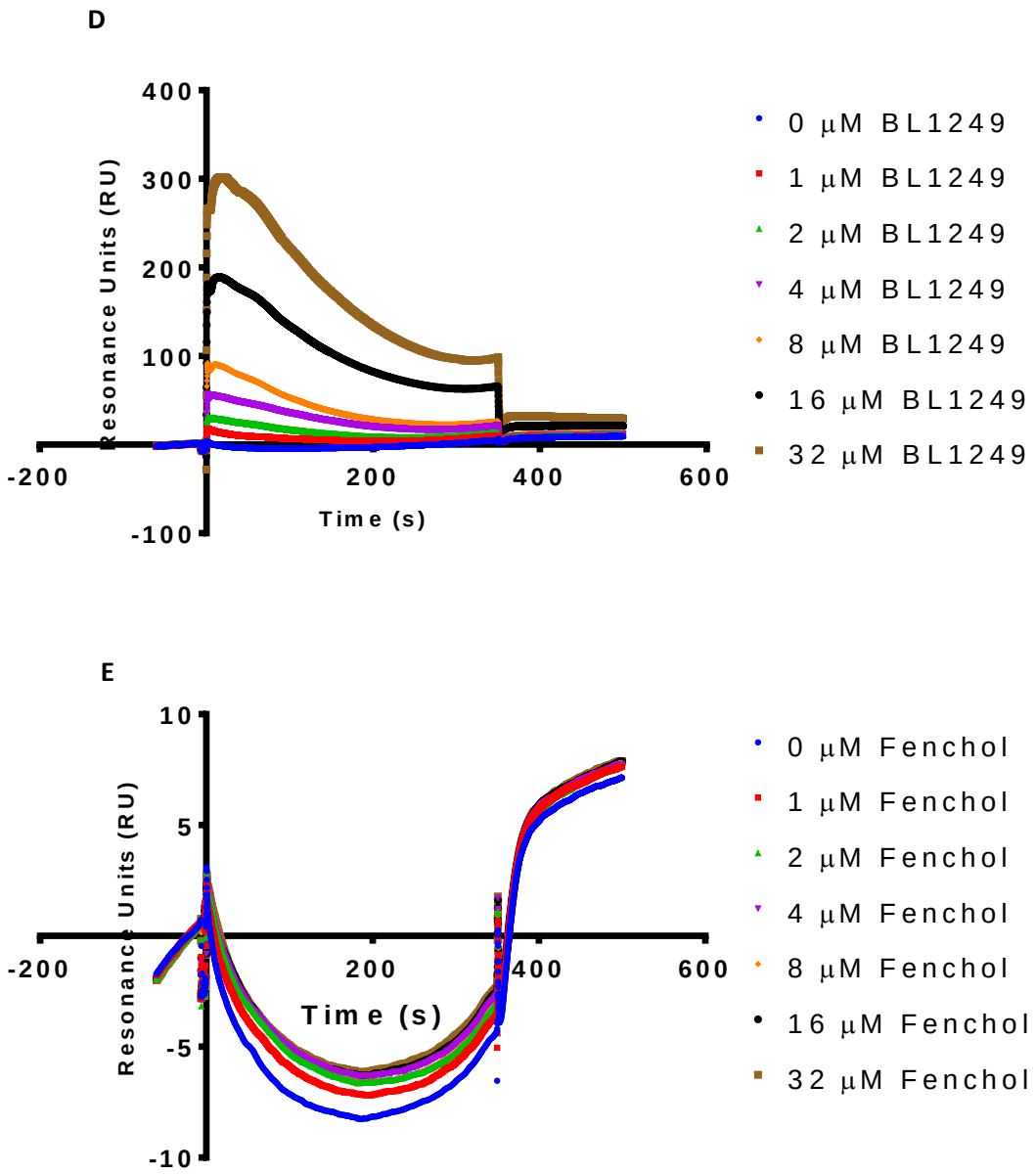

Figure 9.2: Sensorgrams for SPR of known ligands with TREK2. *Figure 9.2A shows data with norfluoxetine, figure 9.2B shows data with penfluridol, figure 9.2C shows data with fluoxetine, figure 9.2D shows data with BL1249 and figure 9.2E shows data with fenchol, a TRPV3 ligand.*

Appendix 3

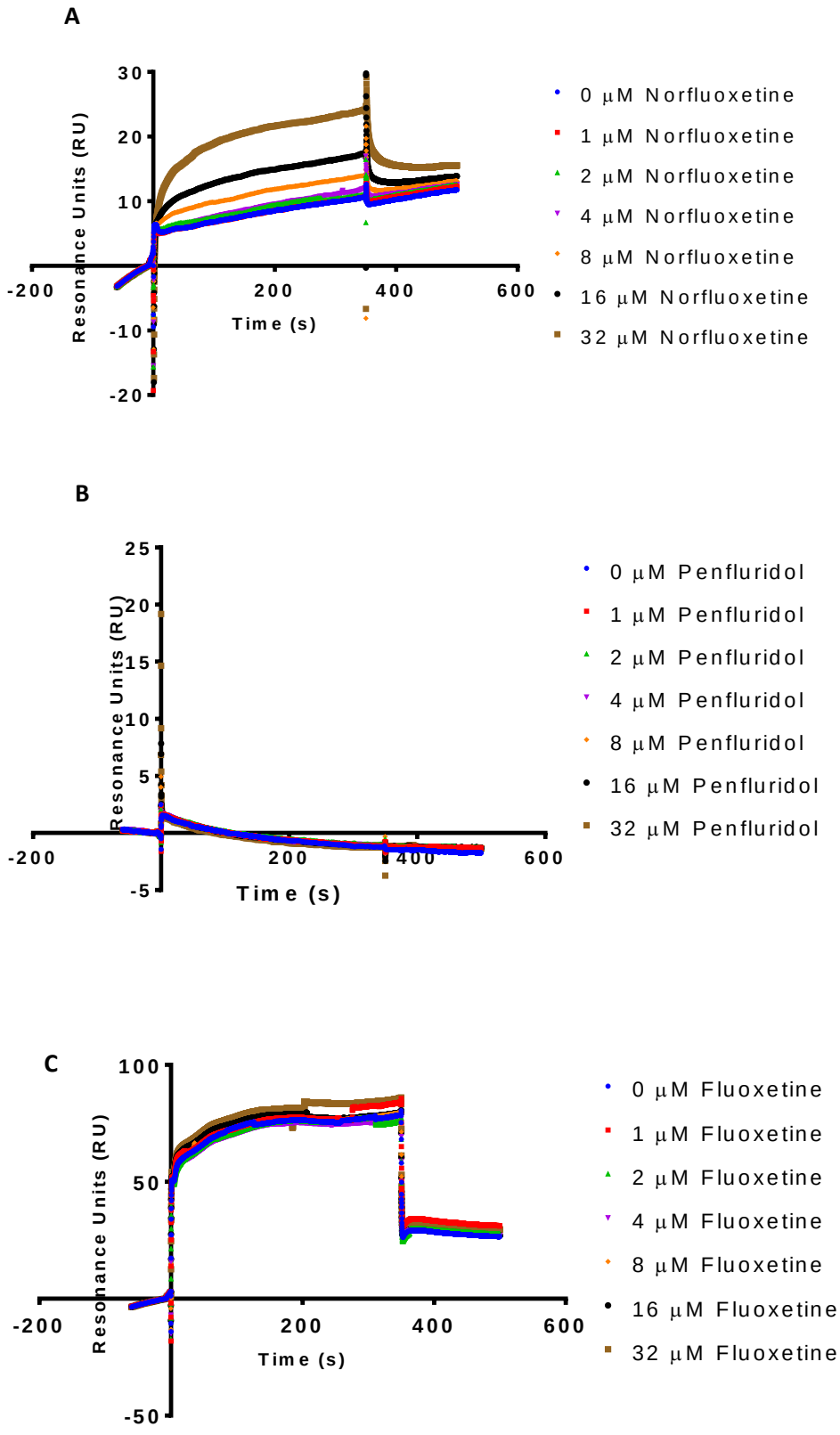
A
Resonance Units (RU)
Time (s)
0 µM Norfluoxetine
1 µM Norfluoxetine
2 µM Norfluoxetine
4 µM Norfluoxetine
8 µM Norfluoxetine
16 µM Norfluoxetine
32 µM Norfluoxetine
B
Resonance Units (RU)
Time (s)
0 µM Penfluridol
1 µM Penfluridol
2 µM Penfluridol
4 µM Penfluridol
8 µM Penfluridol
16 µM Penfluridol
32 µM Penfluridol
C
Resonance Units (RU)
Time (s)
0 µM Fluoxetine
1 µM Fluoxetine
2 µM Fluoxetine
4 µM Fluoxetine
8 µM Fluoxetine
16 µM Fluoxetine
32 µM Fluoxetine

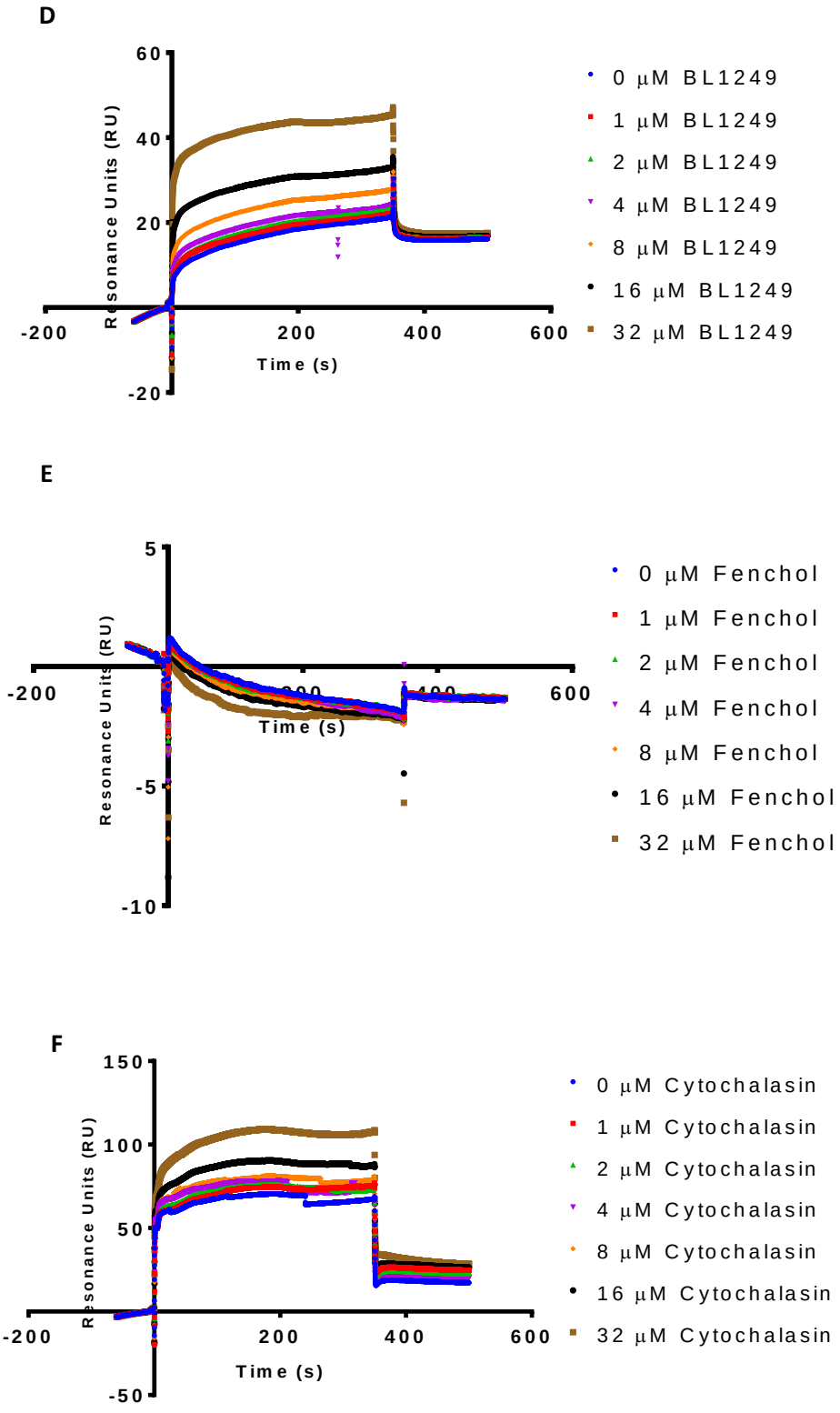

Figure 9.3: Sensorgrams for SPR of known ligands of TREKs with GLUT3. *Figure 9.3A shows data with norfluoxetine, figure 9.3B shows data with penfluridol, figure 9.3C shows data with fluoxetine, figure 9.3D shows data with BL1249, figure 9.3E shows data with fenchol, a TRPV3 ligand and figure 9.3F shows data with the GLUT3 ligand cytochalasin.*

Appendix 4

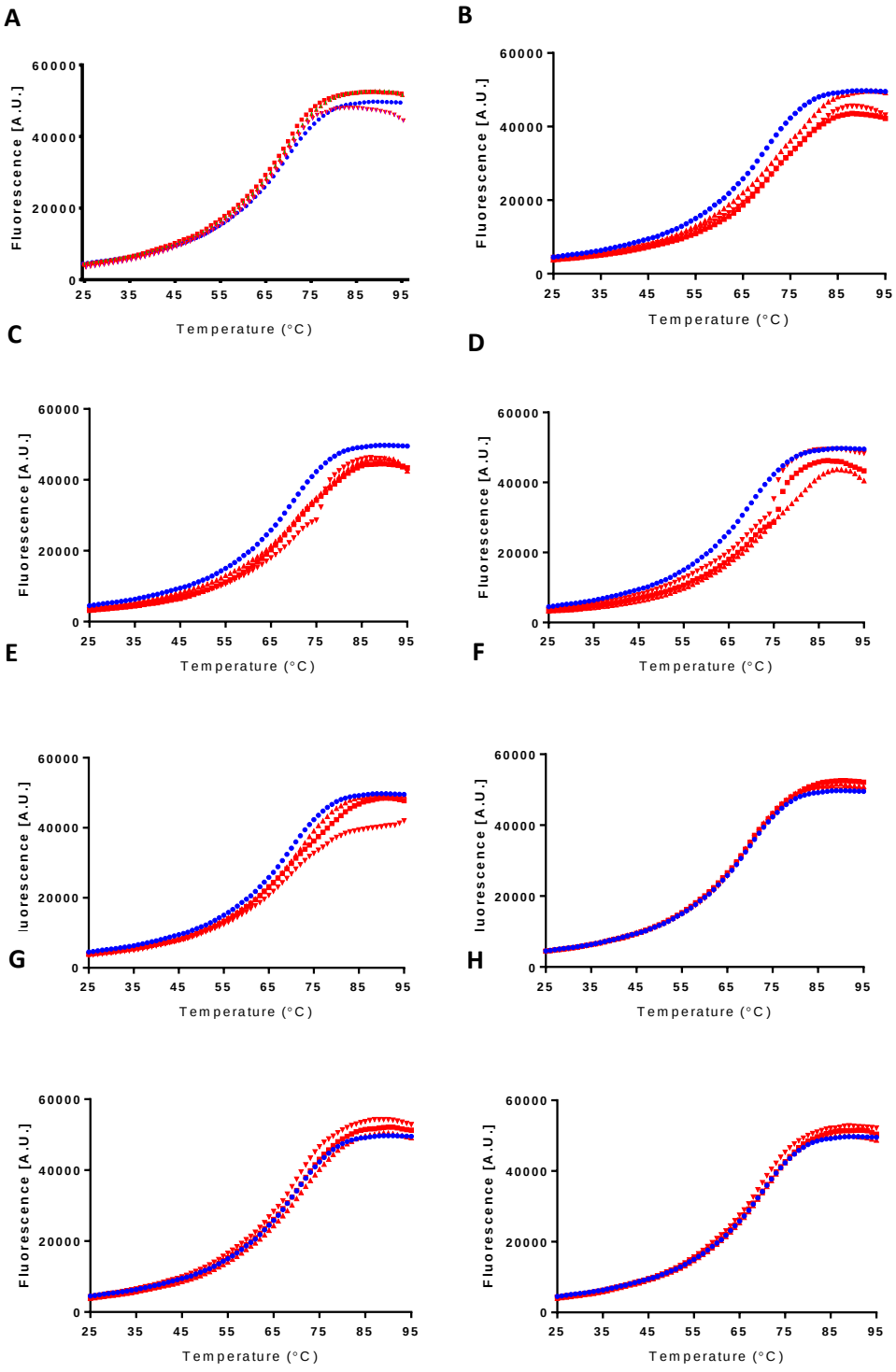
A
B
C
D
E
F
G
H
Fluorescence [A.U.]
Temperature (°C)
60000
40000
20000
0
25
35
45
55
65
75
85
95

I

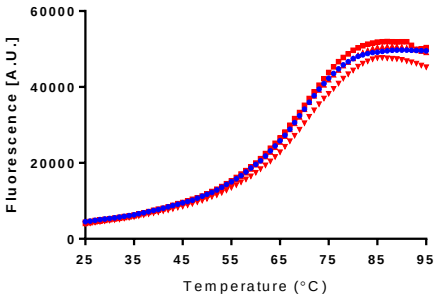
60000
40000
20000
0
Fluorescence [A.U.]
25 35 45 55 65 75 85 95
Temperature (°C)

J

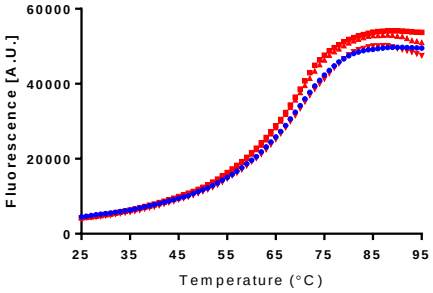
60000
40000
20000
0
Fluorescence [A.U.]
25 35 45 55 65 75 85 95
Temperature (°C)

K

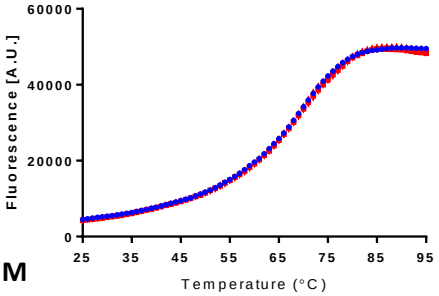
60000
40000
20000
0
Fluorescence [A.U.]
25 35 45 55 65 75 85 95
Temperature (°C)

L

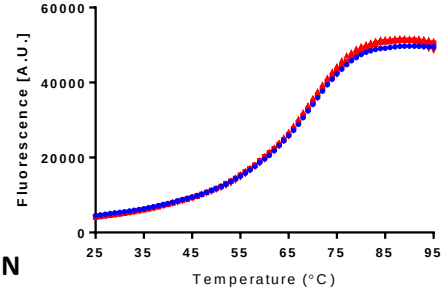
60000
40000
20000
0
Fluorescence [A.U.]
25 35 45 55 65 75 85 95
Temperature (°C)

M

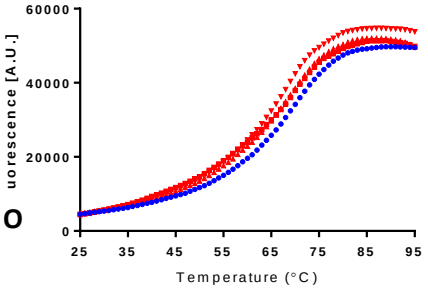
60000
40000
20000
0
uorescence [A.U.]
25 35 45 55 65 75 85 95
Temperature (°C)

N

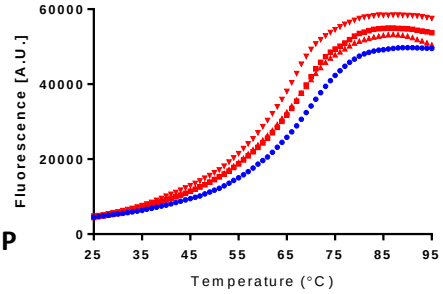
60000
40000
20000
0
Fluorescence [A.U.]
25 35 45 55 65 75 85 95
Temperature (°C)

O

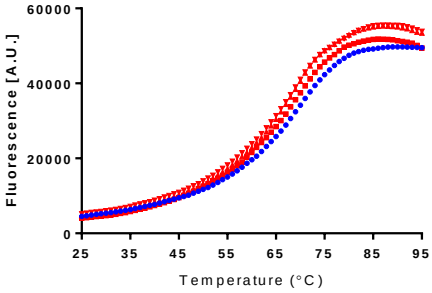
60000
40000
20000
0
Fluorescence [A.U.]
25 35 45 55 65 75 85 95
Temperature (°C)

P

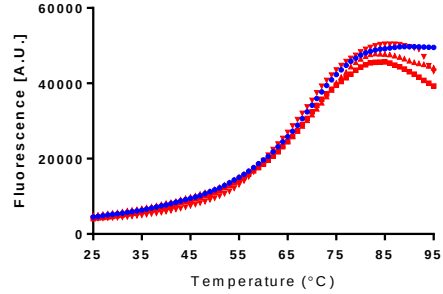
60000
40000
20000
0
Fluorescence [A.U.]
25 35 45 55 65 75 85 95
Temperature (°C)

60000
40000
20000
0
Fluorescence [A.U.]
25 35 45 55 65 75 85 95
Temperature (°C)

60000
40000
20000
0
Fluorescence [A.U.]
25 35 45 55 65 75 85 95
Temperature (°C)

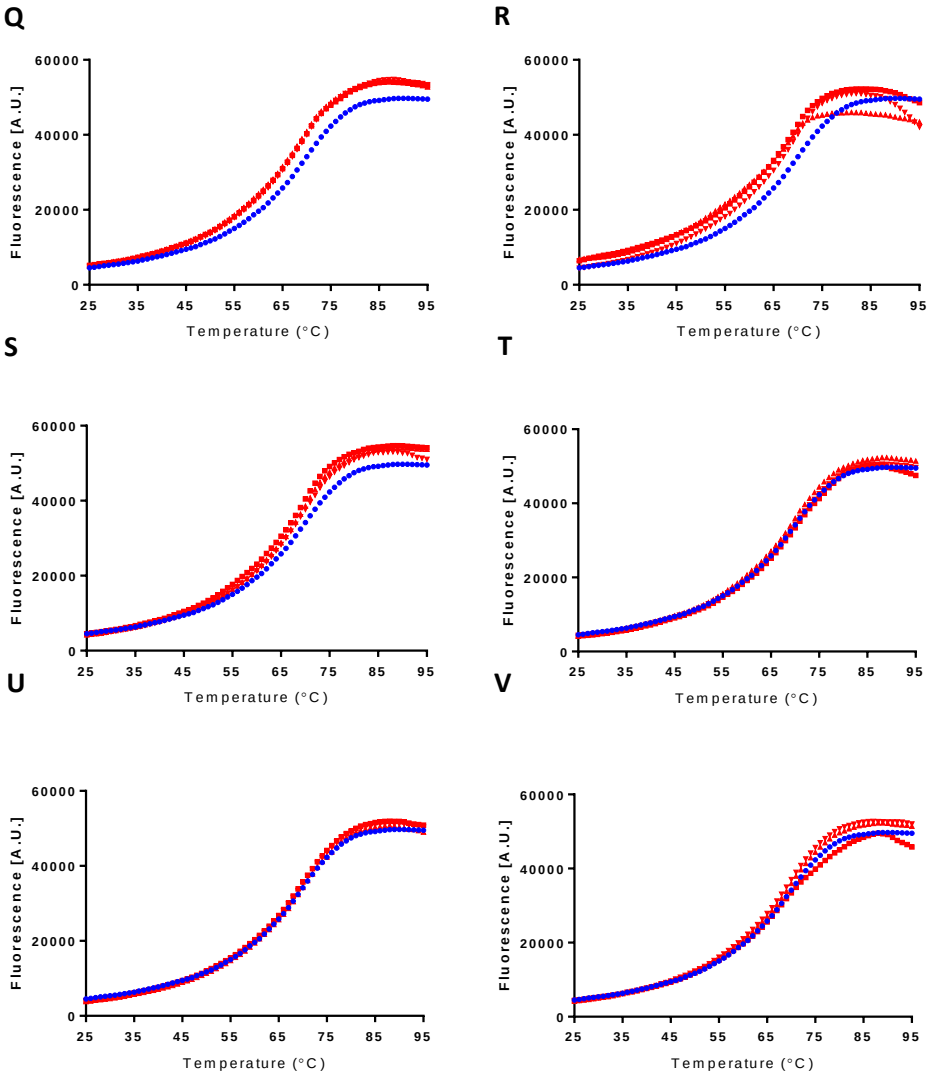

Figure 9.4: Raw CPM Fluorescence Data for Selected Compounds with TREK2. *TREK2 only fluorescence curves are shown in blue while curves in red are those of TREK2 with the addition of 20 µM compound. The compounds added in the various figures are as follows: A: Penfluridol, B: BL1249, C: Sulfasalazine, D: Idebenone, E: Cilnidipine, F: Rimonabant, G: Ondansetron, H: Cetirizine, I: Mesalamine, J: Tolperisone, K: Resveratrol, L: Argatroban, M: Prasugrel, N: Genipin, O: Mizoribine, P: Methyldopa, Q: Amoxapine, R: Pomalidomide, S: Duloxetine, T: Flavoxate, U: Isoniazid, V: Ticlopidine. All compounds were tested with 3 biological replicates of TREK2.*

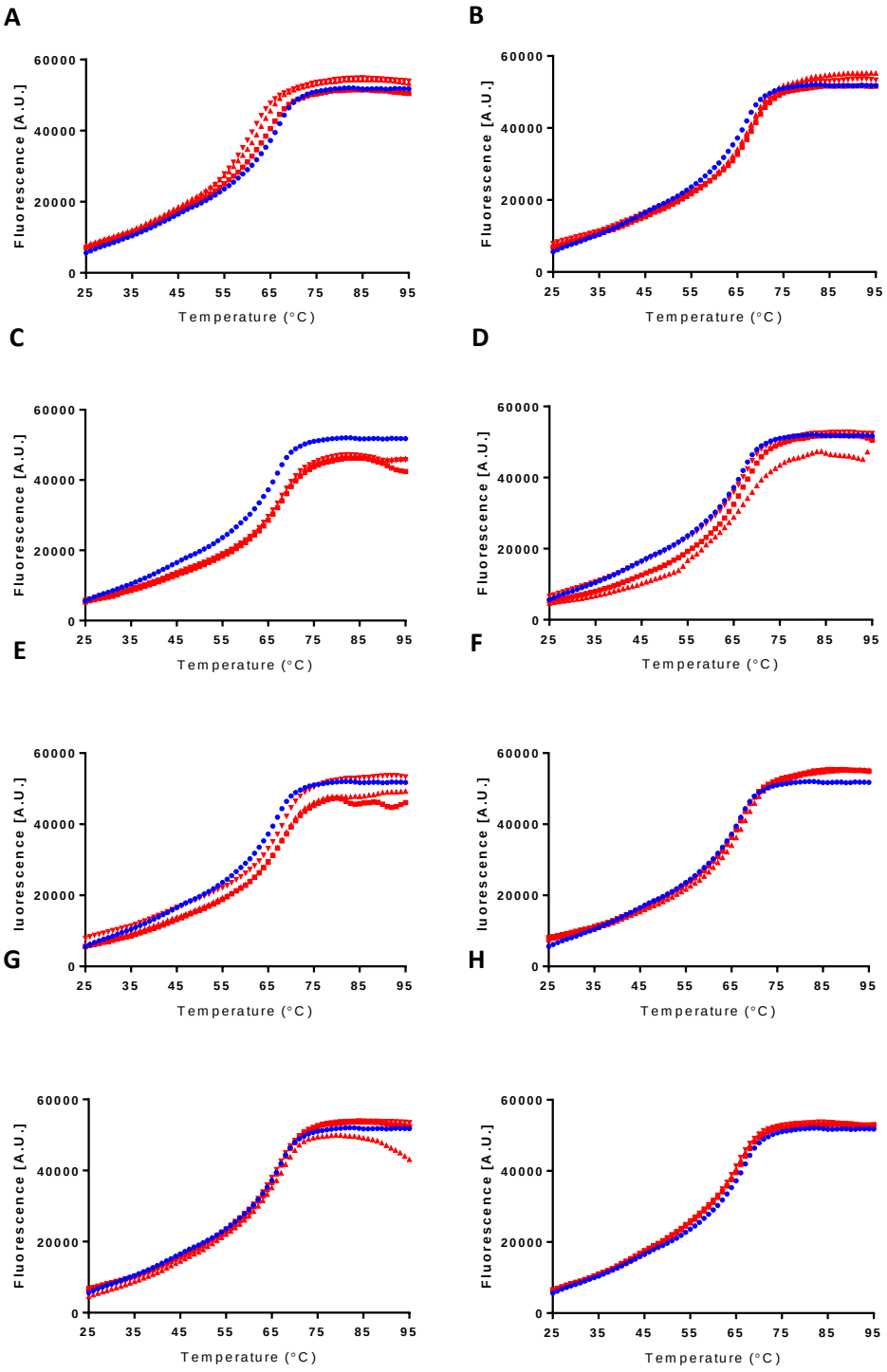
A
B
C
D
E
F
G
H
Fluorescence [A.U.]
Temperature (°C)
0
20000
40000
60000
25
35
45
55
65
75
85
95

I

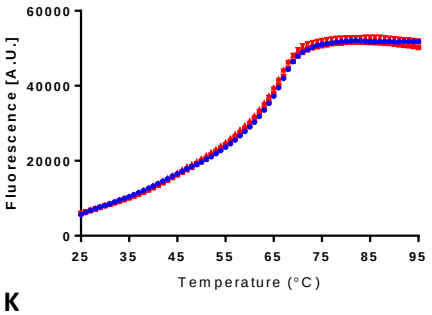
60000
40000
20000
0
Fluorescence [A.U.]
25 35 45 55 65 75 85 95
Temperature (°C)

J

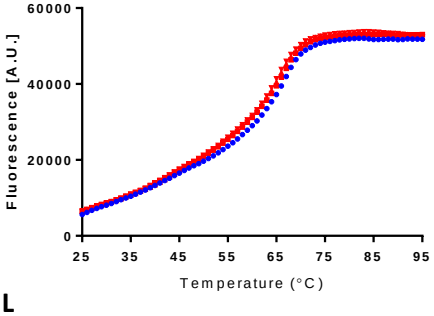
60000
40000
20000
0
Fluorescence [A.U.]
25 35 45 55 65 75 85 95
Temperature (°C)

K

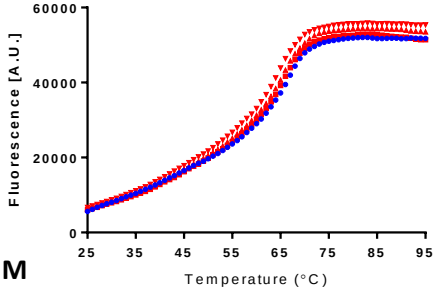
60000
40000
20000
0
Fluorescence [A.U.]
25 35 45 55 65 75 85 95
Temperature (°C)

L

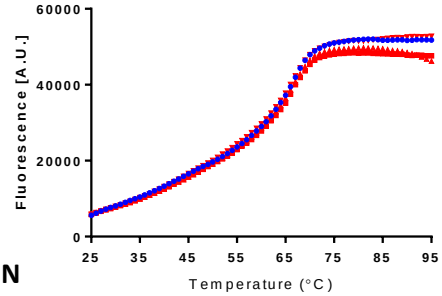
60000
40000
20000
0
Fluorescence [A.U.]
25 35 45 55 65 75 85 95
Temperature (°C)

M

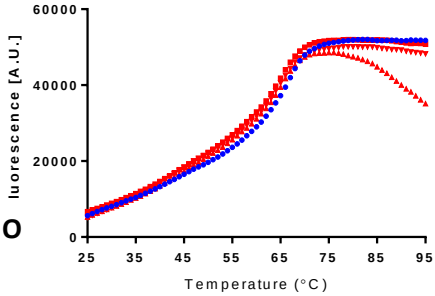
60000
40000
20000
0
luorescence [A.U.]
25 35 45 55 65 75 85 95
Temperature (°C)

N

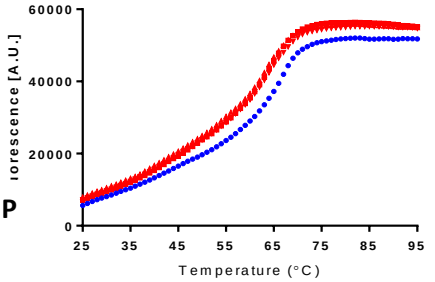
60000
40000
20000
0
Fluorescence [A.U.]
25 35 45 55 65 75 85 95
Temperature (°C)

O

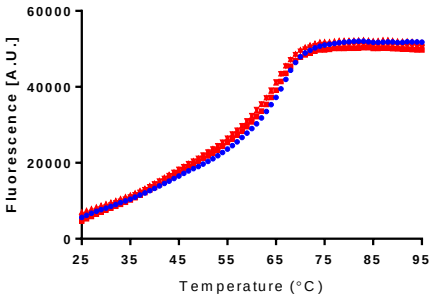
60000
40000
20000
0
Fluorescence [A.U.]
25 35 45 55 65 75 85 95
Temperature (°C)

P

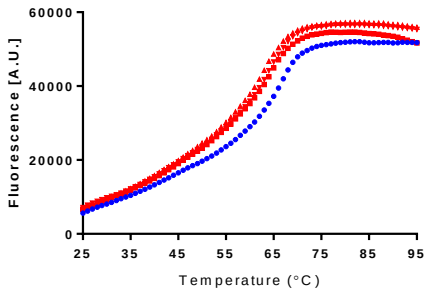
60000
40000
20000
0
Fluorescence [A.U.]
25 35 45 55 65 75 85 95
Temperature (°C)

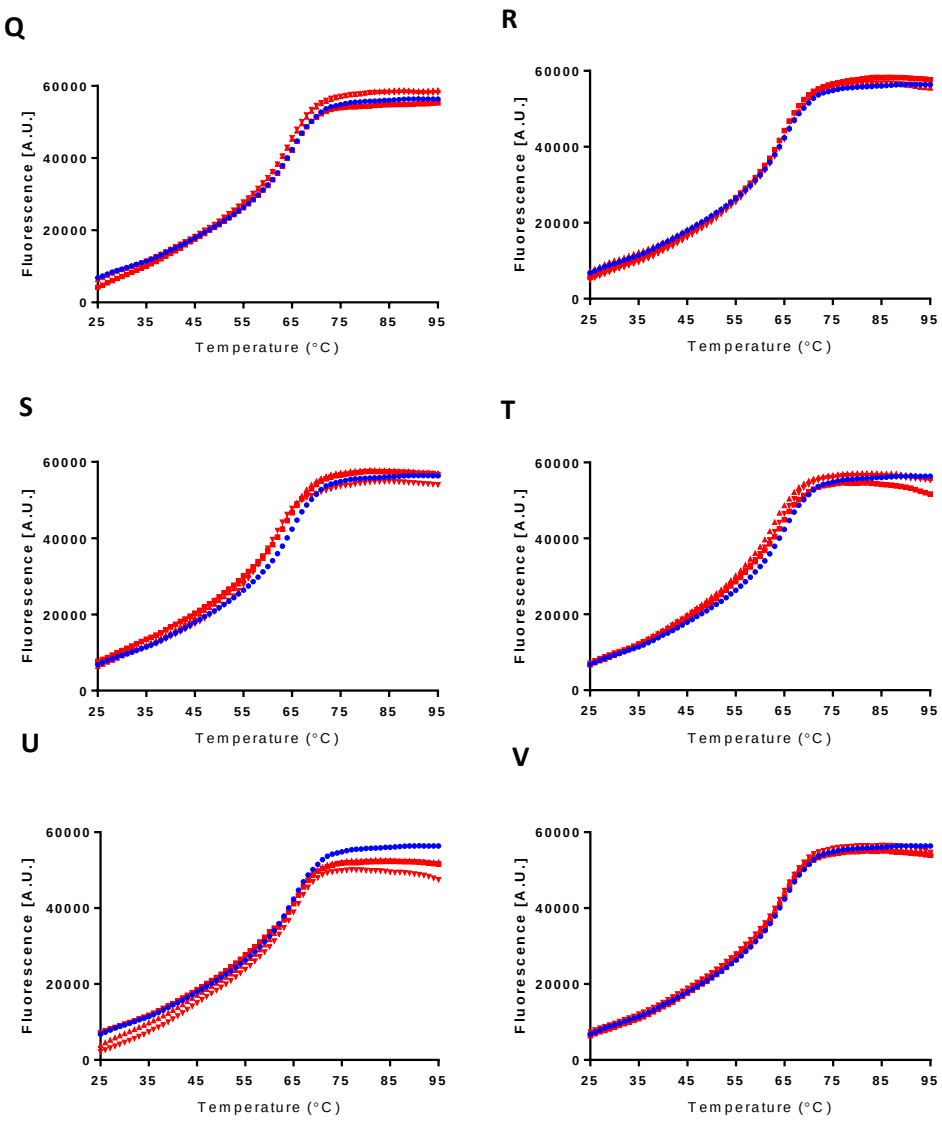

Figure 9.5: Raw CPM Fluorescence Data for Selected Compounds with TREK1. *TREK1 only fluorescence curves are shown in blue while curves in red are those of TREK1 with the addition of 20 µM compound. The compounds added in the various figures are as follows: A: Penfluridol, B: BL1249, C: Sulfasalazine, D: Idebenone, E: Cilnidipine, F: Rimonabant, G: Ondansetron, H: Cetirizine, I: Mesalamine, J: Tolperisone, K: Resveratrol, L: Argatroban, M: Prasugrel, N: Genipin, O: Mizoribine, P: Methyldopa, Q: Amoxapine, R: Pomalidomide, S: Duloxetine, T: Flavoxate, U: Isoniazid, V: Ticlopidine. All compounds were tested with 3 biological replicates of TREK1.*

Appendix 5

A

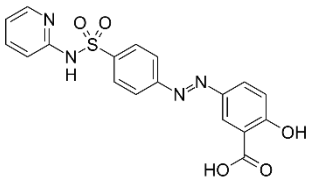

B

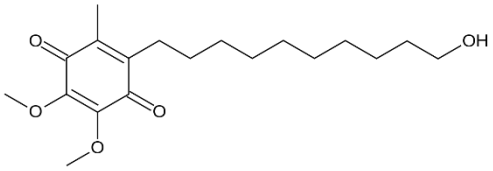

C

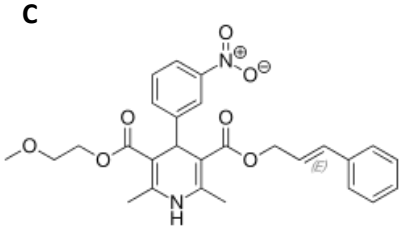

D

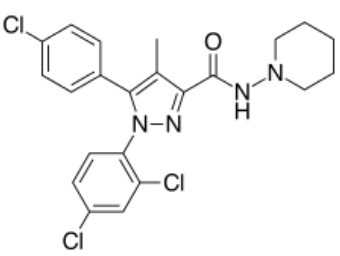

E

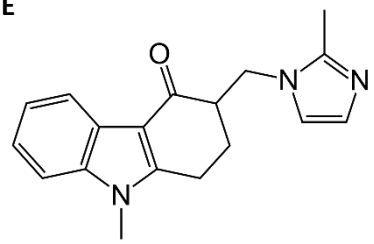

F

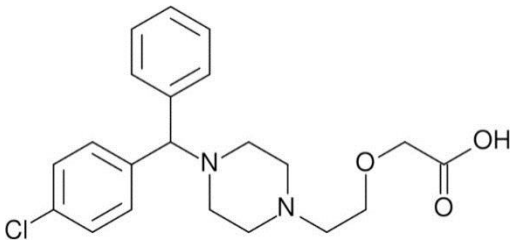

G

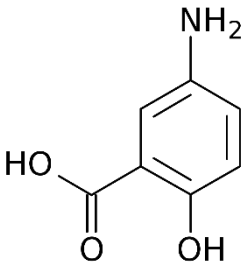

H

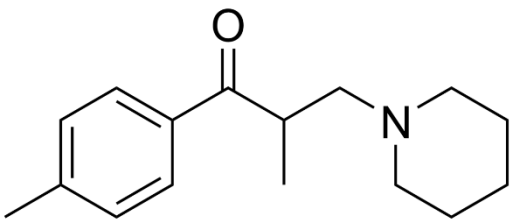

I

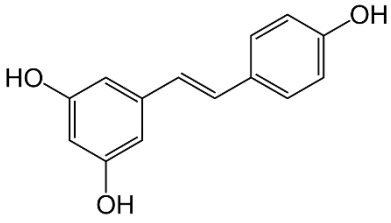

J

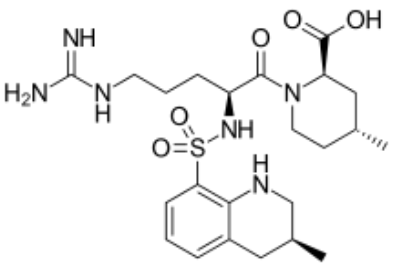

K

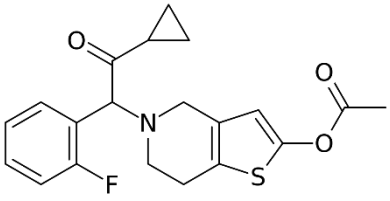

L

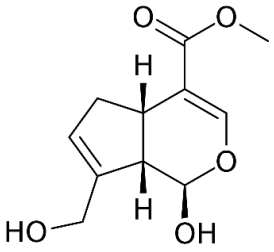

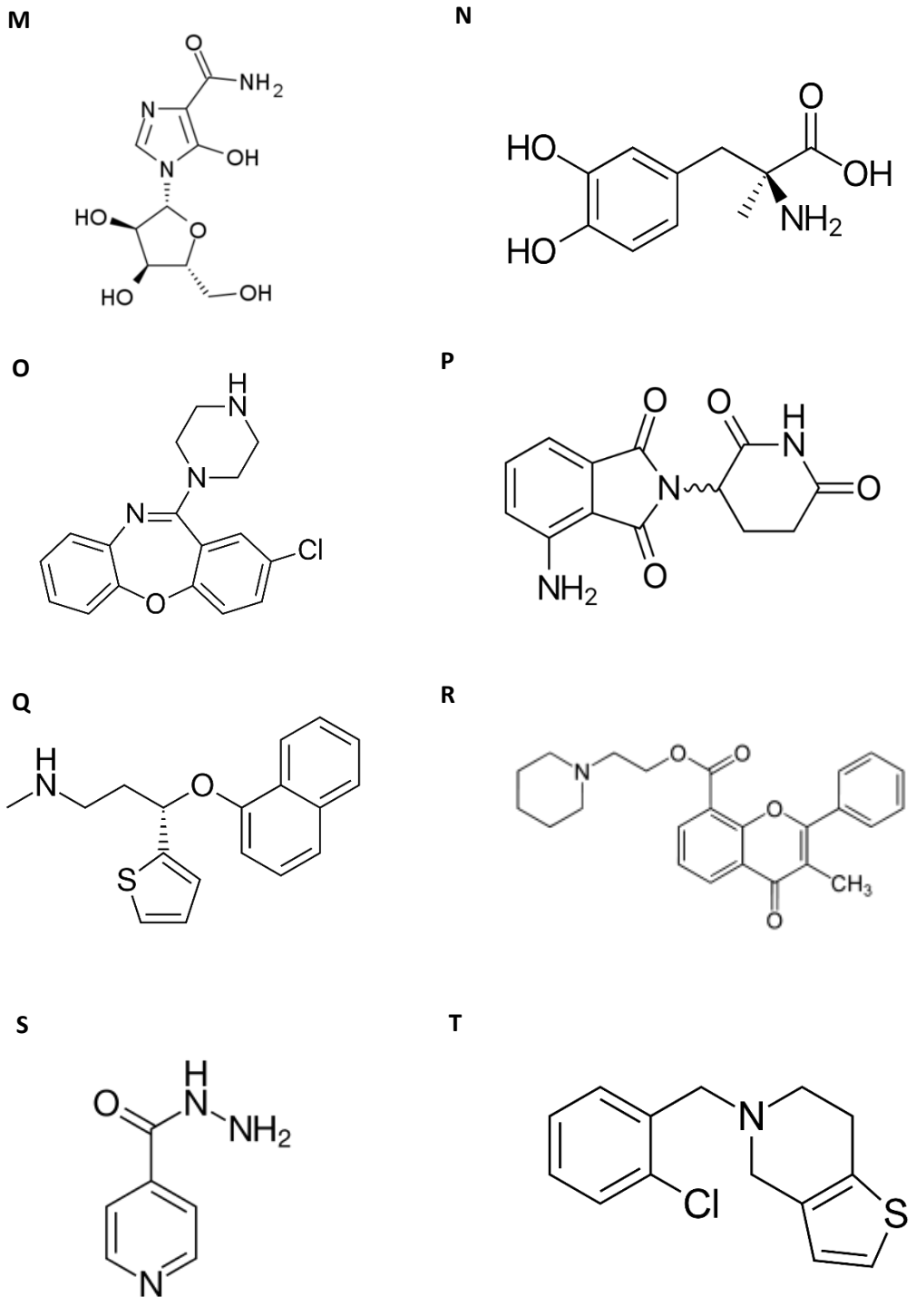

Figure 9.6: Structures of Selected Compounds for Label-free DSF and TEVC analysis. *The compounds shown in the various figures are as follows, A: Sulfasalazine, B: Idebenone, C: Cilnidipine, D: Rimonabant, E: Ondansetron, F: Cetirizine, G: Mesalamine, H: Tolperisone, I: Resveratrol, J: Argatroban, K: Prasugrel, L: Genipin, M: Mizoribine, N: Methyldopa, O: Amoxapine, P: Pomalidomide, Q: Duloxetine, R: Flavoxate, S: Isoniazid, T: Ticlopidine.*